SIMULATION OF THE GENERATION AND PROPAGATION OF BLAST INDUCED SHOCK WAVES

by

GAVIN JOHN YUILL, B.Eng

Submitted in accordance with the requirements for

the degree of Doctor of Philosophy

Department of Mining and Mineral Engineering

THE UNIVERSITY OF LEEDS

MARCH 2003

The candidate confirms that the work submitted is his own and that appropriate credit has been given where reference has been made to the work of others.

Gavin John Yuill

Simulation Of The Generation And Propagation Of Blast Induced Shock Waves

Doctor of Philosophy : March 2003

ABSTRACT

Hybrid modelling of blast vibration uses the signal produced from a single hole test shot to simulate the vibration that would be produced by a full-scale production blast. This simulation can be used to determine optimum hole timings to minimise the vibration generated at a point of interest. This thesis studies the assumptions that are made to facilitate the use of hybrid modelling with emphasis placed on near to mid field applications.

A highly accurate seismograph is developed and used to monitor a series of test blasts carried out in limestone and chalk. The repeatability of single hole test shots is investigated. It is shown that in the near field single holes are generally highly repeatable even with relatively major differences in design. It is also shown that an inversion of the radial and transverse vibration traces may occur. The factors which affect the vibration magnitude are also explored, showing that the level of confinement can have a large effect on the magnitude of vibration.

Two, three and five hole production blasts are examined to determine the signal generated by each hole in the blast. It is shown that in a two hole blast the second hole can produce an inverted signal in the radial and transverse components.

The three and five hole are disassembled by using a computer program to test every possible combination of convolved single holes and select the best. It is concluded that the complex interaction of the vibration generated by each blast hole makes it very difficult to model the vibration generated by a production blast in the near field.

CONTENTS

ABBREVIATIONS

π	The ratio of a circle's circumference to its diameter
ac	Alternating current
A/D	Analogue to digital
DC	Direct current
FFT	Fast Fourier transform
Hz	Hertz
Kg	Kilogramme
m	Metres
mm	Millimetres
ms	Milliseconds
PPV	Peak particle velocity
s	Seconds
USBM	United States Bureau of Mines
VoD	Velocity of detonation

LIST OF TABLES AND ILLUSTRATIVE MATERIAL

CHAPTER 1

CHAPTER 2

CHAPTER 3

List of Tables and Illustrative Material

CHAPTER 5

CHAPTER 7

Chapter 8

List of Tables and Illustrative Material

1. INTRODUCTION

1.1 The environmental impact of blasting

In The United Kingdom, it is inevitable that occupied structures will be in close vicinity to quarrying and mining operations which utilise explosives to break rock. It is an unavoidable side effect of these blasting operations that unused energy from an explosion will be dissipated in the form of ground vibration.

It has been widely agreed that there are two potential problems related to blast vibrations. These are structural damage and human response.

Much work has been done on identifying vibrations levels which cause structural damage. The most widely quoted research to identify safe vibration levels from blasting was undertaken by the United States Bureau of Mines (Siskind et al, 1980). This reports from case history data that a Peak Particle Velocity (PPV) limit of 12mms^{-1} will provide protection from blast damage in greater than 95 % of cases.

Unfortunately the human body can detect vibrations at a much lower level than 12mms^{-1} and have a much higher perception of low frequency vibration, (Bellman et al, 1999) such as that generated by blasting operations. This fact means that complaints made by members of the public are likely at levels of vibration far below anything which can cause damage and far below any planning constraints placed on an operation. This has led to local planning authorities imposing more and more stringent planning limits for blast vibration on mining and quarrying operations.

To ensure compliance with these regulations mines and quarries must use some manner of prediction technique which will give an indication of vibration levels at a certain distance from the blast.

There are several methods available to predict and minimise blast vibration. These range from simple equations to complex models of vibration generation and transmission. The following is a brief review of some of the more popular techniques along with their strengths and weaknesses.

1.2 Prediction of peak particle velocity using scaled distance methods

The most widespread method of determining the level of vibration generated at a point of interest is by using scaled distance methods. Scaling of distance relates the maximum charge weight per delay and the distance from the point of interest to the peak ground particle velocity or PPV. The basic scaled distance equation takes the form:

$$PPV = K\left(\frac{D}{C^n}\right)^{-A} \qquad (1.1)$$

Where: D = Distance

C = Charge weight Per Delay

K and A are site constants which can be determined empirically

n is an exponent, usually either 0.5 for square root scaling or 0.33 for cube root scaling.

The site constants have to be determined empirically by conducting test blasts at the site and measuring particle velocities with seismographs at several different distances in different directions. By varying the charge weight for each blast a log-log plot of peak particle velocity versus scaled distance may be constructed. The slope of a best fit straight line through the data is equal to the constant A and the value of velocity at a scaled distance of 1 is equal to the constant K.

Equation 1.1 appeared in the square root form in a paper by Devine et al (1966), and various other investigators have published formulae which are basically the same equation (Morris and Westwater, 1953, Crandell, 1960)

Many investigators (Duvall and Folgeson, 1962; Attewell and Farmer, 1964) have also proposed a more general scaled distance equation of the form:

$$\text{PPV} = KD^{-A}C^{nA} \qquad (1.2)$$

which avoids assuming an ideal relationship between distance and charge weight.

There are two most commonly used cases of equations 1.1, where n is equal to 0.5 or 0.33. These, for obvious reasons, are known as square root scaling and cube root scaling respectively. These two methods will, obviously, give differing predictions of PPV based on the same field measurements. This clearly leads to problems and is therefore unsatisfactory.

It has been suggested that these empirical laws be shaped by dimensional analysis (Ambrasyes and Hendron, 1968, Newmark, 1968). Dimensional analysis results in cube root scaling laws for explosions of different magnitude in the same medium. This approach has led to the widespread use of cube root scaling.

However, many investigators (Devine and Duvall, 1963, Devine, 1966) have found by experimentation that square root scaling gives a higher correlation coefficient than cube root thus indicating that it is a better model. Attewell and Farmer (1964) also explain that the peak amplitude of particle velocity caused by an explosion should be proportional to the square root of the energy released and that under elastic conditions it should decrease inversely with distance for body waves or as the square root of the distance for surface waves. This would mean that a square root scaling would be more appropriate.

In fact, however, as site conditions rarely comply with assumptions made in dimensional analysis neither scaling method is strictly appropriate. The best estimate of relative scaling between distance and charge weight is site specific.

Blast vibration data is usually presented in graphical form with a line of best fit obtained by regression analysis. Much data in this form is available in literature and almost without exception the PPV is adequately represented by a power law decay with scaled distance. That is, the measured PPV decay can be represented by a straight line on a log-log plot although the slope and intercept may vary considerably from site to site. Figure 1.1 shows a typical scaled distance versus PPV log-log plot.

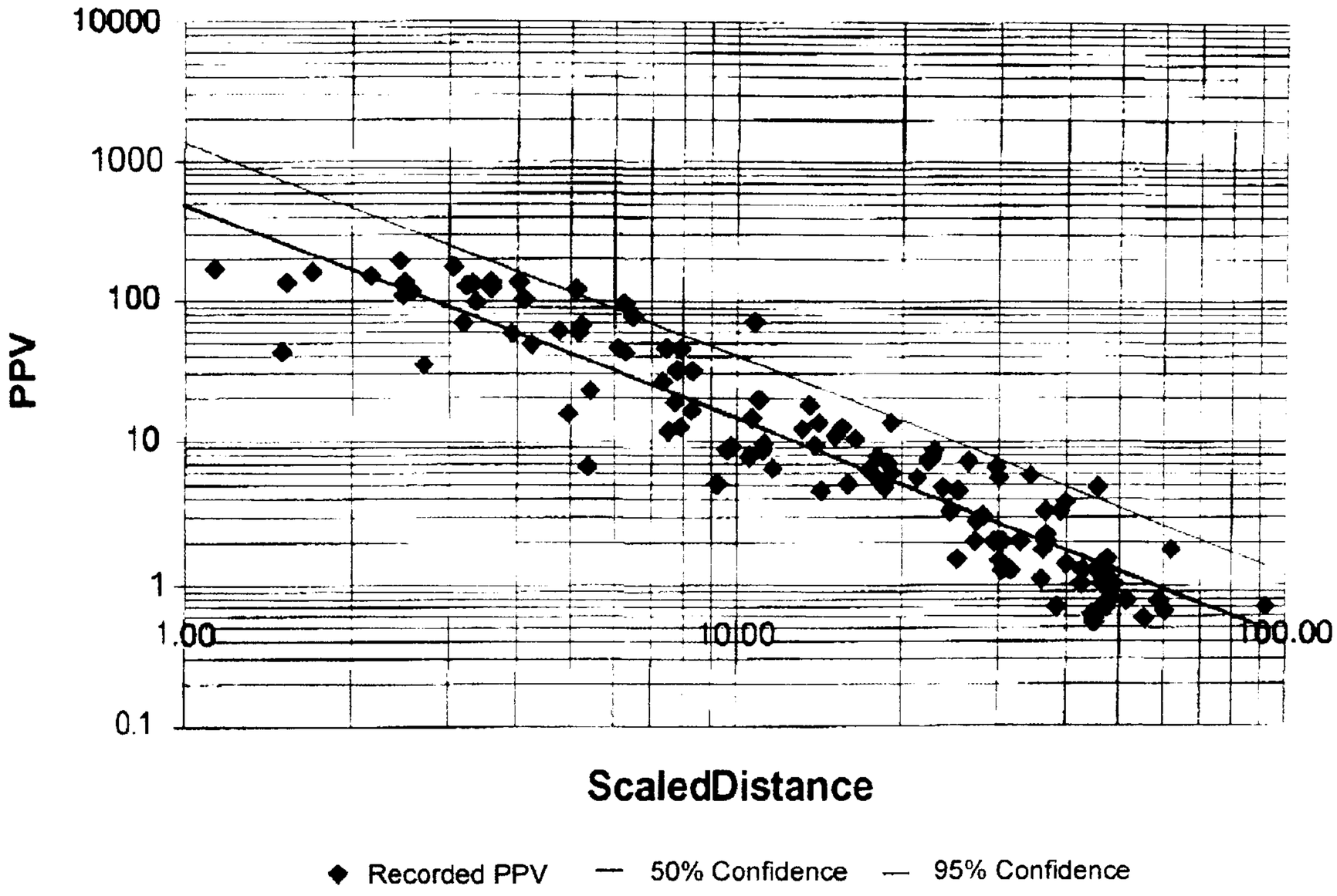

Figure 1.1 Typical scaled distance chart on log-log paper

The scaled distance technique is, however, a far from ideal method of predicting vibration levels. Problems occur due to the amount of scatter encountered in the levels of vibration recorded. This can be clearly seen in figure 1.1. Walker (1981) describes a dataset recorded at an opencast mine with a standard error of 3.52mms^{-1} in a range of PPV's between 0.254 and 4.51mms^{-1} with a correlation coefficient of 0.9660.

Outliers on the scaled distance charts push the mean maximum charge weights down. As the operator will have a limit above which no more than 5% of the blasts may exceed they must blast conservatively by ensuring that their charge weight falls

beneath their 95% confidence line on the scaled distance plot. This can mean in effect that the operator is imposing a further limit on the already stringent limits put in place by the planning authority.

It has also been noted by many investigators, including Siskind et al (1980) and Dowding (1985), that not only the magnitude of vibration but the frequency is also important. It is difficult but not impossible to predict the dominant frequency in a blast from its predicted PPV. In order to predict the dominant frequency, acceleration and displacement must also be predicted and the results plotted on tripartite paper. Tripartite paper graphically represents the mathematical interaction between frequency and maximum amplitude.

This method of frequency prediction is at best a crude indicator of the dominant frequency of a blast. Coupled with the fact that scaled distance PPV predictions can be highly inaccurate to start with, the reliability of the frequency prediction must be questioned.

Even with its major flaws, scaled distance prediction of peak particle velocity remains the most popular technique employed in the blasting industry. This is mainly due to its simplicity to understand and ease of use.

Other prediction and control techniques are however available. These are described in the following sections.

1.3 Mathematical Modelling of Blast Induced Shock Waves.

Mathematical modelling of blasting vibration is an alternative to extensive field tests and empirical formulae. It is far more time and cost efficient to be able to run a number of numerical models to gain an insight into the effects of different design parameters before carrying out a field evaluation.

The biggest problem with numerical modelling is that the theoretical foundation of cylindrical charges is currently not well developed. The United States Bureau of Mines (USBM) has done much work using very short cylindrical charges. These can be considered as spherical charges. The theory of spherical charges is far more advanced than that of cylindrical charges. (Duvall and Petkof, 1959; Aitchison and Tournay, 1959). The results gained from these experiments have shown that in the far field a spherical charge can represent a cylindrical quarry blast with reasonable success. In the near field, however, the technique fails to model the vibration with any degree of success.

1.3.1 Numerical Modelling of Cylindrical Charges

In the near field there are very few analytical solutions for cylindrical charges available and those which have been published are highly complex and have very special conditions attached to them. They are therefore of little use in real blasting conditions.

Heelan (1953) described a theoretical model for the radiation of vibration from a finite length cylindrical charge in a homogenous, isotropic and linearly elastic half space. This model would have been important to the seismic field but unfortunately he made some fundamental errors in his equations which rendered the model unusable.

Jordan (1962) considered a hole of infinite length in an infinite homogenous material over which a finite length instantaneous uniform pressure of constant magnitude is applied. By using a double Fourier integral technique the solution can be determined in the form of a double integral. The solution does not take into account damping or dispersion and there is no provision for the velocity of detonation.

Abo-Zena (1977) proposed a similar model to Jordan which claims to provide an analytical solution for cylindrical sources but only when the radius of the cylinder is small when compared to that of the smallest wavelength of interest.

1.3.2 Finite Element Modelling of Blast Holes

Another possible way of modelling the vibration generated by a cylindrical charge is to use computer based dynamic finite element modelling (DFEM) techniques to examine stress and strain waves around a blast hole. In this application a mesh of elements is constructed to represent the area to be modelled. Impulses representing the detonating charge are then applied. The software then gives a graphical output at certain time steps of the forces throughout the mesh. At the moment these techniques are in their infancy but are becoming more important. The biggest

drawback of these techniques currently is the amount of time required to run a model. A 3D model of a single blast hole with a fine mesh can currently take over a week to run on a fast PC. Once multiple holes are taken into account the processing time can be months. Blair and Minchinton (1996), Hirai et al (1998) and Dare-Bryan et al (2001) all give good overviews of this technique and its various applications within blast modelling.

1.3.3 String charge modelling of blastholes

A third approach to the numerical simulation of blasting is based upon replacing a cylindrical charge with a string of spherical charges. This technique was first developed by Plewman and Starfield (1965) and expanded by Starfield and Pugliese (1968) and Harries (1983) amongst others.

The basic premise relies on dividing the charge length into finite length elements and replacing these with spheres of the same volume as the finite length elements and then reducing these to point sources at the centre of the sphere which can be used to initiate a seed waveform based on either the empirical or analytical model for spherical charges, according to the velocity of detonation. Figure 1.2 shows the steps in forming this model. The seed waveform used as a source function by Plewman and Starfield from each spherical charge was developed using empirical means as an approximation of the stress wave produced by a spherical charge. They defined the function as:

$$f(t) = \frac{Be^{-\beta t} \sin \omega t}{r^n} \tag{1.3}$$

Where: B is the amplitude constant

β is the damping constant

ω is a the angular frequency

n is the attenuation factor

r is the radius

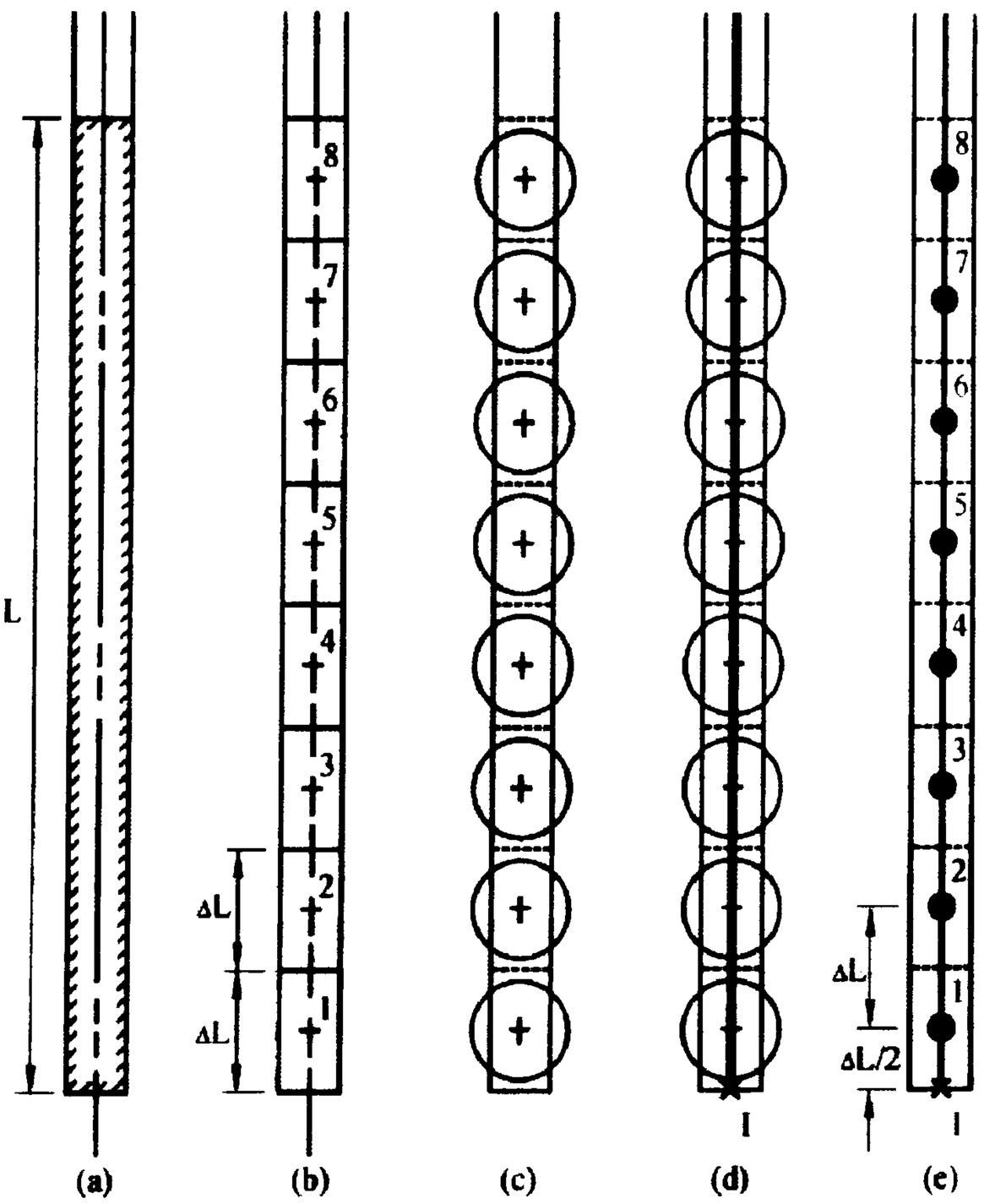

Figure 1.2 Development of a string charge model, (a) the full cylindrical charge, (b) division into finite length segments, (c) replacement by spheres, (d) connection by detonating line, (e) reduction to point charges.

The corresponding waveform of this equation is that of a damped sine wave. This model, which although gives reasonable results, takes no account of the effect of changes in the properties of the explosive or changes in the dimensions of the charge.

Shortly after Plewman and Starfield published their work using the empirical model, Favreau (1969) released his analytical solution for the vibration generated by an explosive contained within a spherical cavity. Favreau defined his solution as:

$$V_r = e^{-\alpha^2 \tau / \rho c b}\left[\frac{Pb^2 c}{\alpha\beta r^2} - \frac{\alpha P b}{\beta \rho c r}\sin\frac{\alpha\beta r}{\rho c b} + \frac{Pb}{\rho c r}\cos\frac{\alpha\beta r}{\rho c b}\right] \qquad (1.4)$$

where $$\alpha^2 = \frac{2(1-2\sigma)\rho c^2 + 3(1-\sigma)\gamma P}{2(1-\sigma)}$$

$$\beta^2 = \frac{2\rho c^2 - 3(1-\sigma)\gamma P}{2(1-\sigma)}$$

$$r = \tau - \frac{(r-b)}{c}$$

The value of V_r is the particle velocity at a distance r from the centre of the charge. The properties of the rock are defined by the Poissons ratio, σ, the mass density, ρ and the wave velocity, c. The explosive properties are defined by the detonation pressure, P and the ratio of the specific heats of the explosion gases in the vicinity of P, γ. The radius of the cavity is defined as b.

This model predicts the waveform at the borehole wall and as such does not have any mechanism for applying attenuation to the signal. This means that this model alone cannot be used to determine vibration levels at a distance.

1.3.3.1 Constant Q attenuation

Harries (1983) used a method called constant Q attenuation in order to allow the use of this model with the Starfield and Pugliese string charge model with good results.

The attenuation of a shock wave can be represented by the seismic quality factor, Q. This factor is inversely proportional to the energy loss in the rock per cycle:

$$\Delta E = \frac{KE}{Q} \tag{1.5}$$

Where ΔE is the energy loss

K is a dimensionless constant.

E is the source energy

Q is the seismic quality factor

Equation 1.5 can be rewritten in terms of Q with K equal to $1/2\pi$:

$$\frac{1}{Q_{AB}} = \frac{2\pi\Delta E}{E} \tag{1.6}$$

Where Q_{AB} is the seismic quality factor applying to the distance AB

The use of Q was first suggested by Born (1941) who suggested that the value of Q was independent of frequency and attenuation was a process of linear friction. This is in contradiction to experimental behaviour of the friction of rocks which has been shown to be non-linear (Dietrich, 1972). The frequency independence of Q, however, seems to be confirmed by experimental evidence. Kjartansson (1979) developed the first real constant Q model which fits with most experimental data including that of Ricker (1953) who was a strong advocate of the theory that Q was indeed frequency dependant. Although Kjartansson's model cannot be explained using elastic theory there is no doubt that the Constant Q model most closely fits experimental data.

The string charge model is lacking in two major areas. Firstly, as only spherical charges are used no shear waves are produced. As Blair and Minchinton (1996) have pointed out the shear wave contribution for cylindrical charges is significant and in fact may be dominant. The model also does not take into account the action of gas pressure. The model is also designed to be used with single hole sources with no provision being made for using multiple holes.

For these reasons the results gained from this model can be called into question even though very satisfactory agreement with experimental data has been obtained.

Numerical models of blast vibration are in general a useful tool but all the techniques described here have major shortcomings which prevent their use in real life situations. DFEM modelling will become more important when computing power allows 3D multiple hole shots to be modelled within a timely manner with any

degree of accuracy. Until then, numerical modelling will stay on the sidelines of blast vibration prediction.

1.4 Hybrid Modelling of Blast Vibration

The importance of the delay between holes in a multi-hole blast has been well documented for a number of years (Kissingler, 1963; Langefors and Khilstrom, 1978). The technology to take this knowledge and apply it to a model is something which did not really become available until the late 1980's.

1.4.1 Basics of Hybrid Modelling

Hinzen (1988) was one of the first to develop a usable model based upon the recording of a single hole "signature" vibration recording. Hinzen realised that the biggest problem with simulation of blast vibration is that the formation of seismic waves from cylindrical charges is not well understood. By assuming a linear superposition of the seismic effects of the individual holes in a row shot the vibration generated by a production blast could be simulated.

Hinzen stated that the ground movement at a specific location could be represented as

$$u(x,t) = m(\xi,\tau) \otimes G(x,t,\xi,\tau) \tag{1.7}$$

where $m(\xi,\tau)$ is the source time function of the row shot

$G(x,t,\xi,\tau)$ is the elastodynamic greens function

x is the observation point

ξ is the source location

The resulting ground velocity can be determined by a differentiation of equation 1.7. Under the assumption that the displacement field of a row shot is a linear superposition of the displacements produced by individual holes the source time function can be separated into two parts. (The mathematical dependency on x, ξ, τ and t has been dropped in all following equations)

$$m = m_s \otimes m_R \tag{1.8}$$

where $m_R = a_i \delta(t - t_i),\ i = 1,\ldots\ldots N$ (1.9)

N = Number of Charges

t_i = Firing time of charge i

The source time function of a single hole is m_s whereas m_R is an impulse series. The amplitudes of the impulses a_i in equation 1.9 are the scaling factors of individual holes.

The superposition of the individual waves is expressed mathematically as a convolution. The arrival times of the vibration from the detonation of the individual

holes at the observation point is expressed by the position of the impulses in the series.

The displacement history of a single hole at the specified location can therefore be written as

$$u_s = m_s \otimes G \tag{1.10}$$

Combining equations 1.7 and 1.8 the displacement for a complete row shot can be determined

$$u = m_s \otimes m_R \otimes G \tag{1.11}$$

due to the commutative character of the convolution process this can be reduced to

$$u = u_s \otimes m_R \tag{1.12}$$

The impulse series m_R can be calculated and the convolution in equation 1.12 combines the single shot measurement and the model calculation.

Figure 1.3 shows a flow chart of the steps involved in Hinzen's model. Figure 1.4 shows a typical hybrid model of a 4 hole shot with 25ms delays.

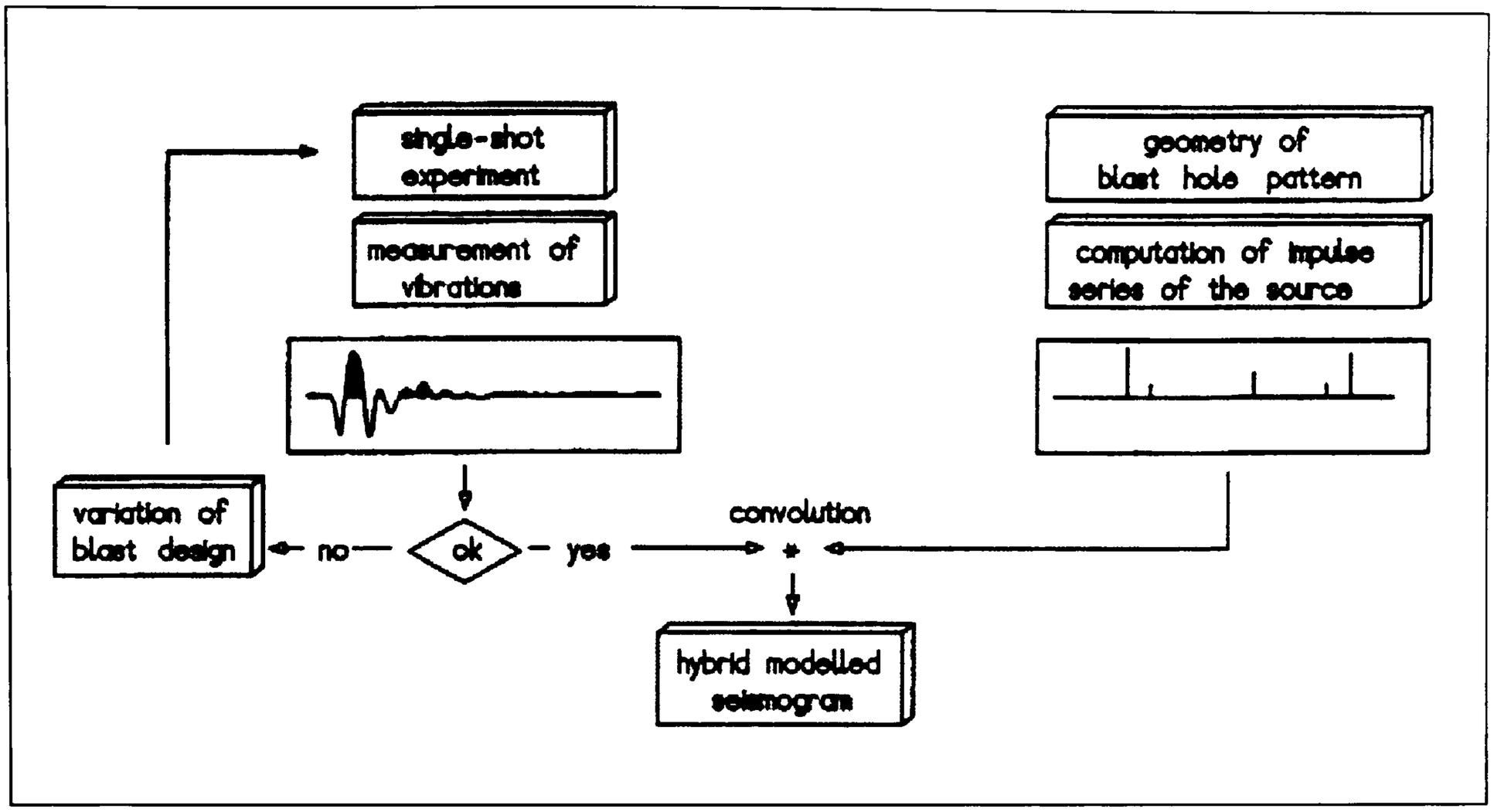

Figure 1.3 Flow Diagram of the Hybrid Modelling of Blast Vibrations in the Time domain. (After Hinzen, 1988)

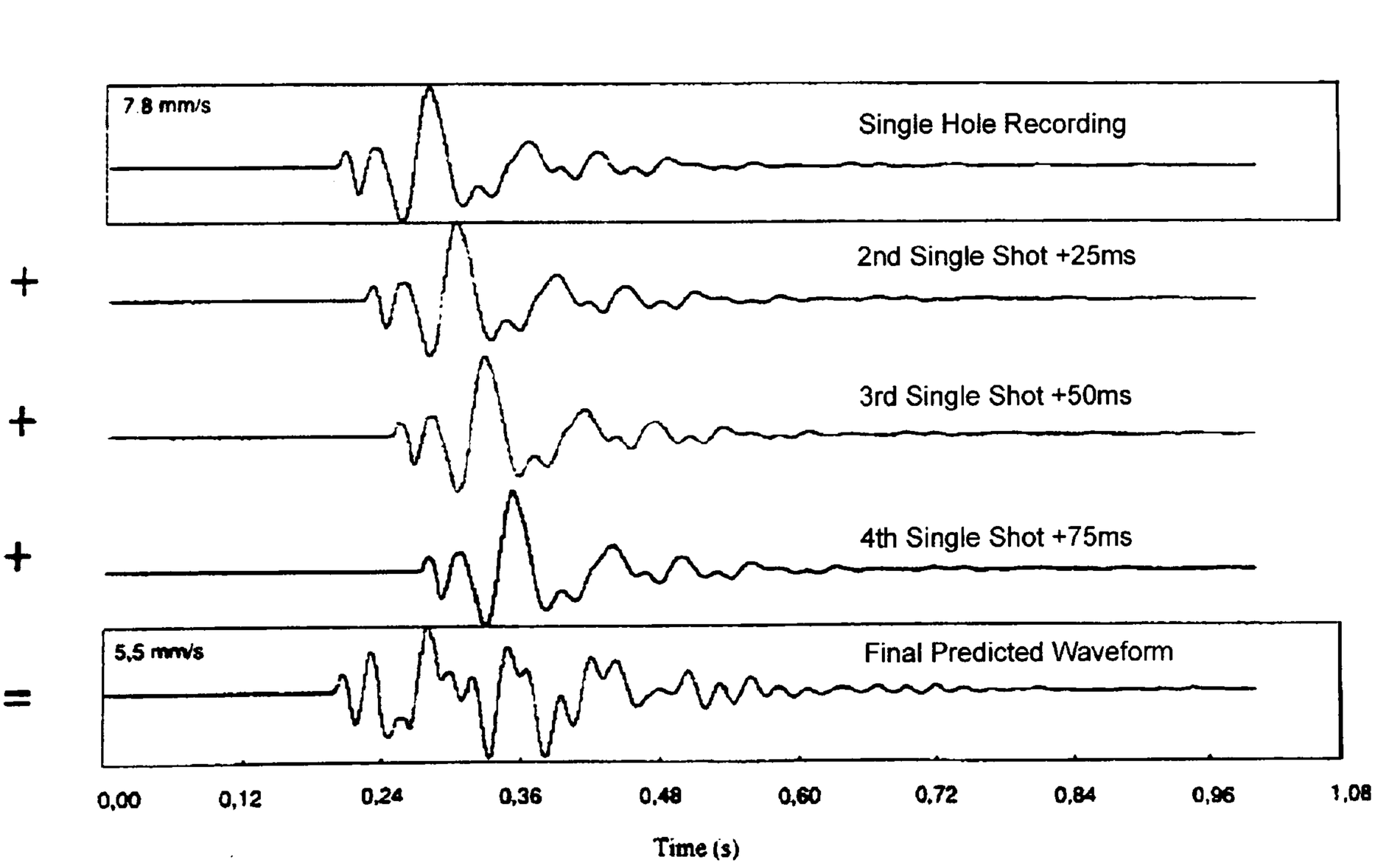

Figure 1.4 Example of Hybrid Model of 4 Hole Shot Using 25ms Delays.

1.4.2 Examination of the Hybrid Model

The main advantage of Hinzen's model is that as it provides a full blast waveform in the time domain it is possible to determine the phase and frequency components of the blast through the use of Fourier transforms as well as the magnitude of the blast vibration.

The model can also be used as a system to minimise vibration by running the model with varying delay times between the holes. The delay time which minimises the PPV can then be selected. Reamer et al (1993) describe two case studies where the firing time has been optimised using hybrid modelling and the resulting vibration was reduced by up to 50%.

Mogi et al (2000) take firing time optimisation a step further. They describe a method of reducing the dominant frequency of a blast by examining the dominant frequency in the signature single hole recording and selecting a time delay corresponding to half the period of that frequency with which to convolve the second hole. That in turn lowers the energy in that part of the spectrum. The two hole signal is then examined for the dominant frequency and the process repeated until a full blast has been designed.

One of the main drawbacks of this system is that highly accurate detonator firing times are required; Reamer et al (1992) note that for the system to be valid detonator delay error must be no more than 1%. Standard pyrotechnic detonators are highly inaccurate. Small (1986) describes a batch of detonators under test having a mean

firing time over 50ms away from that specified. Modern electronic detonators can overcome this problem. They are microprocessor controlled thus ensuring that they initiate at exactly the specified time. They also allow simple programming of the initiation time enabling systems like that described by Mogi et al. (2000) to be used with ease.

Another major drawback to this system is the assumption that each hole in a blast produces the same vibration waveform. Most investigators in this area of work quote this assumption with minimal work being available to back it up. The repeatability of single holes and the signals generated by individual holes of a multi-hole shot will be studied in greater depth throughout this thesis. Most investigators claim that hybrid modelling will give more consistent results when used in the far field. The reasoning that is put forward for this is that there will be less effect generated by the different wave-paths of the vibration. Investigators often blame problems with a model on this effect.

Many investigators (Firth, 1992; Farnfield and White, 1994; Coursen, 1995; Sifre and Bernasconi, 1996; Mogi et al, 2000) have attempted to use hybrid modelling with varying degrees of success. Farnfield and White (1994) describe a blast with 6 holes initiated 50ms apart with a charge weight of 170kg. The simulated PPV was 5.4 mm/s and the actual recorded PPV 9.4 mm/s. Figure 1.5 shows the predicted waveform generated using hybrid modelling with a single hole shot charged with 270kg of explosive. Figure 1.6 shows the recorded waveform. A large difference can be clearly seen between the waveforms.

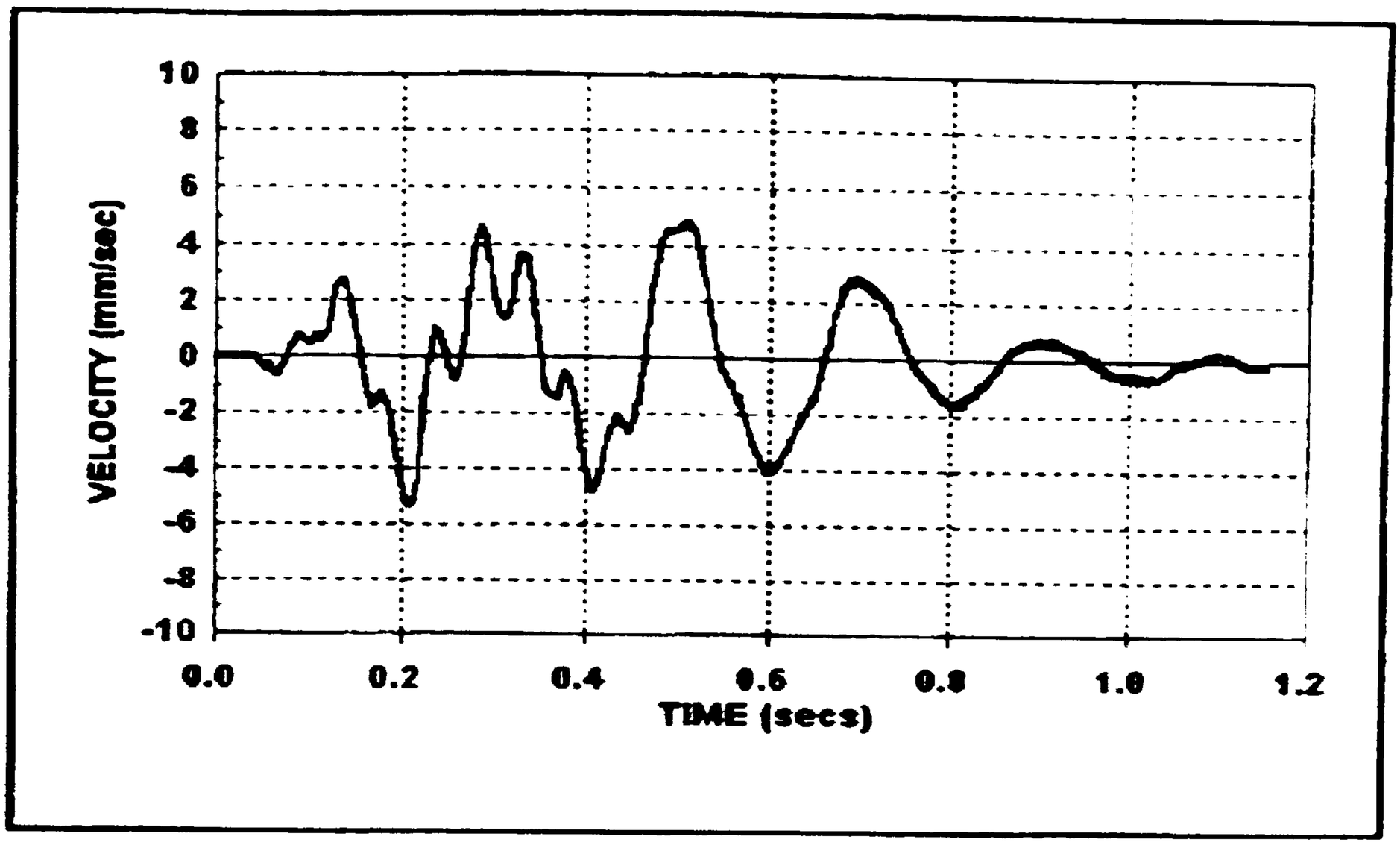

Figure 1.5 Hybrid Model Prediction of 6 Hole Shot with 50 m/s delays. (After Farnfield and White, 1994)

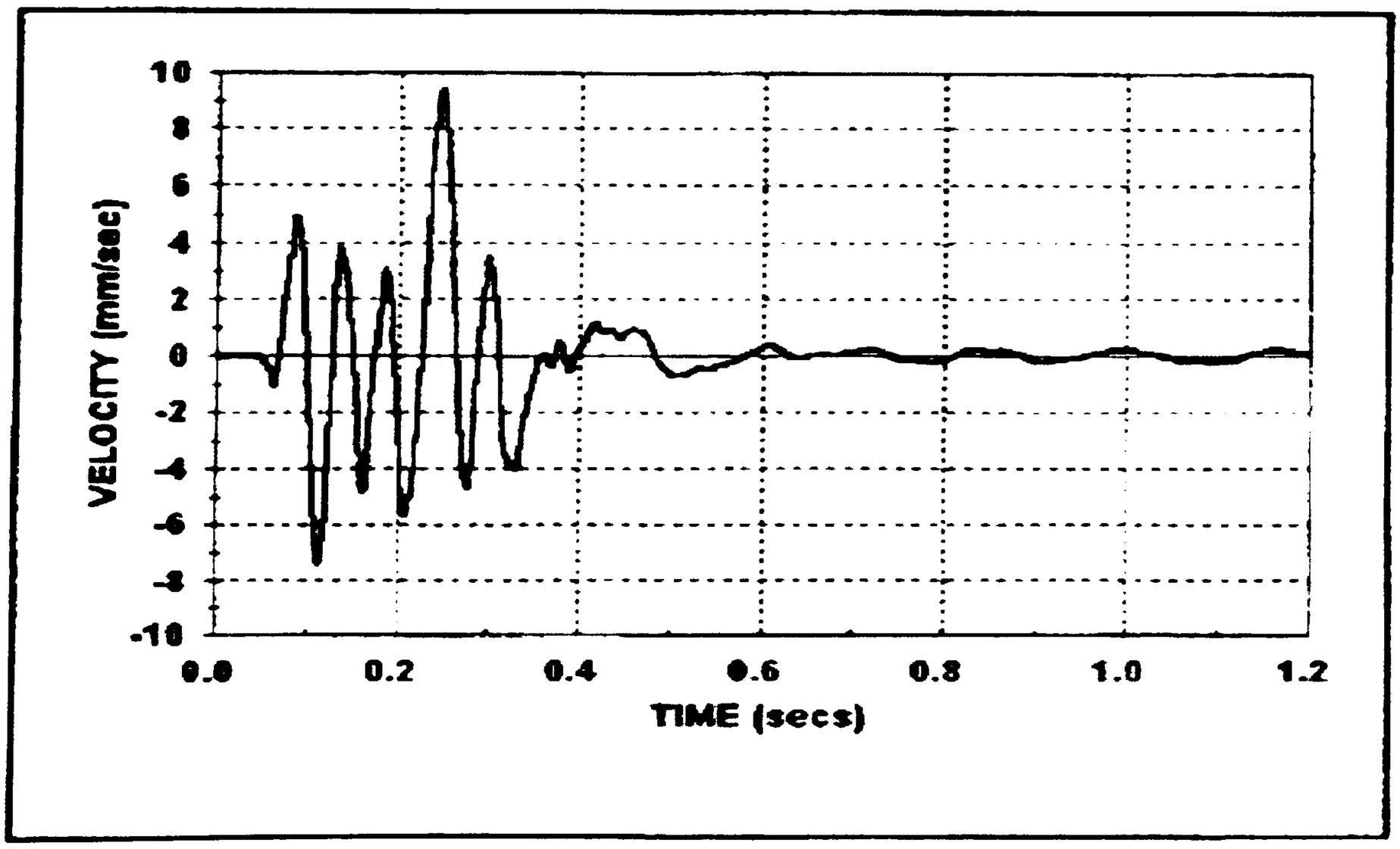

Figure 1.6 Actual Recording of Blast Modelled in Figure 1.5 Using 175Kg Charges. (After Farnfield and White, 1994)

Farnfield and White repeated the experiment using the model shown in figure 1.5 but this time with a charge weight of 190kg. The resulting waveform is shown in figure 1.7. There is clearly more correlation between the model and the recorded waveform and the recorded PPV of 5.4 mm/s is exactly the same as that predicted by the model. However, the model is still different from that recorded and cannot be said to accurately describe the recorded waveform.

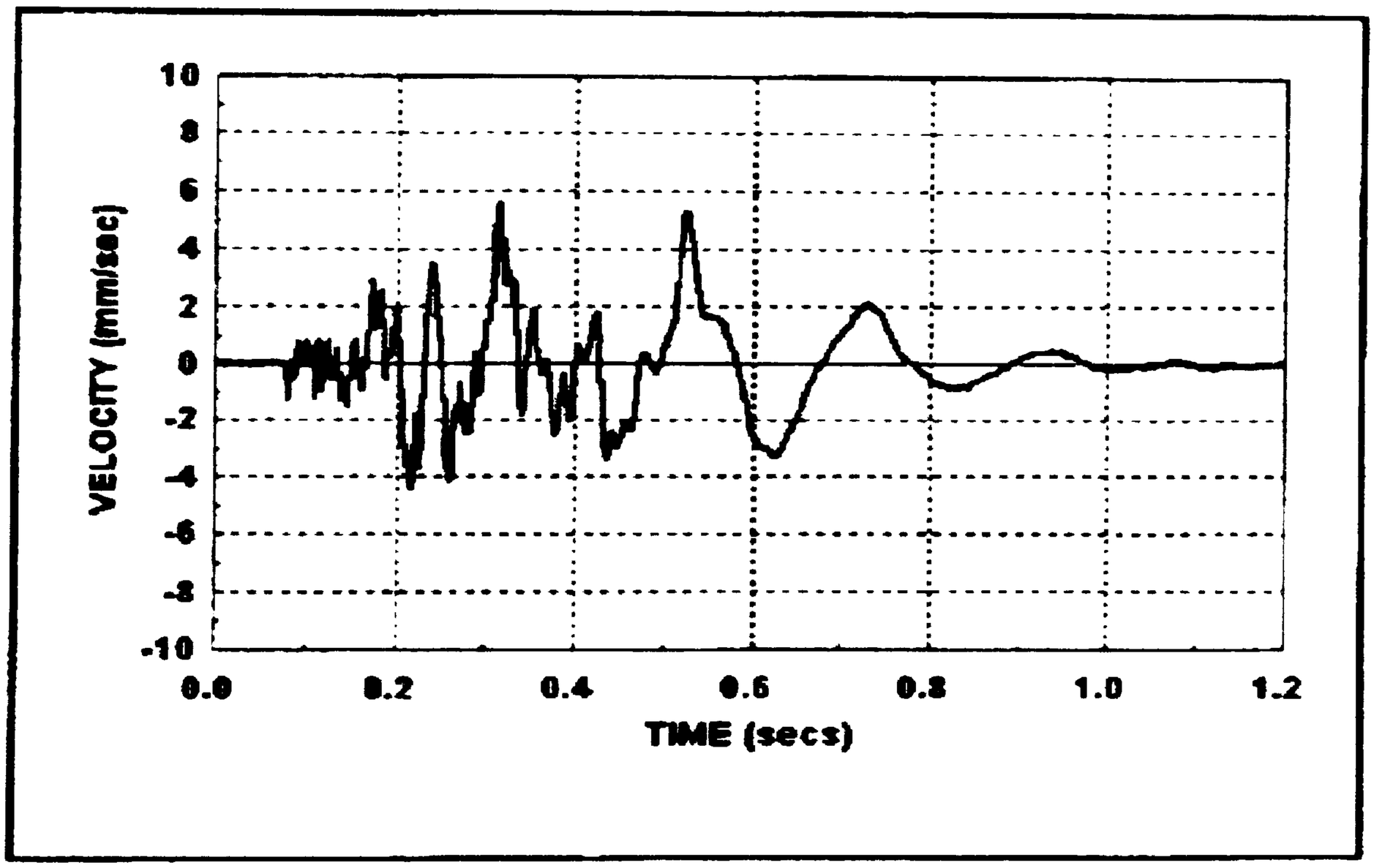

Figure 1.7 Actual Recording of Blast Modelled in Figure 1.5 Using 190Kg Charges. (After Farnfield and White, 1994)

The major differences between the two recorded waveforms perfectly illustrate the problem with hybrid modelling. When two very similar blasts can give two completely different waveforms it becomes very difficult to model.

1.5 Simulation Of The Generation And Propagation Of Blast Induced Shock Waves

In the author's opinion hybrid modelling of blast vibration is currently the most promising usable technique for predicting full vibration waveforms generated by a multi-hole shot. Many investigators have claimed that it is currently a usable tool to accurately predict blast vibration wave-shape and magnitude although it is clear that this is not the case in all situations

This research project has been primarily concerned with the study and refinement of the technique of hybrid modelling through the examination of single hole shots and simple multi-hole shots.

To facilitate the study of this technique a high quality multi-channel seismograph was constructed and a novel technique for the calibration of the seismograph was refined and applied. Chapters 2 and 3 examine the details of these processes.

A series of single holes were fired in a limestone quarry. The repeatability of the vibration signals generated by the single holes was examined. The factors which affect the magnitude of the vibration generated were also examined. Chapters 4, 5 and 6 detail each stage in this study

To examine the assumption that each hole in a production blast is repeatable a series of two hole shots were fired both in a limestone quarry and a chalk quarry. The results of this study are given in Chapter 7.

The final part of this research was to attempt to use the findings from the earlier chapters in order to model larger shots. Chapter 8 details the attempt to disassemble various three hole shots in a chalk quarry using computer simulations. A five hole shot in a limestone quarry is also modelled.

2. EQUIPMENT SELECTION AND CONSTRUCTION

2.1. Introduction

In order to accurately model vibration using hybrid methods it is important that as true a recording of ground vibration as is possible is made. Any parameters which may influence the blast must also be recorded. In order to do this, high quality equipment is required.

This Chapter details the equipment which was utilised in this research along with reasoning behind the choices. Also detailed is the construction of a multi-channel seismograph which was designed especially for this research.

2.2 Vibration recording systems

Two recording systems were used in this research - a multi-channel digital seismograph designed and built in the University and a commercially available seismograph made by White Industrial Seismology, Incorporated. Each system has its strengths and weaknesses which will be discussed below.

2.2.1 Multi-Channel Seismograph

When beginning this research it was decided that a bespoke digital seismograph should be designed and built rather than use commercially available units. The reasons behind this are follows:

i) Versatility - A bespoke piece of equipment could have several types of transducer connected to it. If it was decided that air overpressure should be monitored instead of vibration it can be written into the software to be able to choose between a microphone or geophone. Similarly, an accelerometer or LVDT could be connected if acceleration or displacement was to be measured.

ii) Cost - It was decided that for less than the cost of five individual commercial triaxial digital seismographs a single unit with 5 separate triaxial blocks could be constructed.

iii) Accuracy - Many commercial seismograph manufacturers use cheap geophones with high resonant frequencies and use frequency dependant amplifiers to compensate. This reduces the accuracy of the system. An alternative system using low resonant frequency geophones and signal processing techniques to improve accuracy is examined in Chapter three.

iv) Continuity - Having all five triaxial arrays recorded by a central unit has the advantage that all channels can be triggered by the closest unit. This means that spurious signals can be almost eliminated by setting the trigger to a suitably high level. It also has the advantage that all channels are recorded on the same time base allowing direct comparison of arrival times and signal length.

v) Quality - Many commercial blasting seismographs are produced to be used to monitor vibration levels for compliance with local regulations and as such are not intended for use in complex analysis. Digital resolution and recording speed are often kept to the minimum required and the data is often difficult to extract from the proprietary software provided with commercial seismographs.

2.2.2 Construction of Seismograph

The seismograph was designed around a laptop computer in a ruggedised housing and fitted with an analogue to digital converter (ADC) card. The ADC card allows the signals generated by the geophones to be captured by the computer and stored for later processing.

The software to control the seismograph was written in Hewlett Packard Virtual Engineering Environment (HP-VEE) which is an object orientated language specialising in data capture and processing. The modular format of the software makes it very easy to add and remove features giving a very flexible system for use with a multitude of transducers. The basic system has 15 channels of inputs each of which can be set as a trigger. Every channel is set to the same input sensitivity which means that transducers must be calibrated to the same sensitivity or post processing calibration must be carried out It was decided that post processing calibration was the simplest way forward. This is examined further in Chapter 3. The recorded data is stored in ASCII format which makes it easy to import into external software for processing.

The channels are arranged in five groups of three and brought out to connectors on the side of the seismograph case. This allows the triaxial geophone units to be connected easily and quickly in the field, without having to note which triaxial direction is connected to which channel. Figure 2.1 shows the laptop computer in the ruggedised housing

Figure 2.1 Digital Blasting Seismograph based on a laptop computer with ADC card.

Each channel is recorded using an analogue to digital converter. Digital sampling is an area where care must be taken to select parameters otherwise grave errors may be made. The next section describes these errors and how to avoid them.

2.2.3 Sampling Theorem

A typical time dependant signal, such as ac voltage, is continuous with respect to time and magnitude. Such a signal is called analogue. If equipment such as a tape recorder or oscilloscope is used to record this we get an analogue representation of such a signal.

Today it is far more widespread that digital equipment is used to record electrical signals. Digital signals are discrete with respect to time and magnitude. Therefore, conversion of an analogue to a digital signal means the value of the analogue signal function $F(t)$ is measured at discrete times $t_i = t_0 + i \cdot \Delta t$ during a time interval $t_m = t - t_0$, and the indicated values changes with steps ΔF. Mostly the measured value is represented by a binary number and the step ΔF depends on the number of bits processed by the analogue to digital converter.

The correct use of this sampling technology relies on knowing how often a signal must be measured during a time interval t_m in order to properly reconstruct its shape. The answer is given by the sampling theorem of time functions or Nyquist criterion described by Rost (2000) thusly:

> A function $F(t)$ with a limited bandwidth B, assuming the time interval of measurement is infinite can be correctly described when sampled with a time step of:

$$\Delta t \leq \frac{1}{2B} \qquad 2.1$$

This theorem essentially states that it is necessary to sample the function more than two times per period. For example if a resolved bandwidth of 100Hz is required it is necessary to sample at more than 200Hz.

If this criterion is ignored there is a risk of errors induced by aliasing. Lynn (1973) describes aliasing as the phenomenon whereby high frequency components are mistaken for lower frequency components due to an inadequate sampling rate. Figure 2.2 shows how a 300Hz sine wave can be mistaken for a 100Hz wave when sampled at an inadequate sampling rate of 500Hz. The solid lines are the original signal. The points are where a 500Hz sampling rate would take a measurement and the dotted line is the interpretation of the measurements. To accurately describe the 300Hz signal it is necessary to sample at more than 600Hz.

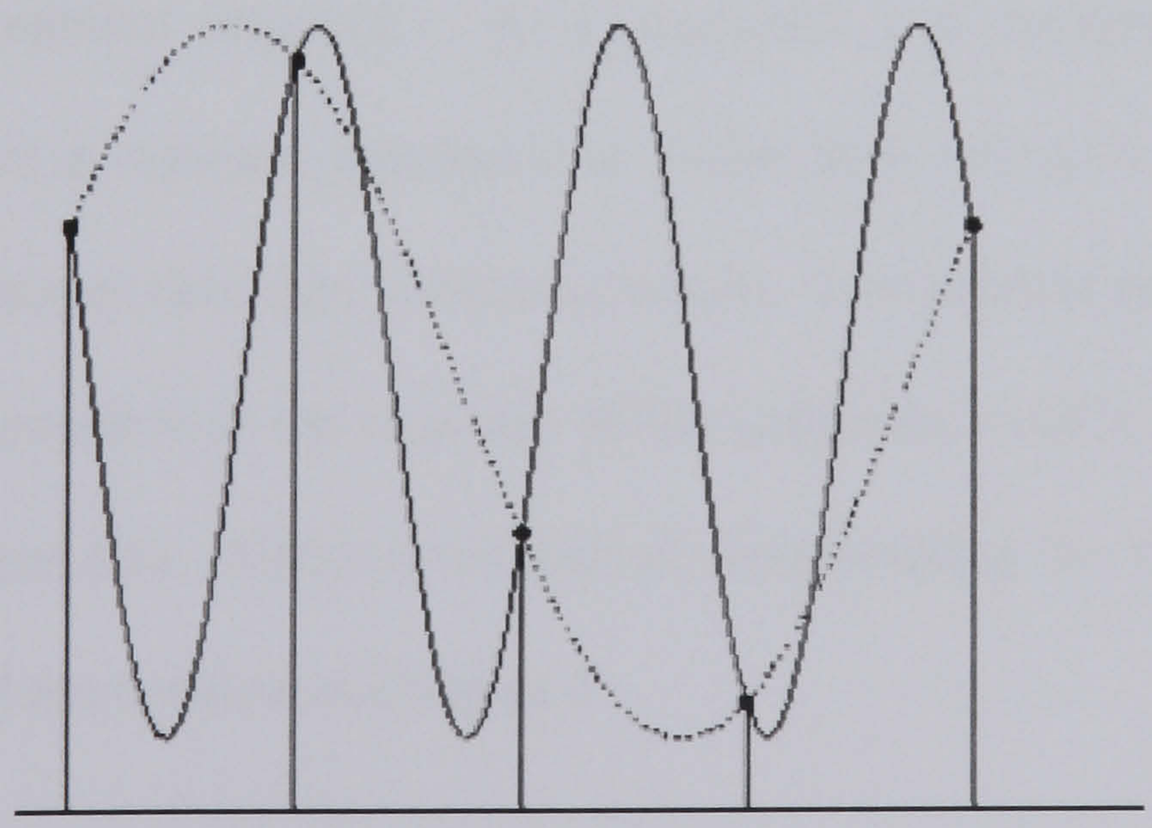

Figure 2.2 Diagram showing how a 300Hz sine wave can be mistaken for a 100Hz sine wave due to aliasing errors.

It was decided to use a sampling rate of 1024Hz with the digital seismograph. This gave a maximum possible resolved frequency of 512Hz. From past work (Dowding 1992, Siskind 1996, Crenwelge 1987) the highest observed frequency from blast generated ground borne vibration is around 100Hz. By over-sampling at 1024Hz it is possible to gain a much more defined waveform at 100Hz as there will be 10 measurement points per cycle. If one decided to use the minimum required sampling rate of 200Hz there would be only two points per cycle. Using a sampling rate of 1024Hz also facilitates the use of the Fast Fourier Transform which is a technique which is explored in depth in Chapter 3.

2.2.4 Construction of Triaxial Geophone Units

It is important that the geophone triaxial units are well designed. There are several sources of error which must be controlled to keep the accuracy as high as possible:

i) Geophone response – As a geophone is a mechanical system they have a resonant frequency at which they will give a much stronger response than they otherwise would. It is prudent to keep this as low as possible as the response of the geophone usually drops off sharply below this. Various methods of compensating for this response exist and are detailed in Chapter 3.

ii) Housing Response – To be mounted in a triaxial array the geophones must be housed in a box or container of some type. This will have a resonant frequency in exactly the same way as the geophone and will

affect the geophone in a similar manner. It is usual for these boxes to be small enough for the resonant frequency to be above the range of frequencies expected to be seen. In Chapter 3 this is examined in further detail. It was found that a housing which would be regarded as small enough to ignore still has an effect on the response of the geophone.

iii) Mounting system – The method by which the geophone is coupled to the ground is very important. The mount needs to keep the transducer fully coupled to the medium at all times without influencing the medium behaviour. It has been found (Johnson 1962) that if the mount is unsuitable then amplification of the signal by up to 5 times may occur. Dowding (1992) suggests that the mounting is least critical when the vertical maximum particle accelerations are less than $0.2g$ and the geophone can be unsecured as long as it is level. From $0.2g$ to $1.0g$ Johnson (1962) recommends that the transducer be completely buried if measuring in soil. He warns against using spikes when measuring in soil as the free response of the mounting system may affect the recorded motion. On rock or concrete Dowding (1992) suggests that the transducer be fastened using double sided tape, epoxy or fast setting cement. For accelerations over $1.0g$ Dowding recommends that bolts are used. It is also important that the mounting system allows for levelling of the transducer. In the field it is rare that you will find perfectly level ground on which to mount the transducer

and unless levelling is possible then the measurements will be affected.

For the above effects to be kept to a minimum and keep within time and cost constraints, it was decided that commercial geophones and geophone housings should be used with a bespoke manufactured base-plate and mounting system.

The geophones and housings that were selected for use are manufactured by Sensor in the Netherlands. The geophones selected were SM-6 4.5Hz versions due to their compact size, low resonant frequency and robust build. The specifications of the geophones are shown in table 2.1. Five triaxial casings to suit the SM-6s were also purchased complete with pond bubbles to aid in levelling. The standard mountings for the Sensor cases are 75mm long spikes which it was decided are of no use as it was intended to monitor close in to the shot-holes and accelerations of over 1g are expected. New base-plates were manufactured with levelling screws arranged in a triangular manner. Provision was also made for securing the base-plate to the medium via bolts.

Washburn and Wiley (1942) note that the larger the area of the base-plate the less of an effect it has on the response of the geophone. It was therefore decided to make the base-plate as large as possible but still maintaining portability. It was decided that 250mm by 170 mm was a good size based on Washburn and Wiley's work and the size of the portable cable reels that would be used with the units.

Parameter	Specification
Natural Frequency	4.5Hz
Frequency Tolerance	± 0.5Hz
Distortion Measured at 12Hz, 1.778 mms^{-1}	< 0.3%
Open Circuit Damping for 365 Ohm Coil	0.265 Ohm
Damping Tolerance	± 5%
Sensitivity	$28V^{-1}ms^{-1}$ ± 5%

Table 2.1 Specification of SENSOR SM-6 4.5Hz geophone (SENSOR 1998)

In total, five triaxial arrays were constructed. Two with 100 metres of screened cable attached. Two with 50 metres of cable and one with 10 metres so giving a maximum spread of 200 metres with a unit every 50 metres. This was decided to be the maximum required spread for the close range monitoring to be undertaken. Figure 2.3 shows a triaxial unit bolted in place ready to monitor a blast.

Even though care was taken in the design and construction of the units the mounting system and case still affect the response of the geophones. Chapter 3 discusses this in more detail as well as describing method for limiting this effect.

2.2.5 Portable Standalone Seismograph

It was noted that the biggest drawback of the multi-channel seismograph detailed above is that it has to be connected with cables to a central unit. It was therefore

decided that commercial portable standalone digital seismographs should also be employed. This was firstly so they could be used in locations which are unreachable by the multi-channel seismograph and, secondly, as a backup system for critical locations.

The units which were used were Mini-Seis 1/8 M manufactured by White Industrial Seismology Inc. The White units have a 12 bit analogue to digital converter and sample at a rate of 1024Hz. The biggest drawback of the White units is that the mounting system is unsuitable for use with close range monitoring, consisting of a single three inch spike which screws in to the bottom.

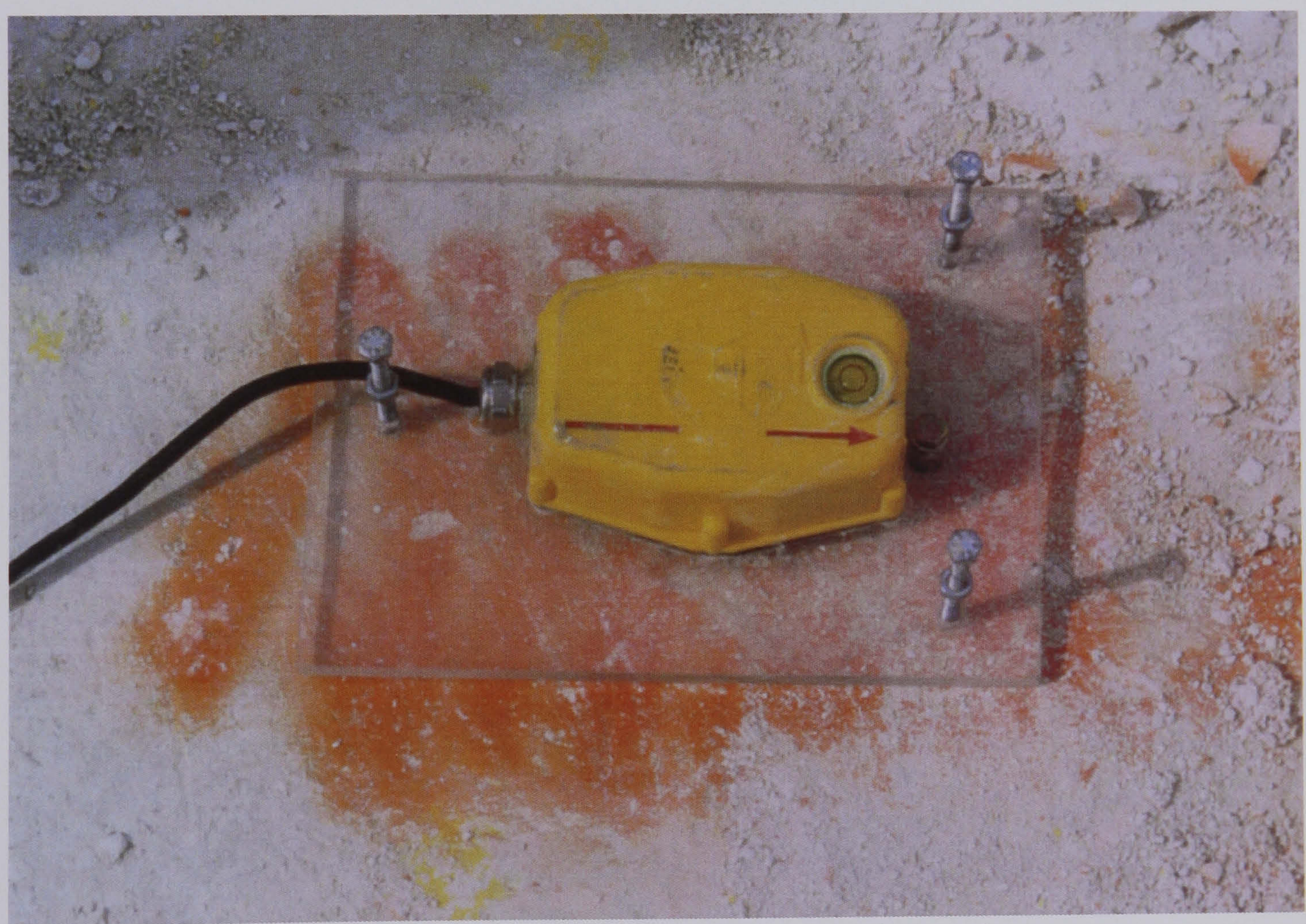

Figure 2.3 Triaxial unit bolted to rock showing new base-plate.

To enable the use of these units at close range a clamp was designed to bolt to the ground either side of the unit and screw down to ensure that no movement is

possible. In side-by-side tests with the multi-channel seismograph this has proved to be sufficient to hold the unit securely.

2.3 Velocity of detonation measurements

The velocity of detonation (VoD) is the rate at which the explosive reacts in the borehole usually measured in metres per second. It is useful to measure this for a number of reasons. Firstly it gives an indication of the quality of explosive. A relatively low velocity of detonation is an indication of a problem such as inadequate mixing of ANFO or waterlogged boreholes. In extreme cases the explosive can fail to detonate and instead deflagrate which in turn will greatly affect any vibration data collected.

The second reason for measuring the VoD is that it can be used to give exact hole timings. With pyrotechnic detonators timing is rarely accurate (Small 1986) and so if multiple hole signals are to be deconstructed then it is important that exact timings are available.

2.3.1 VoD measurement methods

There are several methods which have been put forward for measuring VoD. These are summarised below.

i) Photographic measurement – it is possible to measure the speed of a detonation using high speed photography and flash X-ray methods.

This is however expensive to operate and difficult to set up. It does have the advantage that it is a non-contact method and so nothing is destroyed in the process but even so could not be used for routine testing in the field due to the time taken to set up correctly .

ii) Multi point measurement – this type of instrument is based on a series of high speed digital counters and an accurate crystal clock source. Probes consisting of a pair of wires separated by a small piece of insulating material are placed known distances apart in the explosive column. As the explosive detonated each probe in turn is shorted which starts the timer to which it is connected and stops the previous timer. Since the distance between the probes is known the velocity can be calculated easily from the times between the probes starting and stopping. This system is quite complex to set up and relies on accurate spacing of the probes. It is however very cheap and providing that the probes are set up beforehand can be used with ease in the field.

iii) Continuous Measurement – this system relies on high speed acquisition of data to observe the length of a single cable placed in a column of explosive. There are three methods that can be used to measure the cable length.

The SLIFER (Shorted Location Indication by Frequency of Electrical Resonance) method was originally designed to measure the

propagation of shock waves from nuclear explosions (Heusinkveld and Holzer 1964). It relies on using the cable as part of an oscillator circuit of which the frequency is dependant of the length of the cable. As the explosive detonates the cable becomes shorter and the oscillator frequency increases. By measuring the frequency as a function of time it is possible to calculate the velocity of the detonation.

Radar techniques measure the two way transit time of a voltage pulse along the length of the cable. If the velocity of the pulse in the cable has been previously determined then the length of the cable can be calculated. The rate of change of the length will give the velocity of detonation.

Resistive methods measure the voltage change in the cable as a constant current is applied to it. The voltage increases as the cable shortens. By measuring the voltage as a function of time it is possible to calculate the velocity of detonation. It was this method that was decided upon for this project due to its ease of use, flexibility and relatively low running costs.

2.3.2 Microtrap VoD measurement System

The system that was used in this research was the MREL Microtrap which is a continuous resistive method based unit. This unit is very simple to operate and has

the advantage of four additional channels which can be used to monitor voltage signals from transducers such as geophones or accelerometers. This has two main advantages. The first is that as the Microtrap records at very high speed of up to 1MHz very high resolution recordings can be made to ensure that all features of a vibration trace are captured. The second is that it is possible to determine ground velocity from the point of initiation to the transducer, as the system is triggered by the detonation of the explosive. A Typical VoD recording from the MREL Microtrap is shown in figure 2.4. As can be clearly seen it provides a clear indication of VoD and Firing Times.

2.4 Other equipment

Other equipment which was used in the research includes laser profilers and GPS surveying equipment amongst various other items. No discussion will be made of their selection, as it was based purely on availability. The laser profiling of the benches was more often than not carried out by the quarry where the experiments were taking place.

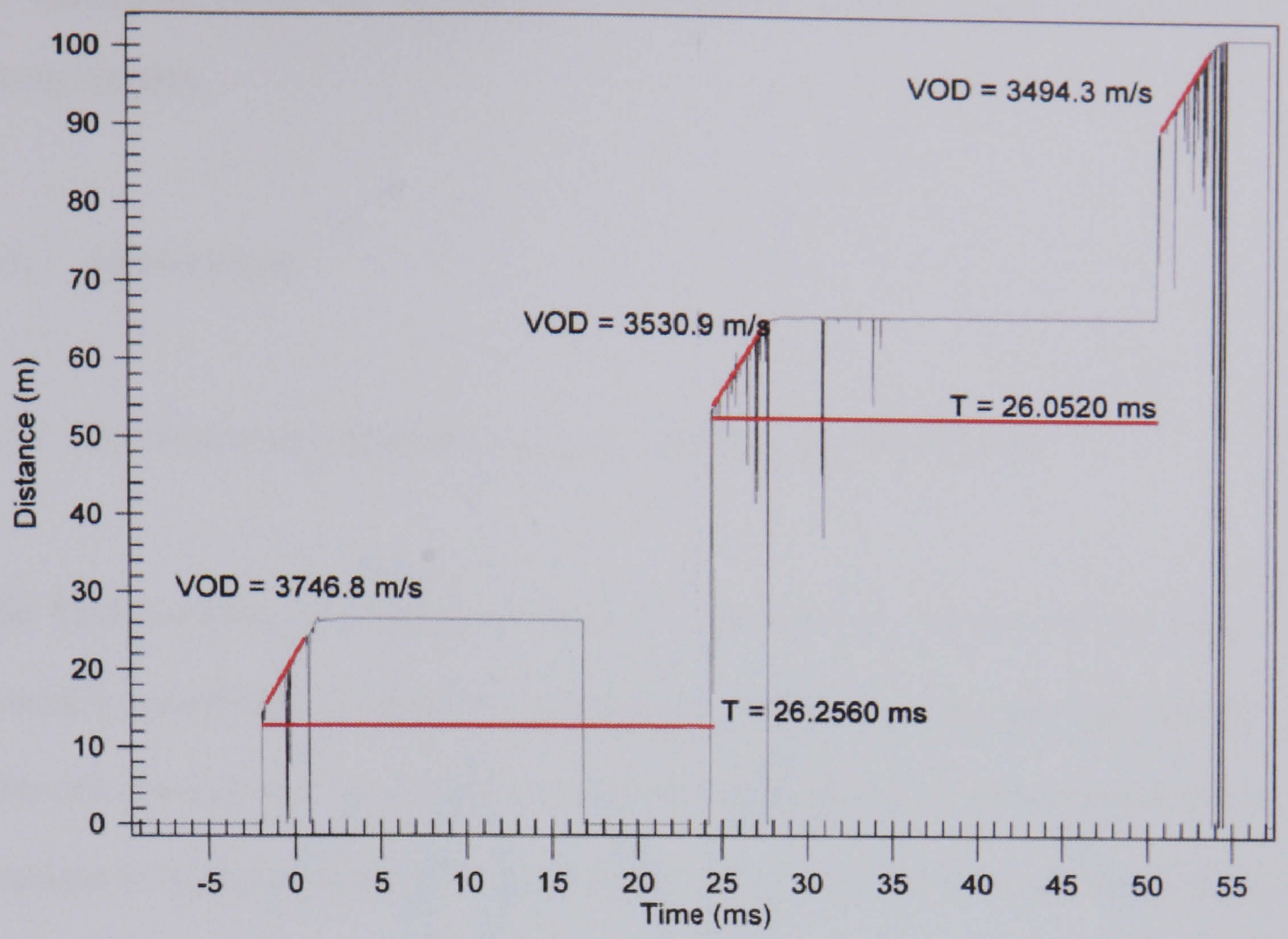

Figure 2.4 Typical VoD recording from an MREL Microtrap.

2.5 Conclusions

The equipment selected and constructed for this project has been chosen to provide the very best performance that can be expected from the small budget available for this project. As will be detailed later in this report there were several teething problems with equipment especially the multi-channel seismograph although ultimately all the equipment performed as well or better than expected.

3. CALIBRATION OF BLASTING SEISMOGRAPH USING TRANSFER FUNCTIONS.

3.1. Introduction

3.1.1 Potential errors induced by ground vibration recording systems

The field recording of blasting vibration for this research was carried out using a specially constructed 15 channel seismograph as detailed in the previous chapter. This unit consists of 5 triaxial geophone arrays connected to a microcomputer via an analogue to digital converter. This system has a high potential for error in two major areas, geophone response and digital sampling errors. Errors due to digital sampling are well documented (Oppenheim and Schafer 1975) and much has also been written for blasting seismographs in particular (Hogg 1992; White and Farnfield 1993). These errors can be eliminated by taking simple precautions when analysing and recording data. Errors due to geophone response cannot be eliminated quite as easily as they are induced by a physical limitation caused by the construction of the geophone.

3.1.2 Geophone frequency response

The majority of blasting seismographs use a triaxial array of geophones as a vibration transducer. Geophones consist of a mechanical system where a coil moves in relation to a fixed magnet (Moving Coil or MC) or vice versa (Moving Magnet or MM). The movement of the geophone causes a relative movement between the

magnet and coil inducing a voltage, relative to the velocity of the geophone, in the coil. Figure 3.1 shows a typical setup of an MC style geophone with the case removed. As a geophone is a moving mass mechanical system the induced voltage is dependent on both the frequency and magnitude of the input signal. This relationship is described by its frequency response. The frequency response of a geophone is a complex function which can be described by the two following functions:

Amplitude response: Describes how the geophone output voltage amplitude varies with frequency. This is usually quoted relative to a calibration transducer.

Phase response: Describes how the output of a geophone lags behind the actual vibration. This is usually quoted in degrees or radians.

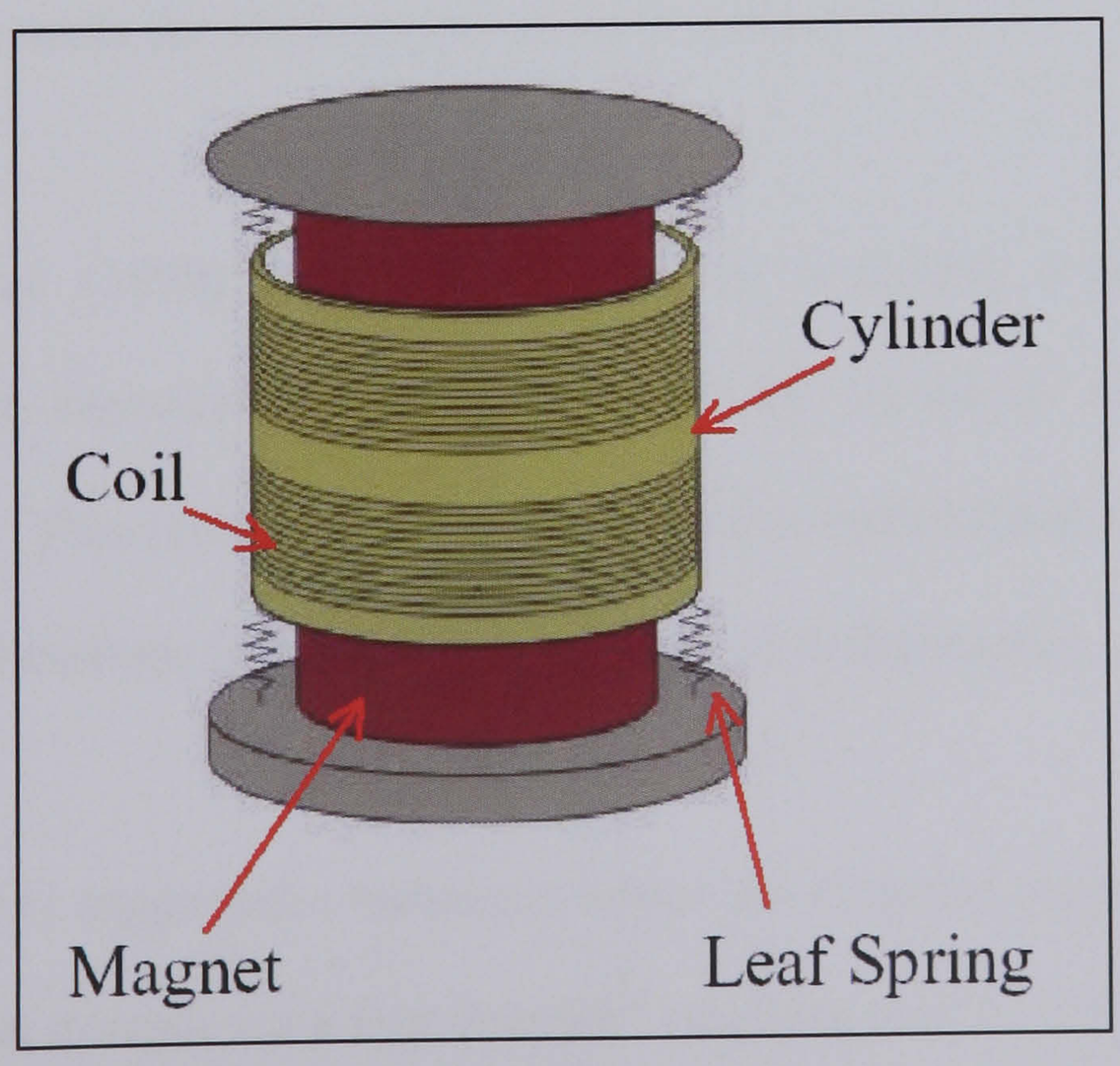

Figure 3.1 Diagram of a moving coil geophone with the case removed.

As geophones are a mechanical system they have a natural resonant frequency at which their response is amplified. The magnitude of the amplification is governed by the resistance of the circuit in which it is installed and often shunt resistors are added to increase this to a specific level. Geophone manufacturers give amplitude response curves for varying resistance values. Below the natural frequency the response of the geophone can be seen to drop off rapidly causing large errors in low frequency measurement. Figure 3.2 shows a typical geophone manufacturer's response curves with varying shunt resistances.

The errors induced by geophone frequency response have been recognised for some time and many techniques for the correction of this have been put forward.

Stagg and Engler (1980) suggested that frequency dependent amplifiers should be employed to correct for geophone low frequency response. Most geophone manufacturers use this technique today. The problem with this technique is that no correction is made for errors due to phase response.

Barzilai et al. (1998) developed a technique to modify a geophone to measure displacement capacitively which increased the resolution and response at low frequencies. This technique although credible is complicated and as expensive as a typical accelerometer/integrator approach and so is discounted.

Walker (1981) suggested a technique where the recorded signal is transformed into the frequency domain via a Fast Fourier Transform (FFT). The relevant frequencies could then be adjusted through multiplication by a factor determined through

experimentation and the time domain signal reconstituted by an inverse FFT procedure. This approach is flawed in that it also took no account of phase response errors.

Farnfield (1998) took Walkers approach and developed it further to include a correction for phase response using a technique known as a Transfer Function. Farnfield proved that a correction for amplitude response without a phase response correction did not increase geophone accuracy but when a phase response correction was applied a marked improvement in accuracy was seen.

It is Farnfield's approach which is going to be investigated for use with the 15 channel blasting seismograph developed for this research. Each choice he made in his method will be examined and modified if necessary.

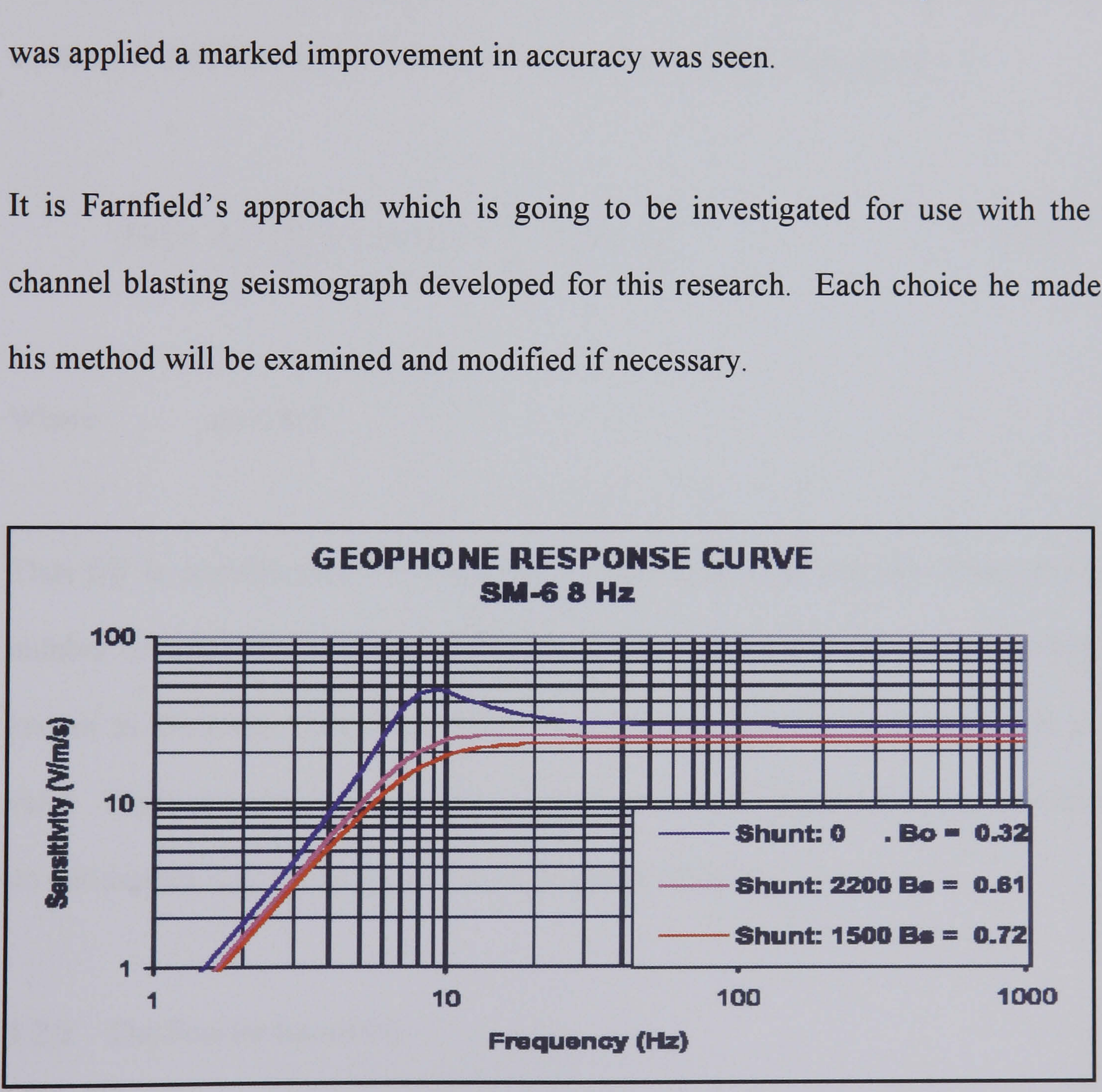

Figure 3.2 Response curves for a SENSOR SM6 8 Hz geophone.

3.2 Transfer function theory

3.2.1 Fourier analysis

The signal processing technique known as Fourier analysis was first described by Baron Fourier in 1822. The basis of the Fourier series is that a complex periodic waveform may be analysed into a number of harmonically related sinusoidal waves which constitute an orthogonal set. If we have a periodic signal *f(t)* with a period equal to *T*, then *f(t)* may be represented by the series give in equation 3.1

$$f(t) = A_0 + \sum_{n=1}^{\infty} A_n \cos n\omega_1 t + \sum_{n=1}^{\infty} B_n \sin n\omega_1 t \qquad (3.1)$$

Where $\omega_1 = 2\pi/T$.

Thus *f(t)* is considered to be made up by the addition of a steady level (A_0) to a number of sinusoidal waves of different frequencies. There are certain restrictions known as Dirichlet Conditions which must be satisfied for the above series to be valid. These are widely documented (Champeney 1973, Lynn 1973) and fortunately do not exclude any signal waveform of practical interest.

3.2.2. The Fourier transform

The Fourier transform is an extension of the Fourier series allowing aperiodic and sampled waveforms to be analysed. The discrete Fourier transform (DFT) is used

when a function is sampled in both the time and frequency domains. Equation 3.2 shows the forward discrete Fourier transform equation and equation 3.2 shows the inverse transform.

$$G(k) = \frac{1}{N}\sum_{n=0}^{N-1} g(n)e^{-j\frac{2\pi kn}{N}} \qquad (3.2)$$

$$g(n) = \sum_{k=0}^{N-1} G(k)e^{j\frac{2\pi kn}{N}} \qquad (3.3)$$

Where $G(k)$ is the frequency domain function

$g(n)$ is the time domain function

N is the number of data points

Equation 3.1 is used to transfer a signal from the time domain into the frequency domain. The result of applying equation 3.2 is a complex number containing both amplitude and phase data for each resolved frequency. This process is reversible by applying the inverse transform, equation 3.3.

Cooley and Tukey (1965) developed an algorithm, known as the Fast Fourier Transform (FFT), for obtaining a discrete Fourier transform from digital signals. The algorithm greatly reduced the number of mathematical operations required and therefore reduced computational stress thus allowing Fourier analysis to become faster and simpler to use. In a standard DFT equation N^2 calculation are required to calculate the frequency spectrum of a function with N data points. Using Cooley and

Tukey's FFT algorithm this can be reduced to $N \log_2 N$. The FFT is most attractive when N is a factor of 2; using the FFT on a signal of length $N = 1024$ has a computational saving of a factor of 100 over a DFT.

The result of the Fourier transform process on a typical blast induced vibration signal is shown in figure 3.3. The vibration signal consists of 1024 samples recorded at a rate of 1024Hz and is therefore 1 second long. When transformed into the frequency domain using an FFT the resulting spectra have 1024 points with the values apparently being mirrored around the central frequency of 512Hz. The phase component also displays an inversion in this case. This central frequency is called the Nyquist frequency and corresponds to half the sampling frequency. This effect is described by Randall (1977) as being due to having two contra-rotating vectors in a complex plane which in effect means that the frequency values above the Nyquist frequency are negative. There are two frequency values which are unique in the frequency domain. These are at zero frequency, commonly known as the DC component, and the Nyquist frequency.

To avoid confusion it is more common to show the frequency spectra as only one half of the complete spectra but it must be noted that if reconstruction to the time domain is to be performed then the whole spectrum must be retained.

Reconstruction to the time domain can be accomplished if both the amplitude and phase data are retained by application of an inverse Fast Fourier Transform. This fact allows operations to be carried out in the frequency domain before reconstruction.

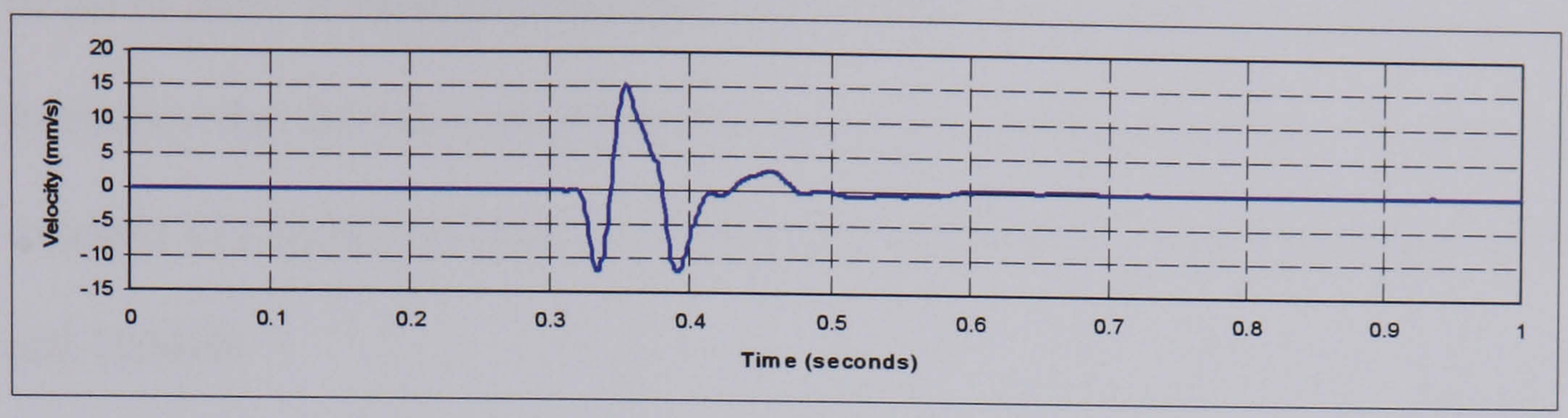

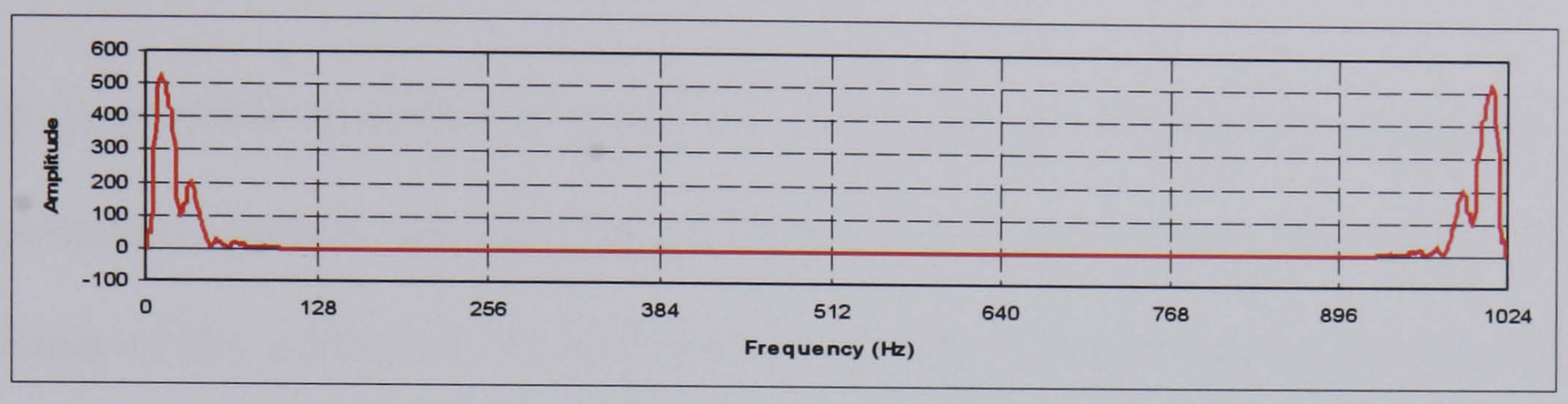

Figure 3.3 Example of the use of the Fast Fourier Transform on a blast vibration transient showing the polar representations of the frequency domain data.

For example, if every value in the amplitude spectra was multiplied by two the resulting reconstructed time signal would have double the amplitude of the original.

A more complex application of this process could be the application of a high pass filter. In this case the signal is transformed into the frequency domain in the usual way. It is then possible to set all unwanted frequencies to zero. For example, if a

high pass filter with a cut-off of 10Hz is required all frequencies below 10Hz would be set to zero. It must be noted that as the spectra are symmetrical about the Nyquist frequency the corresponding frequencies must also be set to zero. In our previous example of a signal recorded at 1024Hz this would be all the values between 1014Hz and 1024Hz.

It is possible therefore to carry out any number of different operations in the frequency domain and then convert it back to the time domain. This effect forms the basis of the calibration system used by Farnfield. By changing the amplitude and phase components of the recordings by an experimentally deduced value it is possible to reduce errors due to the frequency response of the system. The method of applying this correction is known as a transfer function.

3.2.3 Transfer functions

Randall (1977) describes a transfer function as the complex ratio of the output to input of a system as a function of frequency. They suggest equation 3.4 as a simple solution.

$$H_{xy}(f) = \frac{F_y(f)}{F_x(f)} \tag{3.4}$$

Where $H_{xy}(f)$ is the transfer function from x to y.

$F_y(f)$ is the fourier spectrum of the output signal $F_y(t)$ given by the application of equation 3.2

$F_x(f)$ is the fourier spectrum of the input signal $F_x(t)$ given by the application of equation 3.2

Equation 3.4 is the division of a series of complex numbers. The result of this division can be shown in either complex or polar form. The polar form consists of separate information for amplitude and phase and it is in this form a transfer function is most commonly shown.

It can be seen from equation 3.4 that given any of the two functions it is possible to calculate the third. In each case the spectra can be calculated from or converted to the time domain.

3.2.4 Transfer function constraints

Herlufsen (1984) outlined 4 assumptions which must be valid for a transfer function of a system to be sound:

i) Physically Realisable

The system cannot respond to an input before it is applied.

ii) Time Invariant

The properties of the system must not change with time.

iii) Stable

The system should only respond to a limited degree when subject to a finite input.

iv) Linear

The transform must not vary with the amplitude of the input.

As blast vibration analysis is concerned with physical objects it can be assumed that conditions (i) and (iii) will always be satisfied. Conditions (ii) and (iv) can be more problematic and are examined in more detail where required in this thesis.

Herlufsen (1984) also notes a number of other potential problems with transfer function calculations:

i) Multiple input signals

The calculation of a transfer function assumes that there is only one input signal. This is normally the case in electronic circuits but is often not the case with the response of mechanical systems. Multiple input signals, even when generated by one source, are not always well correlated especially in terms of time lag.

ii) Common time base for input and output

For the phase component of a transfer function to be valid both the input and output time domain signals must be recorded with the same time base or at least with a common difference between the time bases. This is not a problem with the multiple channel seismograph that has been developed for this research although a slight lag exists due to the analogue to digital conversion method. Farnfield (1998) suggested a technique to overcome this which is described later in this chapter.

iii) Uncorrelated input or output noise

If there is noise in either the input or output signals used to calculate a transfer function then serious problems can occur, especially if the noise is on the output signal. The division of the output and input spectra can give rise to very high values in the resultant transfer function. Dowding (1985) suggests adding broadband low amplitude noise to both the input and output to overcome the problem. Herlufsen (1984) suggests the use of different equations depending on whether the noise is on the input or the output. As all recordings were taken under laboratory conditions, noise does not present a serious problem in this research. No action was taken to remove noise from the signals recorded.

3.2.5 Transfer function calculation techniques

The calculation of a transfer function from a single set of input and output signals is possible using equation 3.4. It is however desirable to determine a transfer function from a number of input and output signals averaged, so as to remove any spurious signals and minimise the effect of noise. Randall (1977) notes that the transfer function equation 3.4 can be developed to give:

$$H_{xy}(f) = \frac{F_y(f)}{F_x(f)} \cdot \frac{F_x^*(f)}{F_x^*(f)} = \frac{F_{xy}(f)}{F_{xx}(f)} \qquad (3.5)$$

Where $F_x^*(f)$ is the complex conjugate of the input spectra

$F_{xy}(f)$ is the cross spectrum between the input and the output

$F_{xx}(f)$ is the power spectrum of the input signal

Herlufsen (1984) also notes that it is possible to calculate the transfer function from the following equation:

$$H_{xy}(f) = \frac{F_{yy}(f)}{F_{yx}(f)} \qquad (3.6)$$

Where $F_{yy}(f)$ is the power spectrum of the output signal

$F_{yx}(f)$ is the cross spectrum between the output and the input

Equations 3.5 and 3.6 both allow averaging over a number of input and output signals without affecting the operation of the system. Herlufsen (1984) recommends that equation 3.5 be used when there is likely to be noise on the output and equation 3.6 with noise on the input.

3.2.6 Coherence

Randall (1977) notes that with a transfer function calculation it is not known to what extent the output results from the input. It is therefore wise to check the coherence which gives a measure of the validity of the transfer function. The coherence can be calculated as follows:

$$\gamma_{xy}(f) = \sqrt{\frac{|F_{xy}(f)|^2}{F_{xx}(f)F_{yy}(f)}} \qquad (3.7)$$

Where $F_{xy}(f)$ is the cross spectrum between the input and the output

$F_{xx}(f)$ is the power spectrum of the input

$F_{yy}(f)$ is the power spectrum of the output

The resulting spectrum shows the validity of the transfer function against frequency with values ranging from zero to one. A coherence of one shows that the transfer function is entirely valid. Anything less than one indicates that there is noise on either the input or the output or that the signals were sampled on a different time base.

3.3 Geophone linearisation

Farnfield (1998) developed a calibration method for reducing the error induced by geophone response using transfer functions. The system is applied to the calibration of the 15 channel seismograph described in the previous chapter and a small development to the system is suggested.

The calibration technique relies on determining the complex response function of the geophones utilised in the seismograph and using this as a transfer function which can be applied to vibration signals recorded on the seismograph. To determine the response function Farnfield (1998) suggested that the geophones be compared to a calibration accelerometer in a "back to back" test on a shaking table. A signal must be applied to the shaking table so that the response at all frequencies of interest can

be determined. This forcing function can be a number of different signals which have various advantages and disadvantages.

3.3.1 Continuous sinusoidal signals.

Most blasting seismograph manufacturers suggest using a continuous sine wave signal fed into a shaking table to obtain the amplitude response of a geophone compared to an accelerometer.

The main disadvantage of this method is that only one frequency at a time can be employed and so this method requires a large amount of time to determine a complete frequency response function.

This technique is, however, simple and can be carried out with relatively cheap equipment.

3.3.2 Unit pulse

A unit pulse in a digital signal has equal energy at all frequencies and this should make it ideal to determine a geophone's frequency response function. The reality, however, is that it is very difficult to produce a pulse with sufficient energy to be used as a forcing function. The frequency content of the pulse is also distorted by the electronic and mechanical components of the system reducing the frequency range over which it can be applied.

3.3.3 White noise

Randall (1977) defines white noise as a signal which has a power spectral density which is constant with frequency. Such a signal should be ideal for resolving the frequency response of a geophone. Producing true digital white noise is very difficult as all digital systems have a limited dynamic range and contain only a finite number of samples in each time period. An approximation to white noise can be produced by a computer using a random number generator. The resulting frequency content of this type of system will contain energy in a broad frequency range but may result in some frequencies having very low amplitudes.

It is possible to overcome this problem by employing a signal much longer in time. This may not be practical for use with blasting seismographs which usually have a short recording time. Alternatively the problem can be overcome by employing a long term averaging system. Such a method would require that the signal be processed with a time weighted window, which will induce time and frequency domain distortions. A sophisticated signal processing system would be required to realise such a system.

3.3.4 Sine Wave Sweep

A sine wave sweep can be constructed so as to give a reliable vibration input over a required frequency band with ease by employing 2 signal generators. Another advantage of using a sine wave sweep is that the length can be adjusted to fit within a given recording time thus avoiding the need to use windowing techniques.

A sine wave sweep was chosen by Farnfield (1998) as the most effective method of determining the geophone response function and it is this method that was decided upon for the calibration of the 15 channel seismograph that has been developed.

3.3.5 Determination of geophone frequency response

To determine the frequency response of each geophone a unit was constructed to mount them on a shaking table in line with a calibration geophone. Figure 3.4 shows the system. For each geophone a series of ten sine wave sweeps from 1 to 100Hz with constant amplitude of 1Vac peak to peak were played through the table and the outputs recorded on the 15 channel seismograph system. The output of the geophone was matched to that of the accelerometer by adjusting the gain provided by the software on the 15 channel seismograph system.

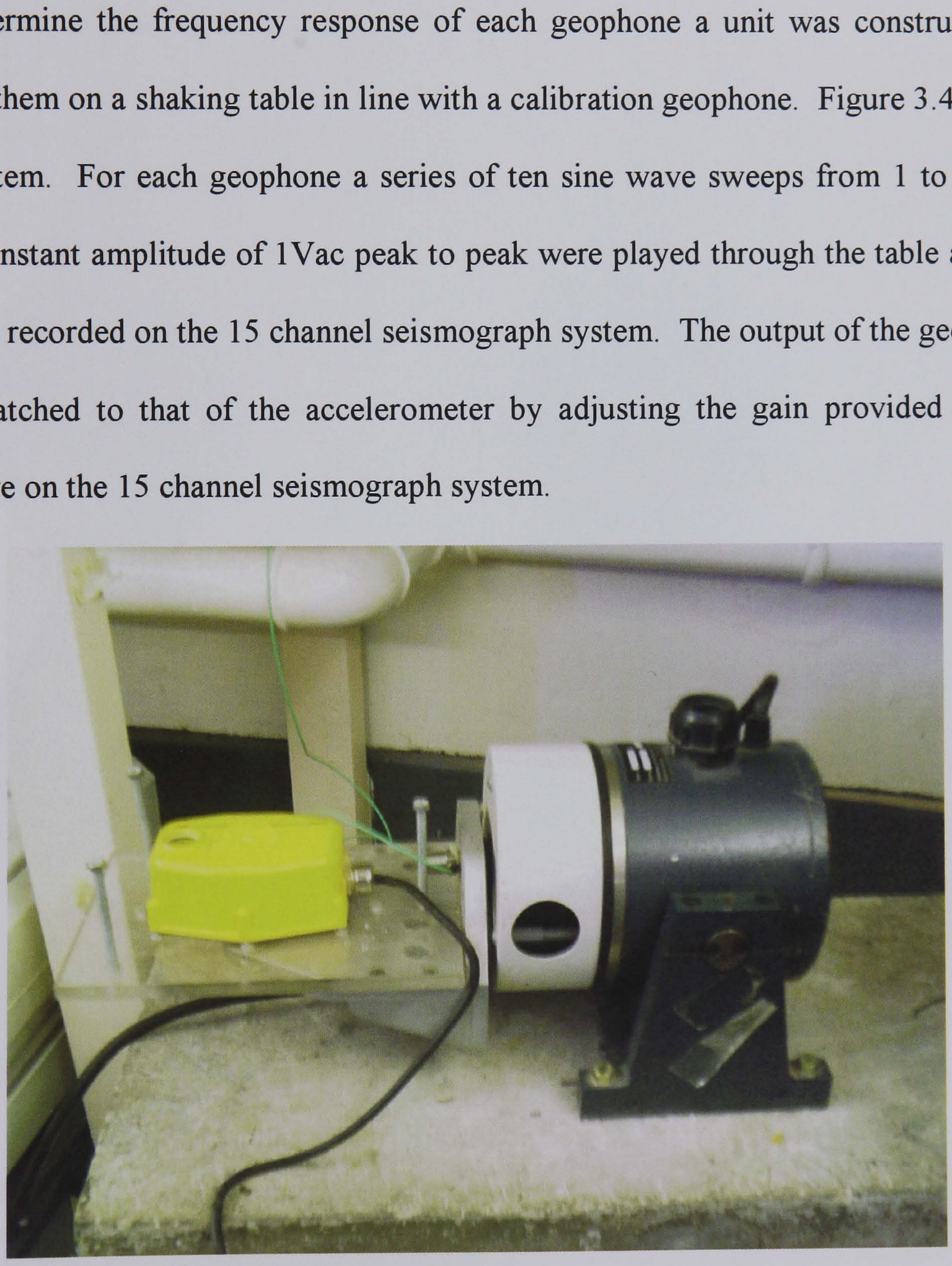

Figure 3.4 Shaking table apparatus for determining frequency response of geophones.

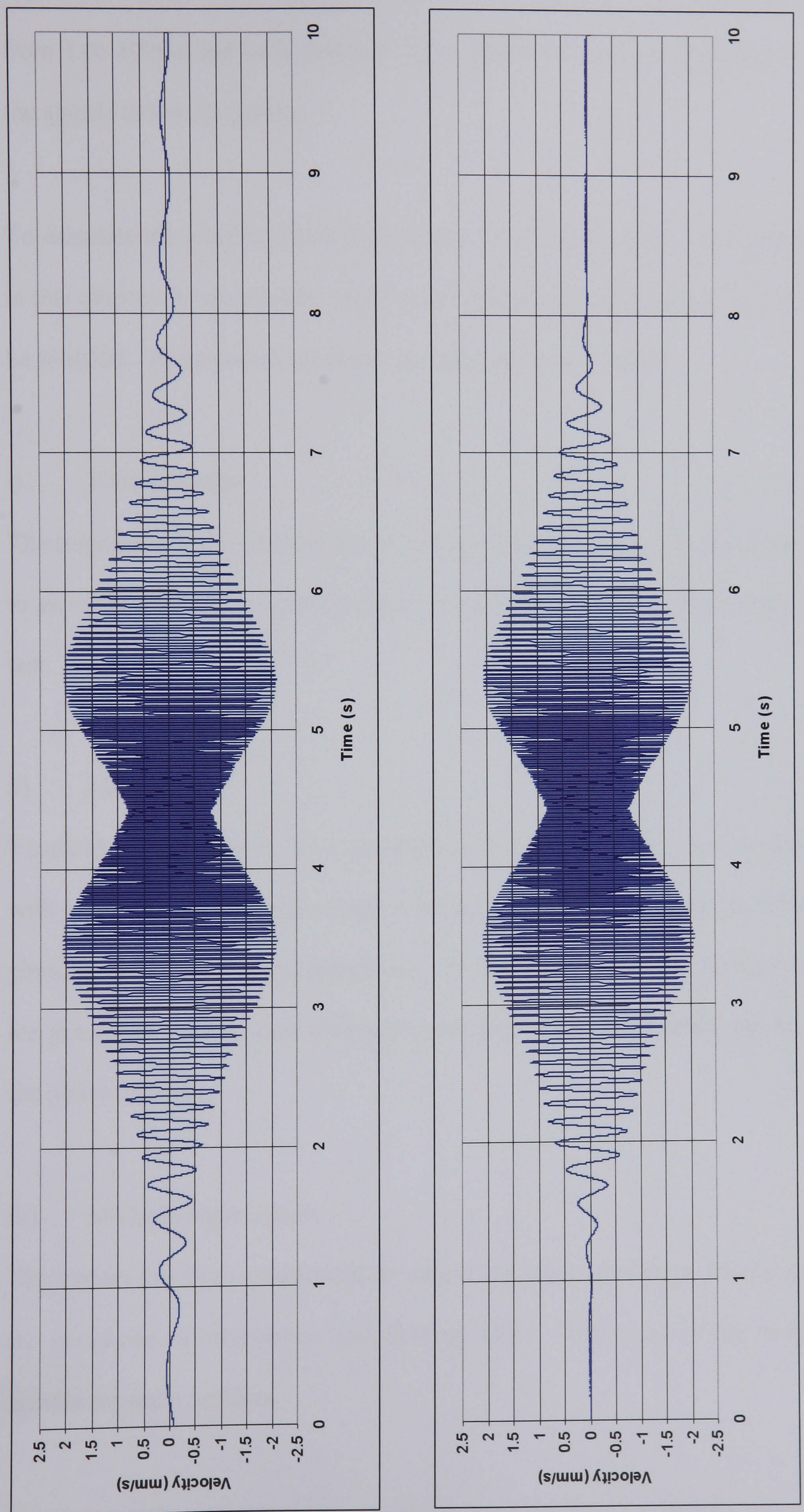

Figure 3.5 Signals recorded from accelerometer (top) and geophone (bottom) when excited with a 1-100-1Hz sine wave sweep.

Figure 3.5 shows one of the recordings made using this system with a sine sweep from 1 to 100Hz and back down to 1Hz. There are obvious discrepancies between the signals at low frequency.

To calculate the transfer function equation 3.6 was employed. As mentioned earlier in this chapter for the transfer function to be valid there are requirements which must be fulfilled. These can be related to the calibration as follows:-

i) Time invariant

The response of a geophone will not change with time unless the geophone is subject to shock or damage. In reality this is checked once a year at an annual calibration test.

ii) Linearity

Farnfield (1998) showed by experimentation that a geophone will respond linearly with amplitude up to approximately $9mms^{-1}$, where the response is limited by the physical dimensions of the geophone. At low frequencies the moving mass inside the geophone can be heard hitting the end stops. The same effect can be seen with the phase response.

iii) Multiple input signals

The system has been constructed to ensure that close contact is maintained between the geophone, accelerometer and shaking table. This ensures that multiple input signals are not a problem

iv) Input and Output on a common time base

The input and output were both recorded on the 15 channel seismograph detailed earlier. The seismograph was set to record on only 4 channels at a rate of 1024 Hz. This gives a lag of approximately 0.25 milliseconds between successive channels. To ensure that the signals were perfectly aligned on the same time base this slight offset must be removed. This was accomplished by calculating the cross-correlation function between the accelerometer response and the geophone response. Herlufsen (1984) notes that the time delay between two time domain signals can be determined from the time at which the cross-correlation function has a maximum. The cross-correlation function is the inverse of the cross spectrum. Randall (1977) gives a technique for calculating the cross spectrum of two signals as follows:

$$F_{xy}(f) = F_x^*(f) \cdot F_y(f) \tag{3.8}$$

Where $F_{xy}(f)$ is the cross spectrum

$F_x^*(f)$ is the complex conjugate of the Fourier spectra generated from the time domain signal X.

$F_y(f)$ is the Fourier spectra generated from the time domain signal Y.

The cross correlation function for the two signals shown in figure 3.4 is given in figure 3.6. The maximum correlation is given at a time of approximately 0.5 milliseconds which coincides with the fact that these signals were recorded on channels 1 and 3 of the blasting seismograph.

v) Uncorrelated noise

As the calibration is carried out under laboratory conditions there is minimal uncorrelated noise other than that generated by the instrumentation.

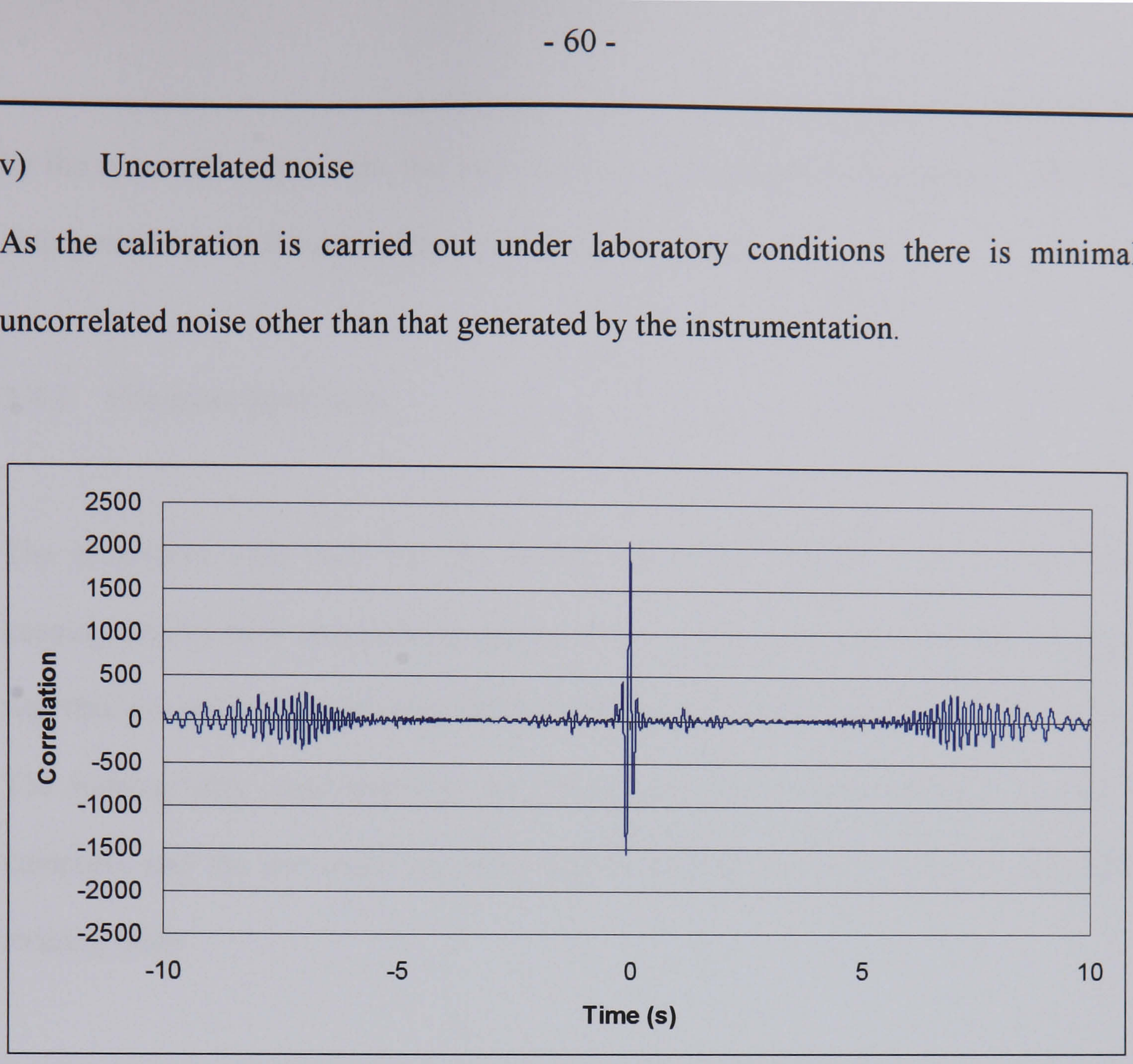

Figure 3.6 Cross Correlation function of the two signals shown in figure 3.4

To ensure that the transfer function calculated is valid the coherence was also calculated. As expected this gave a constant value of 1 above the resonant frequency of the geophone. Below the resonant frequency the coherence drops off sharply. Figure 3.7 shows the transfer function generated for the geophone used in generating the signal shown in figure 3.4, along with the coherence.

3.4 Transfer Function Calibration Testing

Farnfield (1998) tested the calibration system by playing a previously recorded blast vibration signal through the shaking table and comparing the peak velocity recorded

by the corrected output with that recorded by a calibration accelerometer. This was also carried out for the geophones used in this research.

3.4.1 Vibration signal tests

The geophones were built into the triaxial arrays that would be used in the field keeping careful note of which geophone was in which location. The triaxial array was then mounted on the shaking table and the accelerometer mounted in line with it. The shaking table input amplifier was then connected to the analogue output of a computer and the previously recorded signal used as an input signal to drive the shaking table.

Figure 3.8 shows a typical signal recorded on the accelerometer compared with that obtained from a transfer function corrected geophone and the uncorrected geophone. It can be seen that the actual peak particle velocity (PPV) is 13.85mms^{-1} and the correction has increased the PPV recorded by the geophone from 11.95mms^{-1} to 12.60mms^{-1}. This improvement, although significant, is nowhere near the negligible error reported by Farnfield (1998).

Figure 3.9 shows a plot of the accelerometer readings against those recorded by the corrected and uncorrected geophone system for 20 different blasts and shows that the errors induced are still significant. The system was thoroughly checked for anything which could have introduced errors such as loose or uneven mountings and nothing was found.

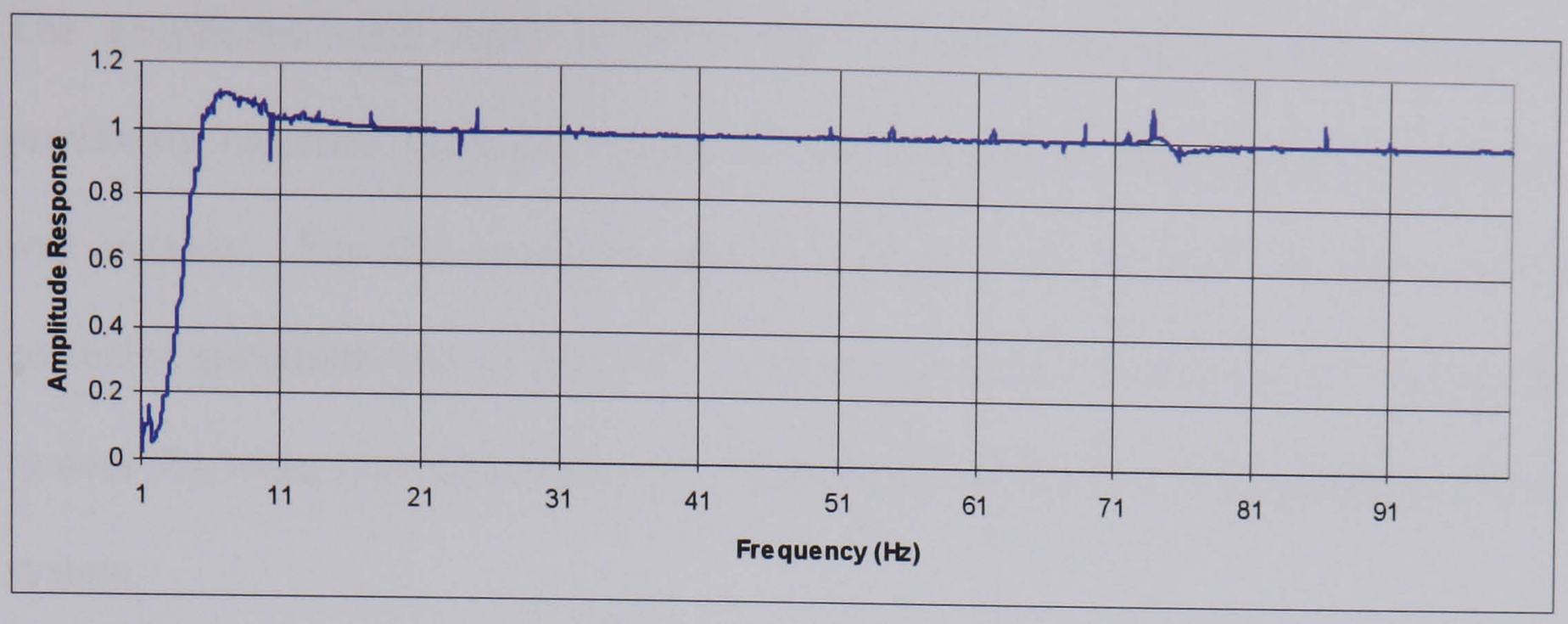

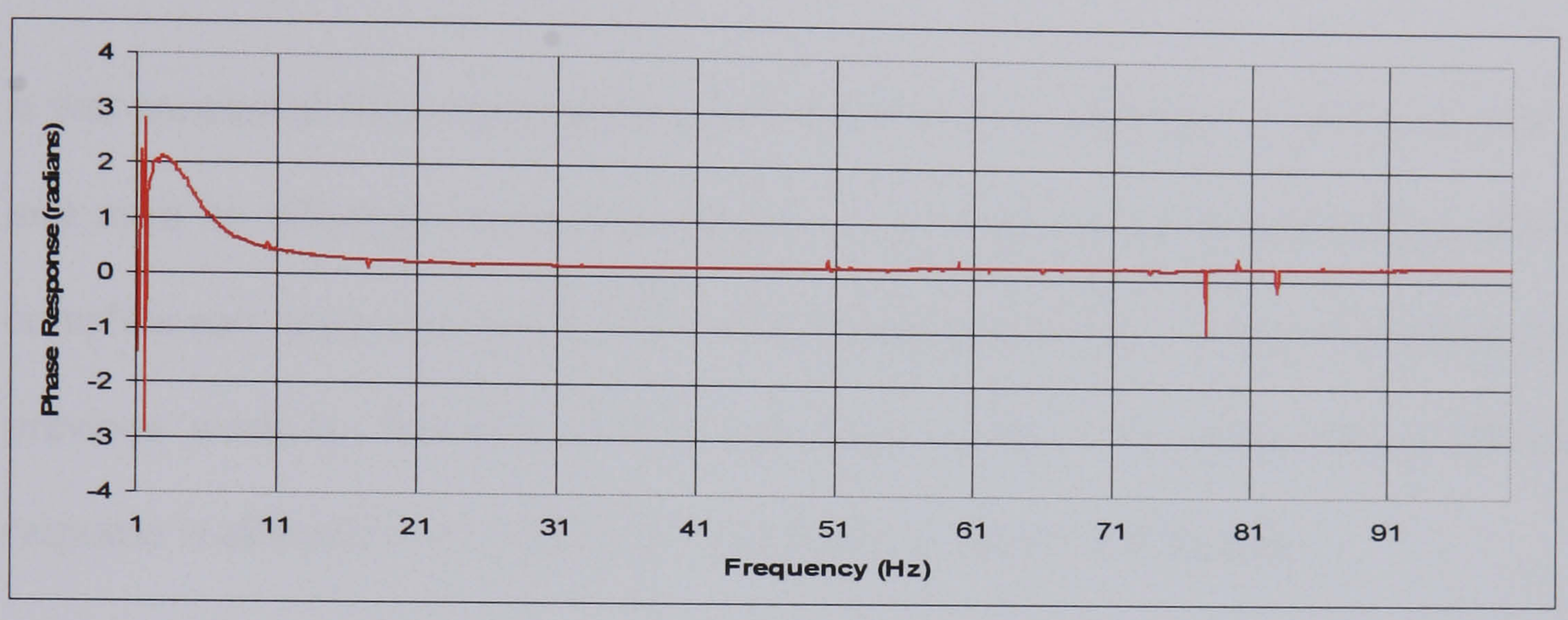

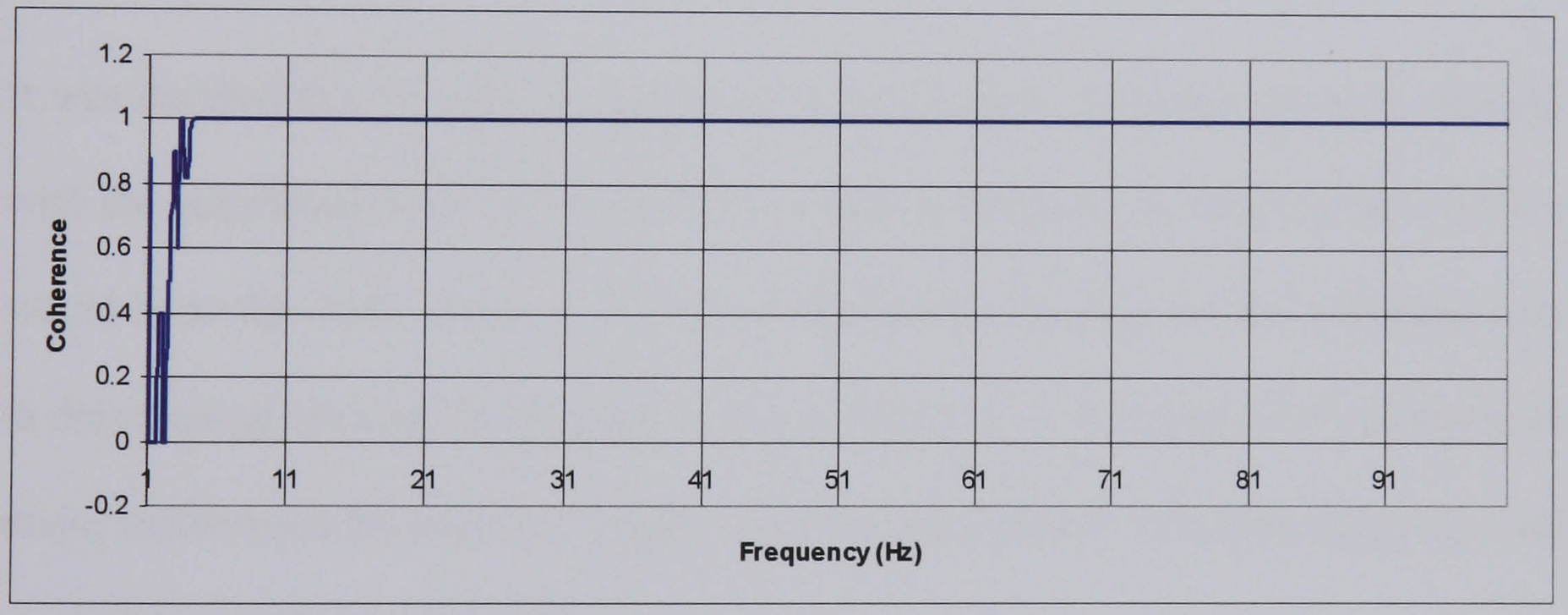

Figure 3.7 Transfer function and coherence for a geophone used in the research work.

The geophones were removed from their casings and retested by playing the previously recorded vibration signals as detailed above. The increase in accuracy was notable. For the geophone shown in figure 3.8 the PPV recorded by the corrected geophone was 13.82mms^{-1}, a percentage error of less than 0.3% compared to over 9% when mounted in the case. The trend was similar for all geophones in the system.

It was concluded from these results that the fact that the geophones were built into a unit must be affecting the transfer function, i.e. the response characteristics of the complete unit were different from that of a single geophone. This is backed up by previous work by Dowding (1992) and Krohn (1985) who note that geophone response is affected by its coupling to the media on which it is located.

It was decided that to improve accuracy the calibration procedure must be repeated with the geophones built into triaxial arrays and mounted to the shaking table as they would be in the field. Figure 3.10 shows the transfer function for the geophone used in determining the transfer function shown in Figure 3.7. It can be seen that there are major differences between the transfer function determined when the geophone was mounted out of the triaxial casing.

The amplitude response shows the greatest difference with a large dip in the response at approximately 45Hz and with a sharp increase shortly after returning to a value of approximately 1 at 55Hz. This is a clear indication of resonance induced by the triaxial casing. The response is also lower over the entire transfer function, indicating that there is a increase in the signal level throughout the frequency range.

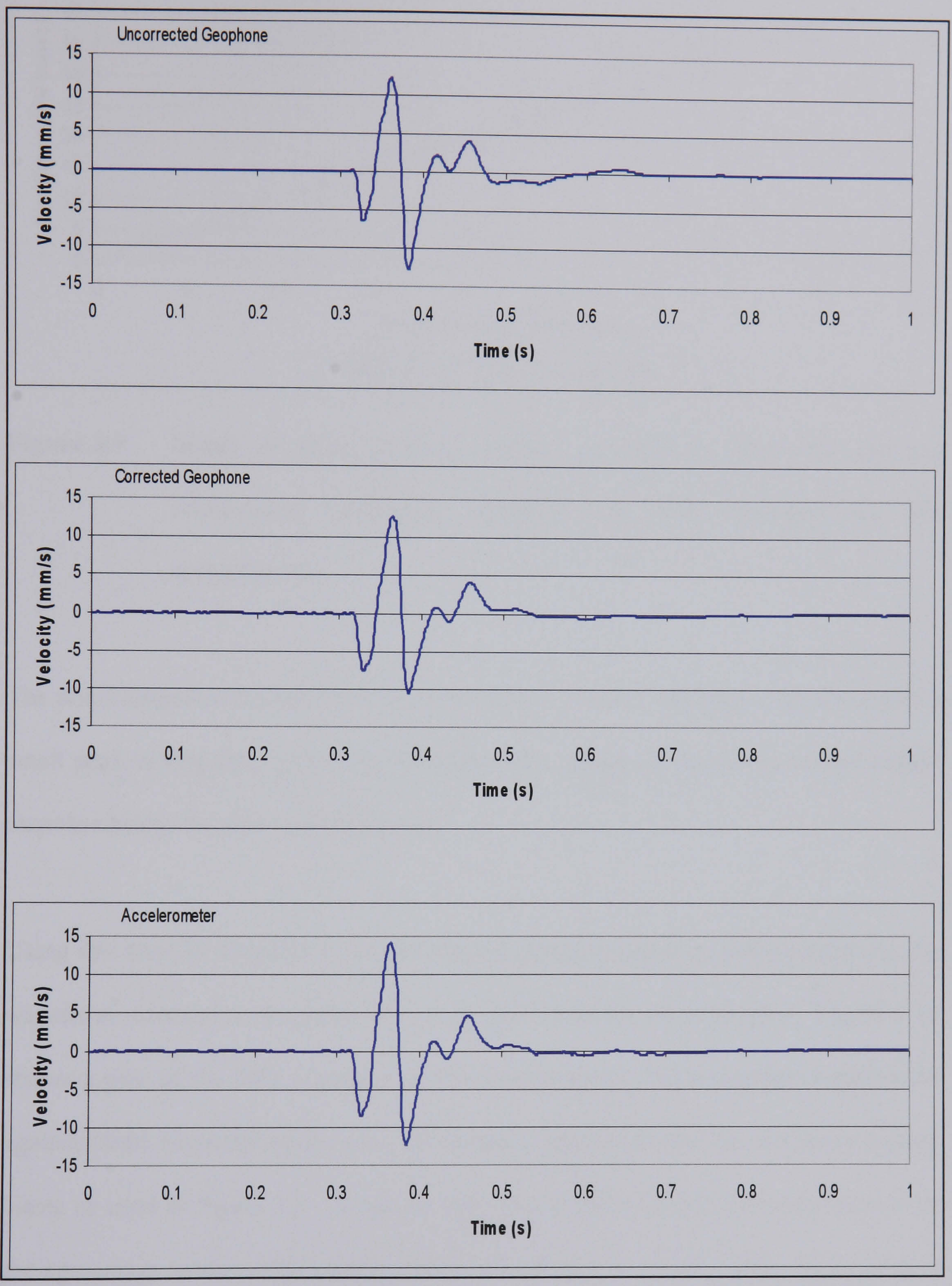

Figure 3.8 Comparison of signals recorded by the uncorrected geophone, corrected geophone and accelerometer.

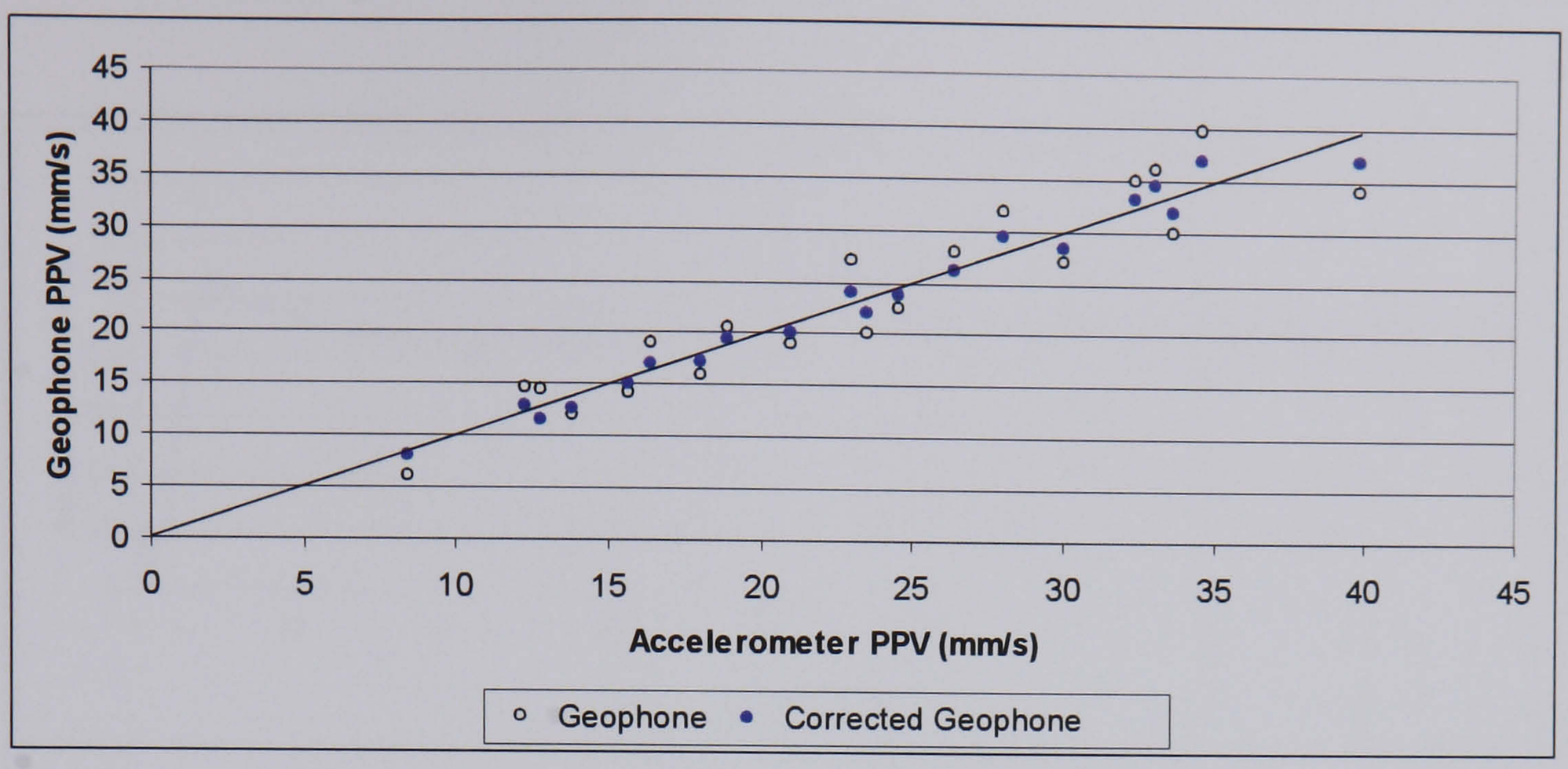

Figure 3.9 Graph of peak particle velocity recorded by the corrected and uncorrected geophone compared to that recorded by the accelerometer.

The phase response is much more similar to the previously calculated function with a small peak in response coinciding with the 45Hz resonance shown on the amplitude response being the only real difference.

Using this transfer function to correct the geophone response as before improves the waveform recorded to the point where any discrepancies are negligible. Figure 3.11 shows a plot of the PPV recorded by the accelerometer and integrator combination against those recorded by the new corrected geophone system for the same twenty blasts as used in figure 3.9. It can be seen that there is significant improvement in the agreement between the accelerometer and geophone results. This observation is confirmed by reference to table 3.1 which shows the regression statistics for figure 3.9 and figure 3.11. It can be seen that the standard error has been reduced from 3.19 to 1.35 for the geophone calibrated out of the case and even further to 0.25 for the

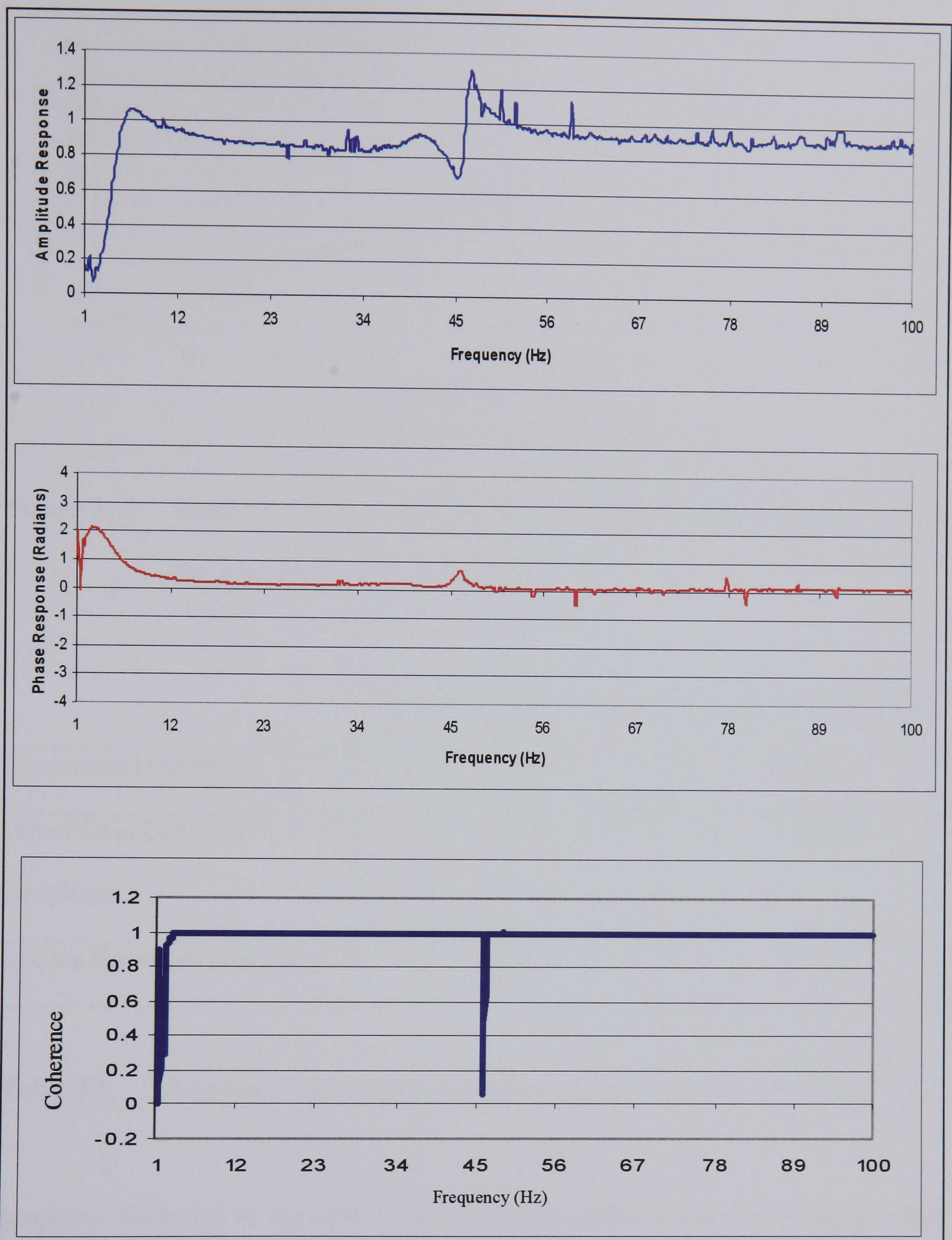

Figure 3.10 Transfer Function determined for a geophone used in the research once enclosed in a triaxial casing with 100 metres of cable.

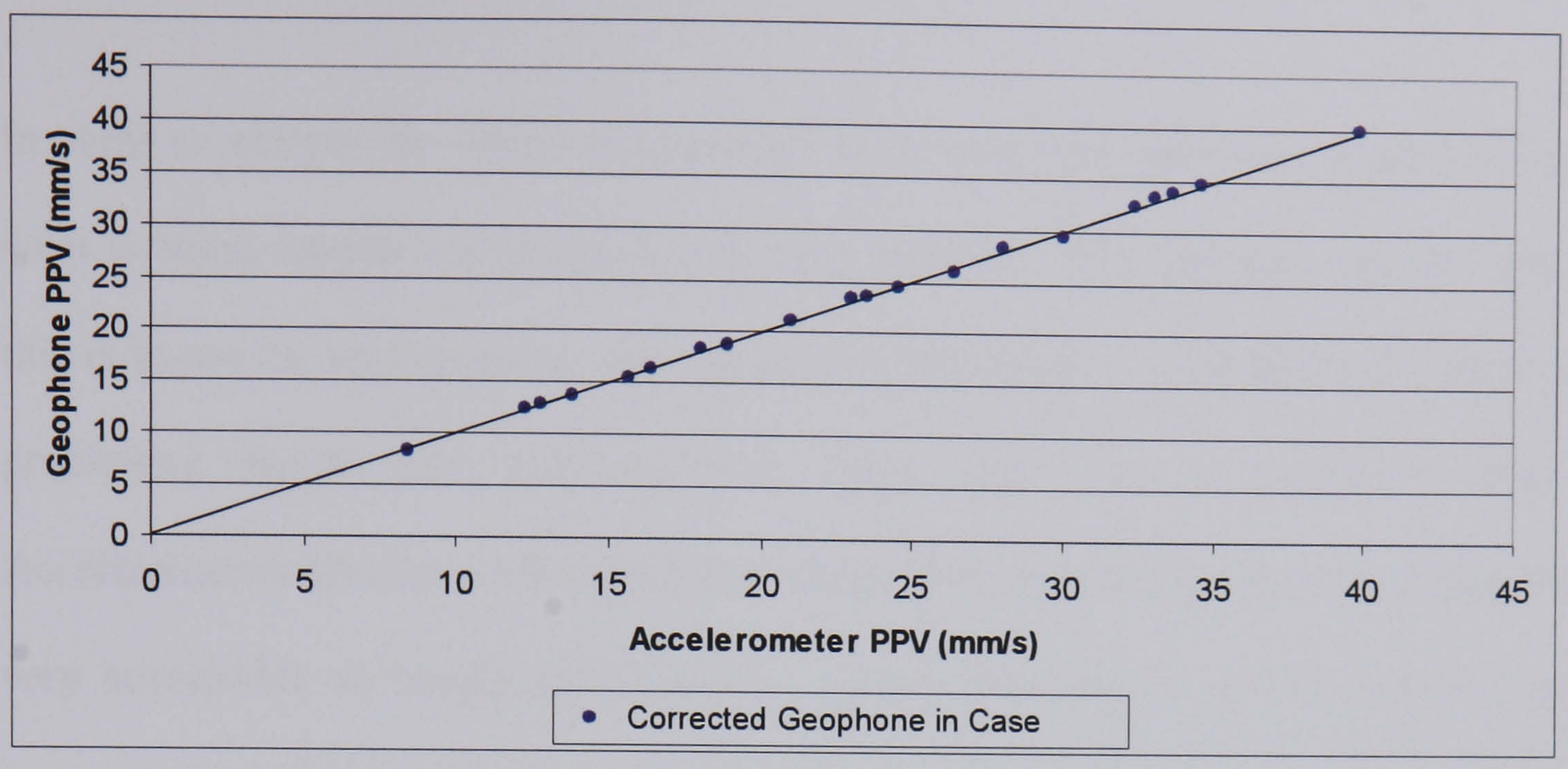

Figure 3.11 Graph of PPV recorded with the in case corrected geophone against that recorded by an accelerometer.

	Standard Error (mms^{-1})	Correlation Coefficient
Uncorrected Geophone	3.19	0.883
Out of Case Corrected Geophone	1.35	0.978
In Case Corrected Geophone	0.25	0.999

Table 3.1 Regression information for the lines given in figures 3.9 and 3.11

geophone calibrated in the case. The correlation coefficient shows a similar trend with improvement from 0.883 to 0.978 for the out of case calibration and to 0.999 for the in case calibration.

3.5 Conclusions on the application of transfer function calibration

In order to analyse the vibration generated by a blast it is necessary to ensure that what is being recorded is as true a picture as possible. The optimum way of doing this is to use an accelerometer and integrator combination. Unfortunately cost is a prohibitive factor with accelerometers much more than a geophone setup. Accelerometers also have other problems in that they require a power source and are very susceptible to temperature changes. Geophones are an economical way of measuring ground vibration but are limited by their resonant frequency below which they give an output which does not represent the true vibration level. A typical quarry blast has significant amounts of energy at low frequencies and so it can be concluded that any recording system utilising geophones will not return a true recording of the vibration generated. Farnfield (1998) outlined a method by which a geophones response could be improved to the equivalent of an accelerometer using transfer functions.

Farnfield's technique was applied to the geophones used to construct the 15 channel seismograph which was developed for this research. Each stage in the procedure was examined and one major shortcoming found.

Whilst Farnfield recommended that each geophone be calibrated in a back to back test on a shaking table with each geophone being mounted separately it can be seen that the casing into which the geophones are placed and the mounting system which is employed will affect the response characteristics. If transfer function calibration is

to be used the transfer function must be determined from the geophone as it will be used in the field.

It can be concluded that through the careful application of transfer function calibration it is possible to get accuracy levels approaching that of an accelerometer and integrator combination with a geophone based unit.

4. FIELD RECORDING OF THE VIBRATION GENERATED BY A SERIES OF SINGLE HOLE TEST SHOTS.

4.1 Introduction

The primary assumption when using hybrid modelling of blast vibration is that each blast hole generates an identical vibration signal. This essentially means that the signal generated by each hole is unaffected by any external effect. Previous work done on validating this assumption appears to be inconclusive with some work reporting that a single hole shot is identical to a production shot hole (Congishi & Qisu, 1990). Other work, however, implies that a single hole does not accurately describe every hole in a production blast (Hinzen, 1988).

To examine whether this primary assumption is correct or not the first step is to look at the repeatability of multiple single-hole shots fired in the same area of a quarry, in the same manner and with similar loading specifications as they would be in a production blast.

A series of tests was undertaken at a limestone quarry in the north of England in order to evaluate the repeatability of single-hole shots. The tests were designed so that certain key parameters would be changed one at a time during the tests giving an insight into which parameters affected the vibration waveform shape and amplitude.

4.2 Field testing of vibration generated by single hole shots

A series of single hole test blasts was designed to be carried out at Coldstones Quarry, in the North Yorkshire dales. Coldstones is a limestone quarry and in that particular location the limestone is unusually thick with several beds coming together without the usual intermediate strata.

4.2.1 Methodology

Six single hole shots were designed, two sets of two near identical holes and two holes with additional design parameters.

The holes were drilled on an 18 metre bench on the bottom bench of the quarry. The location within the quarry was picked as the geology was at its most homogeneous in that area. Each hole was 105mm in diameter and drilled at an angle of 10 degrees.

A series of permanent monitoring locations was set up. Four locations were established on the surface of the test bench at extreme close range varying from 15 to 25 metres away from the shot holes. Each of these locations had a triaxial array of geophones which was bolted to the rock to ensure good ground coupling. Another triaxial array was constructed to be placed down a borehole which had been drilled in the bench for the purpose. This is shown being installed in figure 4.1. The borehole was then filled with quick drying concrete followed by drill chippings. These five locations were designed to be used with the multi-channel seismograph described in Chapter 3.

Another permanent location was established at the site office using a standalone portable digital seismograph. There were no portable seismographs used in the extreme close monitoring for two reasons. Firstly, they cost much more than triaxial geophone arrays and damage or destruction caused by flyrock or other hazards associated with extreme close range monitoring could not be risked. The second reason was due to doubts being cast upon their ability to actually capture high level vibration without clipping as the manufacturers maximum specification was below the level of vibration expected at such close range.

Figure 4.1 Installation of down borehole triaxial vibration transducer

Figure 4.2 shows an aerial photograph of the quarry with the test bench and site office monitoring location marked. The slope distance to the site office monitoring location is approximately 130 metres.

Each of the holes were drilled, loaded and fired at the time the test was taking place. This was to ensure that the boreholes were dry and any problems encountered by the driller or shot firer could be recorded.

Figure 4.2 Aerial photograph of Coldstones Quarry showing test bench and site office monitoring location

The burden in front of each hole was measured using a laser profiling system and the location of the hole was surveyed using standard surveying techniques.

Each hole was also instrumented to measure the velocity of detonation. This involved lowering a cable down the borehole as it is loaded. The cable is taped to the bottom

primer charge and held in the centre of the borehole as the explosive is loaded. This ensures that the cable shorts out cleanly which in turn ensures a clear indication of the velocity of detonation.

Each hole was bottom initiated using a 16L cast primer and loaded using either hand mixed ANFO, packaged emulsion or a combination of both. The holes were all fired using pyrotechnic delay detonators.

Any other data which was thought may be relevant was recorded by visual inspection and is included in the blast logs shown in Appendix A.

4.3 Results of Field Tests

This section details the results gained from the single hole test shots. Included for each hole are examples of the vibration velocity traces measured in the same location. The loading specifications, burden measurements and Velocity of Detonation results are also detailed here. The blast logs in Appendix A give the complete loading specifications and burden measurements for all the blasts.

4.3.1 Test Shot 1.

The first shot was fired on a straight face and so had only one free face excepting the top. As the top of a quarry blast will always be free it will be disregarded in all discussion of the number of free faces from henceforth in this work.

The hole was drilled at an angle of 6 degrees to a depth of 14.7 metres with a subdrill of 0.4 metres. It was then loaded with a base charge of 25 Kg of emulsion and a main charge of 80 Kg of hand mixed ANFO. Drill chippings were then added to a depth of 3.5 metres as stemming.

Figure 4.3 shows the burden as recorded by the laser profiling system. The burden varies between 3.4 and 4.6 metres down the hole with a total cross sectional area in front of the hole of 58.03 square metres.

Figure 4.4 shows the velocity of detonation trace generated as the hole detonated. The two different explosives are clearly defined. The results of 4584 metres per second for the emulsion and 3784 metres per second for the ANFO are typical and show that the explosive was of satisfactory quality and detonated correctly.

Unfortunately the multi-channel seismograph failed to operate correctly and did not record the extreme close up vibration. This left only the vibration from the monitoring point at the site office. The vibration velocity traces from this are shown in figure 4.5.

4.3.2 Test Shot 2.

Test shot 2 was fired in a similar manner as test shot 1, but with two free faces available. The hole was drilled at an angle of 10 degrees to a depth of 15.6 metres with 0.7 metres subdrill.

The hole was then loaded with a base charge of 25 Kg of emulsion followed by 80 Kg of hand mixed ANFO. The stemming consisted of 3.5 metres of drill chippings.

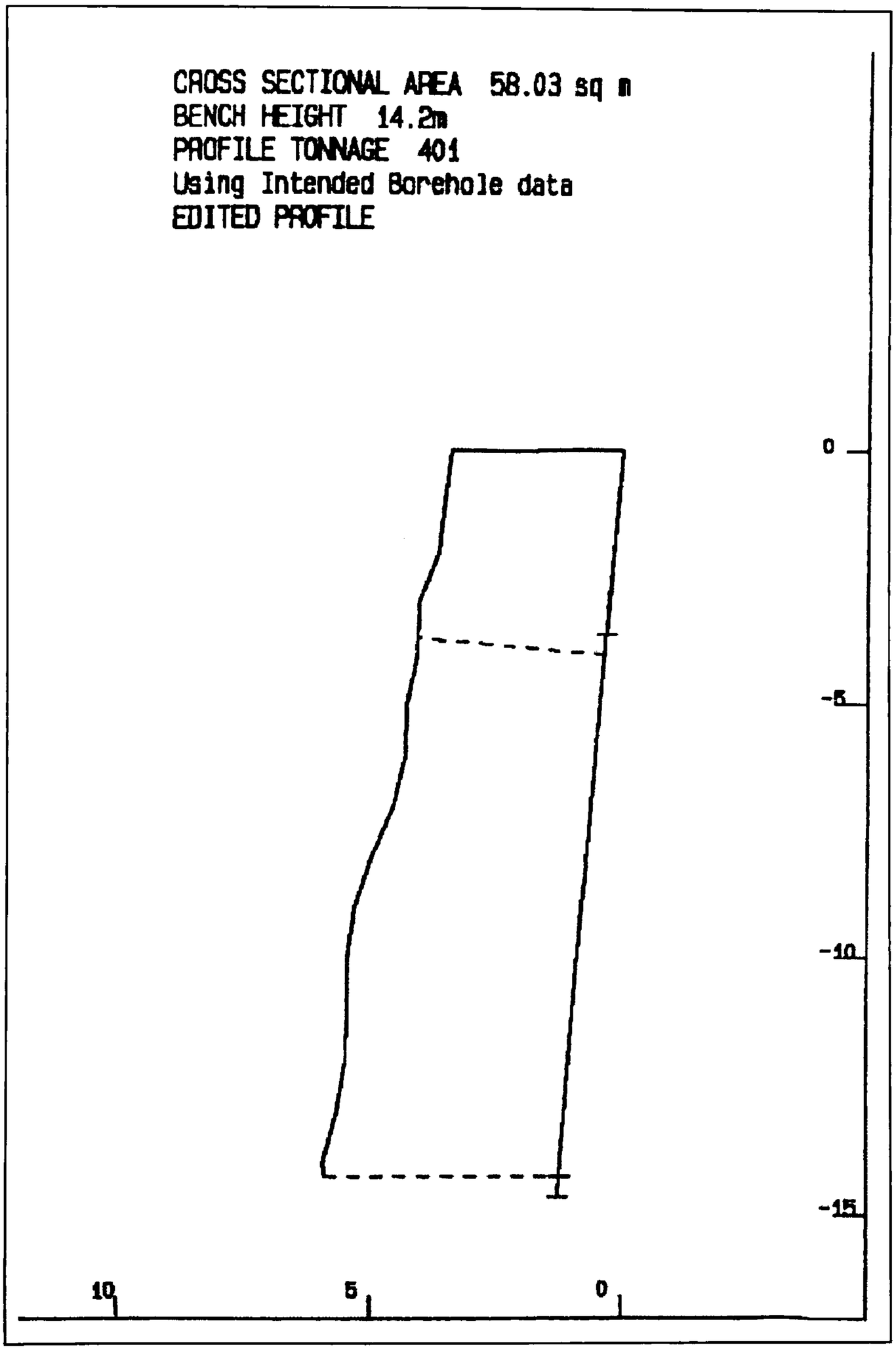

Figure 4.3 Burden of test shot 1 as recorded by laser profiling system

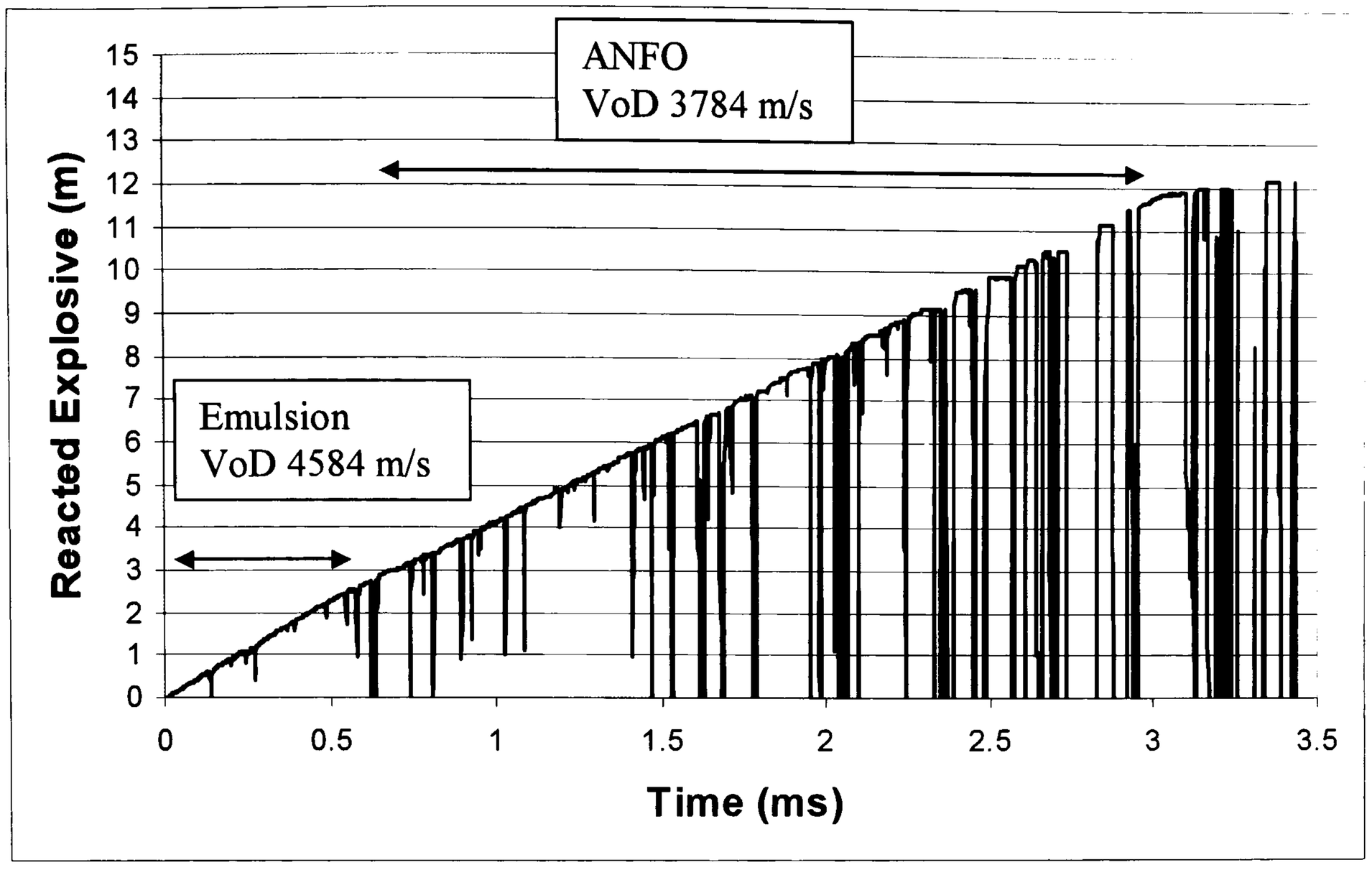

Figure 4.4 Velocity of detonation recording of single hole test shot 1.

The burden of the hole ranged between 2.9 and 4.2 metres, and the total cross sectional area in front of the hole was 52.22 square metres.

The velocity of detonation, Figure 4.6, shows that there is no discernable difference between the explosive types this time even though exactly the same explosives were used as in test 1. The velocity of 3918 metres per second is, however, acceptable for both ANFO and the emulsion.

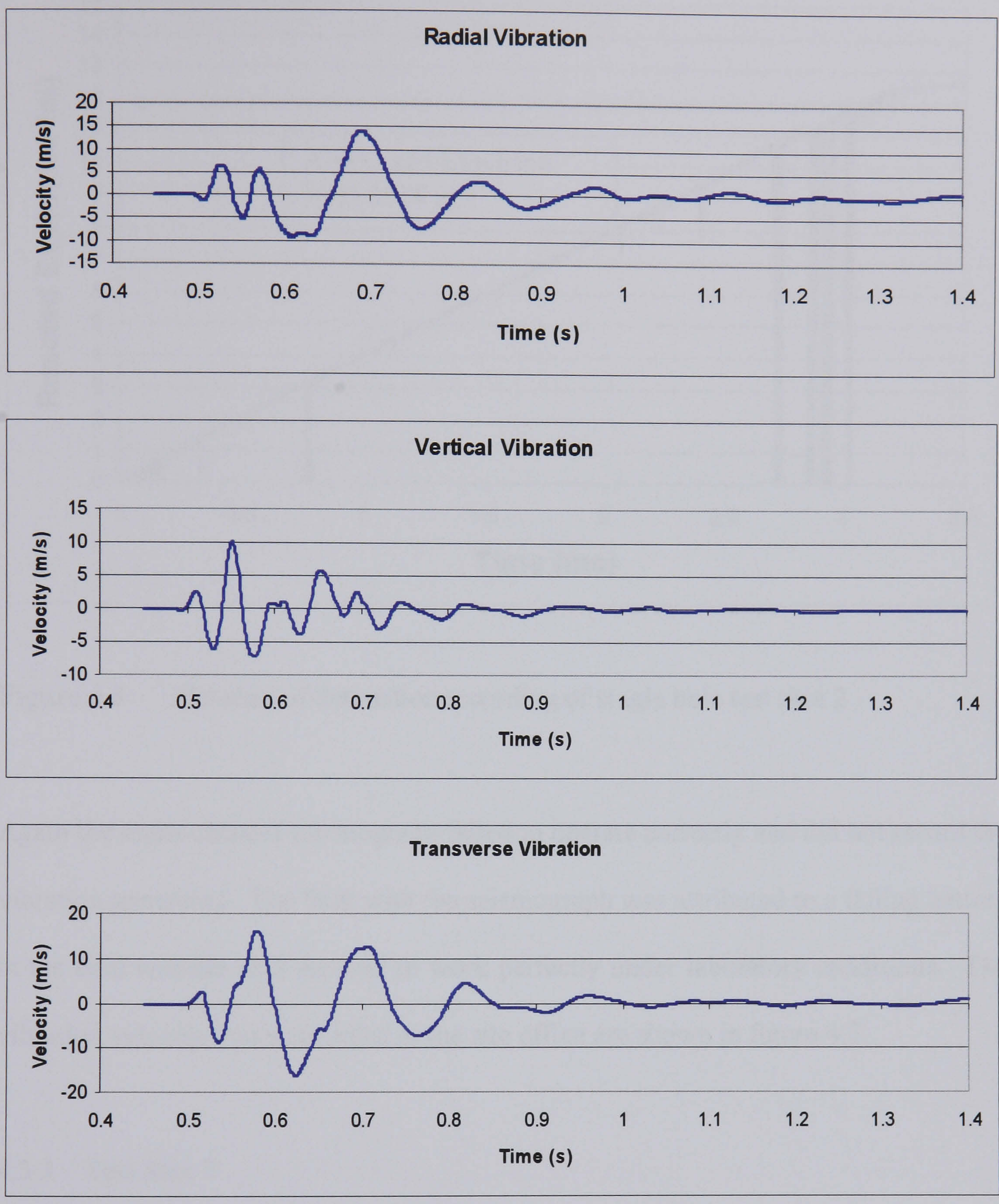

Figure 4.5 Vibration Velocity traces from test shot 1 recorded at site office monitoring point

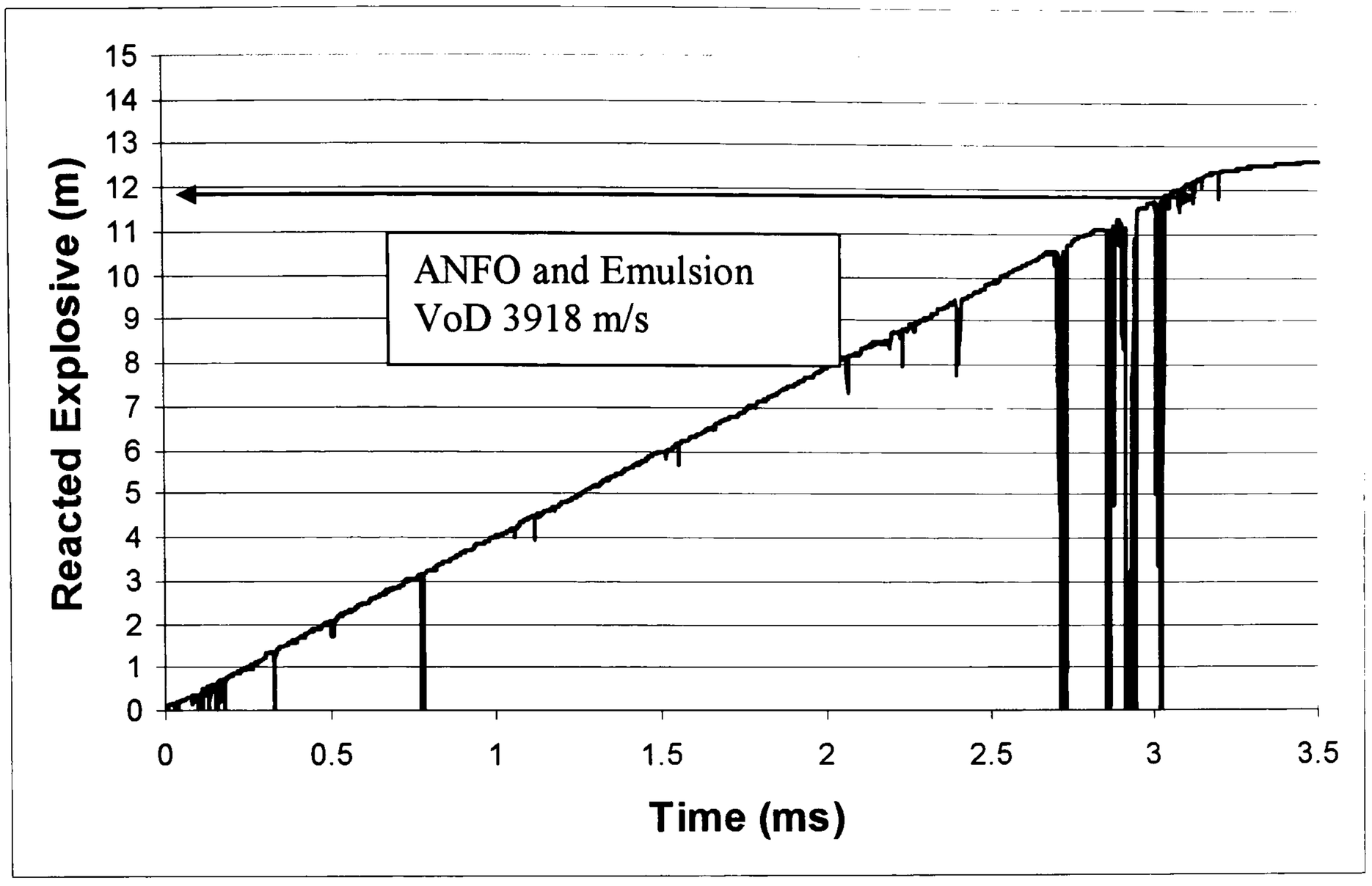

Figure 4.6 Velocity of detonation recording of single hole test shot 2.

Again the multi-channel seismograph failed to operate correctly and did not record the vibration generated. The fault with the seismograph was attributed to a failing battery in the cold weather as it seemed to work perfectly under laboratory conditions. The vibration velocity traces recorded at the site office are shown in figure 4.7.

4.3.3 Test Shot 3

The third test shot was designed to be identical to the second. The hole was drilled at an angle of 10 degrees to a depth of 15.9 metres with 0.6 metres subdrill. The burden ranged from 3.1 metres to 3.7 metres in front of the hole and the total cross sectional area was 52.32 square metres.

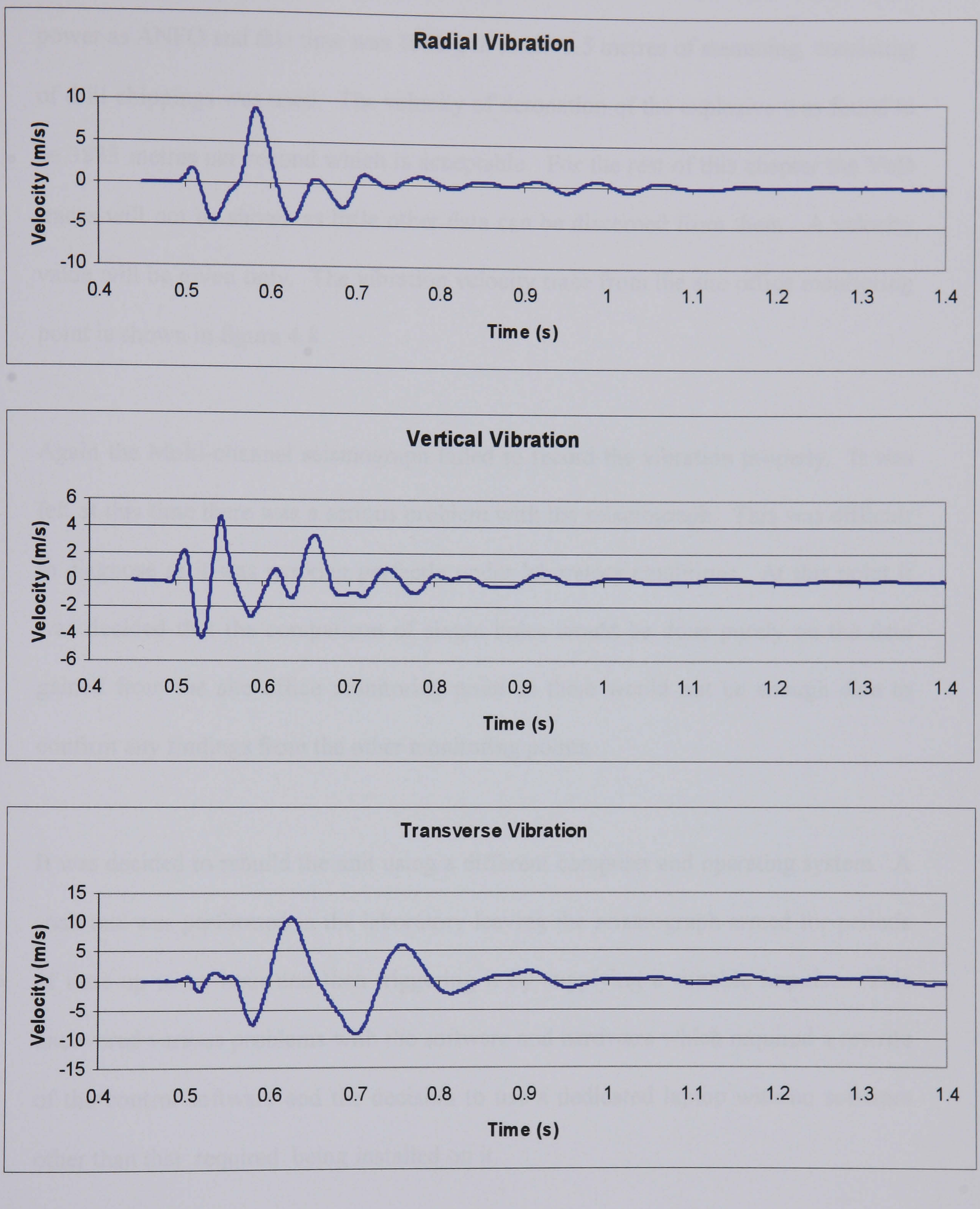

Figure 4.7 Vibration Velocity traces from test shot 2 recorded at site office monitoring point

The hole was this time loaded using only emulsion which was rated as the same power as ANFO and this time was 105Kg in total. 3.5 metres of stemming, consisting of drill chippings was used. The velocity of detonation of the explosive was found to be 3883 metres per second which is acceptable. For the rest of this chapter the VoD traces will not be shown as little other data can be discerned from them. A velocity value will be given only. The vibration velocity trace from the site office monitoring point is shown in figure 4.8.

Again the Multi-channel seismograph failed to record the vibration properly. It was felt at this time there was a serious problem with the seismograph. This was difficult to diagnose as it was working perfectly under laboratory conditions. At this point it was decided that the comparison of single holes would be done purely on the data gained from the site office monitoring point as there would not be enough data to confirm any findings from the other monitoring points.

It was decided to rebuild the unit using a different computer and operating system. A soak test was performed in the laboratory leaving the seismograph armed for periods of time up to an hour and then triggering it by supplying a suitable impulse. This uncovered various problems with the software and hardware which required a rewrite of the control software and the decision to use a dedicated laptop with no software other than that required being installed on it.

Once the system was working with no problems in the laboratory it was decided that the remaining test shots would be instrumented in the same manner as before.

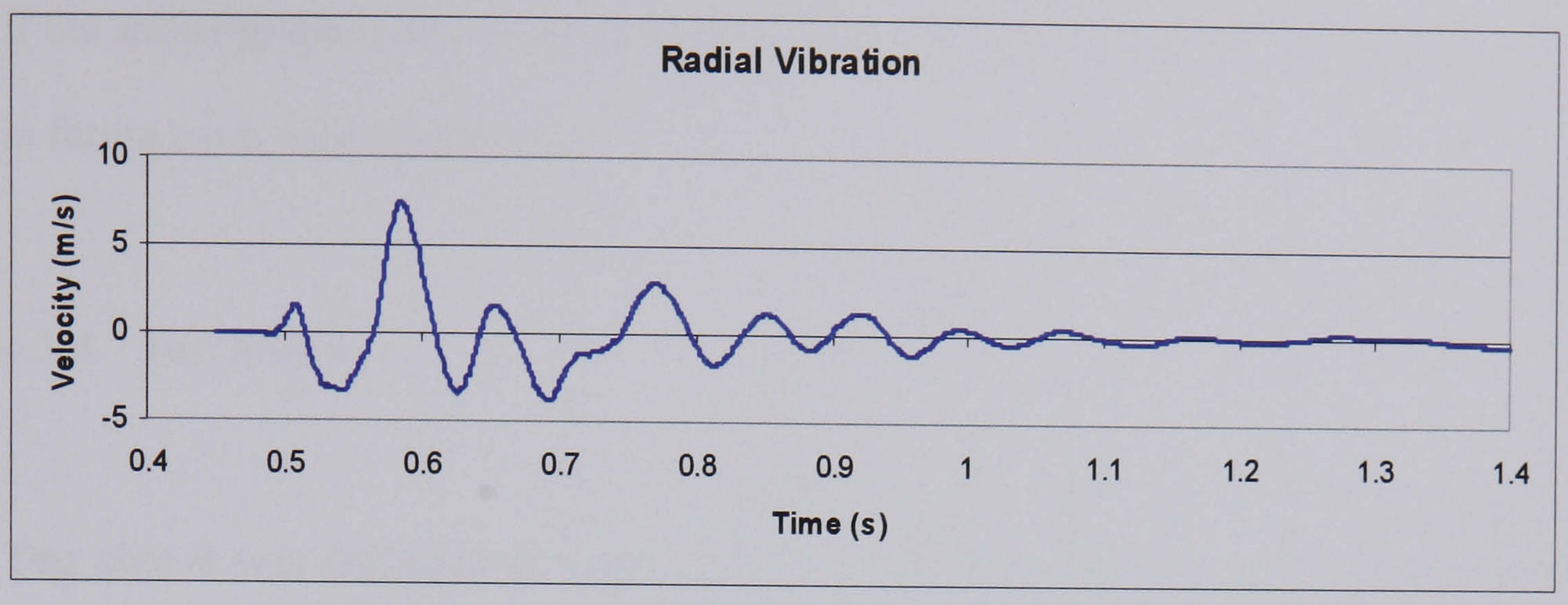

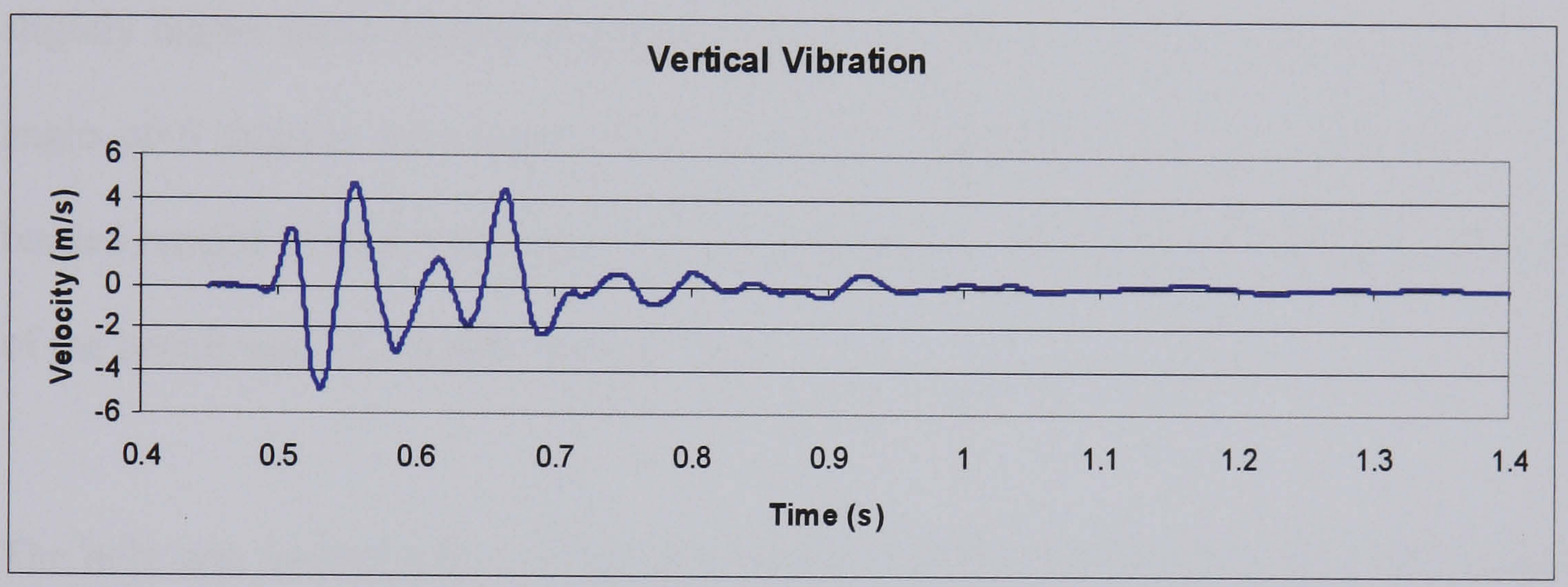

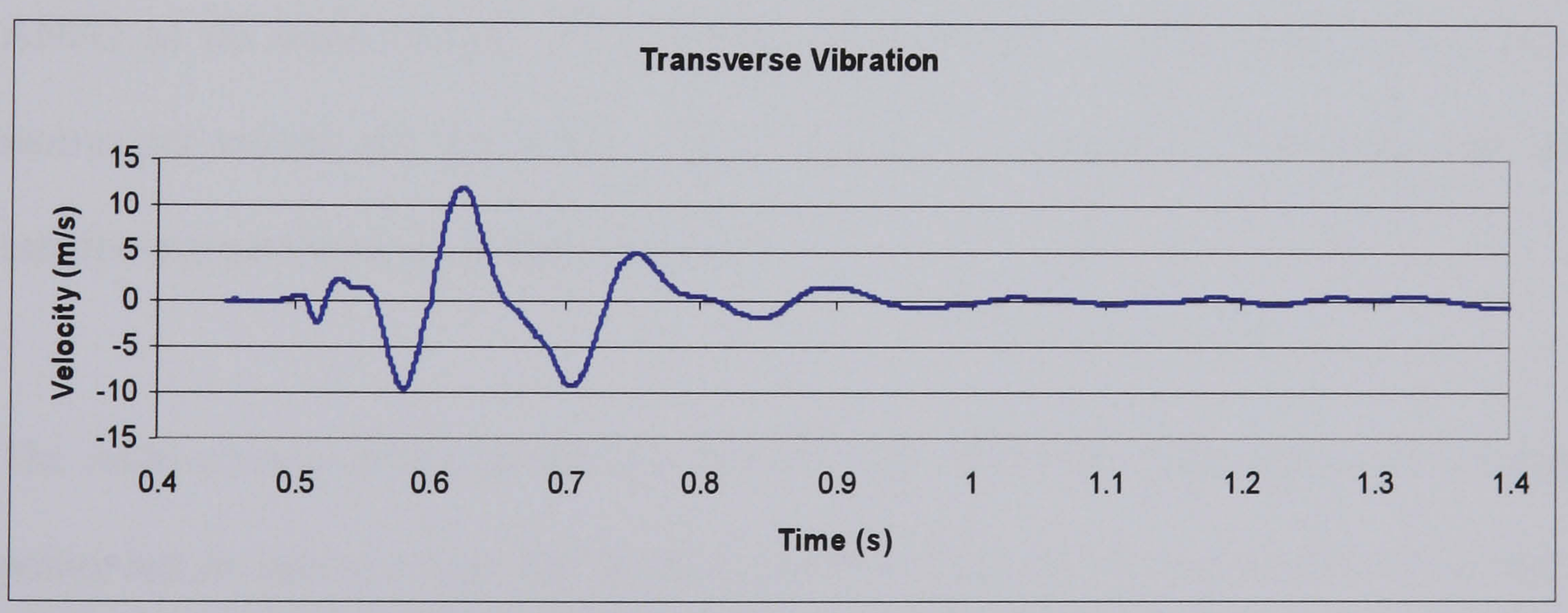

Figure 4.8 Vibration Velocity traces from test shot 3 recorded at site office monitoring point

The seismograph could then be tested in real conditions and any information gained from it could be used to back up the data gathered at the site office.

If the seismograph could be made to record the remaining blasts then it could be used in future work with confidence.

4.3.4 Test Shot 4

Test shot 4 was designed as a direct copy of test shot 1. Due to the bench being slightly higher more explosive was used by the shotfirer. The hole was drilled at an angle of 6 degrees to a depth of 17.2 metres, including 0.9 metres subdrill. The burden ranged from 3.9 metres to 4.9 metres and the total cross sectional area in front of the bench was 73.1 square metres.

The hole was loaded with a 25kg base charge of emulsion and 100kg of hand mixed ANFO as the main charge. The velocity of detonation of the emulsion was 4327 metres per second and the ANFO was 4104 metres per second. These both indicate satisfactory performance of the explosive.

The multi-channel seismograph recorded the blast from the four surface monitoring points but as almost a year had passed since the down borehole transducer had been installed it was no longer functioning. This was most probably due to ingress of water shorting out the transducers. The vibration velocity trace recorded from test shot 4 at the site office monitoring point is shown in figure 4.9.

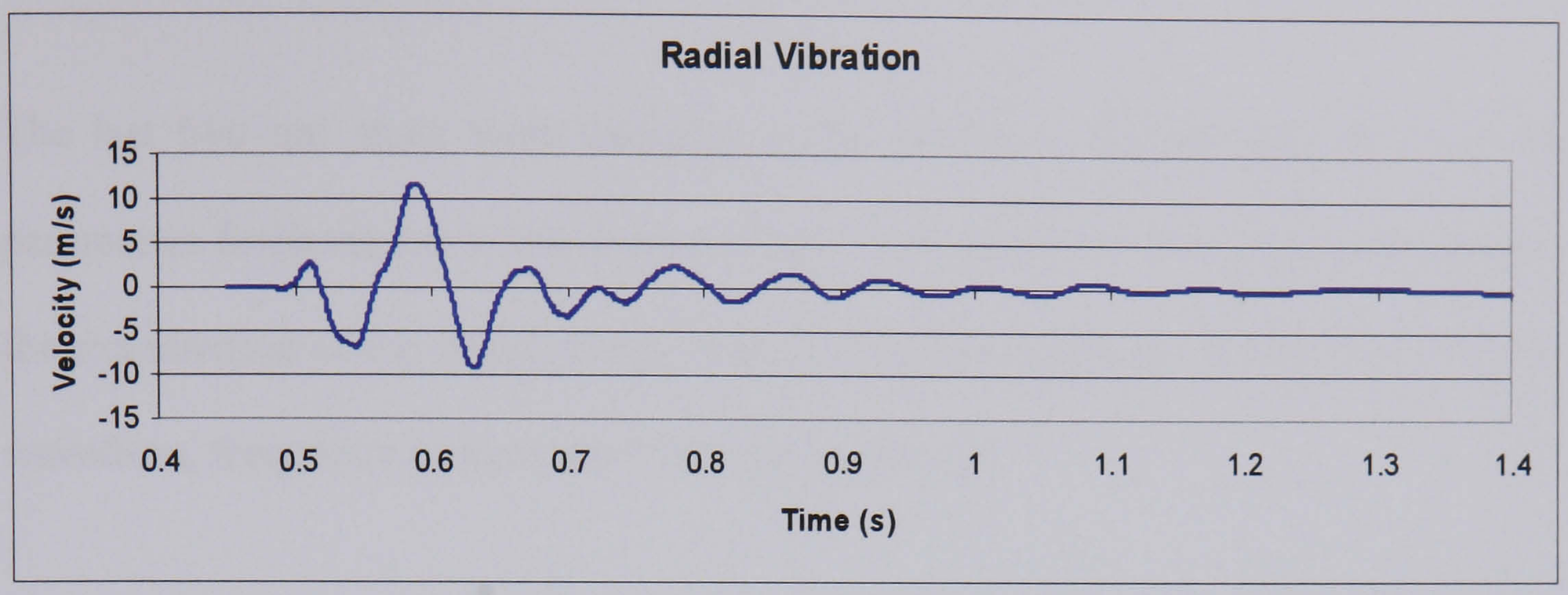

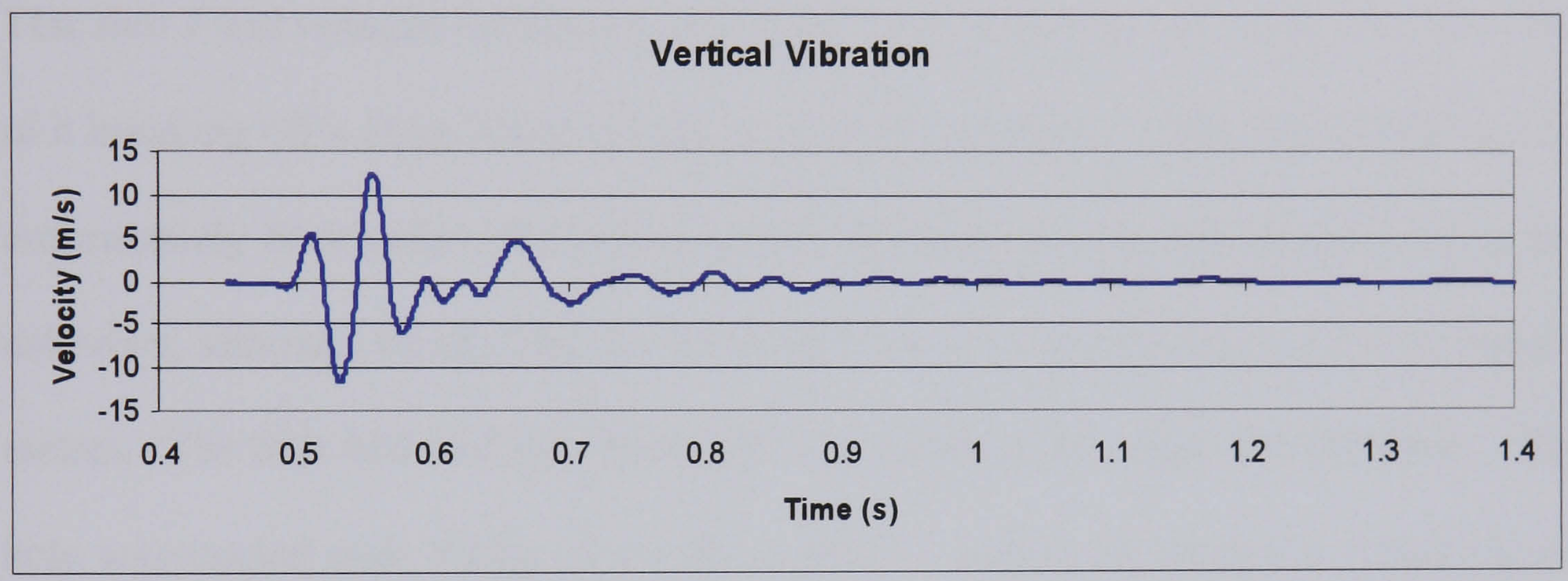

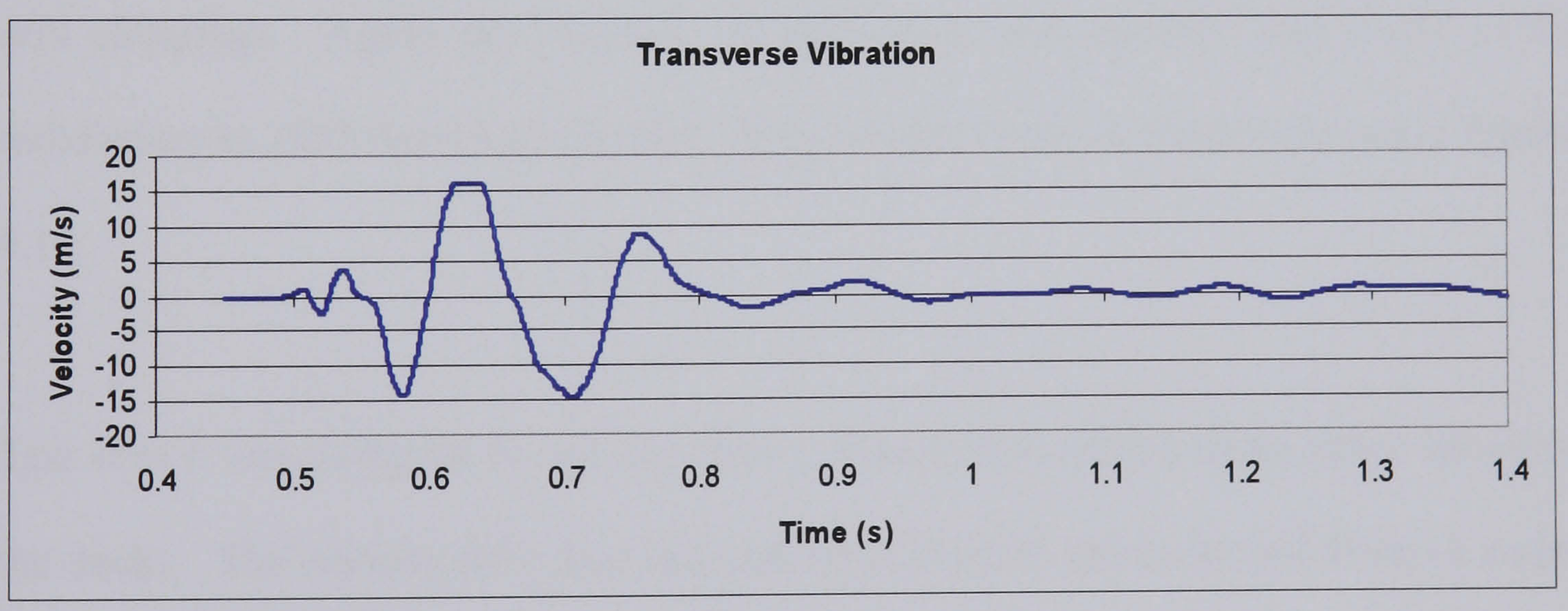

Figure 4.9 Vibration velocity traces from test shot 4 recorded at site office monitoring point.

4.3.5 Test shots 5 and 6

The last two test shots were designed to be similar to the previous four but had parameters fundamental to the design of the blast modified. This was done to allow the examination of the effect, if any, that these parameters have on the blast vibration waveform, frequency content and vibration amplitude.

Test shot 5 had reduced burden on part of the hole. This was caused by the hole next to it breaking off a large block of rock in front of test shot 5. The laser profiling was unfortunately done before the previous shot was fired, so the exact measurements are unknown, although an estimate has been made of a cross sectional area of 50 square metres. The hole had two free faces and was drilled at an angle of 10 degrees. The hole was loaded with 100kg of emulsion and 3.5 metres of stemming consisting of drill chippings. Again the Velocity of Detonation was recorded and found to be satisfactory at 3895 metres per second. The vibration velocity trace is shown in figure 4.10.

Test shot 6 was designed to use two decks of explosive with a 25ms delay between the decks. The bottom deck was charged with 25kg of emulsion and 30kg of hand mixed ANFO. The top deck was charged with 45kg of and mixed ANFO. The velocity of detonation showed the explosive performance to be acceptable. The burden ranged from 3.9 to 4.2 metres and the total cross sectional area was 82.5 square metres. The vibration velocity trace is shown in figure 4.11.

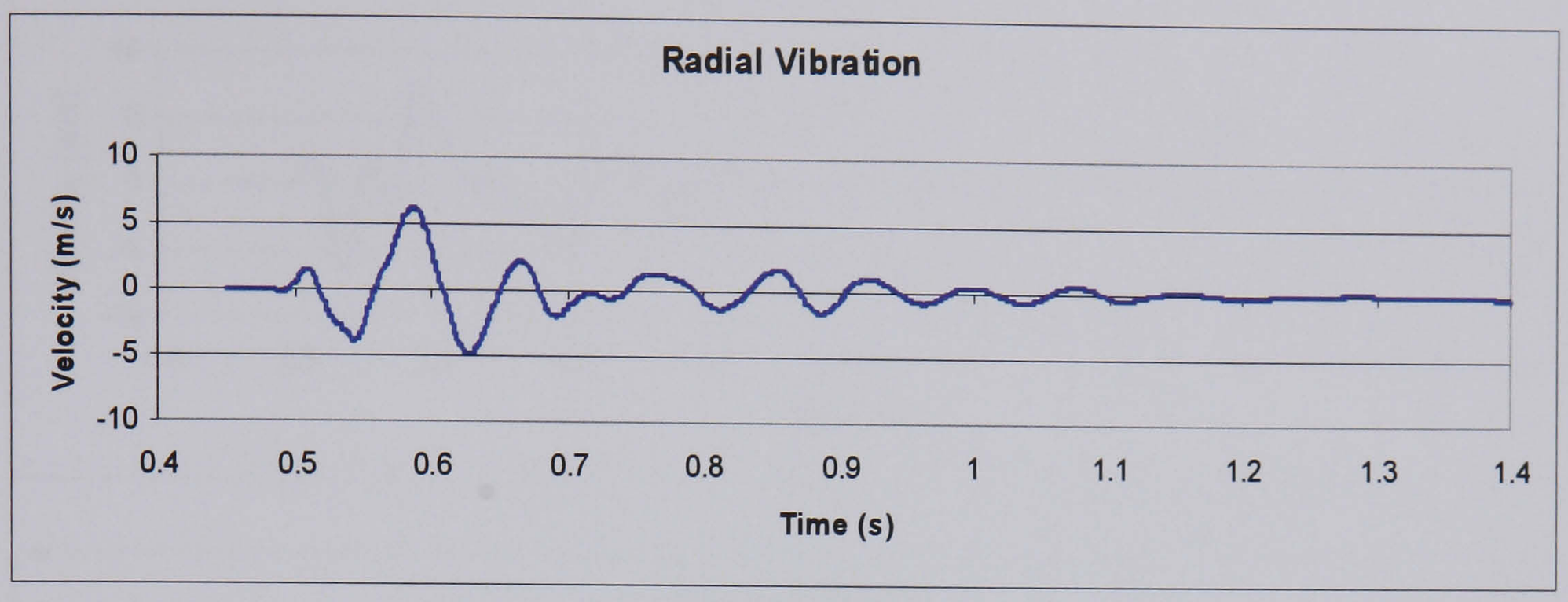

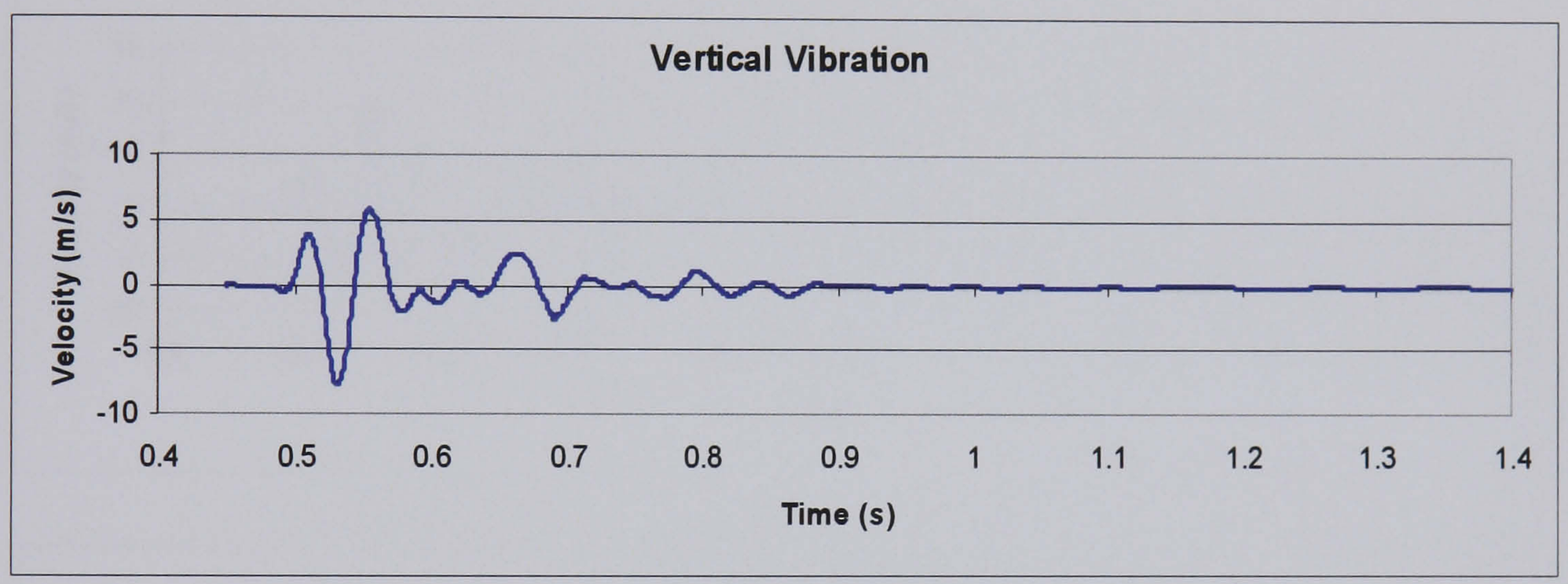

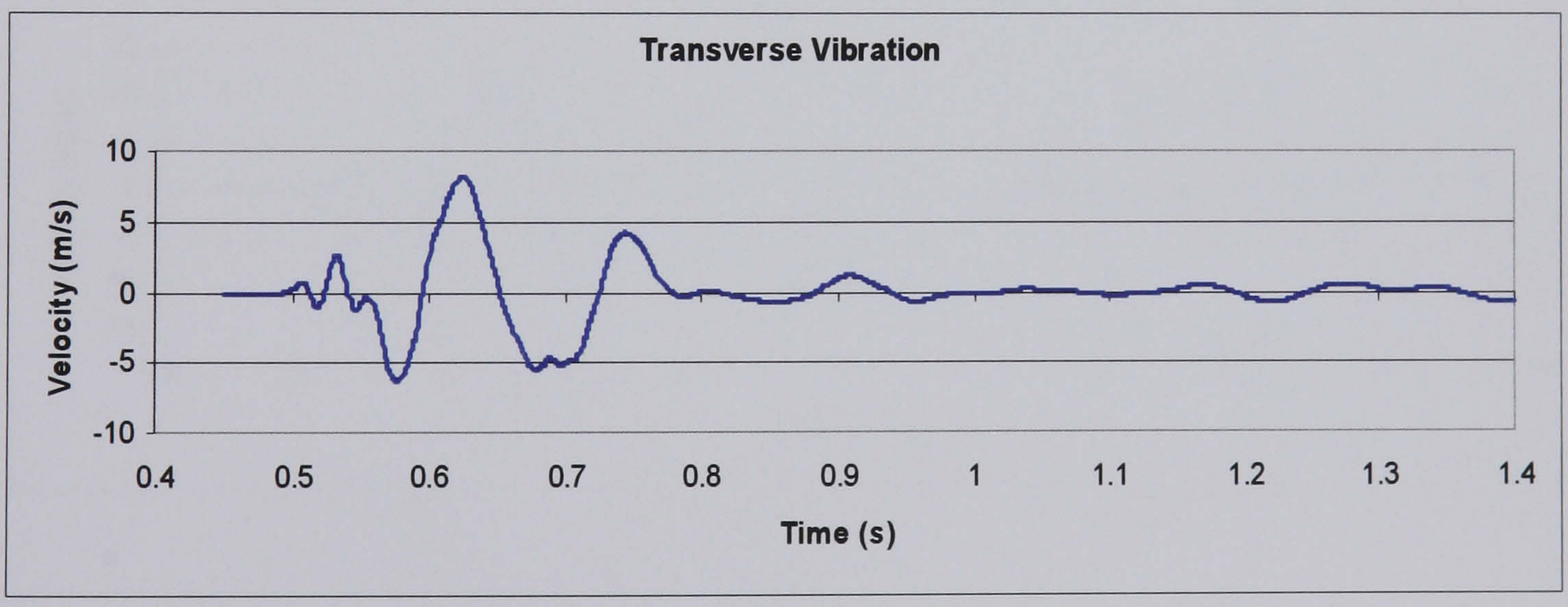

Figure 4.10 Vibration velocity traces from test shot 5 recorded at site office monitoring point.

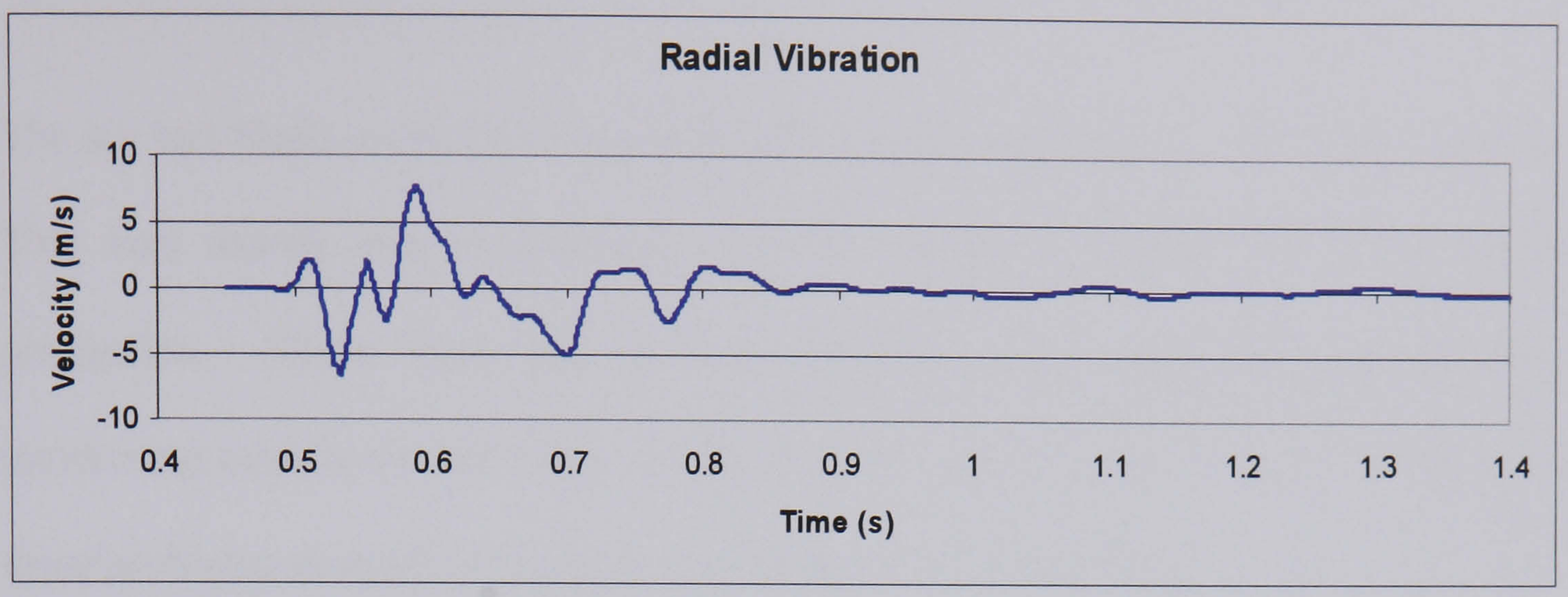

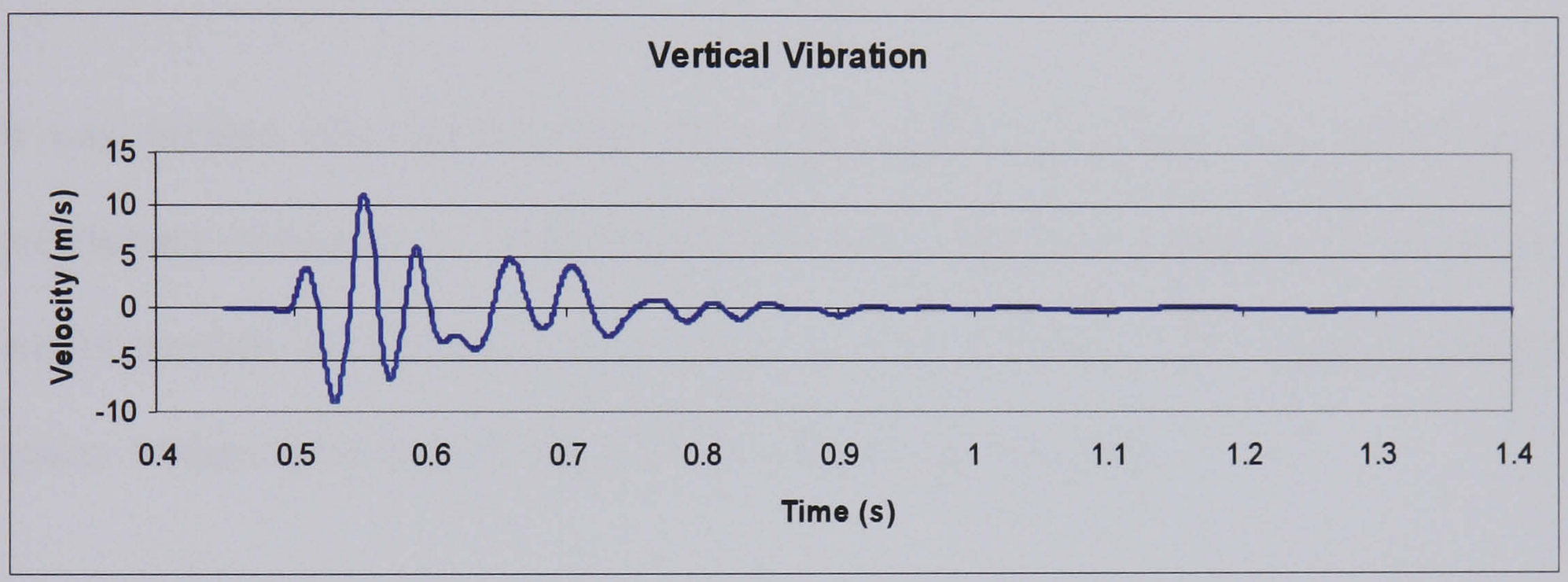

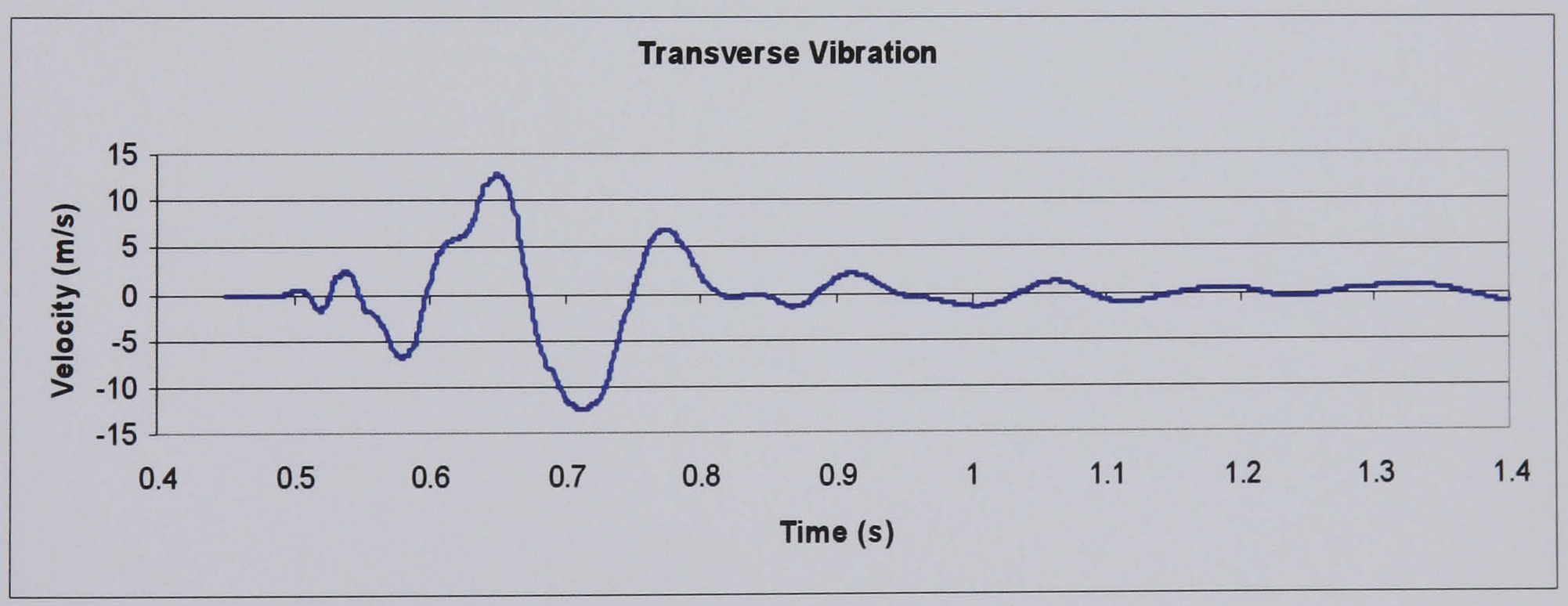

Figure 4.11 Vibration velocity traces from test shot 6 recorded at site office monitoring point.

4.4 Review of single hole test blast recordings

The six test blasts carried out at Coldstones Quarry took almost a year to complete. This was mainly due to problems with the quarry's schedule as it interrupted production. There were also several problems with equipment and the main monitoring equipment had to be redesigned half way through the tests. Because of these problems several of the original ideas had to be abandoned.

It was decided that the data that was collected was sufficient to be able to draw preliminary conclusions. Although a much more intensive campaign of monitoring would provide much more conclusive proof it is difficult to do this in a working quarry without providing compensation for the lost productivity.

5. DETERMINATION OF THE REPEATABILITY OF SINGLE HOLE TEST SHOTS.

The assumption that similar columns of explosive fired in a similar manner in similar material will give a similar vibration waveform is vital to modelling of blast vibration. If similar single holes fired independently cannot be found to be near identical then, by extension, it cannot be valid to assume that each hole in a production shot is identical.

5.1 Background on the repeatability of single hole shots

The repeatability of single holes is an assumption that is often quoted by authors in the field of blast vibration modelling but without giving reference to suitable work which proves this assumption.

Congishi and Qisu (1990) report that single holes with varying hole construction gave similar vibration waveforms and only the amplitude of the vibration varied. They gave no description of methods utilised in determining the similarity and present only a single chart of two waveforms with no scale as an example. Wheeler (2001) also reports a consistency in blast vibration from similar holes, giving three examples in the time domain which appear similar and two examples of the amplitude spectra, in the frequency domain which show similarity. Wheeler, like Congishi and Qisu, does not detail the methods used to ascertain similarity.

Crenwelge (1988) looked at single hole blasts as a method of determining ground transmission characteristics and as part of that work concluded that the holes yielded essentially identical frequency amplitude spectra although no mention is made of the frequency phase spectra or time domain signals.

Repeatability of single holes is clearly a widely agreed upon phenomenon but few detailed studies have been done. The level of similarity between holes does not appear to have been quantified by anything other than by an opinion based on direct visual comparison.

5.2 Existing methods of comparison of single hole test shots.

In order to prove or disprove that similar single hole sources generate a similar signal it is necessary to compare the shape of the waveforms generated. This is a problem because it is difficult to mathematically compare signals which can vary in amplitude as greatly as these signals can. It seems that most authors of work in this field use direct comparison by eye as the only measure of similarity. This is highly subjective and offers no real measure of similarity.

Standard techniques for comparing datasets are available and a brief review of these and why they are not suitable for this application is given below.

5.2.1 Cross-correlation of waveforms

The cross-correlation function is a signal processing technique estimating the degree to which two series are correlated. For two signals $f_x(t)$ and $f_y(t)$ it may be defined as

$$R_{xy}(\tau) = \lim_{T\to\infty} \frac{1}{T} \int_{-T/2}^{T/2} f_x(t) \cdot f_y(t+\tau) dt \qquad (5.1)$$

Where T is the total waveform time

τ is a time interval to shift one of the signals

It is possible to normalise the cross correlation to a maximum value of 1 by dividing equation 5.1 through by $\sqrt{R_{xx}(o) \cdot R_{yy}(o)}$, the product of the RMS values of the two signals.

The normalised cross-correlation gives an output spectrum from $-T$ to T with a value for the quality of fit between the two signals. A value of 1 being a perfect fit, i.e. the signals are identical, sharing all frequency components at the same amplitude and phase. A value of zero shows that the signals have no common frequency values and a value of -1 shows the signals are identical but 180 degrees out of phase.

The problem with using a cross-correlation is that it will only show a high correlation if the relationship between the signals is a linear one. If the relationship is non-linear then it will give false results. For example if we have a signal $f_x(t)=A\ cos\ \omega t$ and another signal $f_y(t)$ which is simply the square of $f_x(t)$. Thus:

$$f_y(t) = f_x{}^2(t) = A^2 \cos^2 \varpi t = \frac{A^2}{2} + \frac{A^2}{2} \cos 2\varpi t \qquad (5.2)$$

It can be seen that $f_y(t)$ contains components at zero frequency and 2ω radians/second but not at ω radians/second as in $f_x(t)$. The resulting cross-correlation will be zero for all values of T.

Because of this limitation the cross-correlation is generally used to determine to what extent a signal measured at one point originates from another or to detect the existence of a known signal buried in extraneous noise.

Figure 5.1 shows the cross-correlation of two single hole signals. It is obvious that the signals are similar by eye but the cross-correlation give a maximum of approximately 0.3. If the original signals were not available, it would be assumed that there is little correlation between the two. For this reason direct cross-correlation cannot be relied upon to give a reliable measure of similarity between two single hole blast transients. Later in this chapter a technique to determine similarity using the cross-correlation function will be described.

5.2.2 Sum of squares of difference

The sum of squares technique is usually applied to regression analysis to find a best fit line by trying various formulations and determining the sum of the square of the

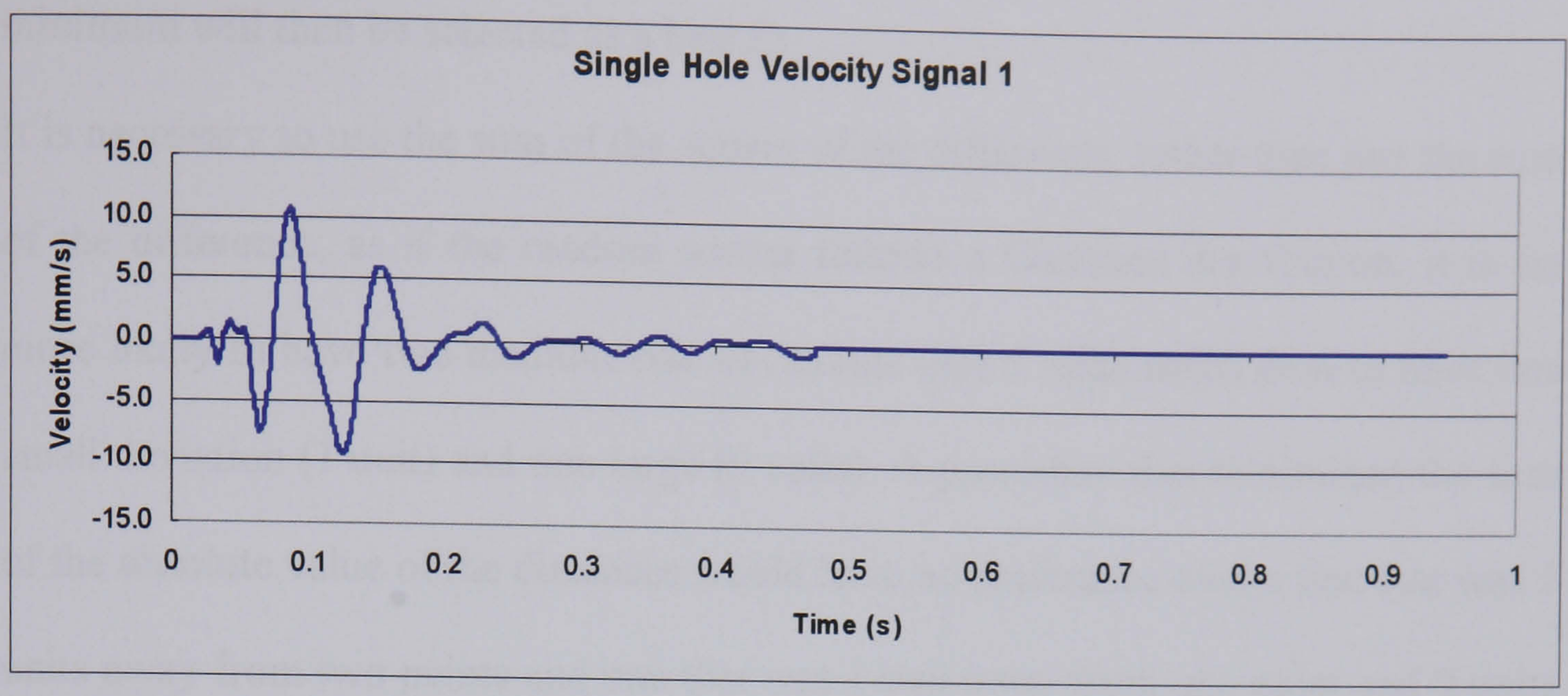

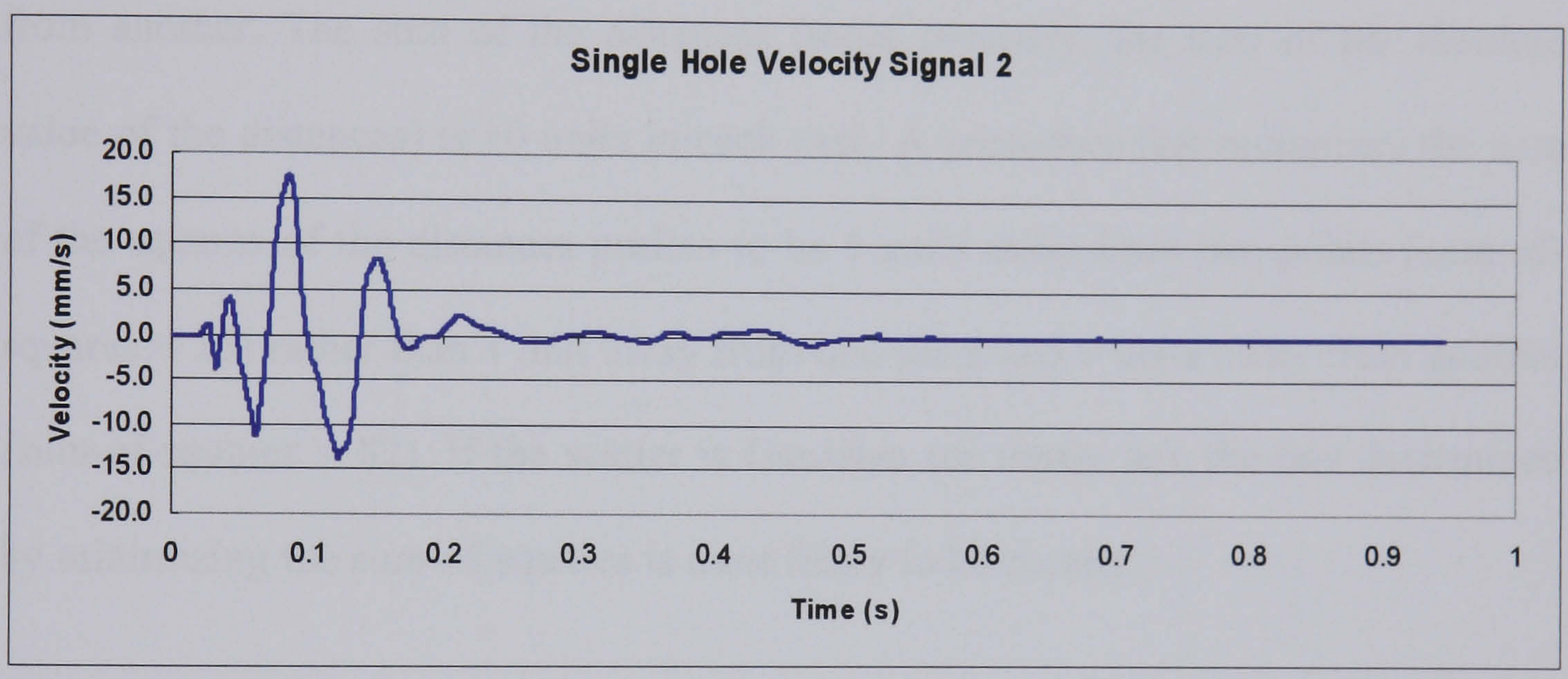

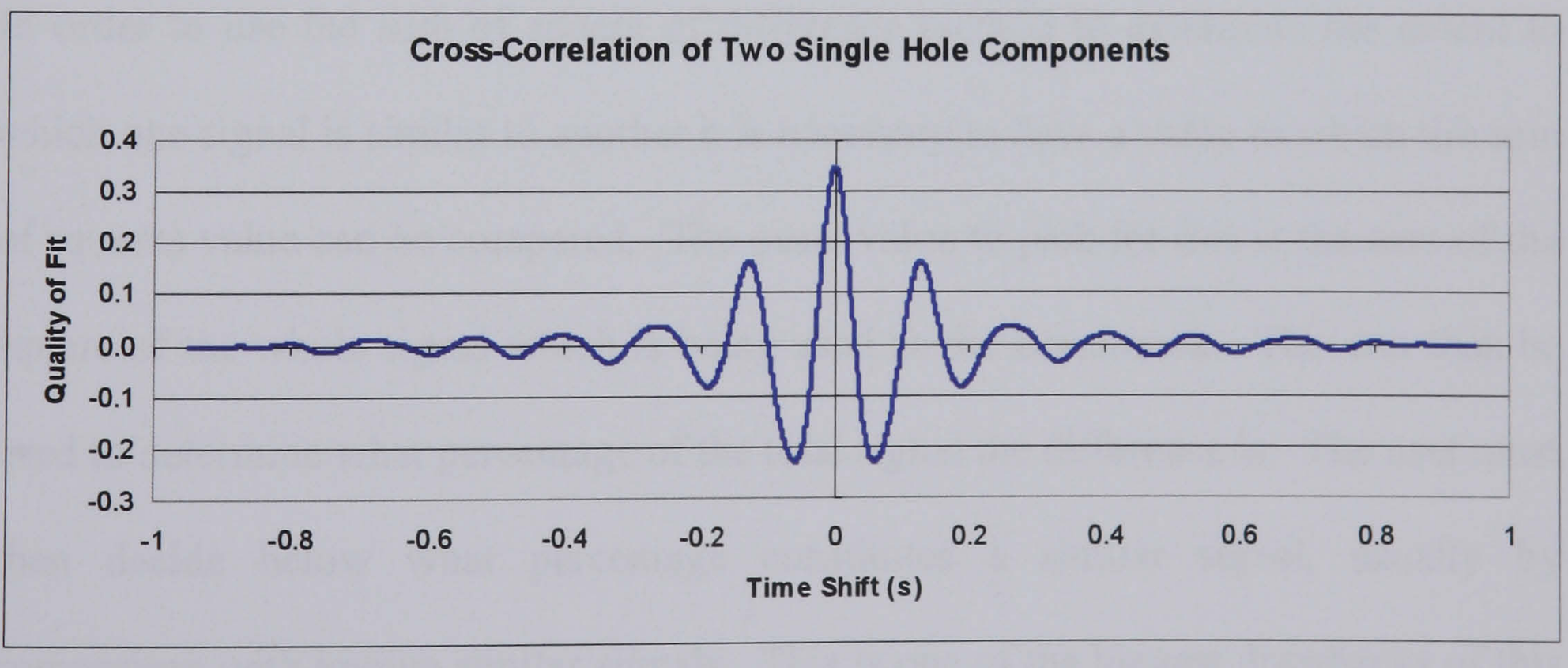

Figure 5.1 Cross correlation of two single hole blast vibration recordings.

deviation on a point by point basis. The line of which the sum of squares of error is a minimum will then be selected as a best fit.

It is necessary to use the sum of the square of the difference, rather than just the sum of the difference, as if the random scatter follows a Gaussian distribution, it is far more likely to have two medium size deviations (say 5 units each) than to have one small deviation (1 unit) and one large (9 units). A procedure that minimized the sum of the absolute value of the distances would have no preference over a line that was 5 units away from two points and one that was 1 unit away from one point and 9 units from another. The sum of the distances (more precisely, the sum of the absolute value of the distances) is 10 units in each case. A procedure that minimizes the sum of the squares of the distances prefers to be 5 units away from two points (sum-of-squares = 25) rather than 1 unit away from one point and 9 units away from another (sum-of-squares = 82). If the scatter is Gaussian (or nearly so), the line determined by minimizing the sum-of-squares is most likely to be correct.

In order to use the sum of square of difference method to determine the extent to which one signal is similar to another it is necessary to have a value to which the sum of squares value can be compared. The usual value to pick for this is the sum of the square of the whole signal which is being used as the benchmark. This can then be used to determine what percentage of the total signal the difference is. The user must then decide below what percentage constitutes a similar signal, usually by comparison with known similar signals. This is one of the biggest drawbacks of this system. Even though it gives a quantative measure of fit it relies on a subjective measure as a calibration.

The other drawback of this system is the fact that it compares the signals point by point. This means that if the signals are out of synchronisation then the sum of square or errors can be huge. For example if you consider two identical sine waves, one 180 degrees out of phase with the other, the resulting percentage error will be 200% This is of course an extreme case but even small amounts of error in the time-base can lead to otherwise similar signals being classified as dissimilar.

5.3 Development of systems to compare single hole blast data

Existing methods of comparison of waveforms have been shown to be inappropriate for use with the single hole blast data that has been recorded.

In order to analyse the data recorded from the single hole test shots two methods were developed to give a quantative measure of similarity. The first is an approach based on the signal processing techniques using a technique which would otherwise be redundant in a novel manner which allows it to be used with success. The second approach is a statistical method which uses the physical shape of the waveform to generate a ranking system which can then be analysed and the probability of similarity determined.

5.3.1 Cross-correlation /autocorrelation method

It has already been shown that the cross-correlation function alone is not suitable for use in determining whether the single hole blast vibration waveforms are similar. A technique has been developed which uses the cross-correlation function along with a scaling system and the autocorrelation function. The autocorrelation function is similar to the cross-correlation function except that it compares a signal with itself rather than with another signal. Essentially, it gives a measure of the extent to which a signal correlates with a displaced version of itself. The autocorrelation of a function $f_x(t)$ is defined by the equation:

$$R_{xx}(\tau) = \lim_{T \to \infty} \frac{1}{T} \int_{-T/2}^{T/2} f_x(t) \cdot f_x(t+\tau) dt \qquad (5.3)$$

It can be clearly seen how this equation relates to the cross-correlation function, equation 5.1.

The basis of the technique is to simplify the signal under study and therefore remove many of the minor differences which increase the probability of the signals being found as dissimilar. The simplified signals can then be scaled and compared.

To illustrate the technique, consider two signals $f_x(t)$ and $f_y(t)$ where $f_x(t)$ is the benchmark signal, and $f_y(t)$ is the signal under test. If the autocorrelation $R_{xx}(\tau)$ of $f_x(t)$ is scaled by dividing through by the root of the sum of the square of

$f_x(t), \sqrt{\sum f_x(t)^2}$,a scaled representation of the correlation of the signal to itself is given. If the non-normalised cross-correlation $R_{xy}(\tau)$ of $f_x(t)$ and $f_y(t)$ is then divided through by the root of the sum of the squares of $f_y(t)$, a scaled representation of the correlation of $f_y(t)$ to $f_x(t)$ is given. Now if the signals were similar then the scaled $R_{xx}(\tau)$ should be similar to the scaled $R_{xy}(\tau)$. Therefore if the normalised cross-correlation of $R_{xx}(\tau)$ and $R_{xy}(\tau)$, $R_{xxxy}(\tau)$ is examined, there should be a high level of correlation. To ensure that the correlation is constant the operation should be repeated using $f_y(t)$ as the benchmark signal and $f_x(t)$ as the signal under test. The two results can then be averaged to give an indication of correlation of the signals to each other.

This system works as the complexity of the signals is decreased by comparing the autocorrelation to the cross correlation. To allow the signals to be directly compared they are divided through by a scaling factor which is proportional to the energy in the system.

Using this system on the same signals shown in Figure 5.1 yields a final cross-correlation factor of approximately 0.8 which shows, as expected a very strong correlation between the signals. The results for these signals are shown in Figure 5.2.

This system is highly effective in determining similarity in signals which may have slight differences but which would cause errors in other techniques. Blast vibrations will never be exactly the same no matter how similar the conditions under which the

blast is fired therefore this technique is well suited to determining similarity between them.

5.3.2 Statistical analysis of similarity between holes using Kruskal-Wallis test

In looking for a method to reliably determine similarity between signals many options were looked at. As has already been seen a method using signal processing techniques has been developed and used with success. However, another technique was also developed based on statistical analysis of the waveform, which gives a probability of similarity based on the Kruskal-Wallis test.

The Kruskal-Wallis test is a one-way analysis of variance method which can be used to test the hypothesis that a number of unpaired samples originate from the same population. West *et al.* (2001) give a good account of this test and its application to detecting similarity between tomograms of flow in pipes.

To use the Kruskal-Wallis test a ranking system must be applied to the signals. This was done by splitting the signals into sections and ranking each section according to the energy content of each slice. The energy of each slice is given by the sum of the square of the signal in each slice.

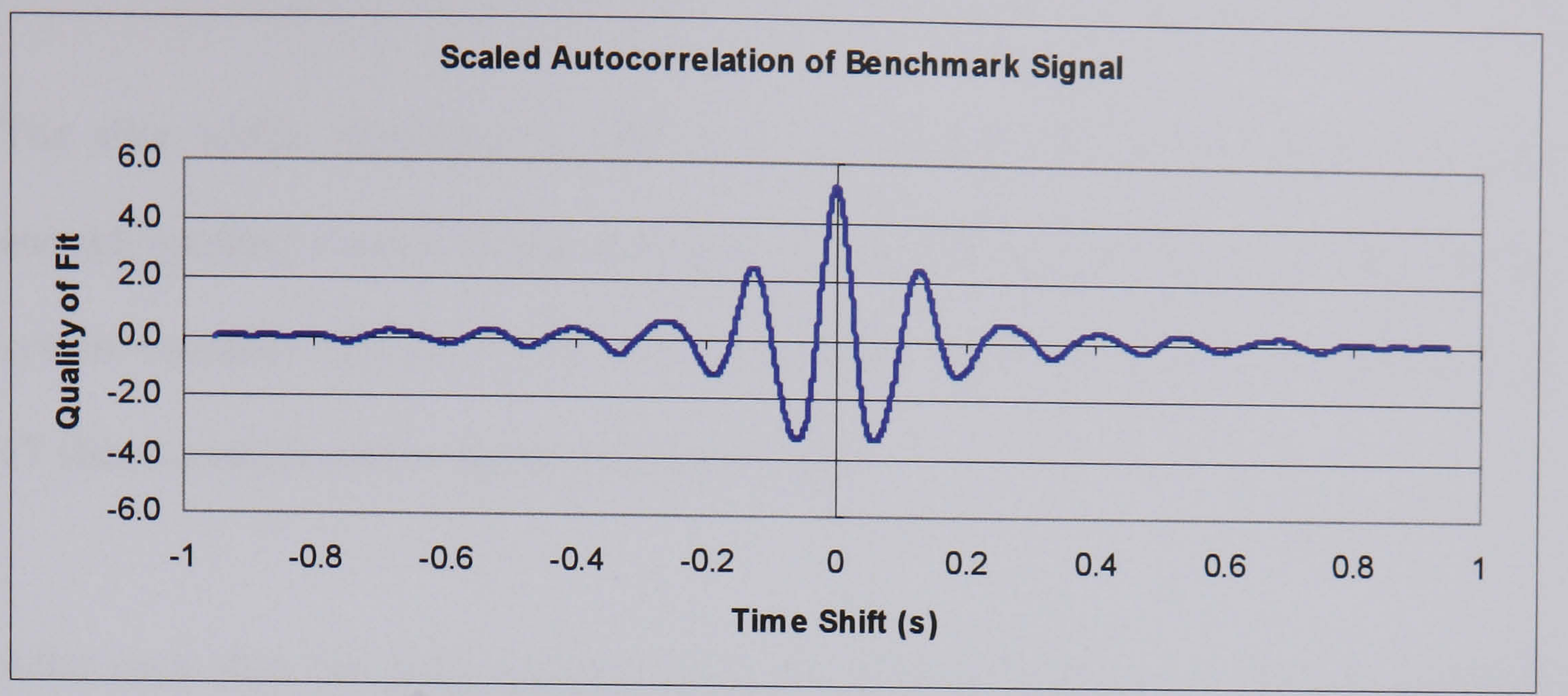

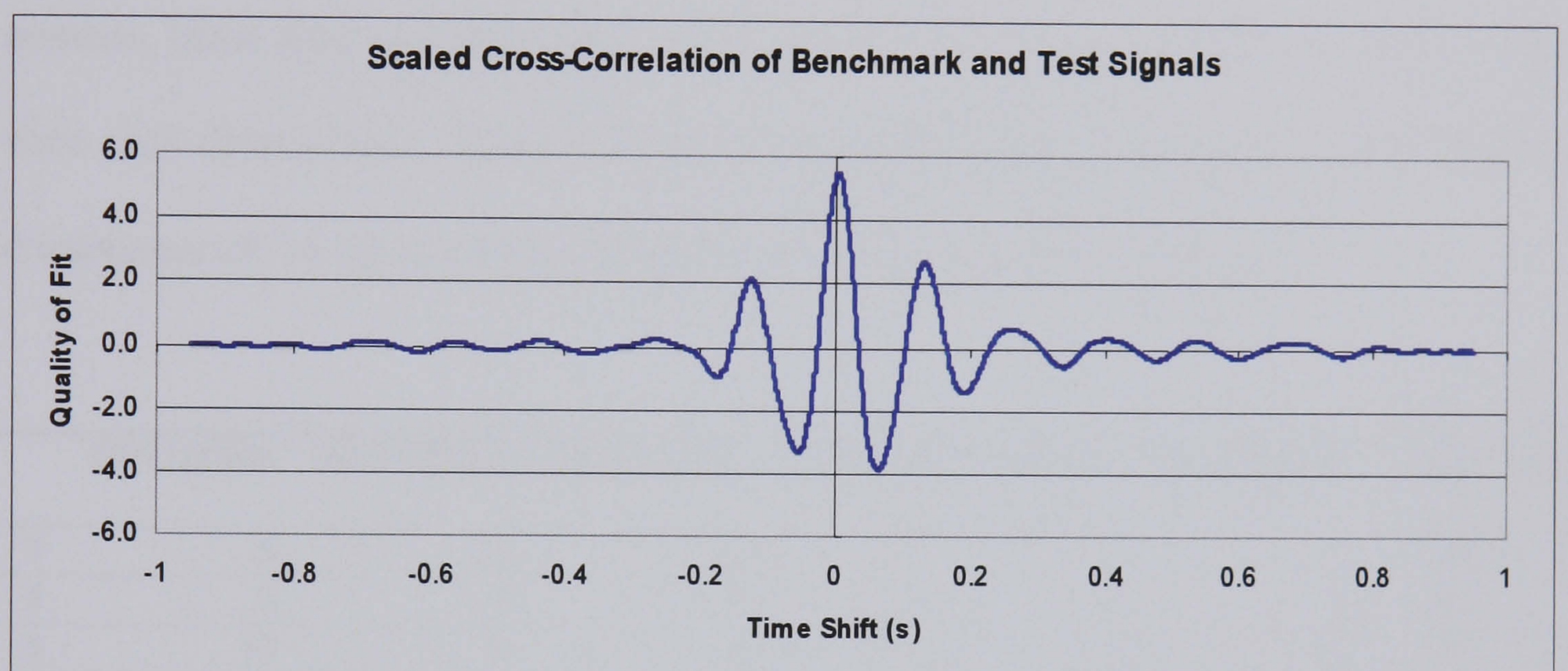

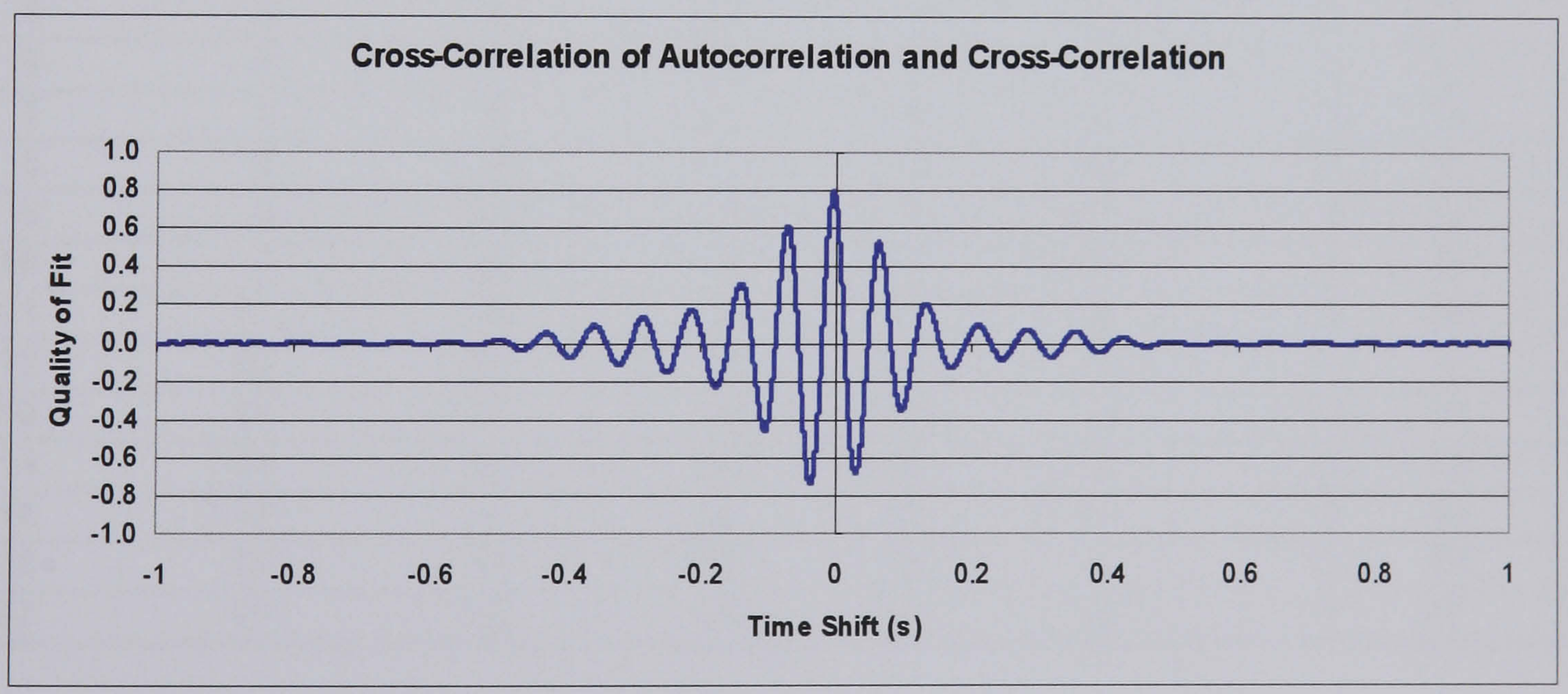

Figure 5.2 Results of autocorrelation/cross-Correlation system using signals shown in figure 5.1

The slice width, although not crucial to the system, was chosen to give a large enough number of slices to give a reliable result without having so much data that the system becomes difficult to use. The slice width chosen was 30ms giving a total of 17 slices over the entire signal length of 510ms.

After each slice has been assigned a rank they are collated into a table of the slice number, blast date and slice rank. Each slice is then given a total and the average slice rank determined. Table 5.1 shows the results from the ranking of the vertical component of the signals recorded at the site office monitoring point.

	08/11/1999	29/11/1999	15/12/1999	17/04/00 - 1	17/04/00 - 2	21/07/2000	Total	Average
1	9	5	8	5	7	5	39	6.50
2	8	3	4	4	4	4	27	4.50
3	10	1	1	1	1	2	16	2.67
4	2	2	2	2	3	1	12	2.00
5	3	4	5	3	2	12	29	4.83
6	5	7	10	8	5	6	41	6.83
7	1	6	3	6	6	3	25	4.17
8	6	9	11	13	16	10	65	10.83
9	4	11	7	9	11	9	51	8.50
10	7	8	6	7	13	7	48	8.00
11	11	16	9	10	10	8	64	10.67
12	13	15	12	12	8	11	71	11.83
13	12	17	16	11	9	14	79	13.17
14	14	14	14	15	12	13	82	13.67
15	16	13	13	14	14	16	86	14.33
16	15	10	15	16	15	15	86	14.33
17	17	12	17	17	17	17	97	16.17

Table 5.1 Ranking of the vertical signals recorded at the site office monitoring point for use with Kruskal –Wallis test.

Once all the data has been collated a null hypothesis is set up:

H_0 = No similarity between wave shapes

H_1 = There is a pattern of energy distribution between blasts

This is then tested by using Friedman's test (Friedman, 1937). This gives an index *W* of the form:

$$W = \frac{12}{Nk(k+1)} \sum_{j=1}^{k} R_j^2 - 3N(k+1) \qquad (5.4)$$

Where *N* is the number of data sets

k is the number of slices in each data set

R_j is the sum of the ranks for each slice

The index W will then be distributed as chi-squared with *k*-1 degrees of freedom.

This technique is a straightforward way of getting statistical proof that a set of single holes are all similar, however, it can only be used to determine the extent of similarity that exists within a whole set of data. It cannot be used to determine to what extent one signal is similar to another.

In this case only a small dataset will be analysed and so it is possible to analyse each signal separately. For this reason the Kruskal-Wallis test will not be used to analyse

the data. If a larger data set was to be analysed, however, this technique would be a good way of quickly determining if the signals were similar or not.

5.4 Results of comparison of single hole test shots

To determine whether a single hole test shot is repeatable a series of six test shots were fired in the same area of a quarry and the resulting vibration recorded at a fixed monitoring point. In order to analyse the data a new technique which disregards minor differences in wave shape has been developed.

Figures 5.3, 5.4 and 5.5 show all the vertical, radial and transverse vibration velocity traces respectively. Visual inspection clearly shows that most blasts share some similar features although it cannot be said just from inspection that all the signals are similar to each other.

To determine the extent of the similarity between the signals the cross-correlation/autocorrelation method detailed above was employed. Each signal was correlated against all others obtaining a series of five results for each hole. Tables 5.2, 5.3 and 5.4 give a summary of the results of the vertical, radial and transverse cross-correlation/autocorrelation tests respectively.

The data given in tables 5.2, 5.3 and 5.4 is difficult to interpret as there are several results for each signal which do not give a definite result as to whether the signals are similar or not.

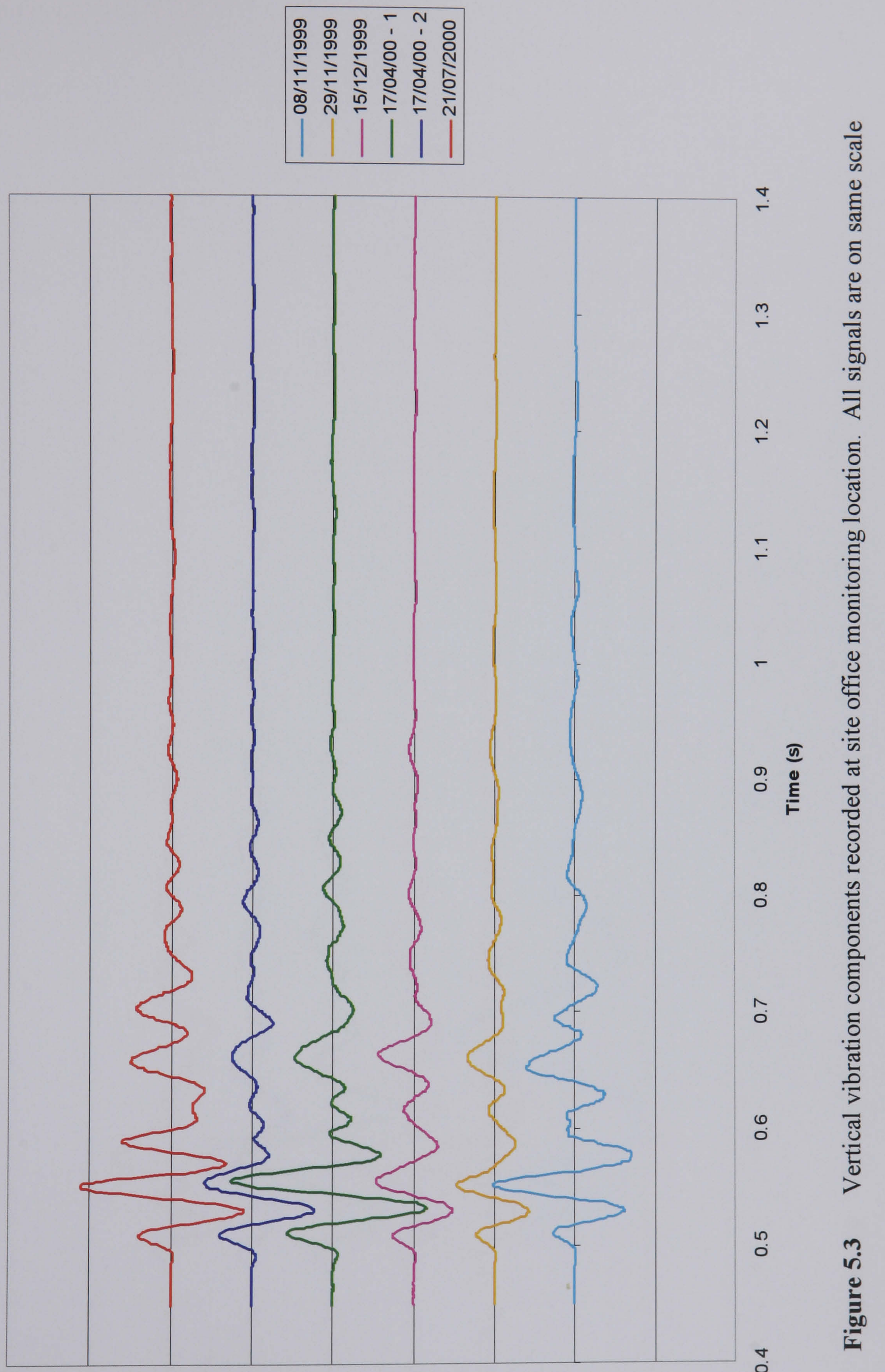

Figure 5.3 Vertical vibration components recorded at site office monitoring location. All signals are on same scale

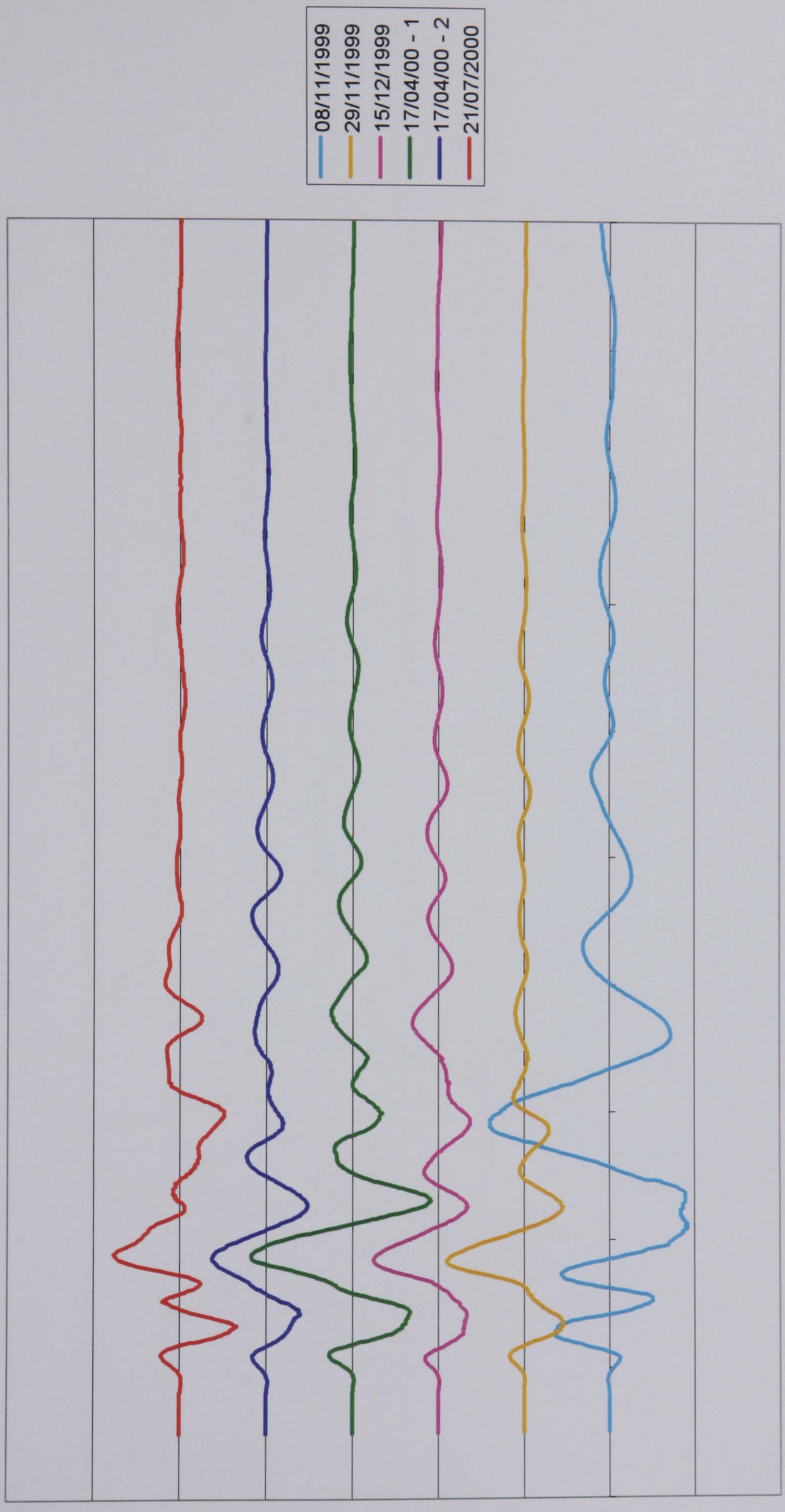

Figure 5.4 Radial vibration components recorded at site office monitoring location. All signals are on same scale

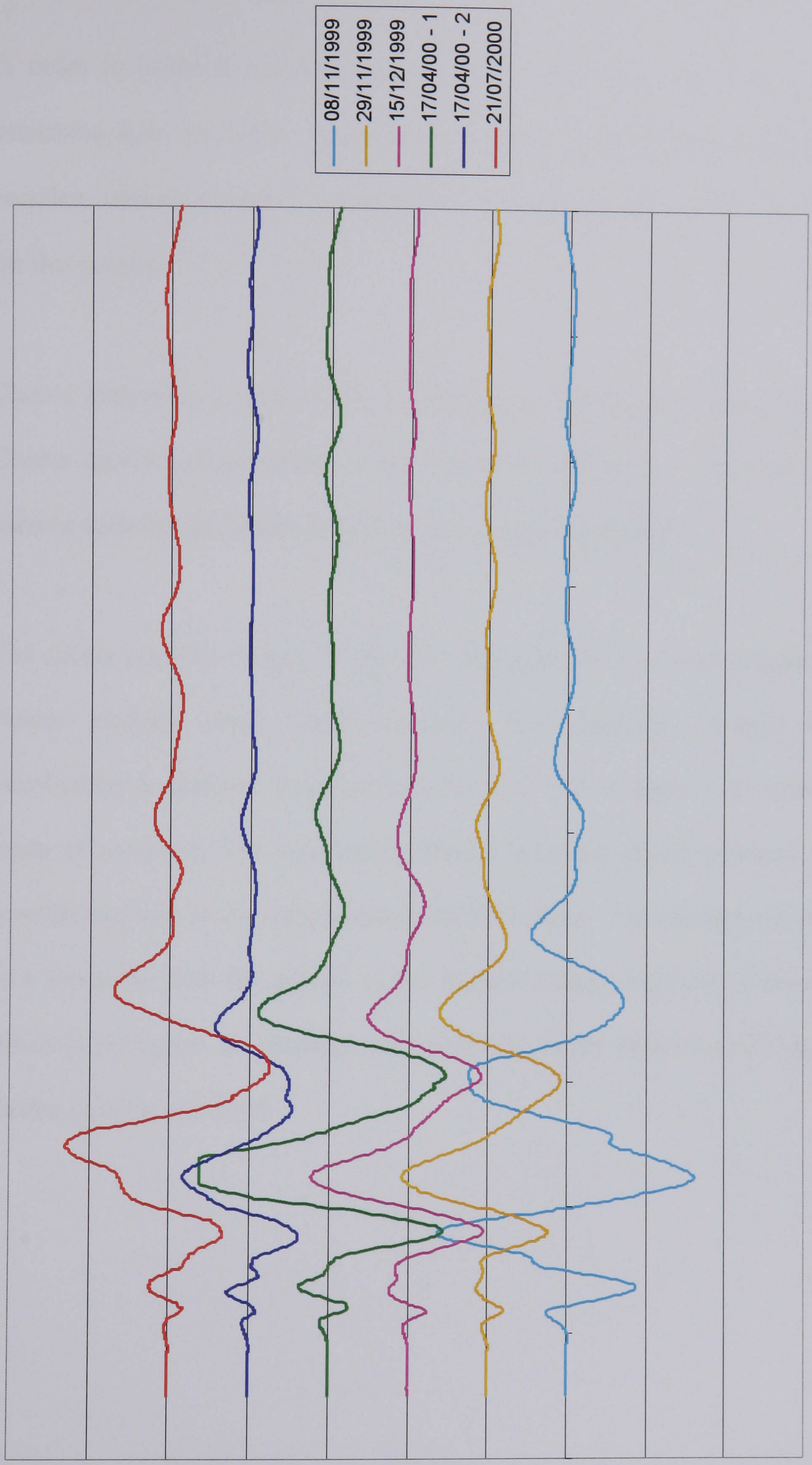

Figure 5.5 Transverse vibration components recorded at site office monitoring location. All signals are on same scale

In order to interpret the data given in tables 5.2, 5.3 and 5.4 it is necessary to determine how the results relate to each other, i.e. to what degree do the signals correlate with each other. A technique known as cluster analysis can be employed for this purpose.

Cluster analysis is a multivariate procedure for detecting natural groupings in data. Cluster analysis classification is based upon the placing of objects into groups in a manner such that the relationship between groups is revealed.

The cluster analysis chosen for use with this application is an ascendant hierarchical cluster analysis using Ward's method. This essentially means that cluster membership is assessed by calculating the total sum of squared deviations from the mean of a cluster. The criterion for fusion is that it should produce the smallest possible increase in the sum of squares of difference. The clusters are then arranged in a hierarchy with the groups of the highest mutual similarity placed at the top. White (1987) gives an excellent description of cluster analysis and its application if further reading is desired.

Benchmark Signal

Test Signal	08/11/99	29/11/99	15/12/99	17/04/01-1	17/04/01-2	21/07/00
08/11/99	1	0.8745	0.8915	0.8708	0.80555	0.8911
29/11/99	0.8745	1	0.9755	0.88475	0.92135	0.6766
15/12/99	0.8915	0.9755	1	0.89105	0.93665	0.7787
17/04/01-1	0.8708	0.88475	0.89105	1	0.95525	0.85455
17/04/01-2	0.80555	0.92135	0.93665	0.95525	1	0.8002
21/07/00	0.8911	0.6766	0.7699	0.85455	0.8002	1

Table 5.2 Results of cross-correlation/autocorrelation of vertical component of vibration signals recorded at site office monitoring point.

Benchmark Signal

Test Signal	08/11/99	29/11/99	15/12/99	17/04/01-1	17/04/01-2	21/07/00
08/11/99	1	0.57975	0.53905	0.5597	0.34995	0.7683
29/11/99	0.57975	1	0.9158	0.9308	0.9021	0.76975
15/12/99	0.53905	0.9158	1	0.93095	0.9512	0.7787
17/04/01-1	0.5597	0.9308	0.93095	1	0.9601	0.58275
17/04/01-2	0.34995	0.9021	0.9512	0.9601	1	0.544
21/07/00	0.7683	0.76975	0.70815	0.58275	0.544	1

Table 5.3 Results of cross-correlation/autocorrelation of radial component of vibration signals recorded at site office monitoring point.

Benchmark Signal

Test Signal	08/11/99	29/11/99	15/12/99	17/04/01-1	17/04/01-2	21/07/00
08/11/99	1	-0.9451	-0.8834	-0.8987	-0.8492	-0.9089
29/11/99	-0.9451	1	0.9861	0.9754	0.9731	0.9721
15/12/99	-0.8834	0.9861	1	0.9848	0.9829	0.7787
17/04/01-1	-0.8987	0.9754	0.9848	1	0.9359	0.9829
17/04/01-2	-0.8495	0.9731	0.9829	0.9359	1	0.9380
21/07/00	-0.9089	0.9721	0.9613	0.9829	0.9380	1

Table 5.4 Results of cross-correlation/autocorrelation of transverse component of vibration signals recorded at site office monitoring point.

The cluster analysis was carried out via a computer spreadsheet and cluster dendrograms of the results obtained. These are shown in figures 5.6, 5.7 and 5.8.

The dendrograms give an indication of the relationships between the signals. The dendrogram is scaled by an index of dissimilarity. This means that the index value increases as the similarity between clusters decreases.

Figure 5.6 shows that there is a high level of similarity within the vertical components of all the single hole blasts. This confirms the assumption that similarly loaded and fired single holes produce similar vibration waveforms, i.e. single holes are reproducible.

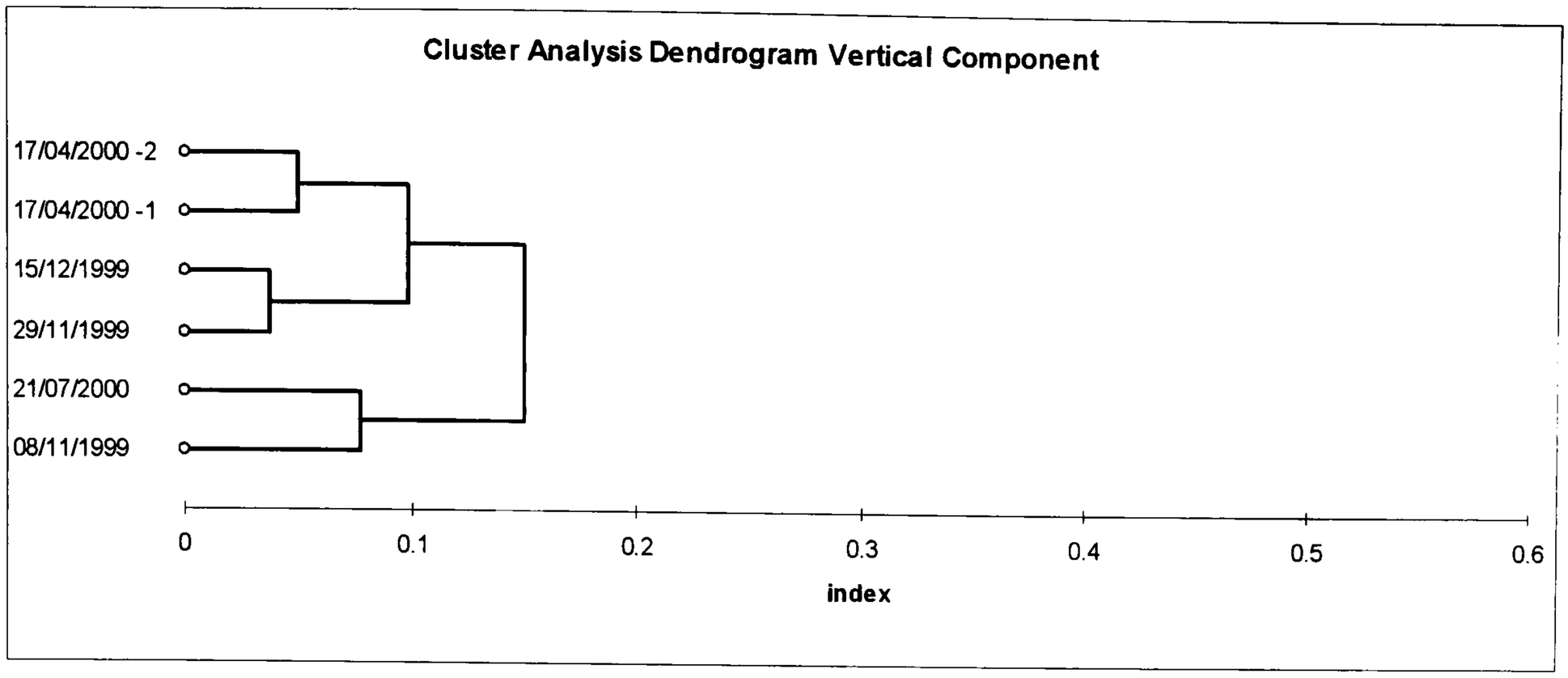

Figure 5.6 Cluster dendrogram showing relationships of correlation coefficients for vertical component of recorded waveforms.

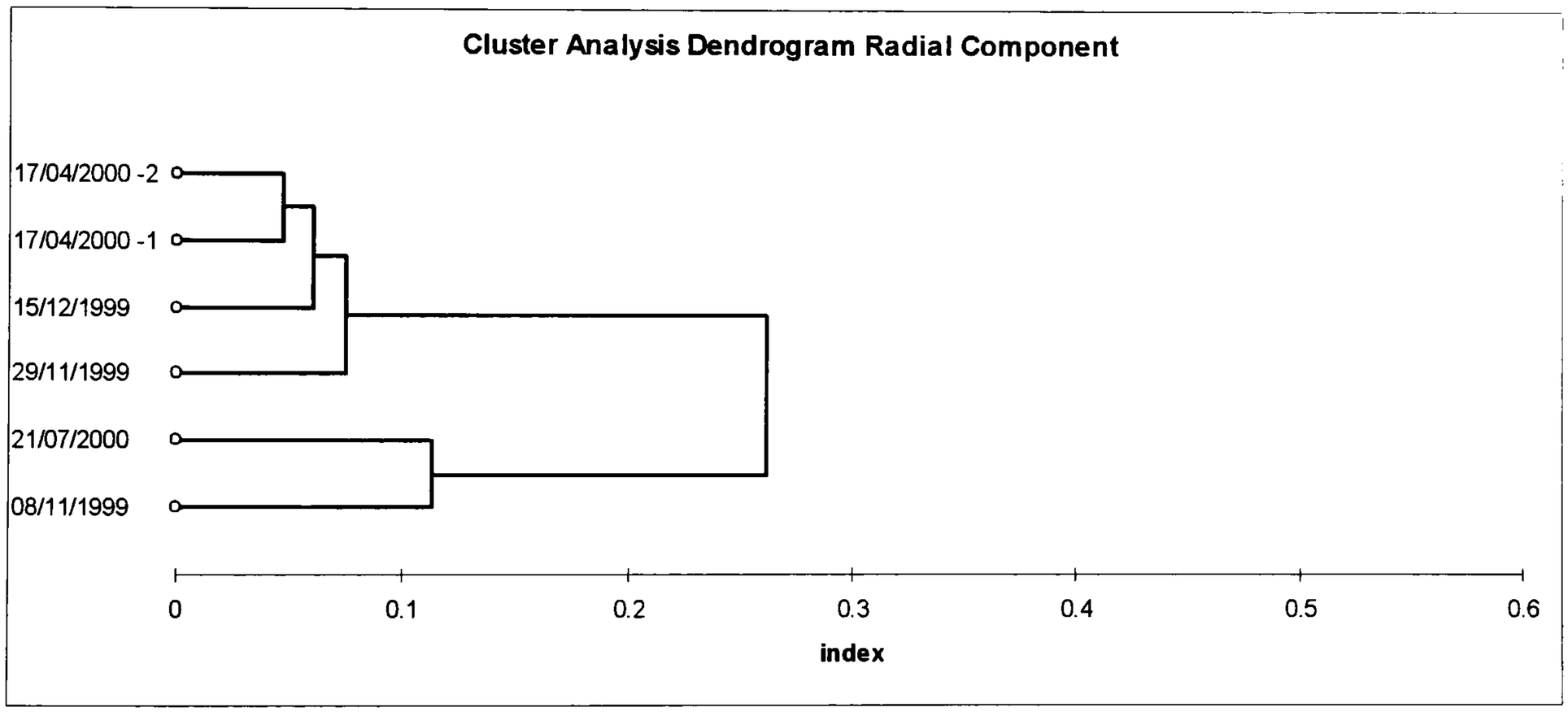

Figure 5.7 Cluster dendrogram showing relationships of correlation coefficients for radial component of recorded waveforms.

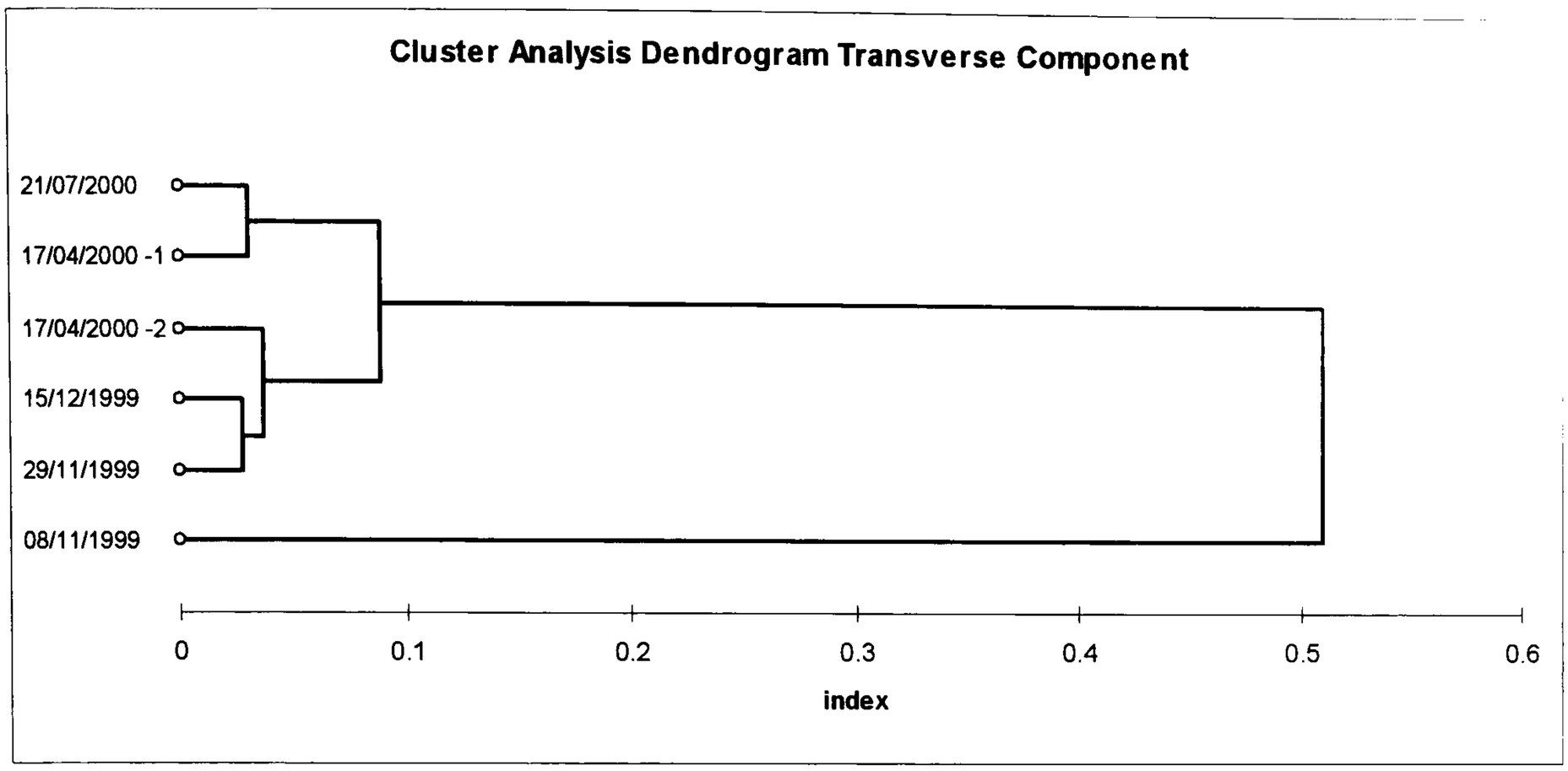

Figure 5.8 Cluster dendrogram showing relationships of correlation coefficients for transverse component of recorded waveforms.

Figure 5.7, however, shows a distinct dissimilarity between the radial component of the two blasts recorded on the 8th November 1999 and the 21st July 2000, and the other four blasts. The blast recorded on the 21st July was double decked and was partly expected to provide a different waveform than those from the other blasts. The blast recorded on the 8th November, however, was very similar in design to the first blast recorded on the 17th April 2000 but there is a small measure of similarity shown in the dendrogram. If one refers to figure 4.16 it can be seen that the waveform recorded on the 8th November appears to have similar features but slightly delayed by an extra feature at the front of the signal. The blast recorded on 21st July has a feature that is clearly caused by the decking of the charge. If one compares it to the four blasts which have a high level of similarity it can be seen that where these four have a single large peak at around 0.6 seconds, the blast from the 21st August has a stepped peak, with two smaller features most probably caused by the individual

decks detonating. If the time between the two smaller peaks is examined it is approximately 25ms which corresponds to the time between decks.

The largest measure of dissimilarity is shown in figure 5.8. The blast recorded on the 8th November 1999 is clearly very different from the other five blasts which all show a reasonably high level of similarity. Looking at figure 5.5 it can be seen that the signal does appear to be very different to the other five blasts. If we refer to table 5.4 the correlation factors for the blast on the 8th November all appear to be in the range of -0.8 to -1. This shows a high negative correlation implying that the signal may be an inversion of the other five.

To examine whether the signal actually was inverted each value in the signal was multiplied by -1, and compared to the other five signals using the autocorrelation/cross-correlation method. Figure 5.9 shows the inverted signal along with the other 5 signals non-inverted. Table 5.5 shows the results of the autocorrelation/cross correlation comparison method.

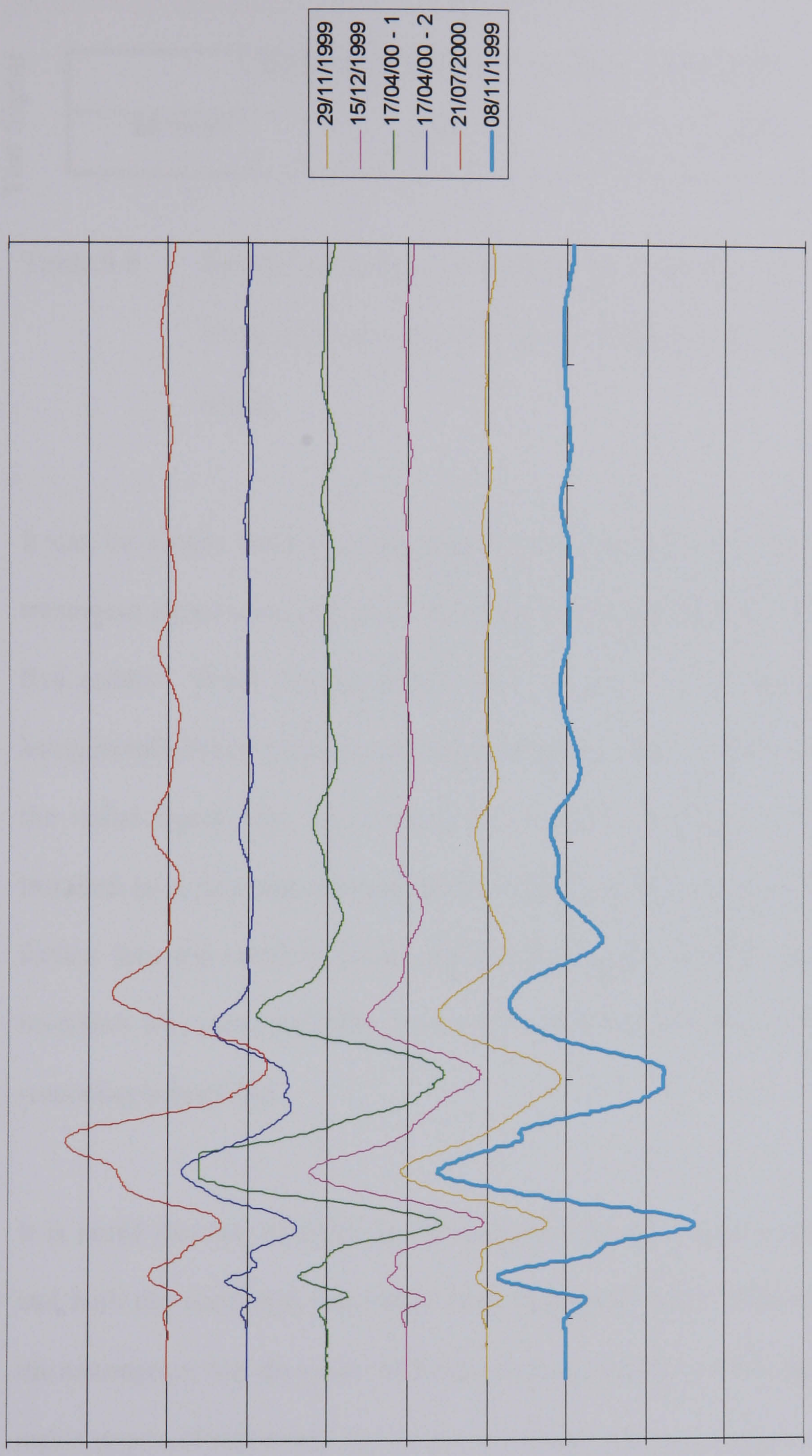

Figure 5.9 Transverse vibration components recorded at site office monitoring location. 08/11/1999 has been inverted

Benchmark Signal

Test Signal

	08/11/99	29/11/99	15/12/99	17/04/01-1	17/04/01-2	21/07/00
08/11/99	1	0.9451	0.8834	0.8987	0.8492	0.9089

Table 5.5 Results of cross-correlation/autocorrelation of inverted transverse component of vibration signal recorded on 08/11/99 with all other test blasts.

It can be clearly seen from the results shown in table 5.5 and figure 5.9 that the transverse signal recorded on 8th November 1999 is indeed an inversion of the other five results. When first examined this inversion was put down to the equipment being installed incorrectly even though it had been thoroughly checked. However, as the radial signal was not inverted as would be expected if the equipment was installed in a reversed manner, some doubt was cast on this theory. Only when further into the research when new findings came to light was the fact that this inversion was most probably a real phenomenon accepted. Chapter 7 details the reasoning behind this.

It is noted that the vibration in the vertical direction seems to be highly repeatable and both the transverse and radial have displayed major differences. This leads to the assumption that the major differences occur mainly in body waves as they are the major source of transverse and radial movement whereas surface waves are primarily Raleigh waves. As body waves are of less importance in the far field this could

explain the reported success of linear superposition in the far field and its apparent failure in the near field.

It is also interesting to note that the blasts which were designed to be as similar as possible in their design, which would be expected to show the highest levels of similarity in the vibration waveforms produced do not always show this. It has already been shown that the signal recorded on the 8th November 1999 was very different to all the others even though it was designed to be as near identical to the first blast on 17th April 2000 as possible. The blasts recorded on the 29th November 1999 and 15th December 1999, however, were also designed to be as similar as possible. As would be expected these two blasts show the highest correlation of any group in the vertical and transverse components. However in the radial component the signal recorded on the 15th December correlates more strongly to both signals recorded on the 17th April. These are very different in design to that recorded on the 15th December and, indeed, each other.

5.5 Conclusions on the repeatability of single holes

Techniques have been developed to allow the analysis of the similarity between vibration waveforms generated by blasting.

Using these techniques a series of six single hole test shots were analysed. The results showed that the majority of vibration signals generated by similarly designed single holes show high correlation in wave shape.

However, not all signals generated were identical. It has been shown that out of the series of six holes one signal was significantly different to the other five in both the transverse and radial components. This difference appears in the form of an inversion of the phase of the signal. This inversion appears to be limited to the body waves due to being only in the transverse and radial directions and so will become less noted in the far field.

It is clear that in the near field not all similar single hole shots produce a similar vibration waveform. This lack of repeatability will hamper any attempt to use hybrid modelling in the near field.

6. FACTORS AFFECTING VIBRATION LEVELS GENERATED BY SINGLE HOLE SHOTS.

It is well known that charge weight per delay and the delay between holes will have a significant effect on the vibration level generated by a production shot (Langefors and Kihlstrom, 1978, Dowding, 1985). What is less clear is the effect that other parameters such as burden and confinement can have on vibration levels and which parameters affect the vibration generated by a single hole in a shot.

6.1 Previous work on factors affecting vibration.

Rosenthal and Morelock (1987) looked at many factors which they thought could affect the vibration level generated by a production blast and produced a table of factors split into three results; significant, moderately significant and insignificant. Their results are reproduced in table 6.1.

It can be clearly seen from table 6.1 that Rosenthal and Morelock found few factors other than the charge weight per delay and the timing between holes which affect the vibration level by any significant amount. Of the four other factors they found to have an effect on the vibration level, two cannot be controlled with the single hole shot experiments that were intended to be carried out; the direction of initiation cannot be modified as there is only one hole to fire and the type of overburden cannot be changed as the tests are all to be carried out in the same part of a quarry.

This leaves burden and spacing, of which only the burden can be modified in a single hole blast

	Influence on ground motion		
Variable	Significant	Moderately significant	Insignificant
Charge per delay	X		
Delay interval	X		
Burden and spacing		X	
Stemming (amount)			X
Stemming (type)			X
Charge length and diameter			X
Angle of borehole			X
Direction of initiation		X	
Charge weight per blast			X
Charge depth			X
Bare vs. covered primacord			X
Charge confinement	X		
General surface terrain			X
Type and depth of overburden	X		
Wind and weather conditions			X

Table 6.1 Factors affecting ground motion (after Rosenthal and Morelock, 1987)

and charge confinement which can be modified and their effects studied.

Rosenthal and Morelock did not take into account the velocity of detonation (VoD) of the explosive or the number of free faces available when blasting.

Whitaker et al. (2001) realised that the VoD was an important factor and attempted to identify the effect that it, along with explosive column length, decked charges and explosive type had on blast vibration amplitude and frequency. They found that their results were very site specific, especially regarding decked charges which in some circumstances produced higher amplitude dominant frequencies than full column shots and in others did not. They also concluded that the VoD and explosive type had little effect on vibration amplitude or frequency. At large distances they found no parameters which had an effect on the vibration, thus concluding that the natural filtering system of the ground is the dominant factor. From their results they produced an updated version of table 6.1 detailing the factors they found to have the most influence on vibration levels. This is shown in table 6.2

Whitaker et al. disagree with Rosenthal and Morelock on several issues. They found that charge length and diameter does indeed have a moderately significant effect on the characteristics of ground motion affecting both the dominant frequency and the amplitude of the vibration. They also concluded that charge confinement, although a highly significant factor, was not as significant as the charge per delay or delay interval in affecting the vibration characteristics. The differences shown are most probably due to the location dependent nature of the results that Whitaker et al. reported.

Parameters	Most Significant	Moderately Significant	Insignificant
Explosive per detonation	X		
Delay	X		
Detonator precision	X		
VOD scatter	X		
confinement	X		
stemming		X	
Charge length	X		
Charge decoupling	X		
Angle of borehole		X	
Direction of initiation	X		
Total charge weight		X	
Shot duration	X		
Charge depth		X	
Bare vs covered detonation cord		X	
Electric vs non electric		X	
Surface terrain	X		
Overburden type	X		
Ground structure	X		
Atmospheric conditions		X	

Table 6.2 Factors affecting ground motion (after Whitaker et al. 2001)

Blair and Jiang (1995) showed that if one attempted to simulate blast vibration without accounting correctly for the VoD and the number of free faces then the vibration levels can be drastically overestimated. Mckenzie et al. (1995) also found that by neglecting the VoD in a blast vibration model could lead to an overestimation of the true vibration level. These findings clearly point to the fact that VoD will have a bearing on blast vibration amplitude.

Whilst it is commonly agreed upon that charge weight per delay is the factor with the greatest effect on vibration levels generated by a single shot hole for a given location, this will be governed more by bench height and geology than anything else and so will remain more or less constant. For specific locations other, often commonly overlooked, variables could possibly make a significant difference to vibration levels.

6.2 Determination of the factors affecting the vibration levels from single hole test shots.

The single hole test shots carried out in this research were designed so that the parameters which affect the vibration level could be determined. From previous literature the five parameters which were deemed to be the most important to study were:

i) Charge weight.

ii) Burden

iii) Number of free faces

iv) Number of decks

v) Velocity of detonation.

In order to be able to relate these five parameters to the peak particle velocity a method of determining the extent to which each individual parameter affects the PPV is required. It should be noted that no rock parameters have been taken into account as the model is being tested in a very localised area of the quarry. The rock is therefore assumed to be homogenous and the structure does not change between test shots.

6.2.1 Multiple regression

The purpose of multiple regression is to determine the relationship between several independent variables and a criterion variable. The basic principle is the same as that for linear regression which was briefly mentioned in Chapter 1. Instead of a regression equation with a single X variable a multiple regression equation is used. This takes the form

$$Y' = A + \beta_1 X_1 + \beta_2 X_2 + \ldots \beta_k X_k \qquad (6.1)$$

Where Y is the criterion variable

A is the intercept parameter

β are regression coefficients

X are the independent variables

One wishes to find the values of A, β_1, $\beta_2 \ldots \beta_k$ that will result in the highest possible correlation coefficient, R, between the observed values of Y and the predicted values Y'.

Multiple regression is advantageous over other methods of analysing data such as analysis of variance in that it allows the determination of the contribution of each independent variable in a model by allowing for partitioning of variance. In other words it is possible to determine how much variance in the criterion variable is accounted for by a specific independent variable. Therefore, in attempting to fit a model to a set of data we may proceed in either of two basic ways:

i) Start with a model that contains all available candidates as independent variables then simplify the model by discarding candidates that do not contribute to explaining the variability in the criterion variable; or

ii) Start with a simple model and elaborate on it by adding additional candidates.

In either case one will wish to compare a "full model" to a "reduced model", following the usage introduced by Bottenberg & Ward (1963). If the difference in variance explained is negligible one will prefer the reduced model and may consider simplifying it further. If the difference is large enough to be interesting one suspect the reduced model to be oversimplified and will prefer the full model. One may then

wish to consider an intermediate model or a model even more elaborate than the present full model.

6.2.2 Application of multiple regression analysis

The data collected from the single hole blasts is given in table 6.3. This data will be used as the basis of the multiple regression analysis. The charge weight has been adjusted to an ANFO equivalent.

Date	**8/11/99**	**29/11/99**	**15/12/99**	**17/04/00 -1**	**17/04/00 -2**	**21/07/00**
PPV (mms^{-1})	18.7	11.8	12.6	18.5	9.5	18.6
Charge weight (kg)	109	109	110	133	113	110
Burden (m^2)	58.03	52.22	52.32	73.10	50.00	82.5
VoD (ms^{-1})	3789	3948	3886	4104	3985	3954
Free faces	1	2	2	1	2	1
Decks	1	1	1	1	1	2

Table 6.3 Data collected from single hole shots to be used in multiple regression analysis.

The technique selected to refine the regression was to start with a full model and compare it with a reduced model by removing the independent variable which has the least effect on the regression. In this manner it should be possible to determine which parameters have the greatest influence on the PPV which is the criterion

variable. The regression analysis was carried using a computer spreadsheet, giving an answer in terms of coefficient estimates. Table 6.4 shows the results of the regression with all 5 independent variables.

Coefficient estimates			
Variable	**Coefficient**	**Std Error**	**t-ratio**
Charge weight	-0.081	0.367	-0.219
Burden	7.15	19.579	-0.194
VoD	0	0.036	0.002
Free faces	-3.132	16.129	0.121
Decks	1.128	9.303	0.365
R2 = 0.9232 R2b = 0.6161			

PPV = -0.081* Charge Weight + 7.15*Burden + 0*VoD - 3.1*Free Faces + 1.128*Decks

Table 6.4 Multiple regression analysis results for all five independent variables.

From this table the most important coefficient is the R2b which is the adjusted R value giving a measure of how well the equation explains the data. The t-ratio and standard error give an indication of each variables influence on the criterion variable.

It is clear from table 6.4 that the variable with the least influence is the velocity of detonation. The t-ratio is extremely low and the coefficient it has determined is zero. This would indicate that the VoD has no effect on PPV whatsoever. This may be misleading however, as there is a very small variance in the values of the VoD which

may artificially influence the regression. What can be surmised is that small differences in the VoD have no effect on the PPV generated. The VoD is therefore removed from the regression analysis and a reduced model is formed. The results of this are shown in table 6.5.

Coefficient Estimates

Variable	Coefficient	Std Error	t-ratio
Charge Weight	-0.08	0.14	-0.571
Burden	7.18	4.01	1.79
Free Faces	-3.106	1.678	-1.851
Decks	1.142	2.111	0.541

R2 = 0.9232 R2b = 0.808

PPV = -0.08* Charge Weight + 7.18*Burden - 3.106*Free Faces + 1.142*Decks

Table 6.5 Multiple regression analysis results for dataset with VoD removed.

It is clear to see that the reduced model is much improved. The R2b value has increased from 0.6161 to 0.808 indicating that the equation describes the linear relationship much more accurately. Looking at the t-ratios now it can now be seen that both charge weight and the number of decks have a smaller effect on the PPV than both burden and the number of free faces. It is a well established fact that this cannot be correct in general terms as the charge weight will quite obviously have a greater effect on the vibration level than any other parameters. Decking of charges is also well known to reduce vibration levels by reducing the instantaneous charge

weight. Removing either of these parameters from an equation which claims to model blast vibration magnitude would therefore be a bold move. What must be understood is that this is not a model to explain blast vibration in general terms. The idea of this part of the research was to determine the effect that various parameters had on blasting vibration generated by very similar holes, i.e. which parameters are the most sensitive and therefore will have a greater effect on the vibration generated by an individual hole in a production shot.

If decking is therefore removed from the equation it is not because it is considered an unimportant parameter in blasting but in this case other parameters have influenced the PPV more. If one refers to table 6.3 it can be seen that the decked blast on the 21st July 2000 has a similar charge weight and PPV to that on the 8th November 1999. Both blasts have one free face. The only differences between the blasts is a drastically increased burden and the decking. It is fair to suggest then that the increased burden has negated the effect of the decking. If another similar blast was fired with no decking and the increased burden one would expect to see a significantly increased PPV.

Table 6.6 shows the reduced model formed from the regression of a dataset containing only charge weight, burden and free faces as independent variables.

Coefficient Estimates			
Variable	**Coefficient**	**Std Error**	**t-ratio**
Charge Weight	-0.102	0.117	-0.87
Burden	8.148	3.318	2.597
Free Faces	-3.014	1.459	-2.065

R2 = 0.912 R2b = 0.8533

PPV = -0.102* Charge Weight + 8.148*Burden - 3.014*Free Faces

Table 6.6 Multiple regression analysis results for dataset with VoD and decks removed.

As can be seen the R2b coefficient has increased again indicating a better fit with the data.

It is plain to see by now that the two factors which affect the PPV the most are the burden and the number of free faces when the holes are very similar.

6.3 Conclusions

It has been found that in the case of similar blast holes where the range of charge weights is small the most important factors to consider will be the burden, number of free faces and the charge weight. It should be noted that no account of rock related parameters was taken and that these findings should not be assumed true for large variations in blast design.

These findings are important for the use of hybrid modelling as it is clear that for a single hole to be able to represent the vibration generated by each and every hole in a blast then the charge weights, burden and number of free faces must be kept identical. This could prove difficult as in a production blast the burden and free faces are changing constantly as each hole detonates and breaks the rock.

In order for hybrid modelling to be used with increased accuracy, the effect of these "dynamic" parameters must be examined. This will be studied in Chapter 7.

7. THE EFFECT OF DYNAMIC PARAMETERS WITHIN A TWO HOLE SHOT

7.1 Introduction

Chapter 6 detailed the large effect that the burden and the number of free faces has on the magnitude of vibration generated by a single hole shot. It is logical to assume that the same effects will be seen in a production blast. However, in a production blast the burden and the number of free faces are constantly changing. Figure 7.1 shows this effect as applies to free faces.

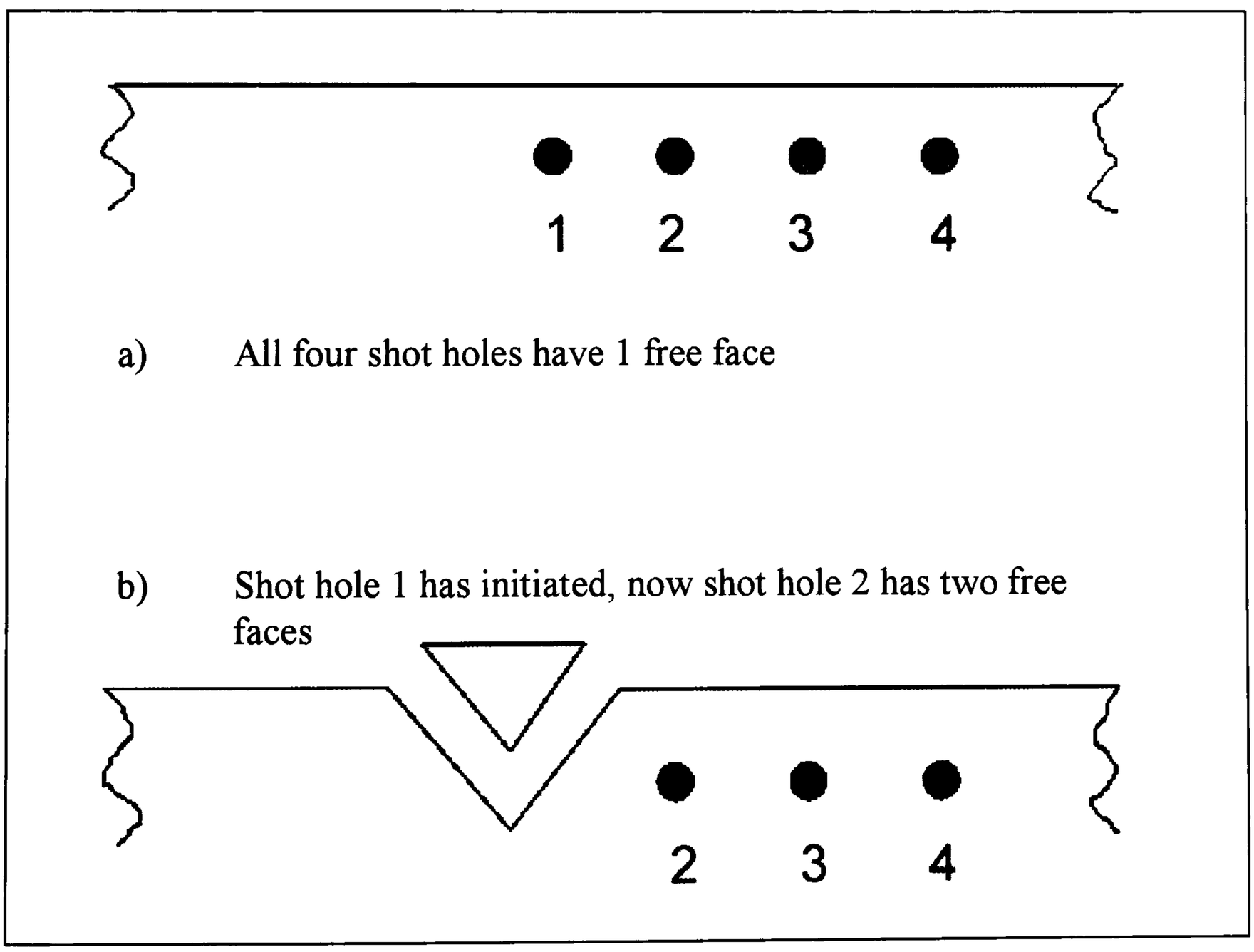

Figure 7.1 a) Shot holes all have one free face. b) After initiation of shot hole 1 shot hole 2 has two free faces.

Figure 7.1 (a) shows a typical small blast consisting of four holes all fired with one free face. If hole 1 is initiated it will create a new free face for hole 2. This means that hole 2 will have two free faces. The same will happen for holes 3 and 4. This is what is meant by the term dynamic - parameters which are constantly changing throughout the blast and cannot be easily quantified. In order to determine the effect that the dynamic parameters have on the waveform generated by a shot hole a series of experiments were devised.

7.2 Determination of the effect of dynamic parameters on the vibration waveform generated from each hole of a two hole shot in a limestone quarry.

To determine the effect of dynamic parameters on each hole of a production blast it was decided that an experiment would be carried out using a two hole shot with identically loaded holes. This would be fired along with a single hole shot which would be loaded identically. Both holes would be fired on straight faces with only 1 free face. As the first hole of the two hole shot will have no dynamic parameters to affect it, it may be possible to assume that it will be identical to the single hole shot. It has been shown in Chapter 5, however, that not all single hole shots produce the same vibration signal. This uncertainty can be minimised by comparison with the earlier recorded holes. Four out of five single decked holes gave near identical blast waveforms and so if the new single hole can be said to be near identical to those, it will be assumed to be identical to the first hole of a production blast. Once a single and a two hole shot have been fired and the vibration traces recorded it is possible to

remove the single hole vibration trace from the two hole so leaving what can be assumed to be the second hole of the shot. Comparison of this shot with the single hole shot will give an indication of the effect that dynamic parameters can have on the vibration trace.

7.2.1 Single hole shot

The single hole was recorded in exactly the same area of the same limestone quarry that had been used for the test work detailed in Chapter 4. The hole was drilled to a depth of 17.5 metres at an angle of 10 degrees and loaded with 50kg of emulsion and 78kg of hand mixed ANFO. The hole was bottom initiated using a 16L cast primer. Figure 7.2 shows the vibration traces generated by the blast as recorded at the site office monitoring point. In Chapter 5 it was concluded that the majority of similar single hole shots gave similar blast vibration waveforms. In order to assume that this single hole will be the same as the first hole in the two hole shot we can compare it to the previously recorded shots. Table 7.1 shows the results gained from the comparison technique described in Chapter 5.

It is clear to see from the high values obtained that the signal is very similar to the other test signals except for that recorded on 8th November 1999. The error associated with this signal has been detailed in Chapter 5 and is discounted. As the test signal recorded for this experiment correlates well with the other four single holes it can be assumed that it is suitable to simulate the first hole of the two hole shot.

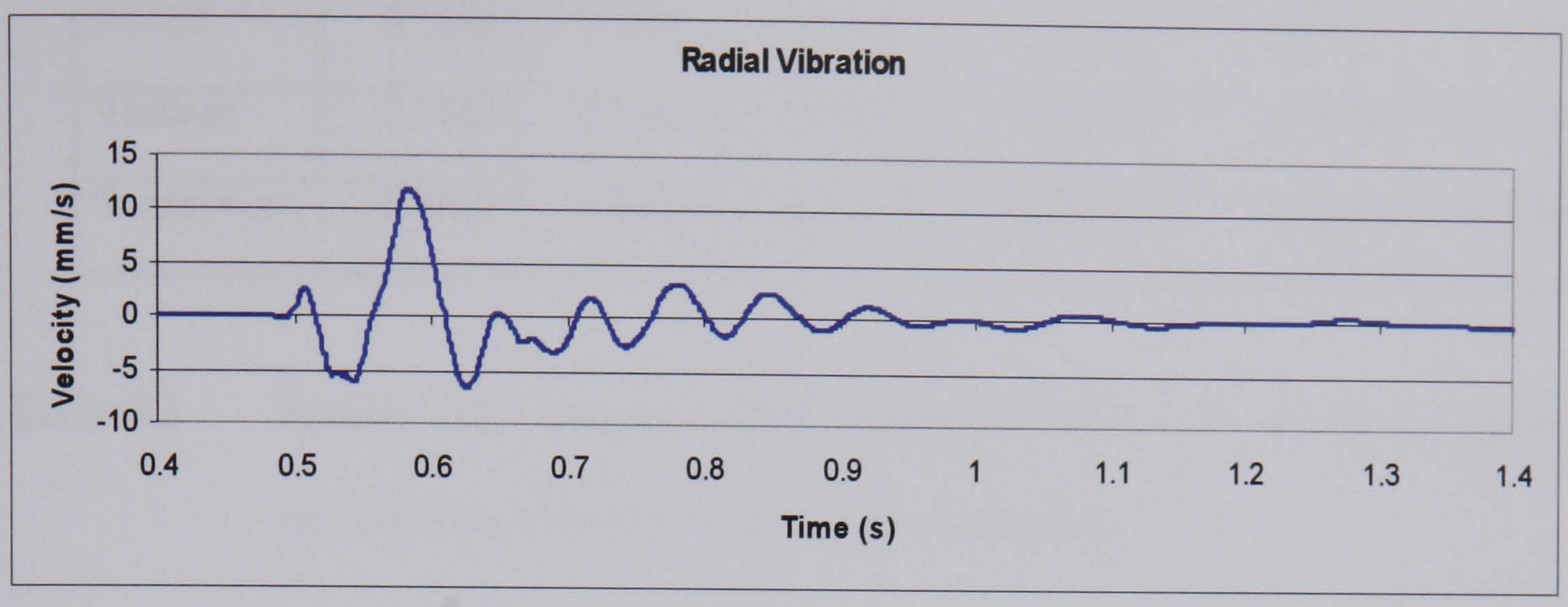

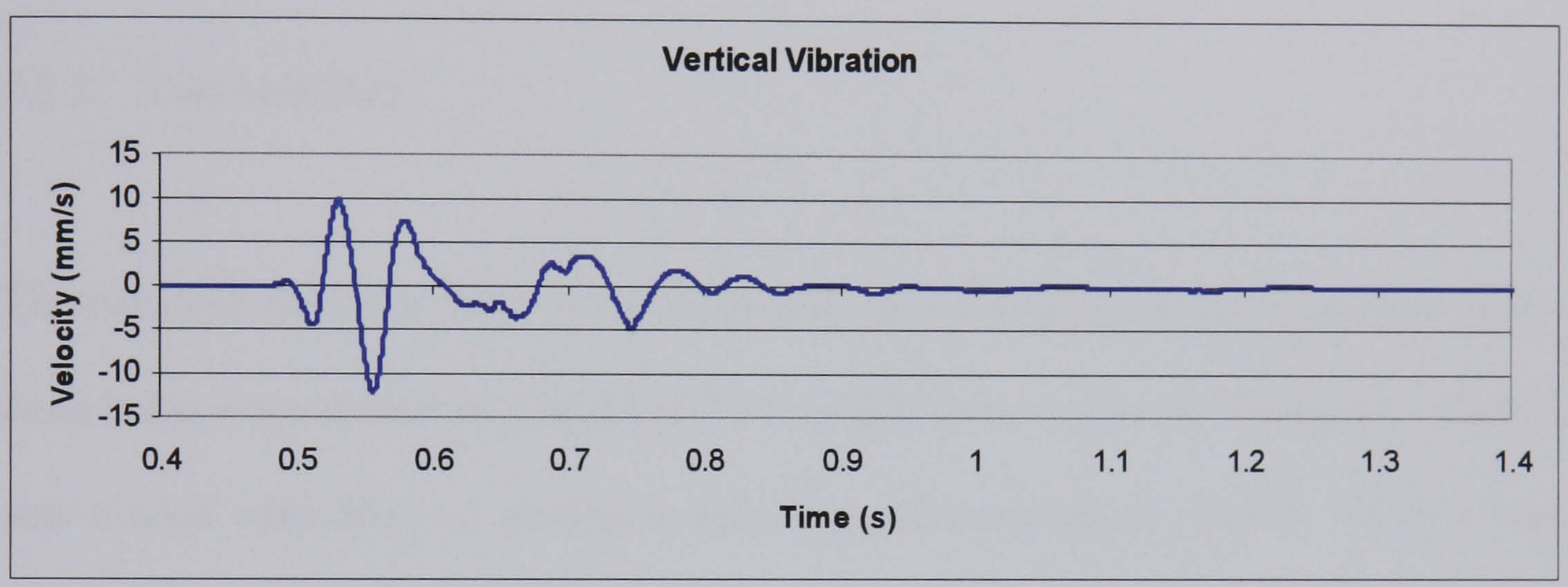

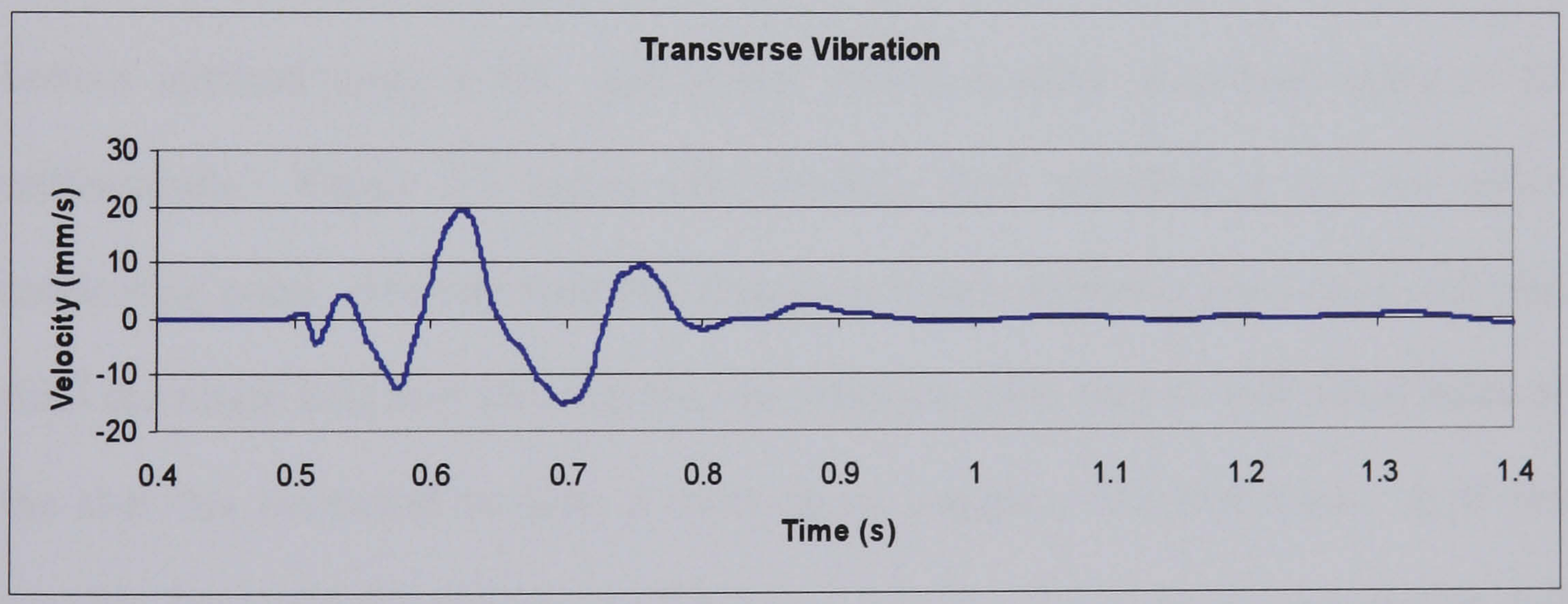

Figure 7.2 Vibration velocity traces from single hole test shot recorded at site office monitoring point

19/01/01	08/11/99	29/11/99	15/12/99	17/04/01-1	17/04/01-2	21/07/00
Radial	0.5342	0.9351	0.9086	0.9187	0.8562	0.7089
Vertical	0.7843	0.7954	0.7592	0.8017	0.7634	0.8124
Transverse	-0.8892	0.9012	0.9143	0.8873	0.8854	0.7182

Table 7.1 Results of cross-correlation/autocorrelation of vibration signal recorded on 19/01/01 with all other test blasts.

7.2.2 Two hole shot

The two hole shot was fired in the same area as the single hole shot detailed above. Both holes were drilled to a depth of 17.5 metres at an angle of 10 degrees. Hole 1 was loaded with 50kg of emulsion and 70kg of hand mixed ANFO. Hole 2 was loaded with 50kg of emulsion and 77kg of hand mixed ANFO. Both holes were bottom initiated using a 16L cast primer with a nominal inter-hole delay of 25 milliseconds. Figure 7.3 shows the vibration trace recorded at the site office monitoring point. The two hole recordings are clearly different from those recorded from the single hole shot showing that the vibration from the two individual holes of the shot has combined to form a much more complex vibration trace. It is not possible from visual inspection to determine how the two holes are interacting and what waveform is generated by each hole.

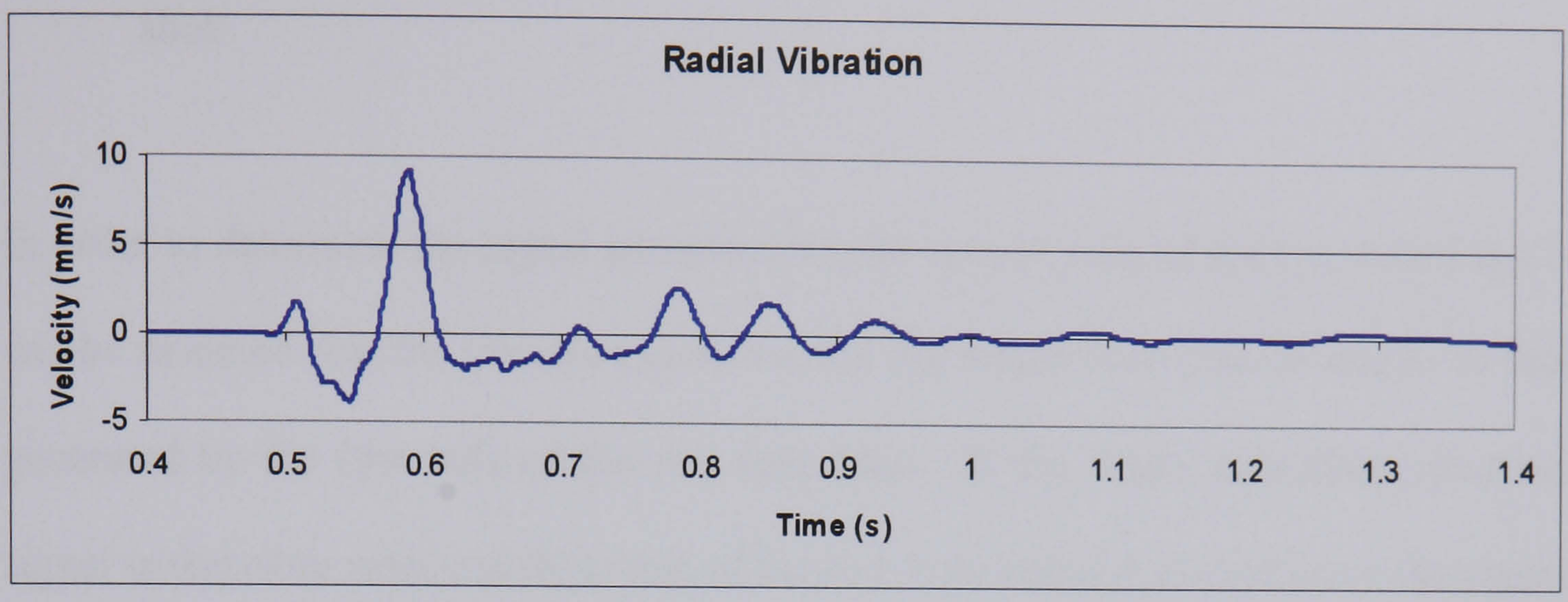

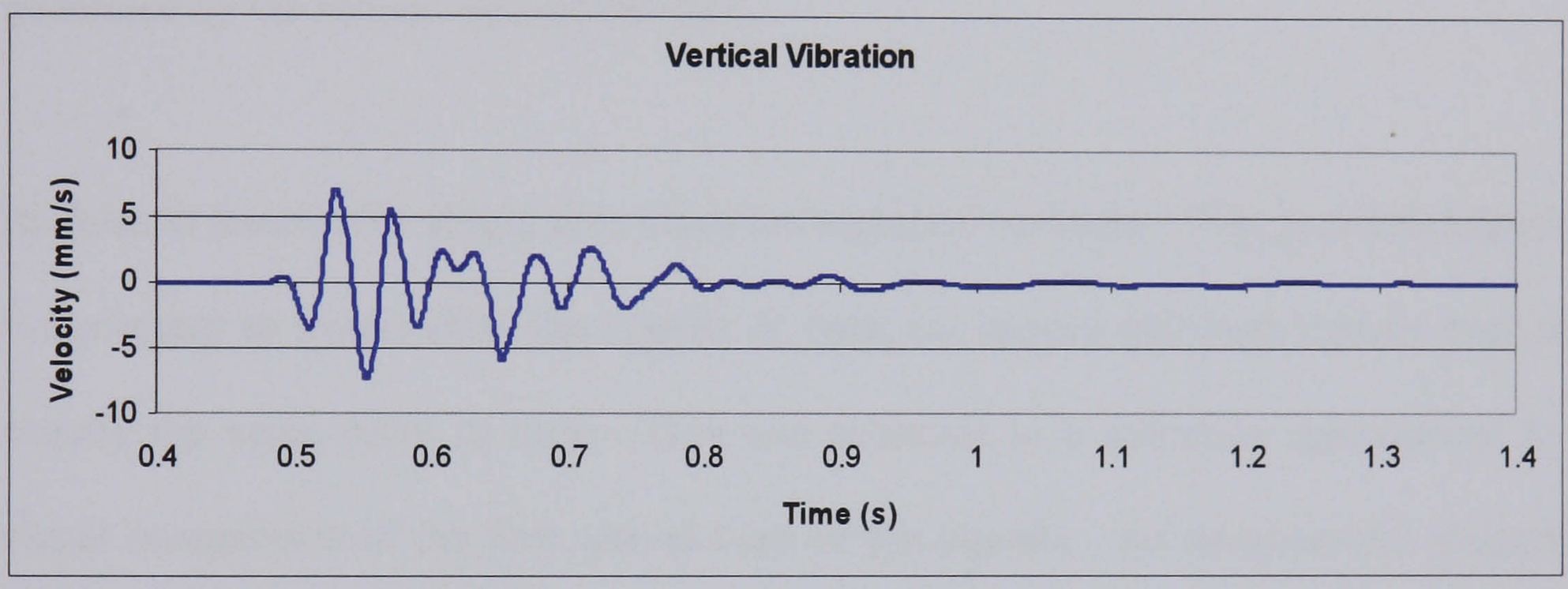

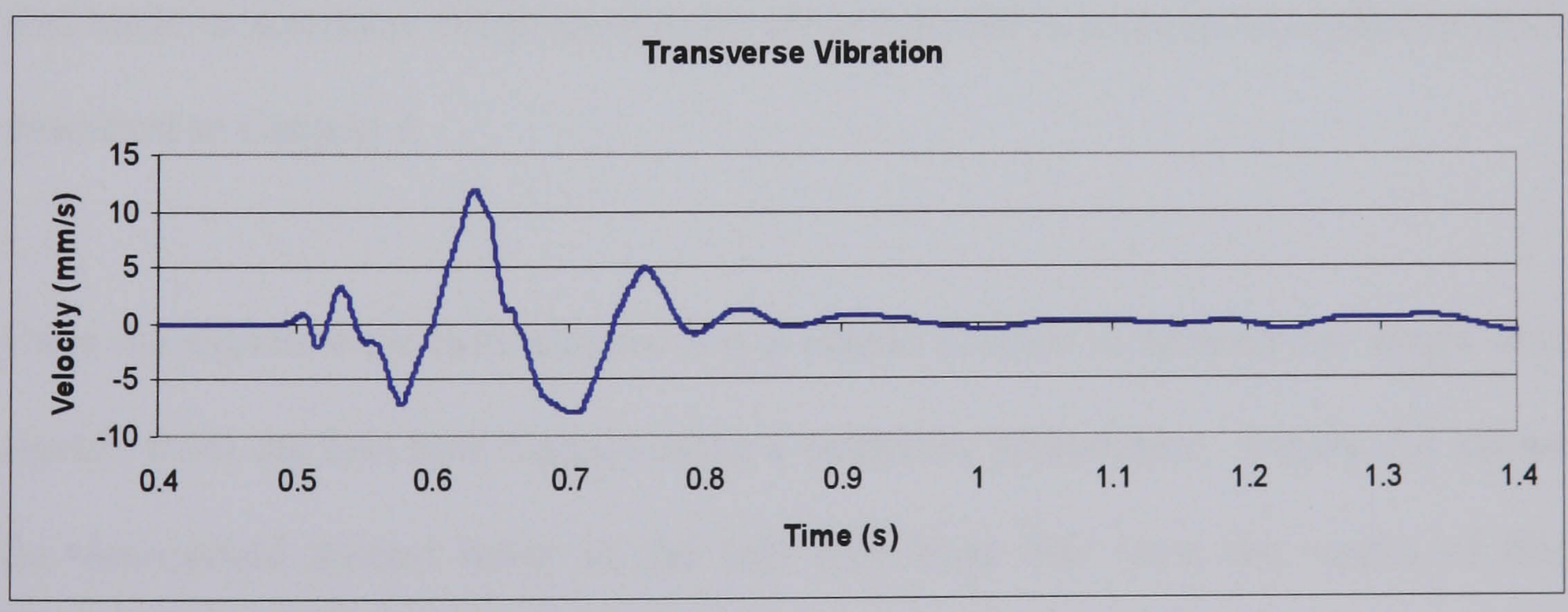

Figure 7.3 Vibration velocity traces from two hole test shot recorded at site office monitoring point

7.2.3 Determination of the signal generated by the second hole of the two hole shot.

In order to determine the signal generated by the second hole of the two hole blast it can be assumed that the vibration generated by the single hole blast is similar to that generated by the first hole of the two hole blast. If the single hole blast vibration signal is therefore removed from that of the two hole signal it should leave the signal generated by the second hole of the shot.

In order to remove the single hole vibration signals from those of the two hole blast it is necessary to synchronise the signals in time, i.e. ensure that both signals start at exactly the same point in time. This was achieved in a computer spreadsheet by visual comparison of the first arrival time of the signals. An unsuccessful attempt was made to automate this process using cross correlation techniques similar to those described in Chapter 3.

Once the signals were time aligned it is a simple process to subtract the single hole signals from the two hole signals using a computer spreadsheet. Figure 7.4 shows the determined second holes of the two hole blast that were the results of this subtraction.

By synchronising the single hole signals with the determined second hole signals in the same manner as above it is possible to compare the signals directly. Any large

differences between the two signals should theoretically be attributed to the fact that it is the second hole of a blast and is therefore subject to dynamic parameters which the first hole is not.

Figure 7.5 shows the vibration generated by the single hole test shot, which it has been assumed is identical to the first hole of the two hole shot, with the determined second hole of the two hole shot. It is clear from visual inspection that the two sets of data share common features.

The vertical components appear almost identical in shape with a reduction in amplitude. This reduction would be expected if the second hole in this blast was following the findings from the single holes detailed in Chapter 6 which conclude that if the number of free faces is increased the vibration amplitude will decrease.

The radial and transverse determined second hole recordings, however, appear to be very different to that from a single hole. This indicates that each hole in a multi-hole blast does not produce a similar waveform and that dynamic effects alter the waveshape as well as the amplitude.

The determined second hole signals were compared to the single hole signal using the autocorrelation/cross-correlation technique described in Chapter 5. The results of this are shown in table 7.2.

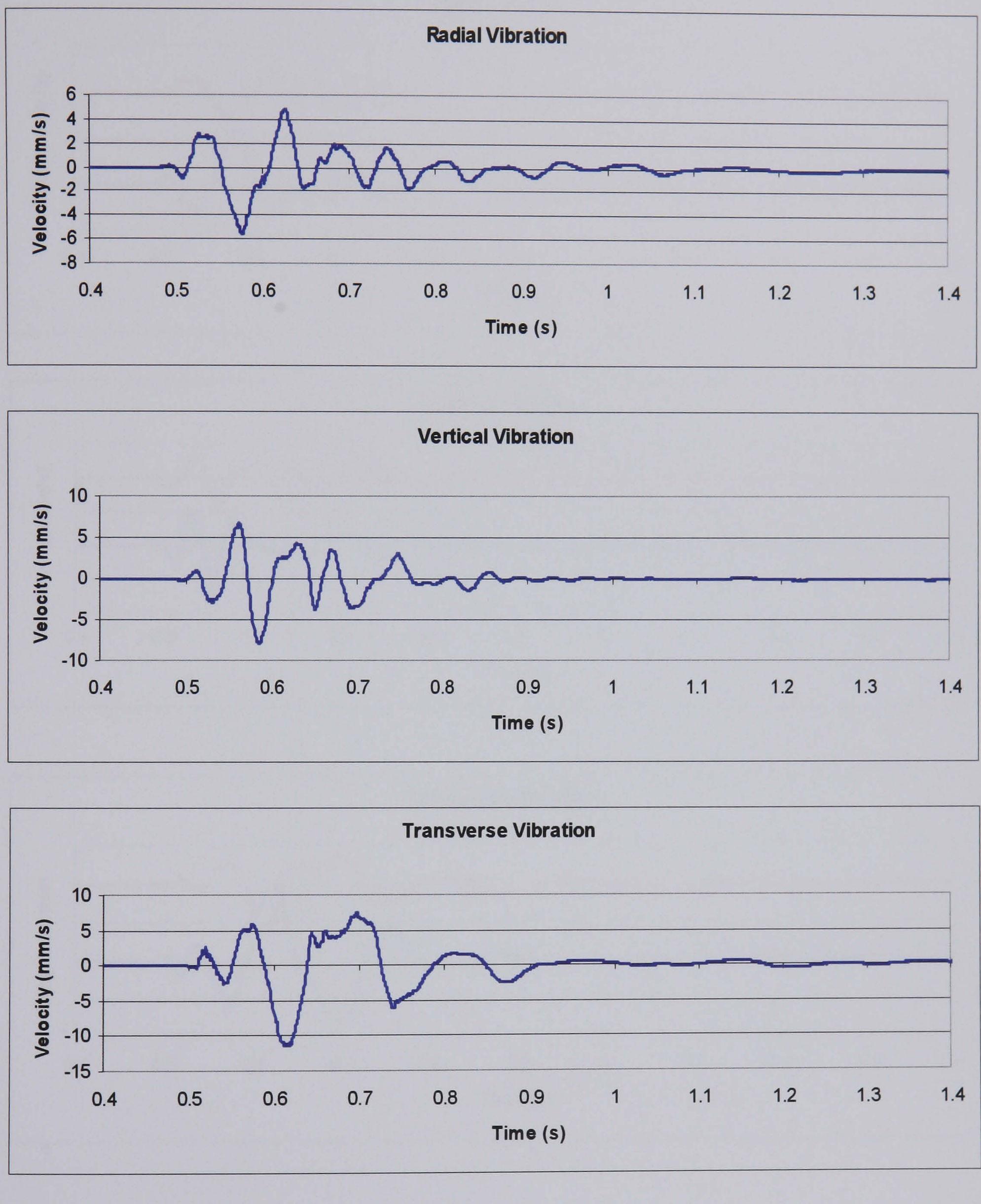

Figure 7.4 Vibration velocity traces showing the result when a single hole test shot is subtracted from a two hole shot.

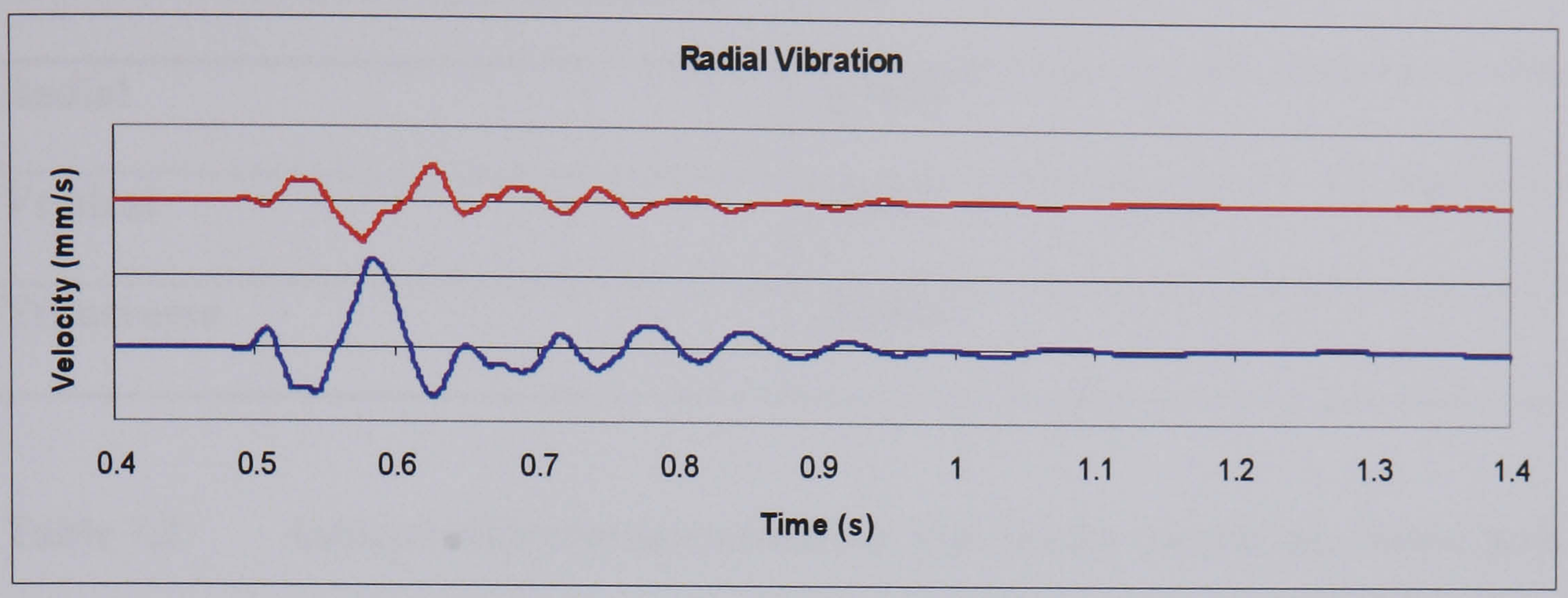

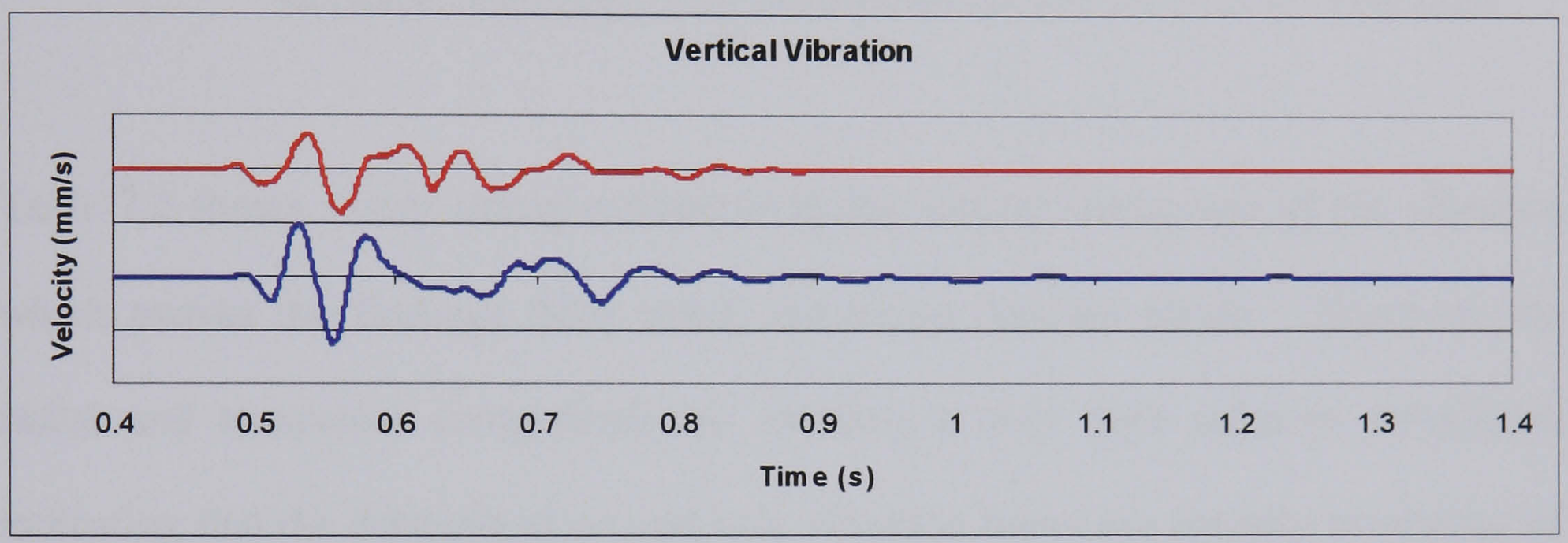

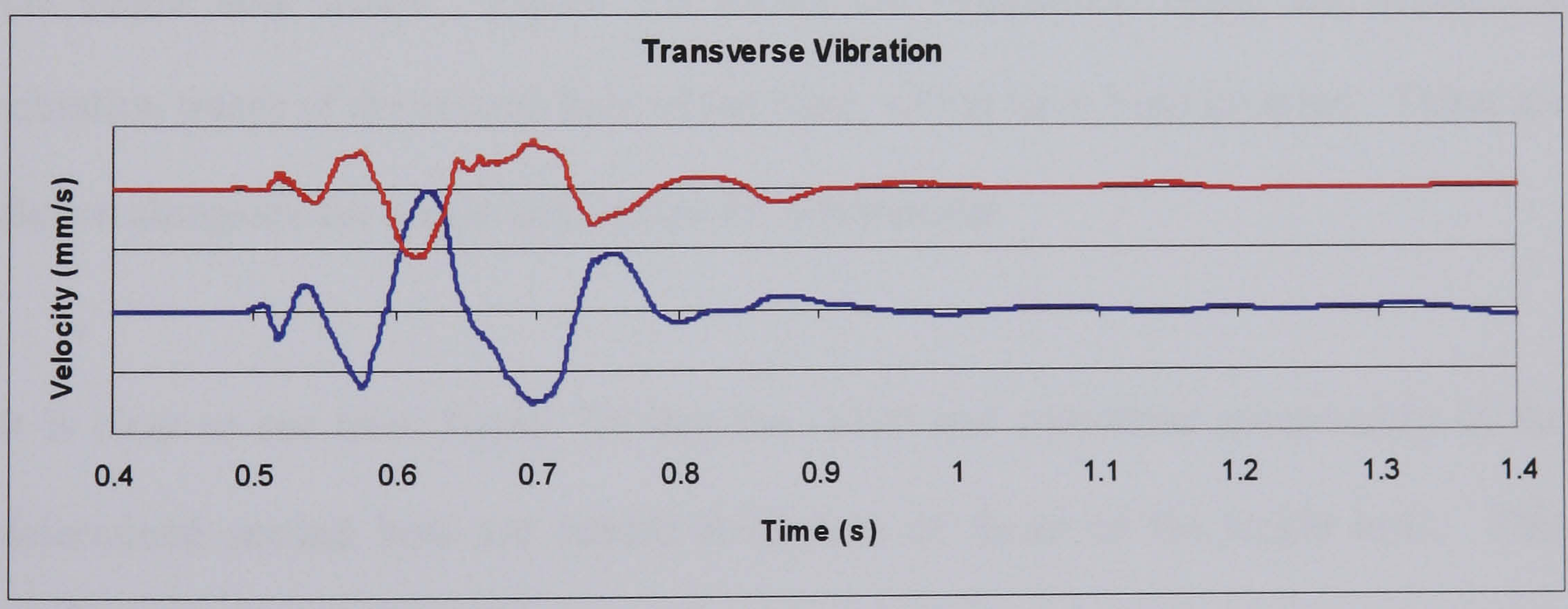

Figure 7.5 Vibration velocity traces showing the recorded single hole shot (lower) compared with the determined second hole shot (upper). both traces are on the same scale.

Autocorrelation/Cross-correlation test results	
Radial	**-0.9023**
Vertical	**0.8945**
Transverse	**-0.9203**

Table 7.2 Autocorrelation/cross-correlation test results comparing single hole vibration recordings with determined second hole of two hole blast.

Table 7.2 shows a very strong correlation in the vertical component of the vibration which proves the findings from visual inspection detailed earlier. However, the radial and transverse components are showing a very high negative correlation indicating that the determined second hole vibration traces are actually inversions of the single hole traces. Figure 7.6 shows the determined radial and transverse vibration traces of the second hole of the blast, which have been inverted. These are shown alongside the single hole traces for comparison.

It is clear to see from figure 7.6 that the radial and transverse components of the determined second hole are indeed inversions of those of the single hole. This inversion was also seen in one of the single holes detailed in Chapter 5. If this inversion is a repeatable effect it will have a large impact on the use of hybrid modelling in the near to mid field. The main issue would be with firing time optimisation. If the inversion is always seen, then what is thought to be the

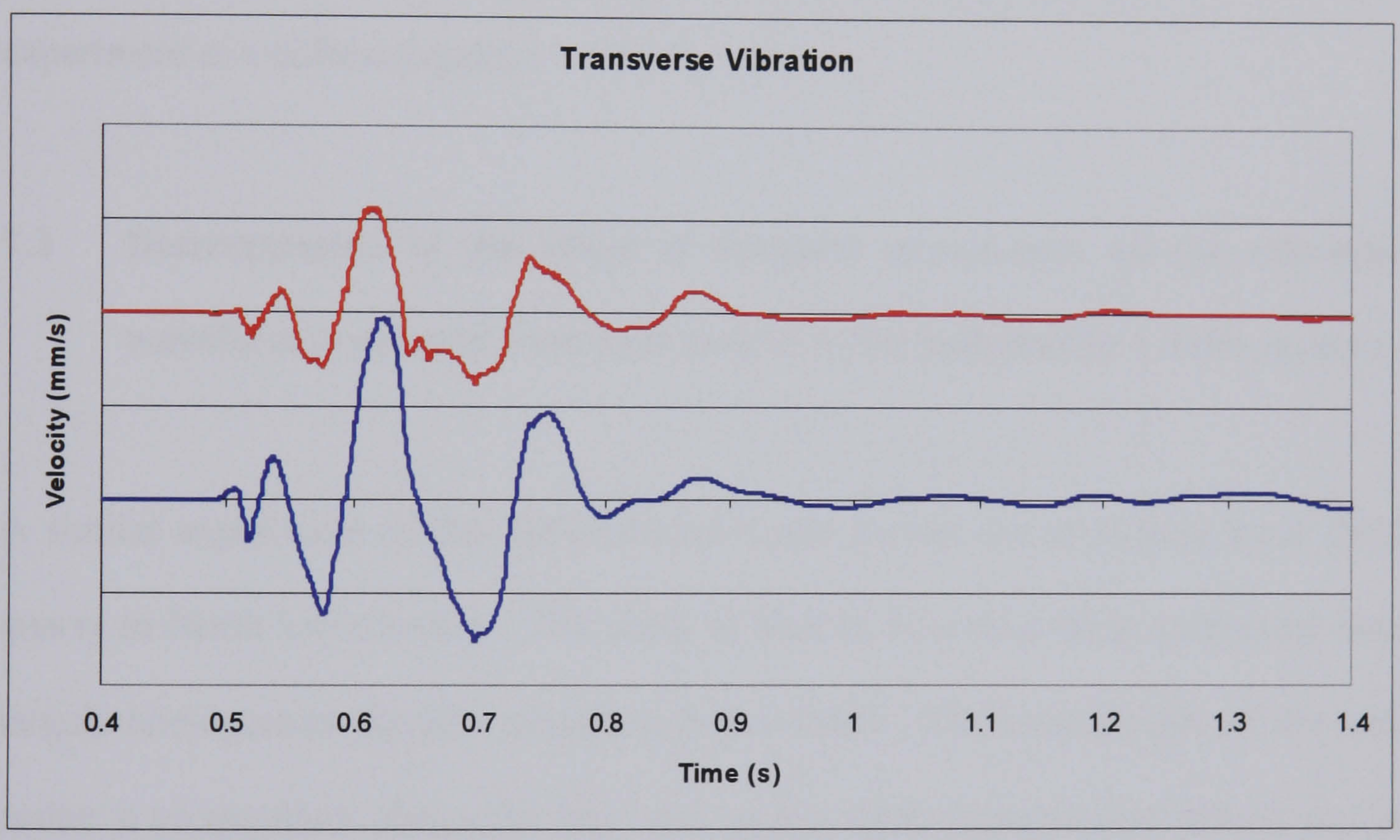

Figure 7.6 Vibration velocity traces showing the recorded single hole shot (lower) compared with the inverted determined second hole shot (upper). both traces are on the same scale.

maximum destructive interference condition, i.e. when the waves cancel each other out to the greatest degree, will in fact be the maximum constructive interference condition, as the waves will be adding to each other, rather than subtracting. This in turn will increase the resulting vibration. This effect could explain findings by Farnfield and White (1984) who reported a 50% increase in vibration levels after the application of firing time optimisation.

In order to study this effect further and determine whether it was a phenomenon local to this particular quarry or experimental setup it was decided to carry out another experiment at a different quarry.

7.3 Determination of the effect of dynamic parameters on the vibration waveform generated from each hole of a two hole shot in a chalk quarry.

A similar experiment to that detailed above was carried out at Melton Ross chalk quarry in North Lincolnshire. The chalk at Melton Ross is a thick, extremely hard largely homogenous deposit containing flint nodules. The homogeneity of the rock makes it an excellent choice for this work as the effect of geological factors can be assumed to be minimal. Melton Ross also has very large benches, thus allowing the equipment to be set out behind the blast on the bench being fired at up to a distance of 80 metres.

7.3.1 Experimental procedure

The blast was set up so that both the single and double holes would be fired with one free face. The face was instrumented with a total of 14 monitoring points varying in distance from the shots from 20 metres to 80 metres. Figure 7.7 shows a plot of the layout of the bench which was taken from the GPS survey that was undertaken. To take full advantage of the opportunity to record small test blasts another student was also recording data for use with another project and so not all the monitoring points were used for this research.

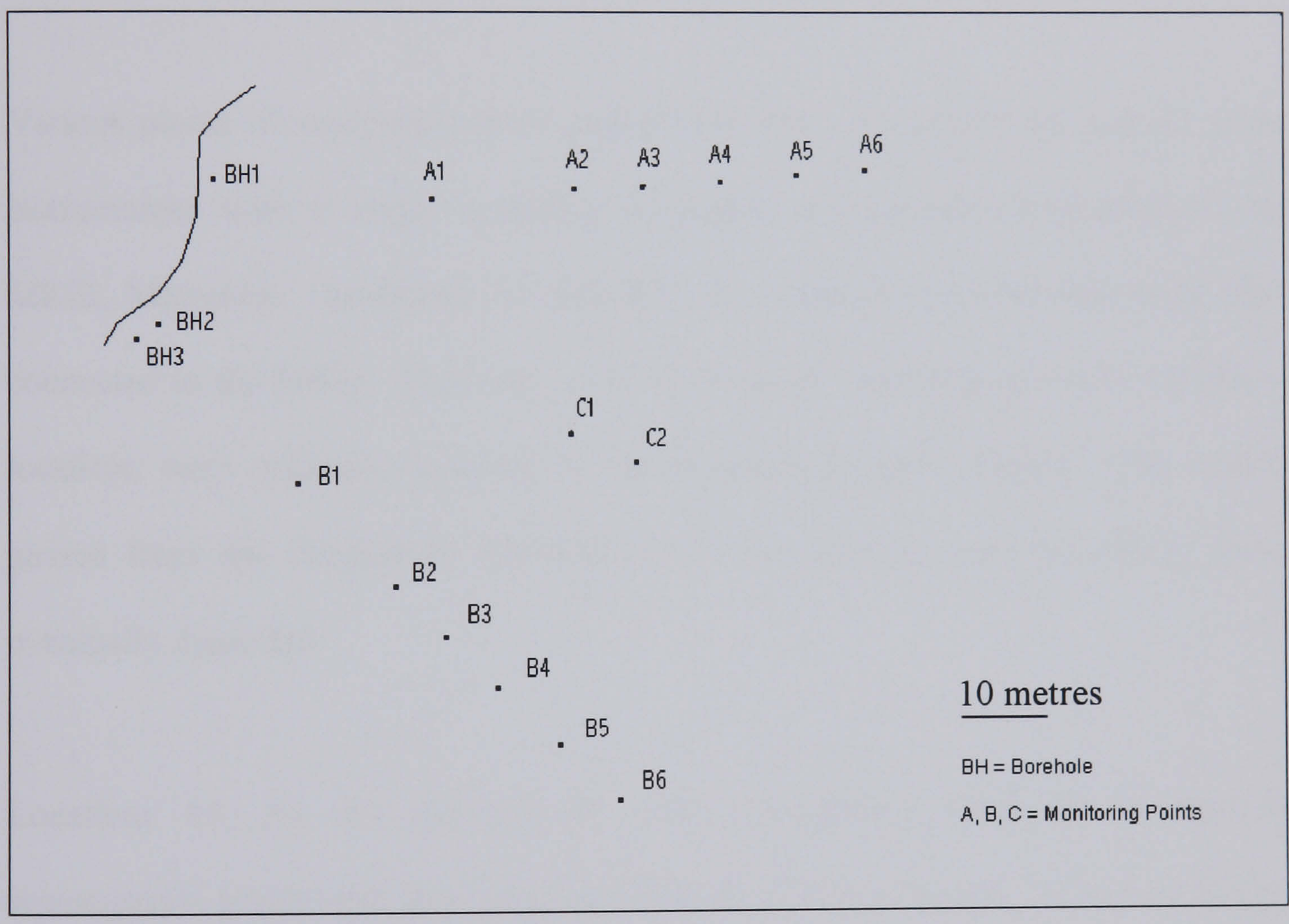

Figure 7.7 GPS survey plot of blast holes and monitoring locations for two hole experiment at Melton Ross Chalk Quarry

The instruments were set up so that location A1 was the same distance from the single hole blast as location B1 was from the two hole shot. This was repeated for

locations 2 to 6. This was to ensure that there were no problems with the direction of the blasts. For each distance from the blast the A locations were used as the single blast vibration recorders which were orientated towards the single hole shot and B locations were used to record the vibration from the two hole shot and thus were orientated towards the first hole of the two hole shot. The C locations were set at identical distances from each blast. The problem with the C locations is that they were not moved in orientation between blasts, but left pointing towards the single hole shot.

Various pieces of equipment were used on the face. Locations A1 and B1 were instrumented with a single vertically orientated accelerometer connected to the MREL Microtrap. Locations A2 and B2 had a triaxial accelerometer array also connected to the MREL Microtrap. The acceleration recordings gained from these locations were originally intended to be integrated to give velocity. The results gained from the integration, however, were unsatisfactory and the results were eventually discarded.

Locations A3, A4, B3, B4 and C1 were instrumented with the 15 channel seismograph, which was now working perfectly. The C location was discarded as there was no opportunity to change its orientation between blasts due to time restrictions. The A and B locations, however, performed as expected and the results are given in section 7.3.2.

Locations A5, B5 and C2 were instrumented with White portable seismographs. Again the C location was discarded for the same reason as previously mentioned. The remaining 2 locations were used and the results given in section 7.3.2.

The final two locations A6 and B6 were instrumented with Geosonics Microseis portable seismographs. The results from these locations were discarded as the resolution of the Microseis is very low giving a castellated appearance to the waveforms. The Microseis were also not secured to the bench and so the results would be of doubtful quality.

The holes were drilled to a depth of 16 metres and each loaded with approximately 110Kg of ANFO from a small automatic mixing hopper and a 16L cast primer. The two hole shot was initiated with a nominal inter hole delay of 25ms.

7.3.2 Results

The results from six of the fourteen locations were deemed suitable for use with this project. This translates into three sets of data as two recordings are needed for each set. Results were obtained at distances of 50, 60 and 70 metres from the blast holes.

Figure 7.8 shows the single hole recorded at 50 metres, Figure 7.9 shows the signal recorded at 60 metres and figure 7.10 shows that recorded at 70 metres. As this is the first test undertaken at this quarry there is no data with which to compare the

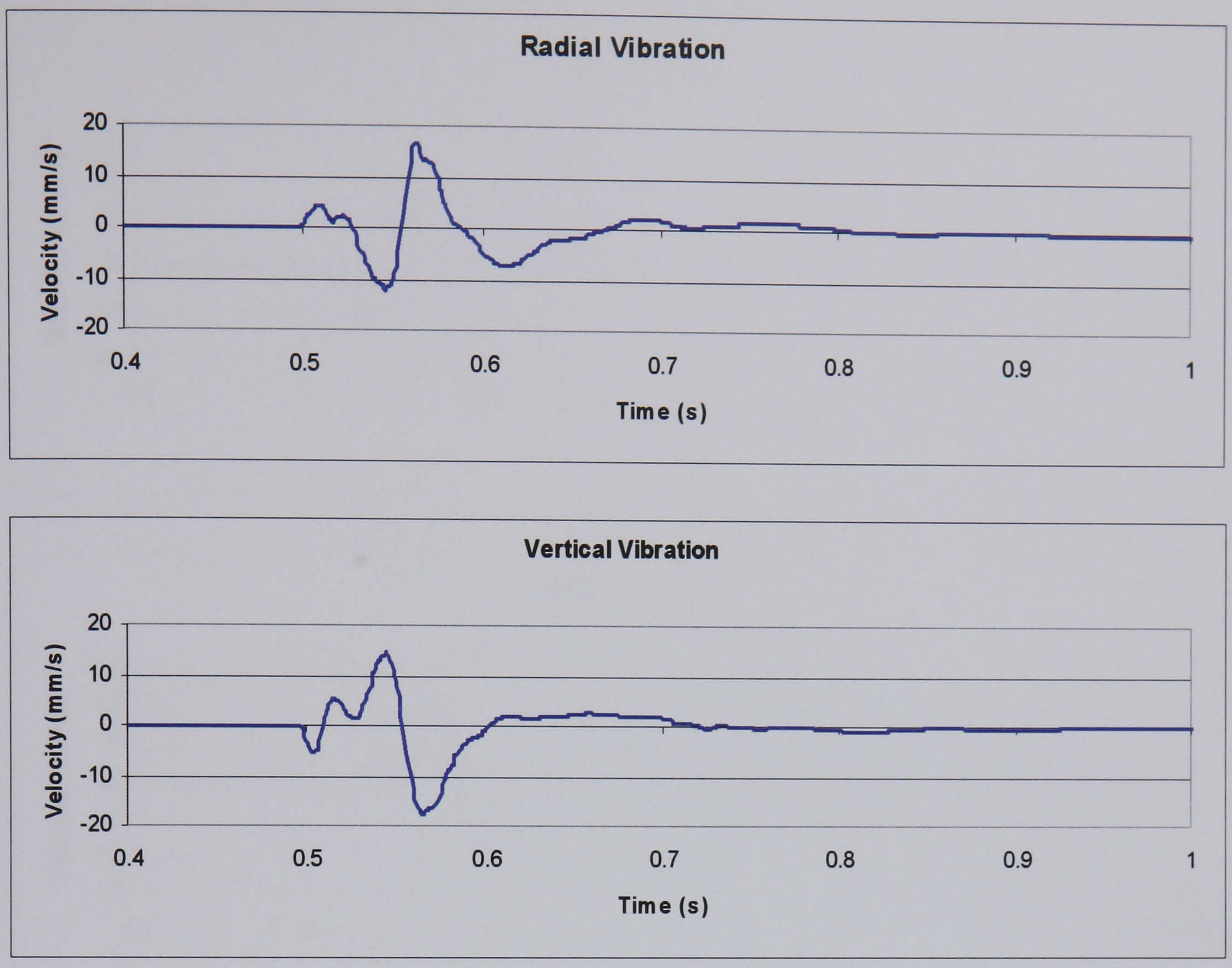

Figure 7.8 Single hole recording from Melton Ross chalk quarry at 50 metres

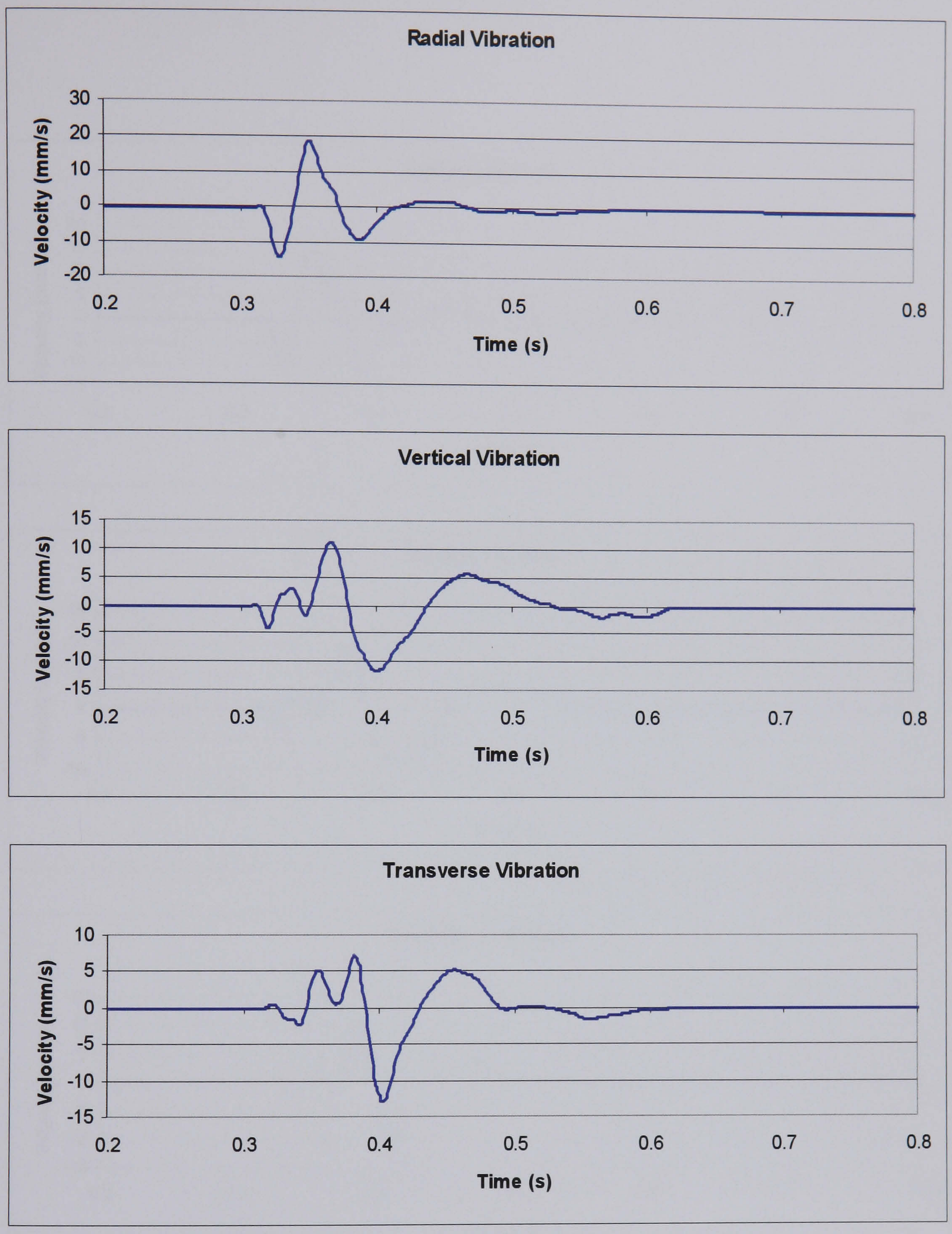

Figure 7.9 Single hole recording from Melton Ross chalk quarry at 60 metres

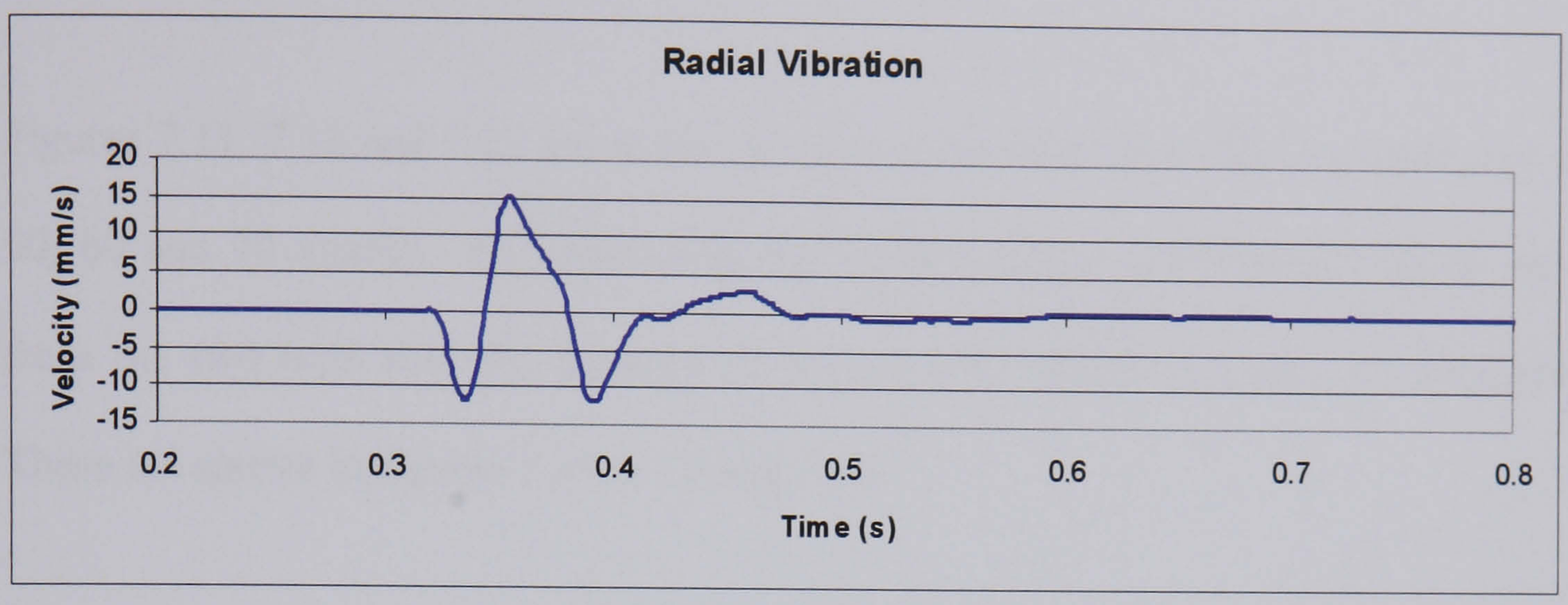

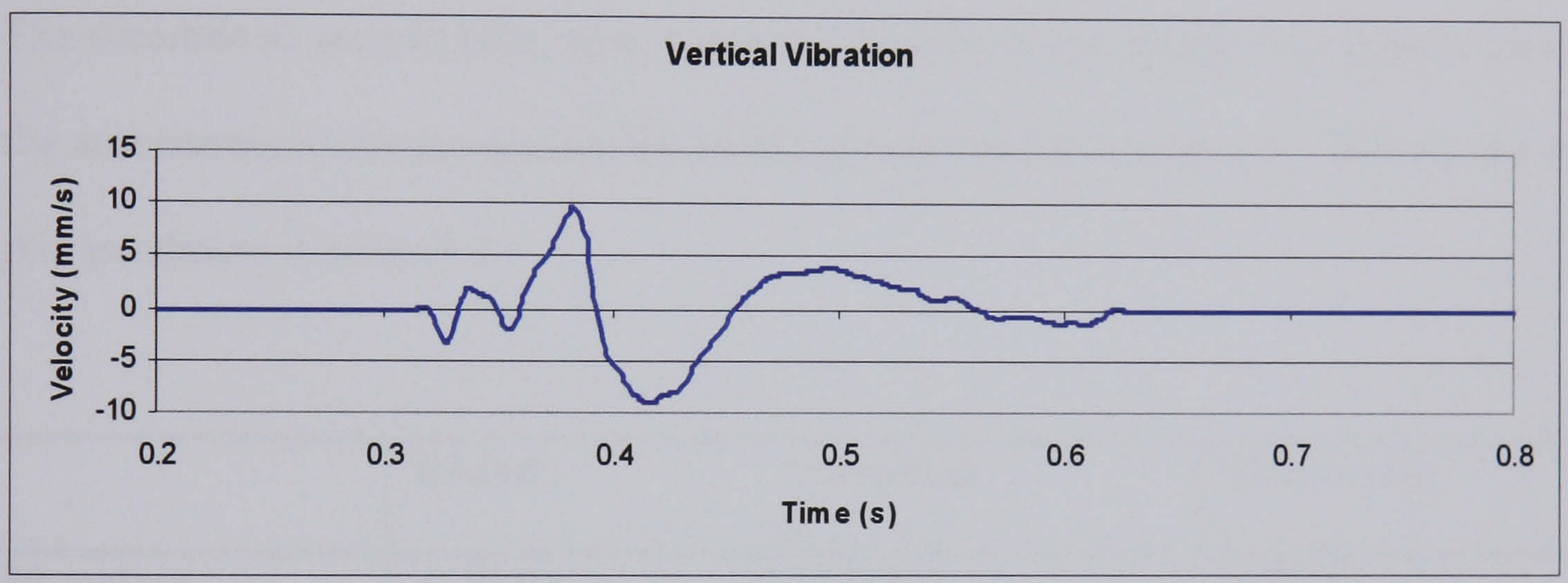

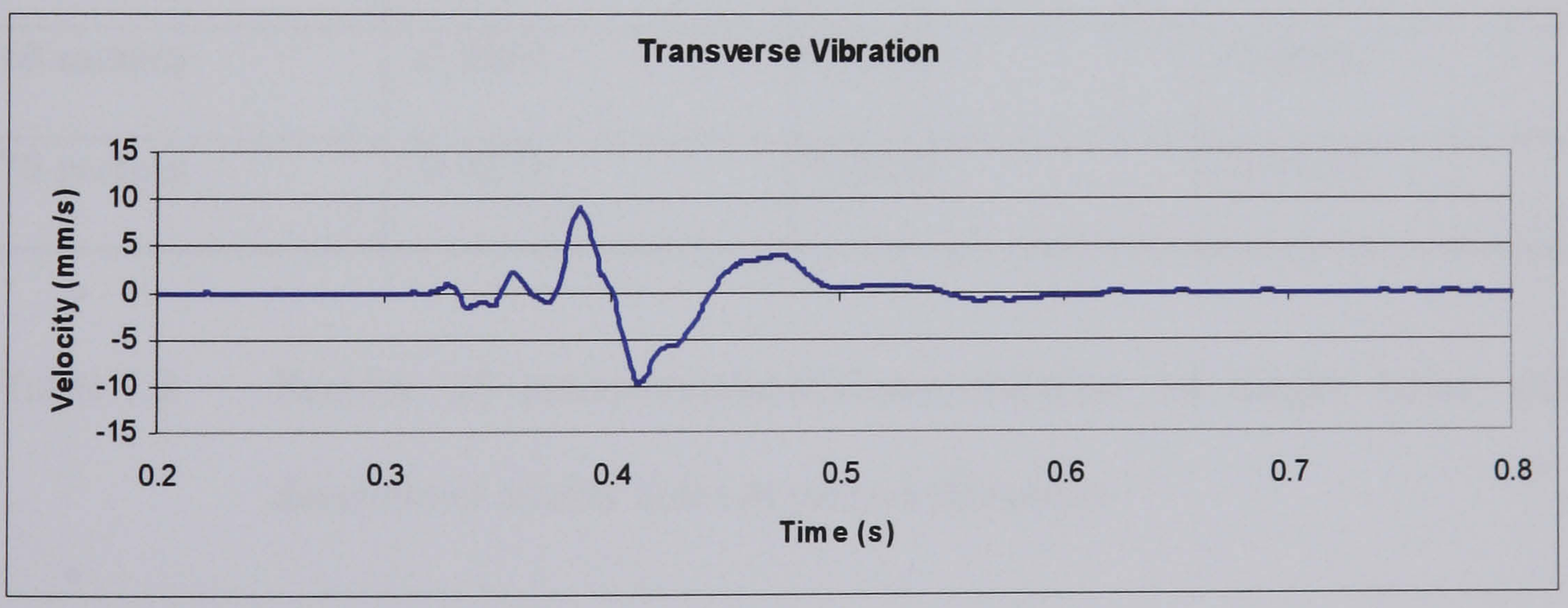

Figure 7.10 Single hole recording from Melton Ross chalk quarry at 70 metres

single hole for repeatability so it assumed that these recordings are representative of the first hole of a multi-hole shot.

Figures 7.11, 7.12 and 7.13 show the vibration recordings from the two hole shot at 50, 60 and 70 metres. By subtracting the corresponding synchronised single hole from the two hole shot the determined second hole vibration traces are obtained. These are shown in figures 7.14, 7.15 and 7.16.

The determined second hole signals were compared to the single hole signals using the autocorrelation/cross-correlation technique outlined in Chapter 5. The results of this are shown in table 7.3.

	Radial	**Vertical**	**Transverse**
50 metres	-0.9130	0.4265	-0.9523
60 metres	-0.9254	0.8934	-0.9823
70 metres	-0.9271	0.8832	-0.9910

Table 7.3 Results of autocorrelation/cross-correlation of single holes and determined double holes at various distances.

It can be seen that the vertical components recorded at 60 and 70 metres fit well as was also seen in the previous test at Coldstones Quarry. The vertical component at 50 metres, however, does not seem to fit well at all. The reason for this poor fit is unknown and without more data it is difficult to draw a conclusion. As both the 60

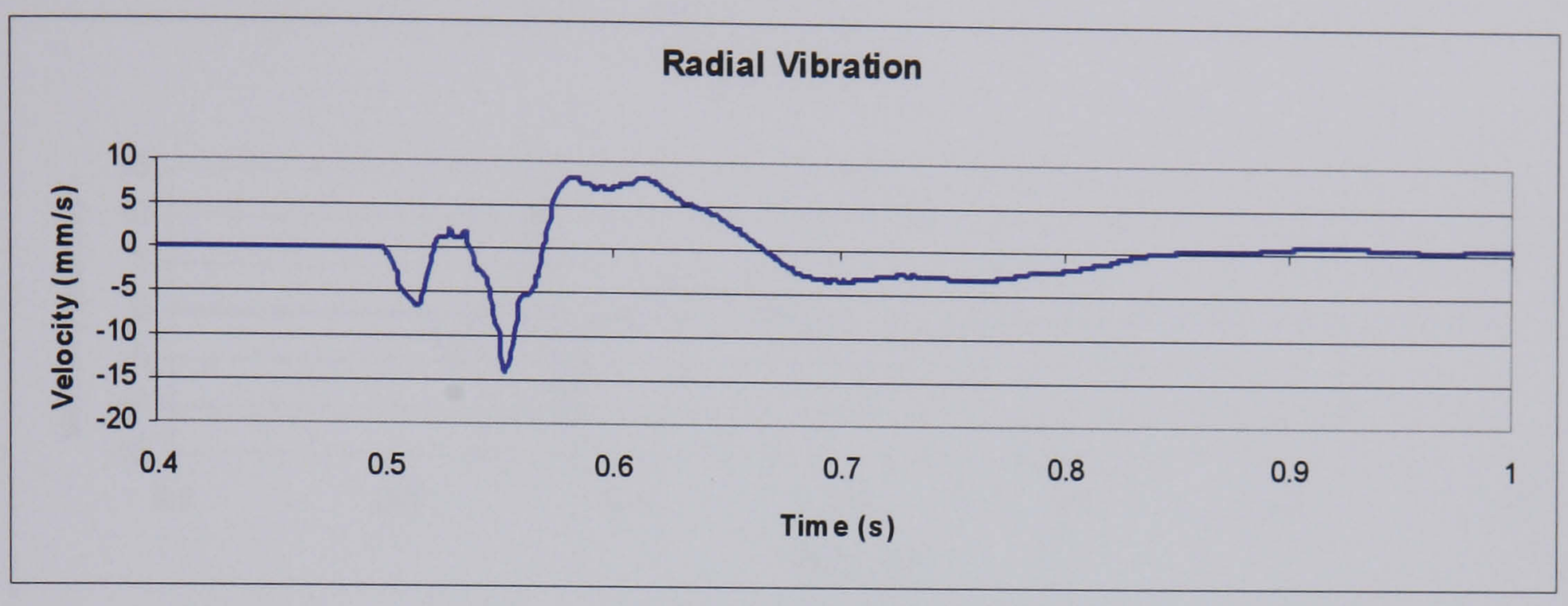

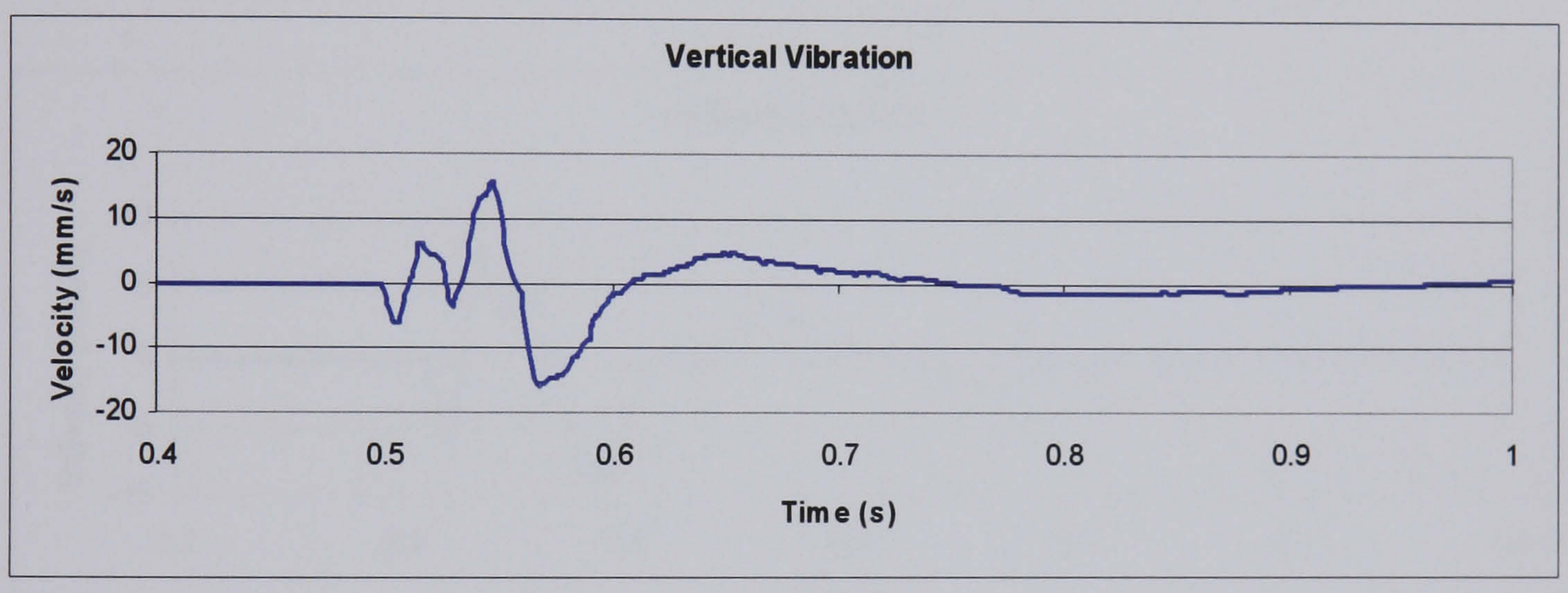

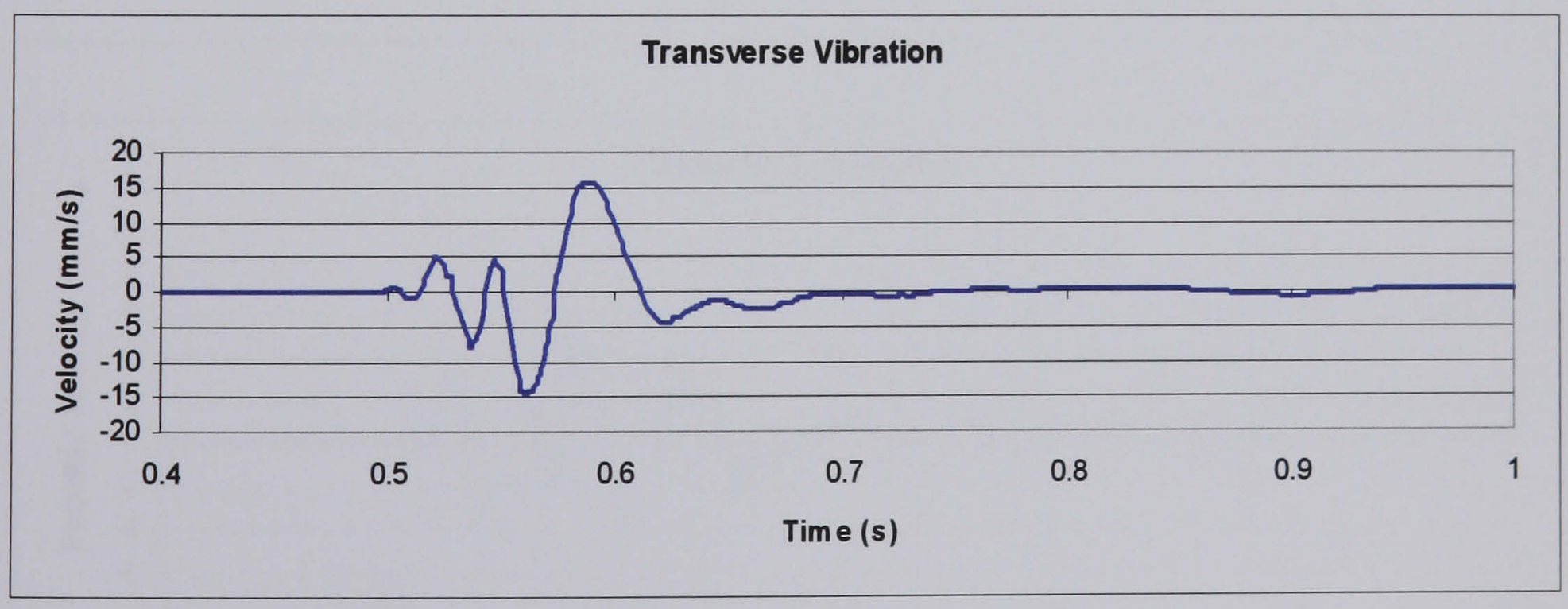

Figure 7.11 Two hole recording from Melton Ross chalk quarry at 50 metres

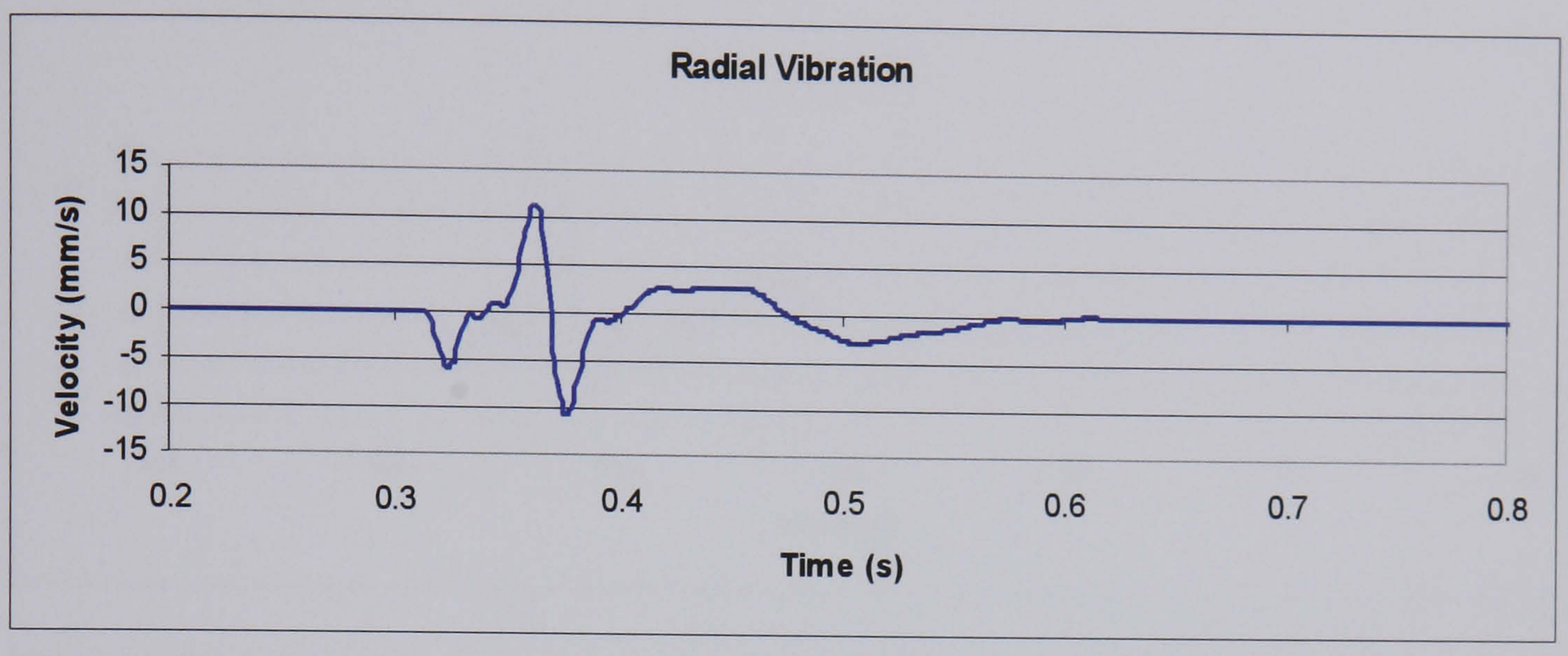

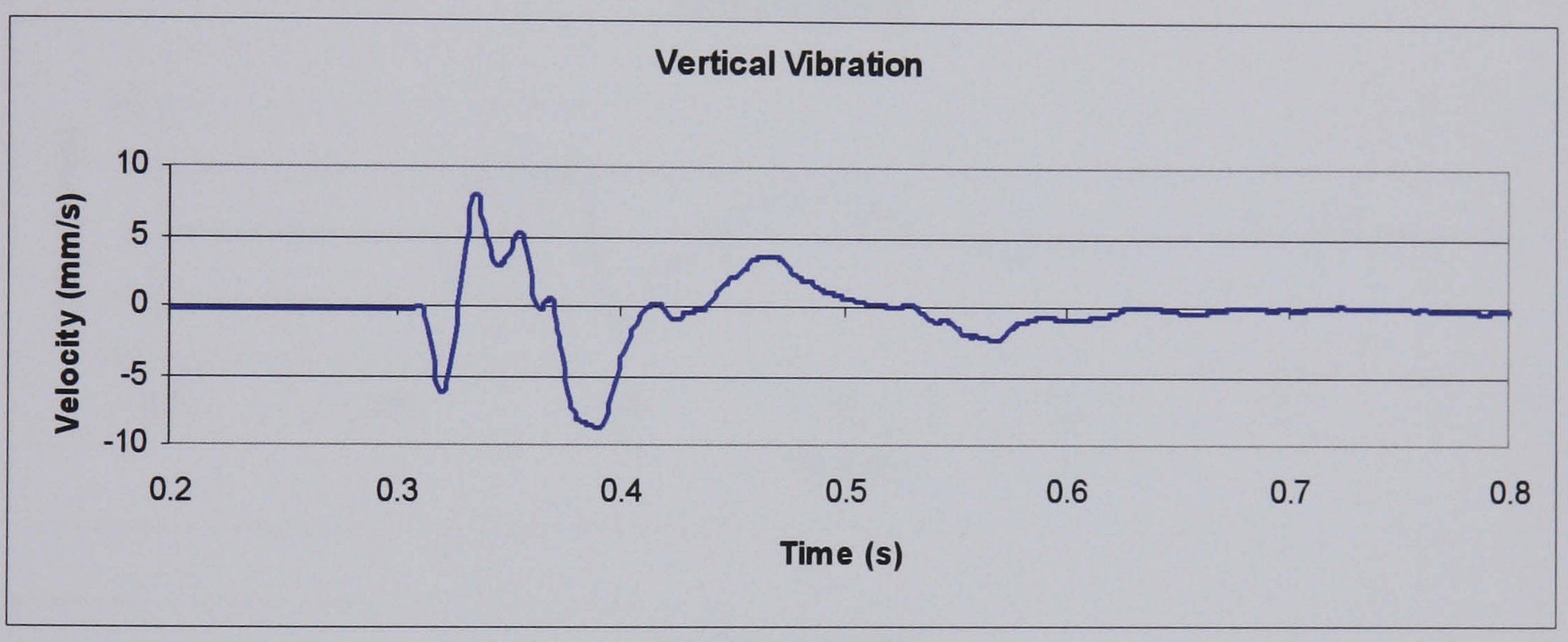

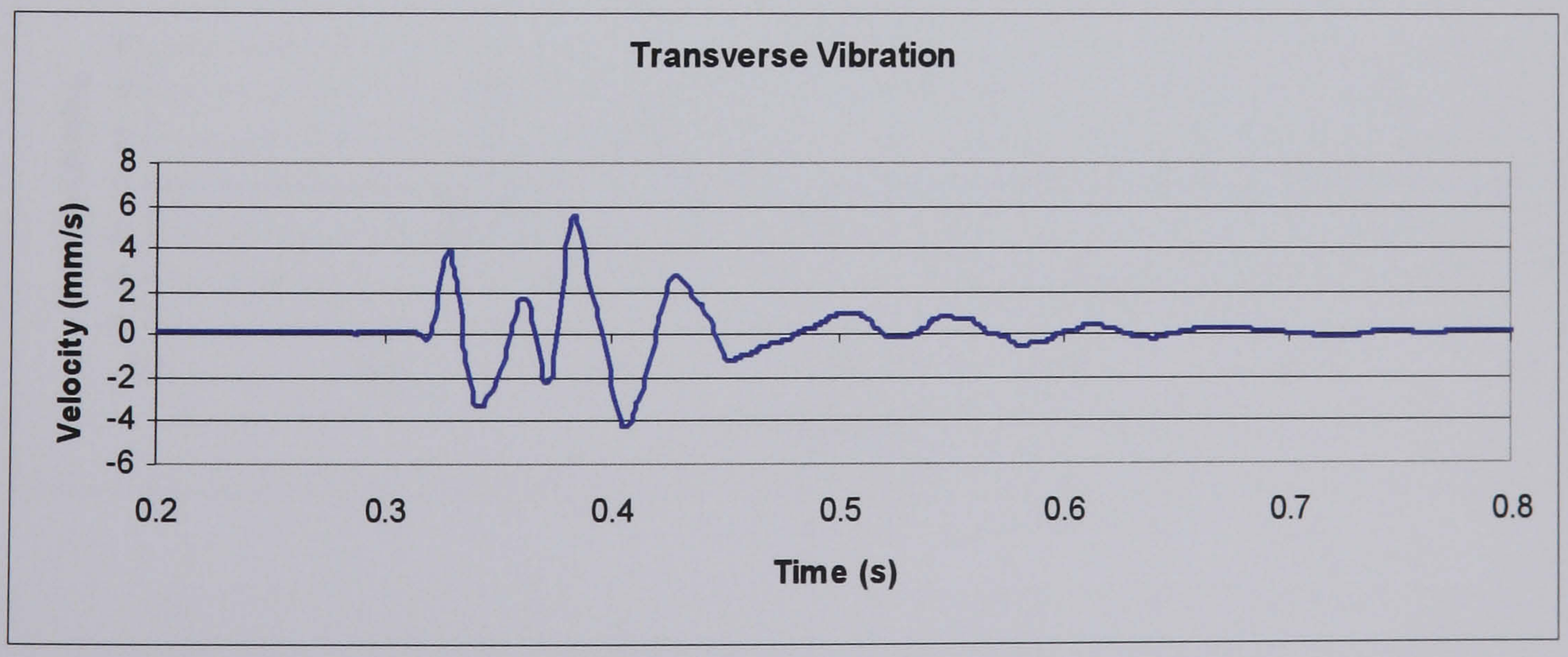

Figure 7.12 Two hole recording from Melton Ross chalk quarry at 60 metres

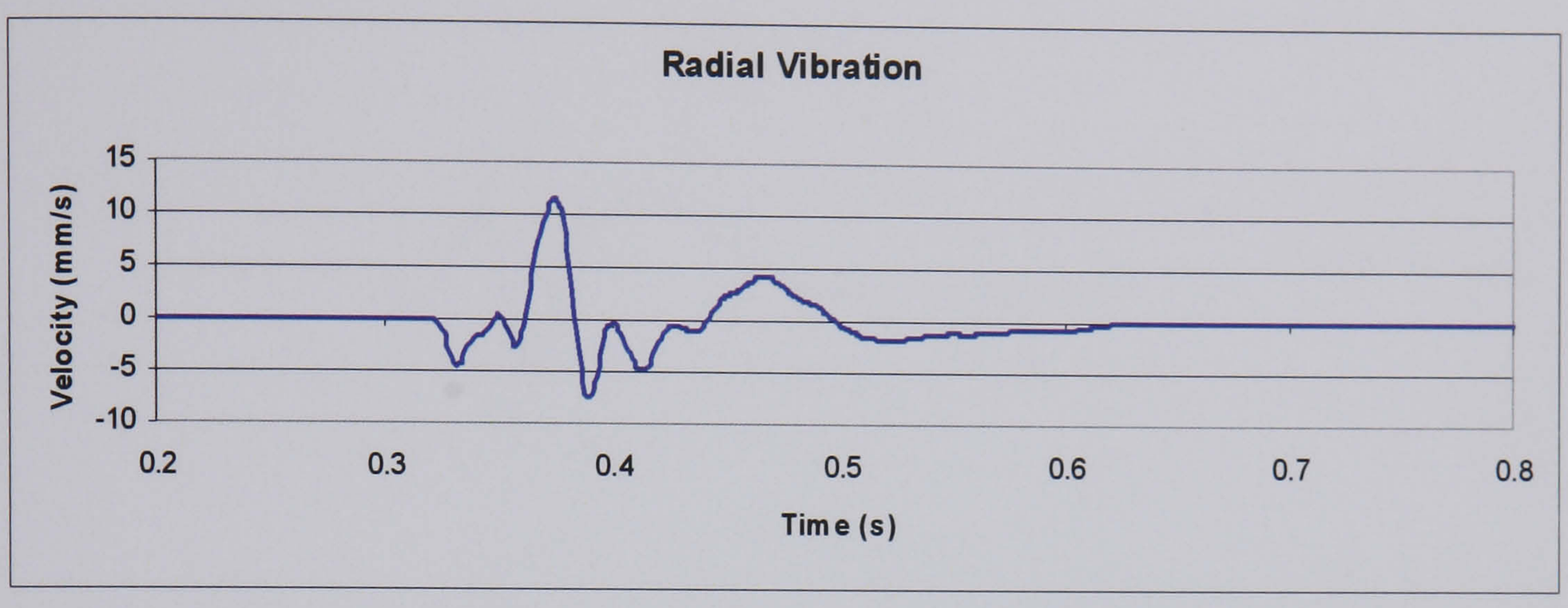

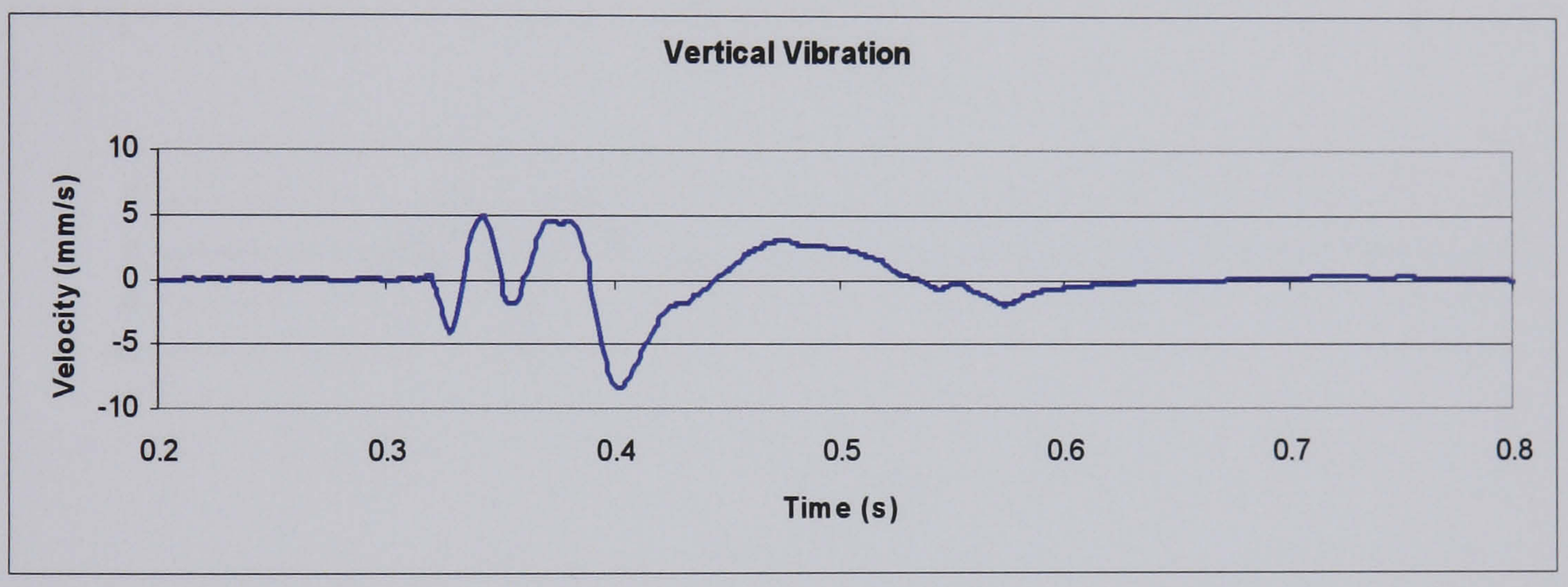

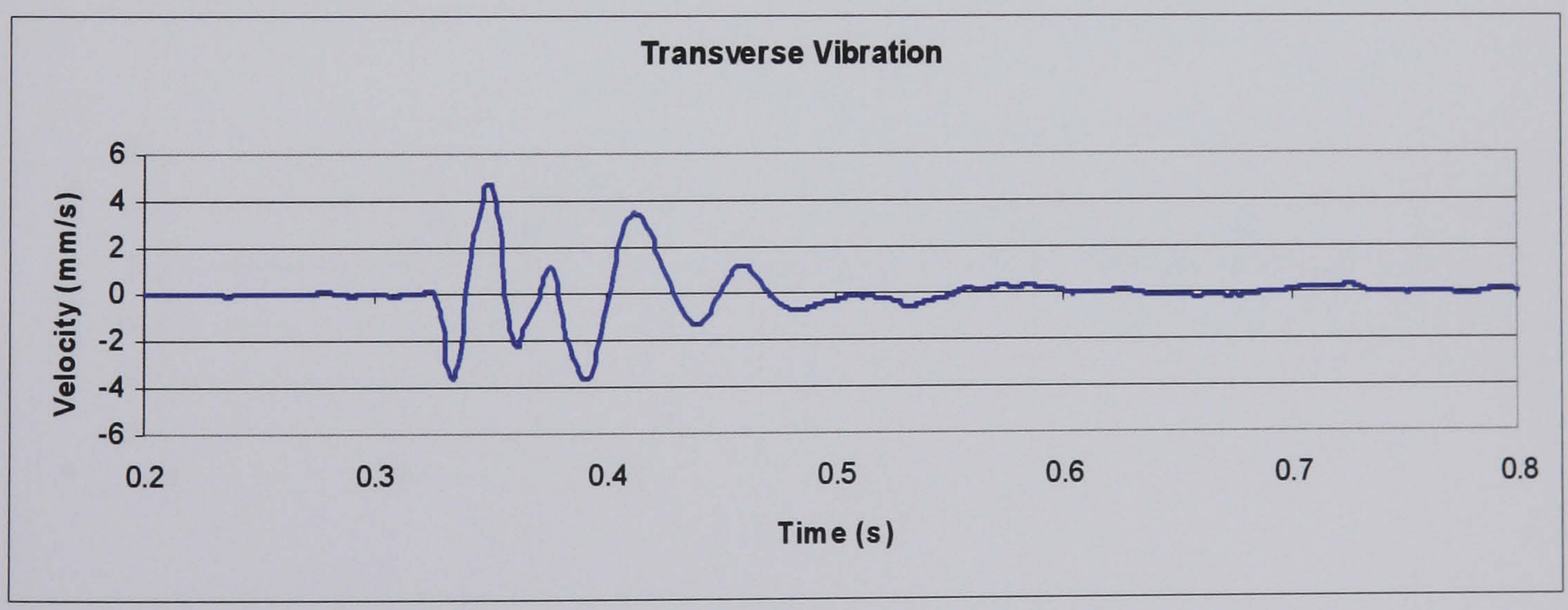

Figure 7.13 Two hole recording from Melton Ross chalk quarry at 70 metres

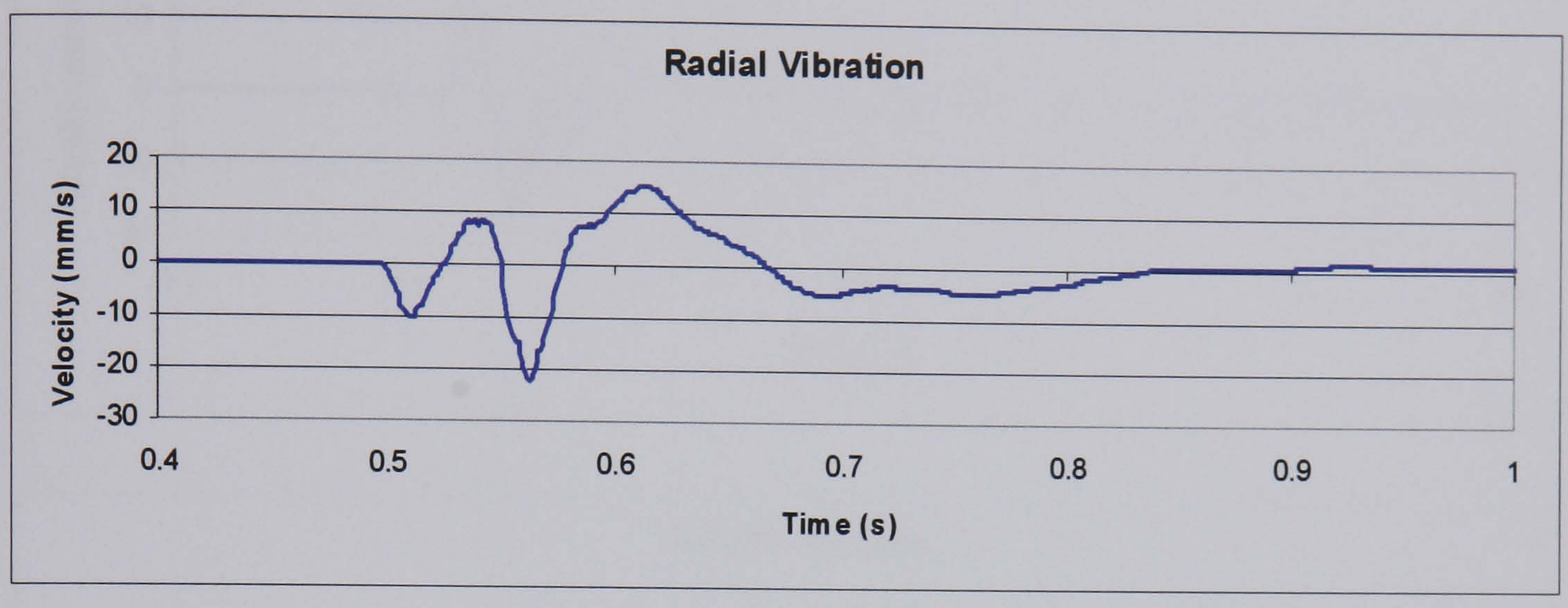

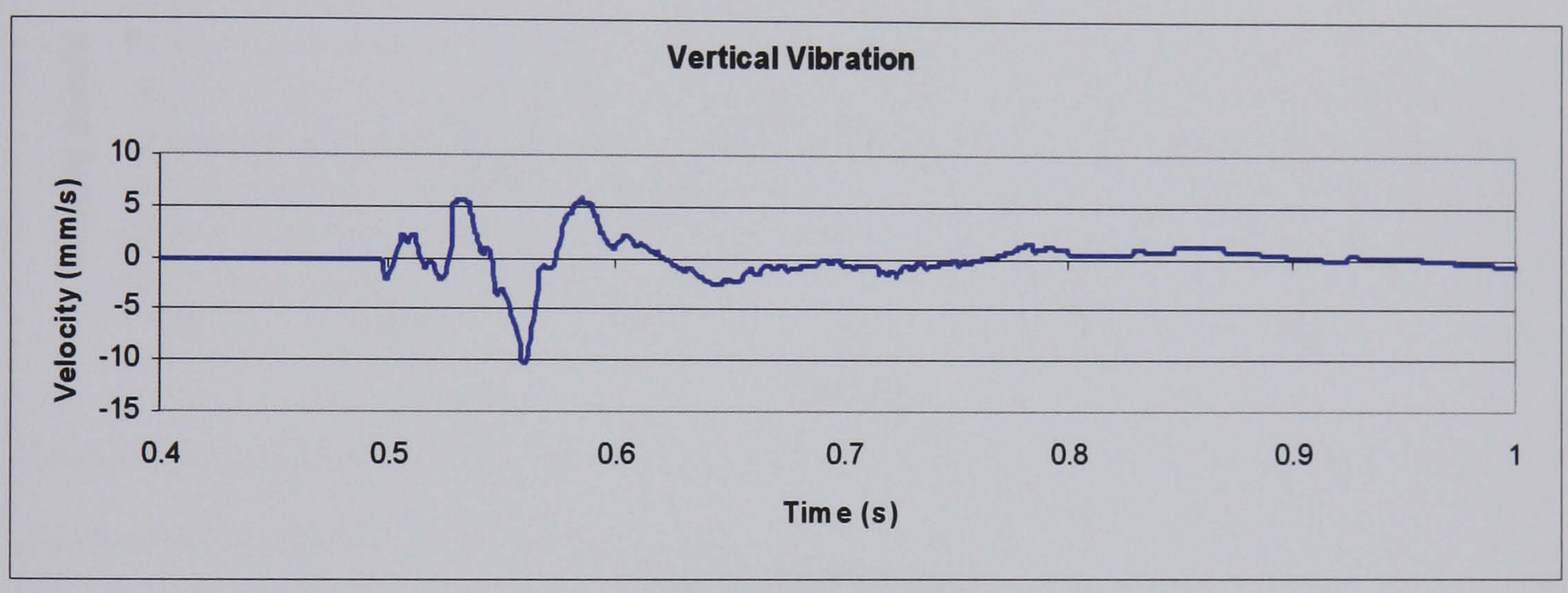

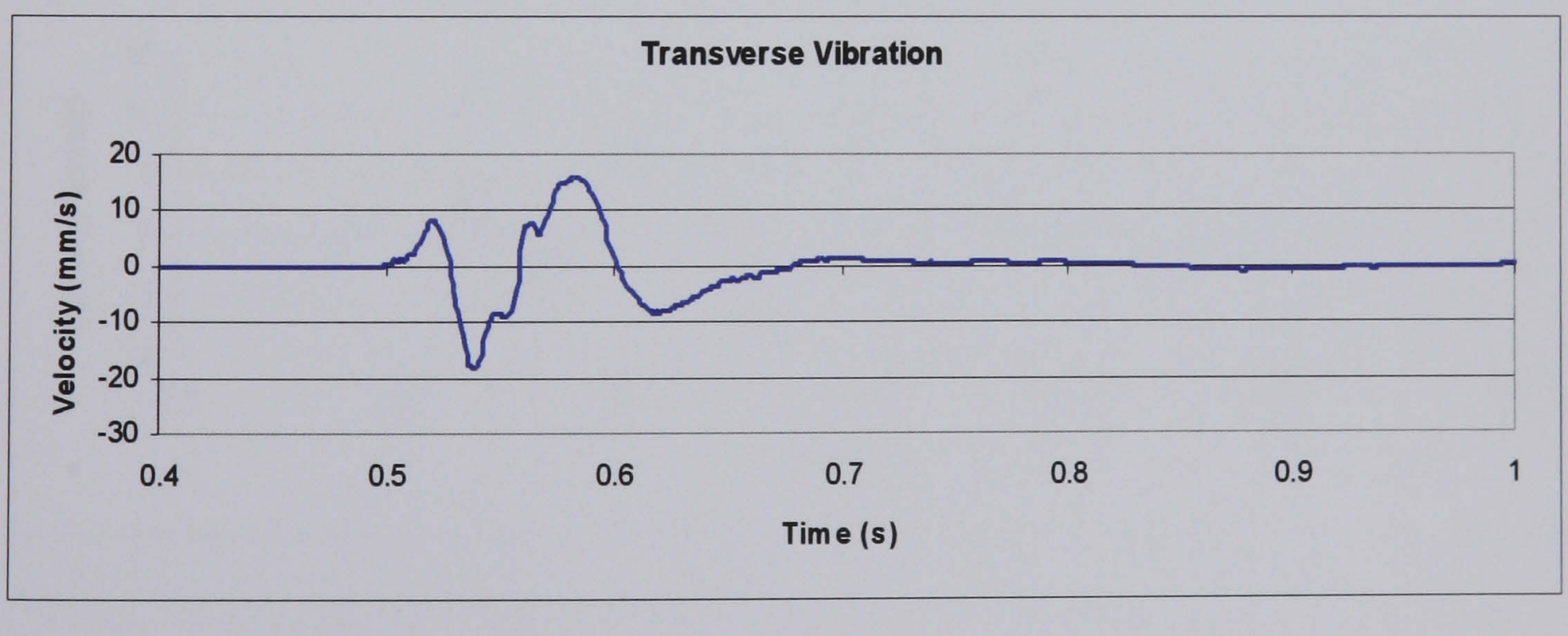

Figure 7.14 Determined second hole of a two hole shot from Melton Ross chalk quarry at 50 metres

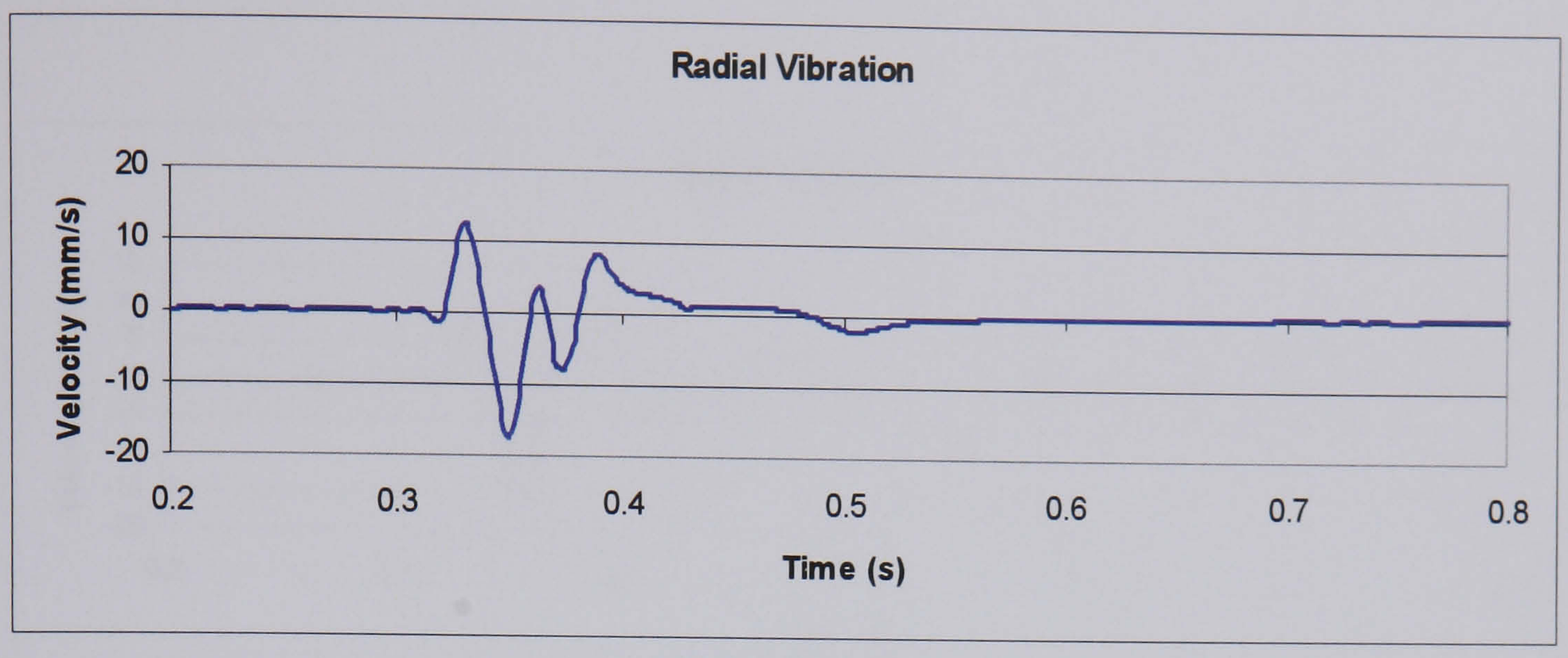

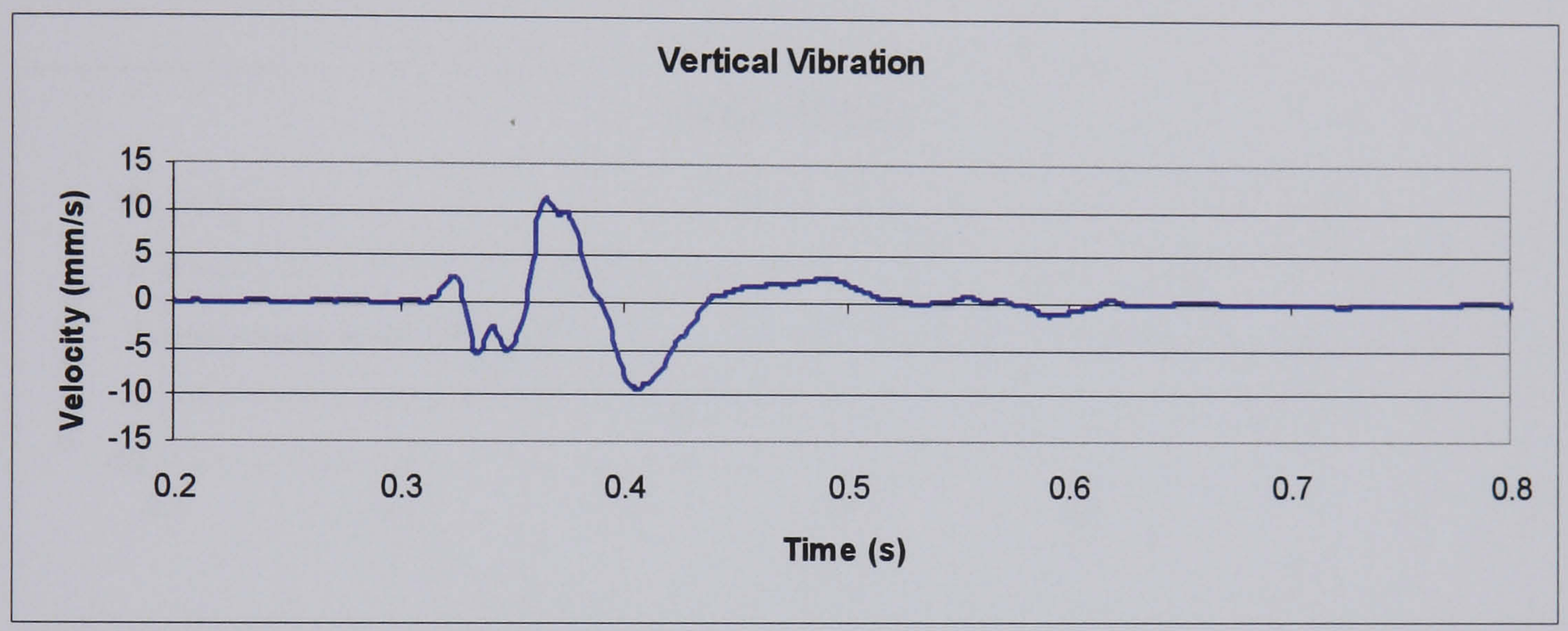

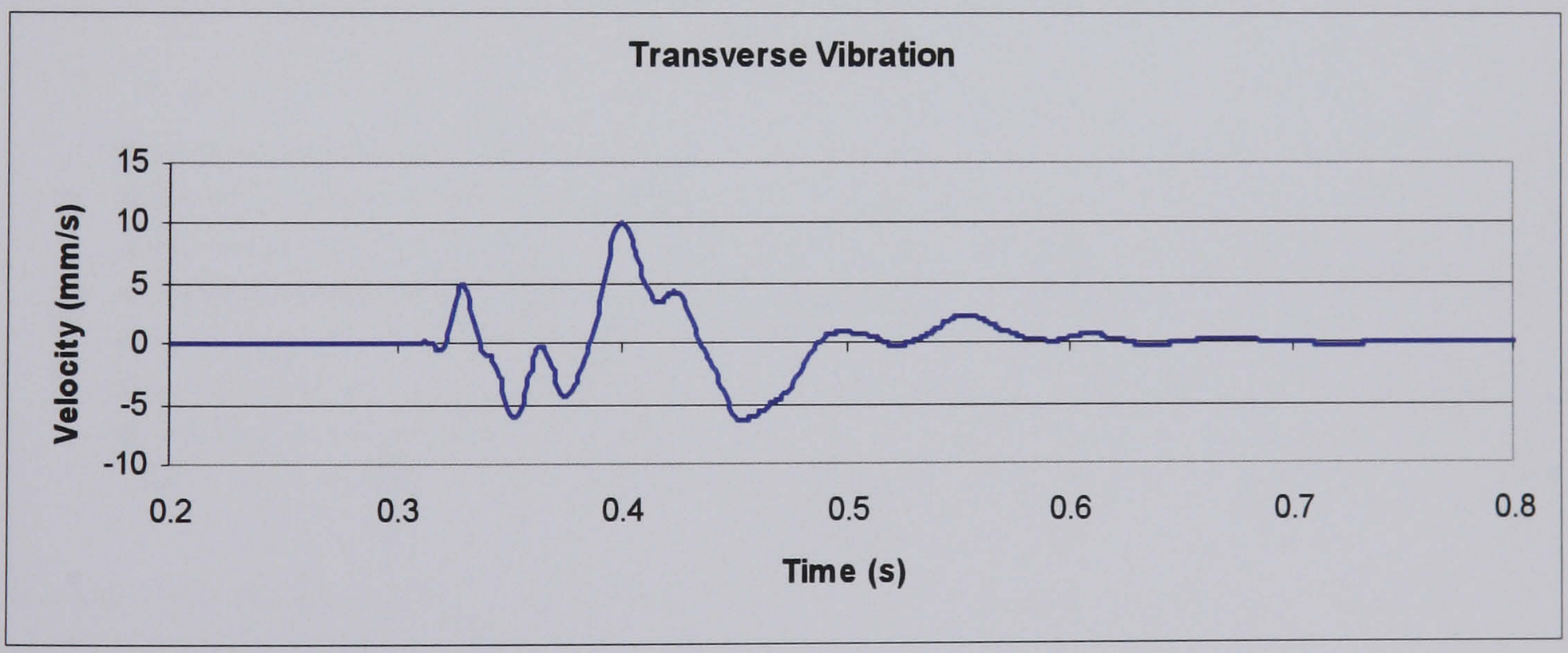

Figure 7.15 Determined second hole of a two hole shot from Melton Ross chalk quarry at 60 metres

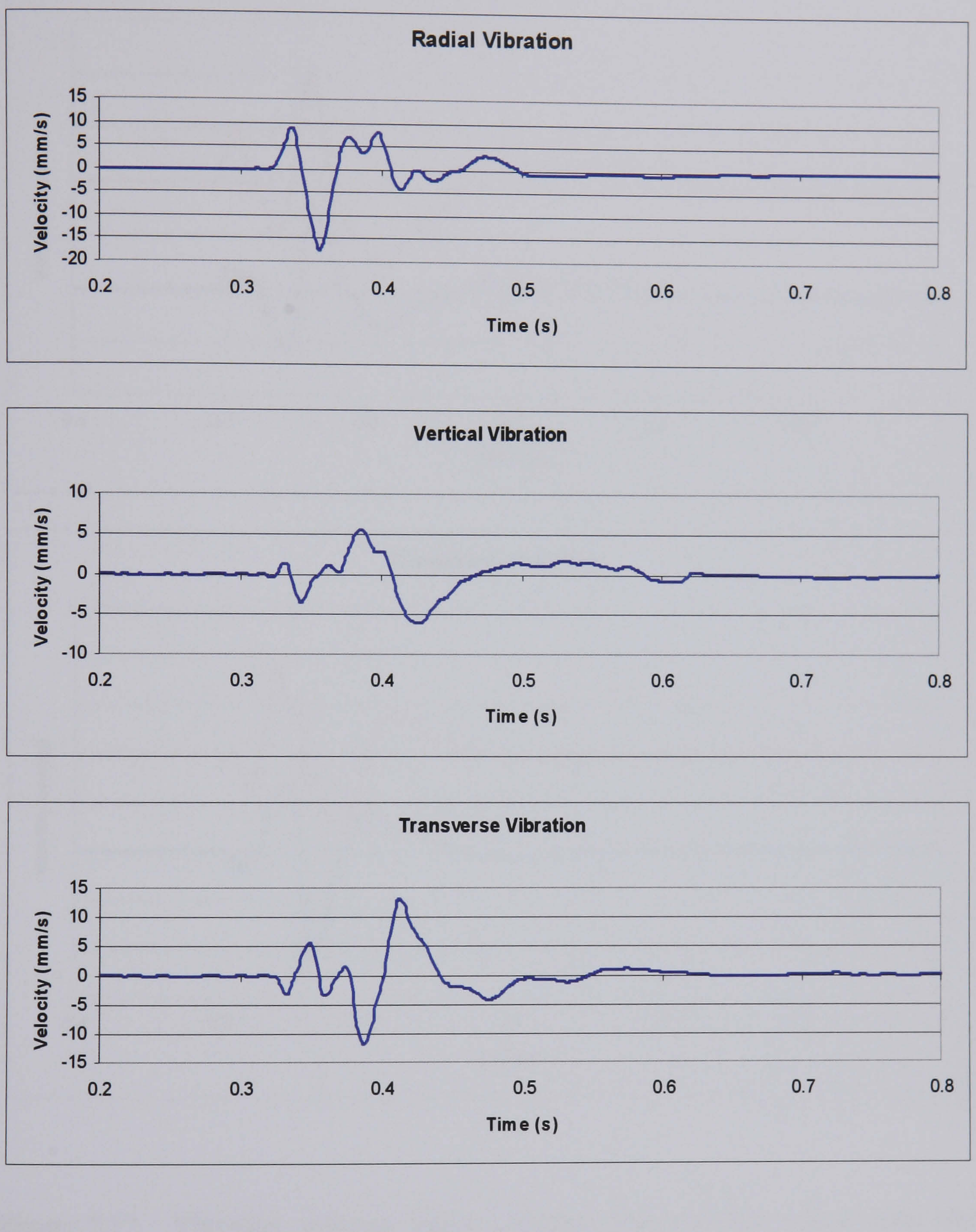

Figure 7.16 Determined second hole of a two hole shot from Melton Ross chalk quarry at 70 metres

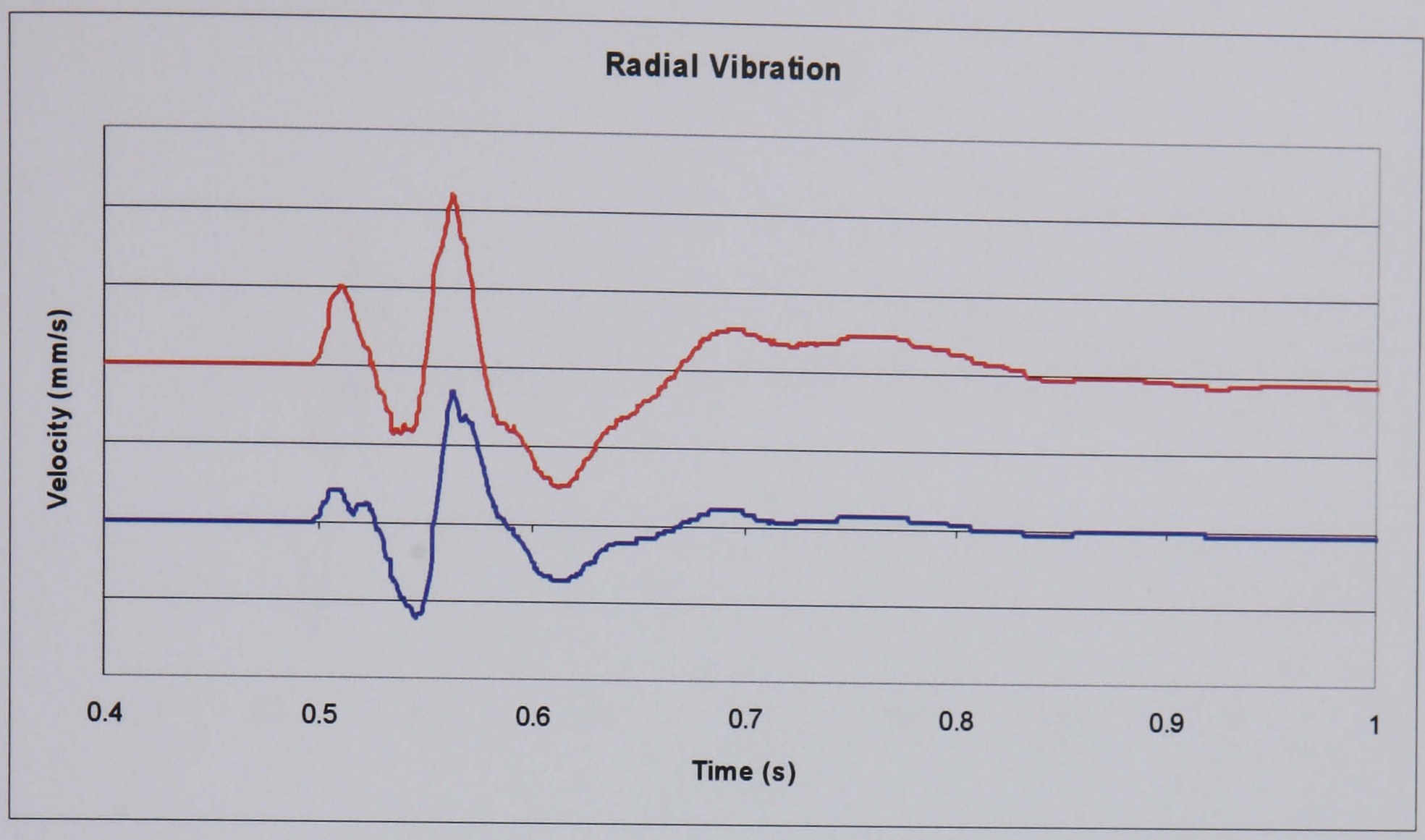

Figure 7.17 Vibration velocity traces showing the recorded single hole shot (lower) compared with the inverted determined second hole shot (upper) at 50 metres. both traces are on the same scale.

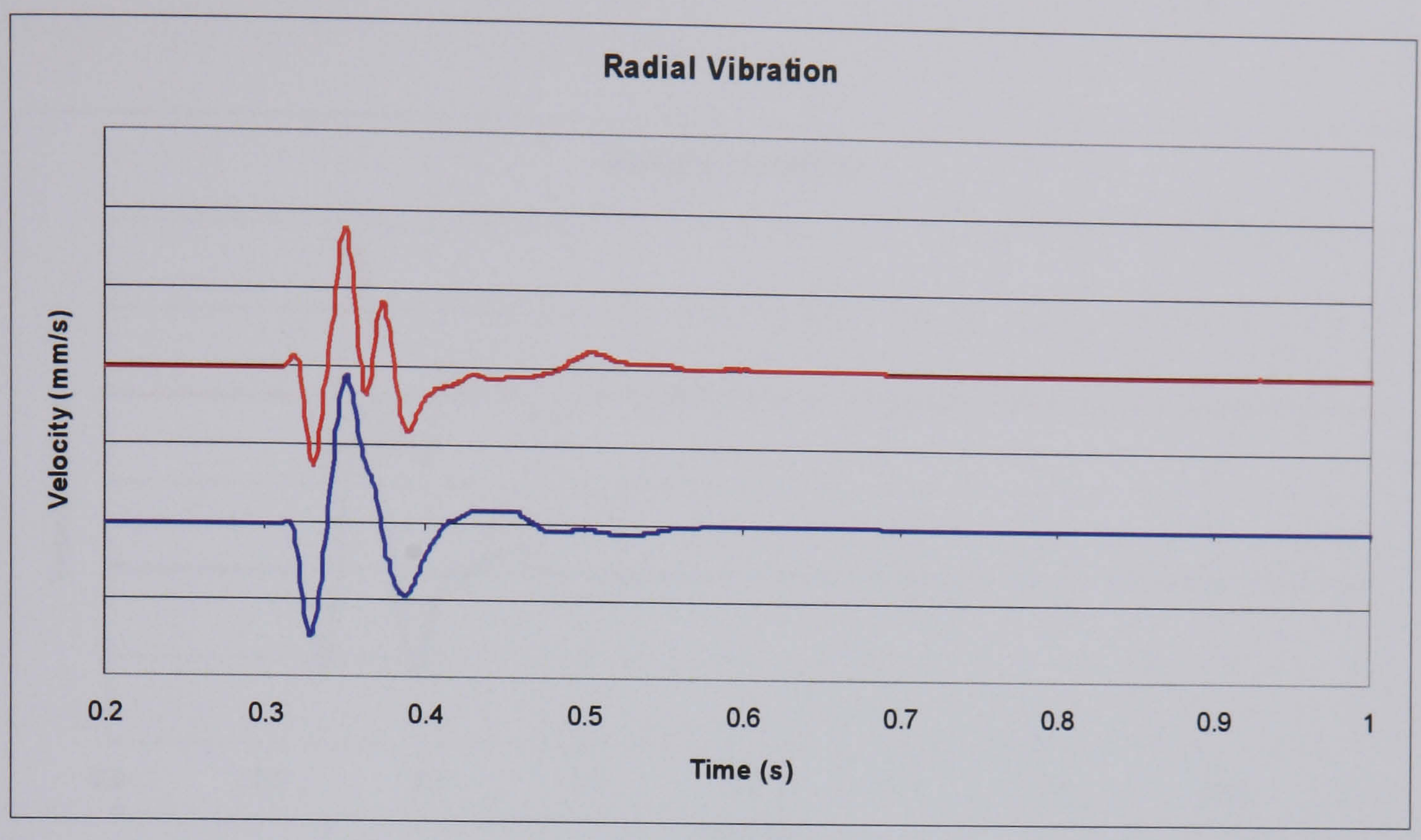

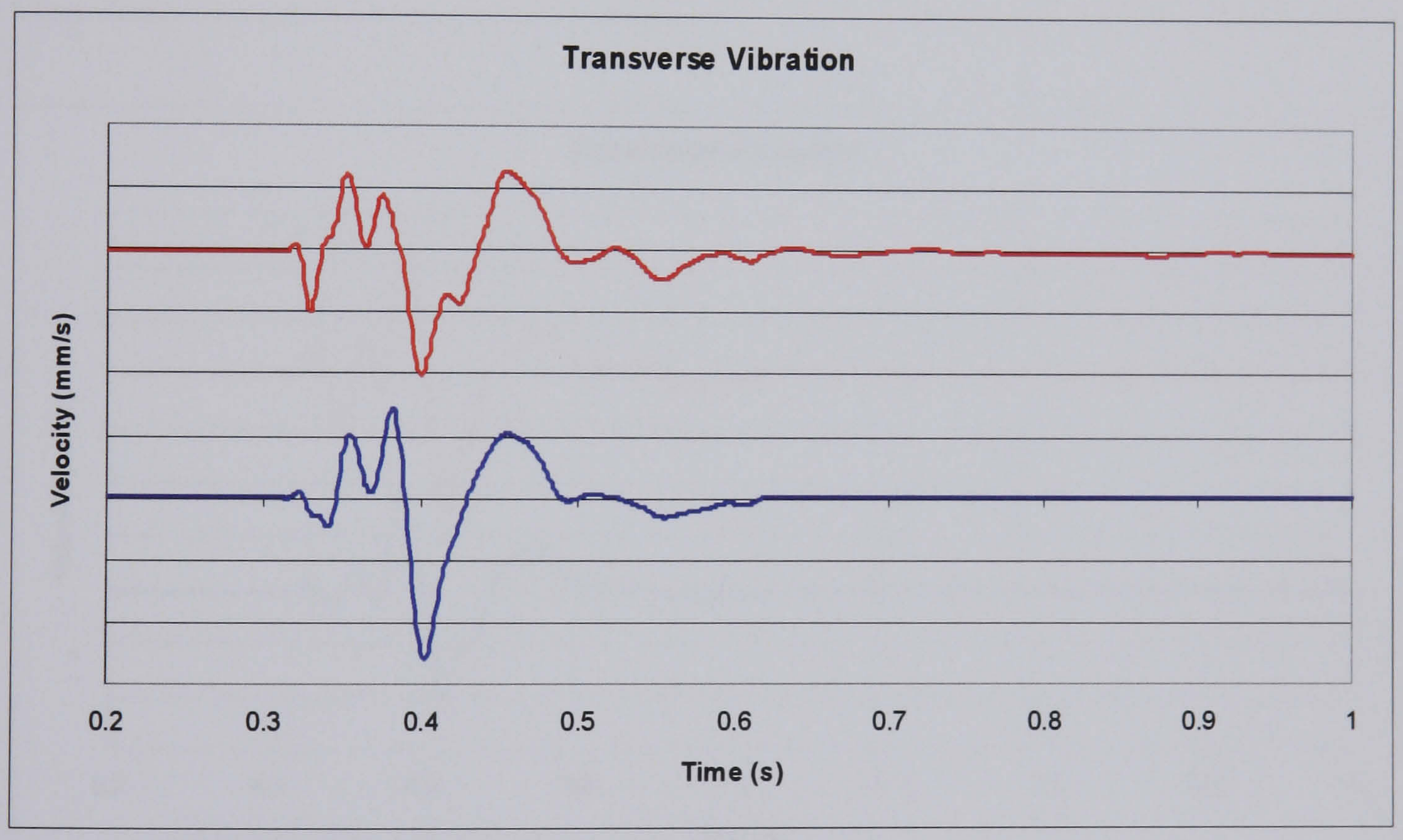

Figure 7.18 Vibration velocity traces showing the recorded single hole shot (lower) compared with the inverted determined second hole shot (upper) at 60 metres. both traces are on the same scale.

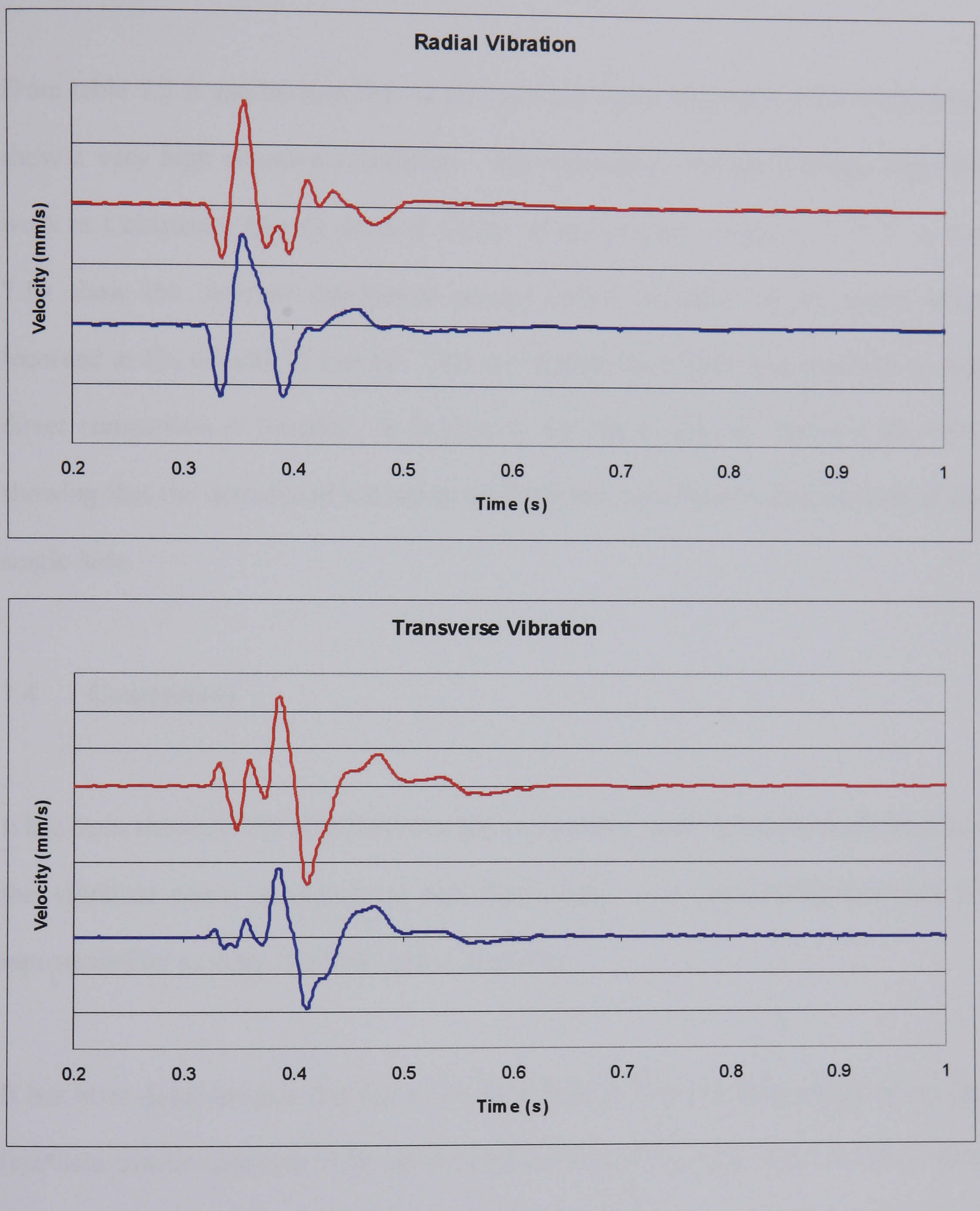

Figure 7.19 Vibration velocity traces showing the recorded single hole shot (lower) compared with the inverted determined second hole shot (upper) at 70 metres. both traces are on the same scale.

and 70 metre recordings show a good fit is it likely that this poor fit can be attributed to an equipment problem however further study may be warranted.

From table 7.3 it can be seen that in all cases the radial and transverse components show a very high negative correlation. This coincides with the findings from the work at Coldstones Quarry detailed earlier in this chapter. Figures 7.17, 7.18 and 7.19 show the inverted determined second holes compared to the single holes recorded at 50, 60 and 70 metres. The two signals have been synchronised so that direct comparison is possible. It is clear to see the similarities between the holes showing that the determined second hole of the two hole blast is an inversion of the single hole.

7.4 Conclusions

It has been shown in the near field that the assumption made in hybrid modelling that the vibration trace generated by individual holes in a production shot can be represented by a single hole test shot is incorrect.

It has been demonstrated that for a two hole blast if the vibration generated by the first hole can be assumed to be represented by that of a single hole test blast, then with an inter-hole timing of 25ms the vibration from the second hole is represented by the inversion of the vibration trace from a single hole test blast in the radial and transverse directions.

The reason for this inversion is not currently understood. It seems that as this effect is only apparent in the radial and transverse directions that it is limited to body waves. This theory is also backed up by the fact that hybrid modelling has been used with much more success in the far field where body waves are far less prominent.

Chapter 7 – The Effect Of Dynamic Parameters Within A Two Hole Shot

.

PAGINATION AS IN ORIGINAL

8. DETERMINATION OF THE SIGNAL PRODUCED BY INDIVIDUAL HOLES OF A MULTI HOLE SHOT.

8.1 Introduction

It was demonstrated in Chapter 7 that in the near field the vibration signal generated by the second hole of a two hole blast is not the same as that generated by the first hole. This finding is important as one of the primary assumptions of hybrid modelling is that every hole produces the same vibration signature.

Before the findings from Chapter 7 can be used in full scale hybrid modelling it is necessary to determine whether all holes after the first in a production blast follow the pattern seen in Chapter 7.

8.2 Subtraction of single hole test shot vibration signatures from a three hole shot at a chalk quarry.

In order to attempt to find the signal produced by each hole of a larger blast a single hole and a three hole blast were fired and the resulting vibration recorded at various points. The single hole was then subtracted from the start of the three hole. The single hole was then inverted and subtracted from the remainder of the three hole signal at times corresponding to the initiation of the holes. This would leave either the second or third hole depending on the inter-hole time used.

The experiment was carried out at the same chalk quarry as described in Chapter 7. For this experiment the top bench of the quarry was used, which was not as wide and the surface more broken than the lower bench which had been used previously. This led to difficulty in laying out equipment. The equipment was finally positioned as shown in figure 8.1.

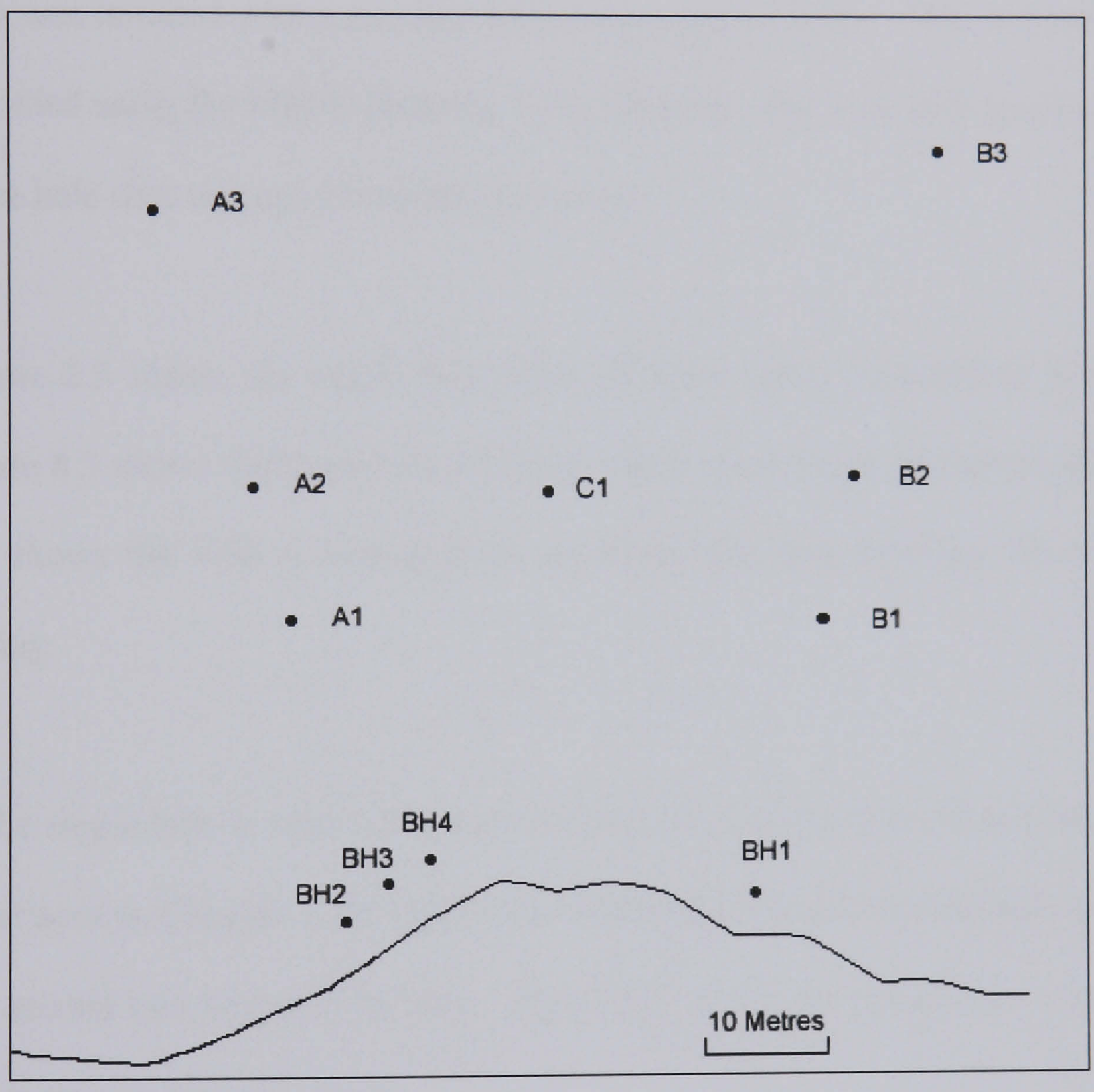

Figure 8.1 GPS survey plot of blast holes and monitoring locations for three hole experiment at Melton Ross Chalk Quarry.

The 15 channel seismograph was laid out in positions A2, A3, B2, B3 and C1, which are all on the same bench as the blasts. Positions A1 and B1 were instrumented with White digital seismographs.

The four holes were drilled to a depth of 16 metres and loaded with approximately 110Kg of site mixed ANFO from a small hopper. The three hole shot was initiated with a nominal inter-hole delay of 25ms. This was accurately recorded using the MREL Datatrap VoD recorder. The inter hole spacing for the three hole shot was approximately 4 metres.

Figure 8.2 shows the single hole blast vibration traces recorded at 60 metres, figure 8.3 shows the three hole vibration traces recorded at 60 metres and figure 8.4 shows the VoD recording from the three hole shot detailing the inter-hole timing.

If the single hole is subtracted from the beginning of the three hole blast, as had been done in Chapter 7, the remainder of the signal should theoretically represent the second two holes of the blast. Figure 8.5 shows the remaining two holes of the recording from 60 metres.

Chapter 8 - Determination Of The Signal Produced By Individual Holes Of A Multi-Hole Shot.

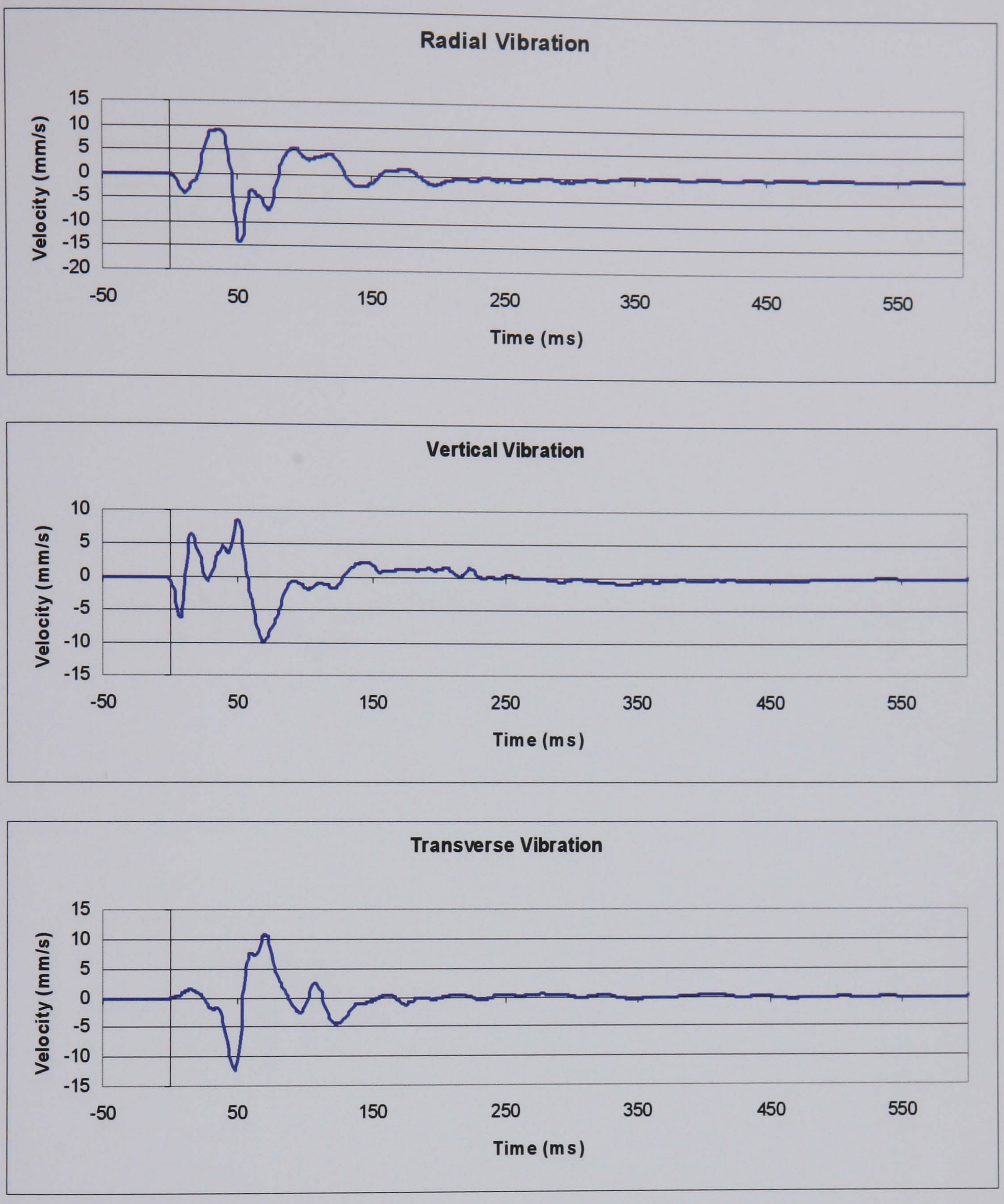

Figure 8.2 Single hole recording from Melton Ross Chalk Quarry at 60 Metres.

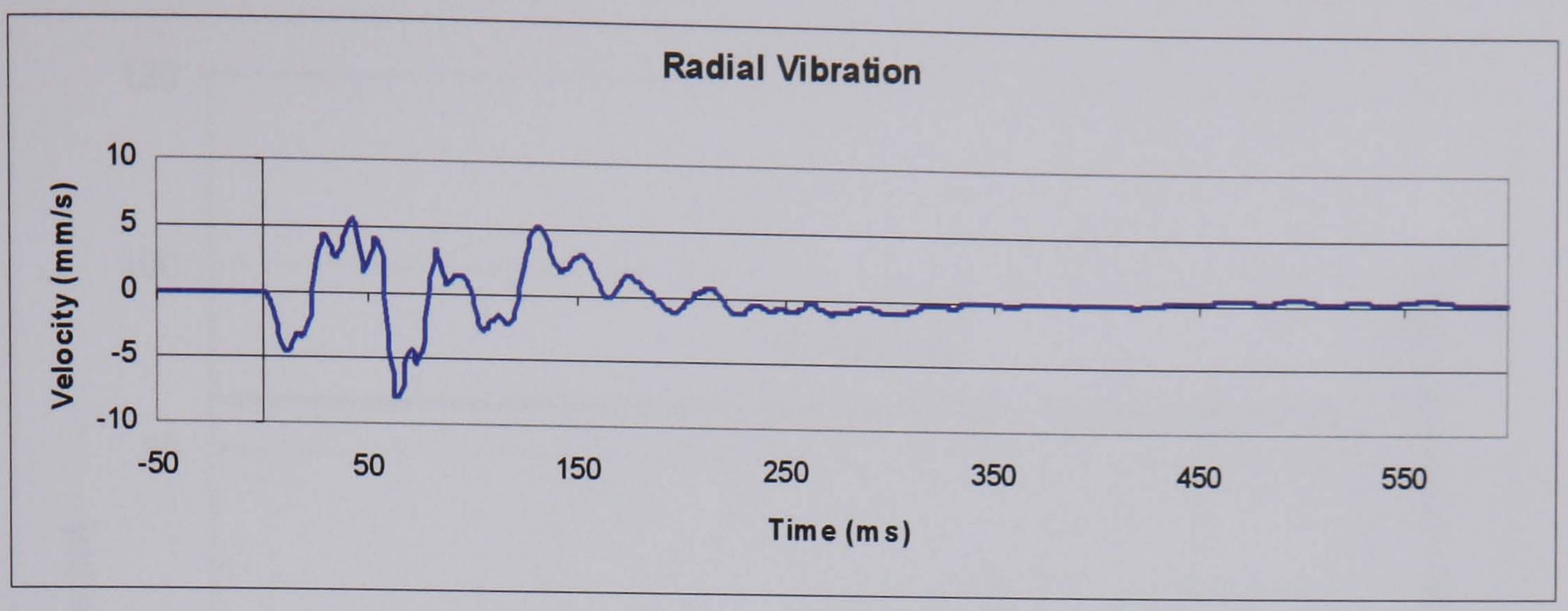

Figure 8.3 Three hole recording from Melton Ross Chalk Quarry at 60 Metres.

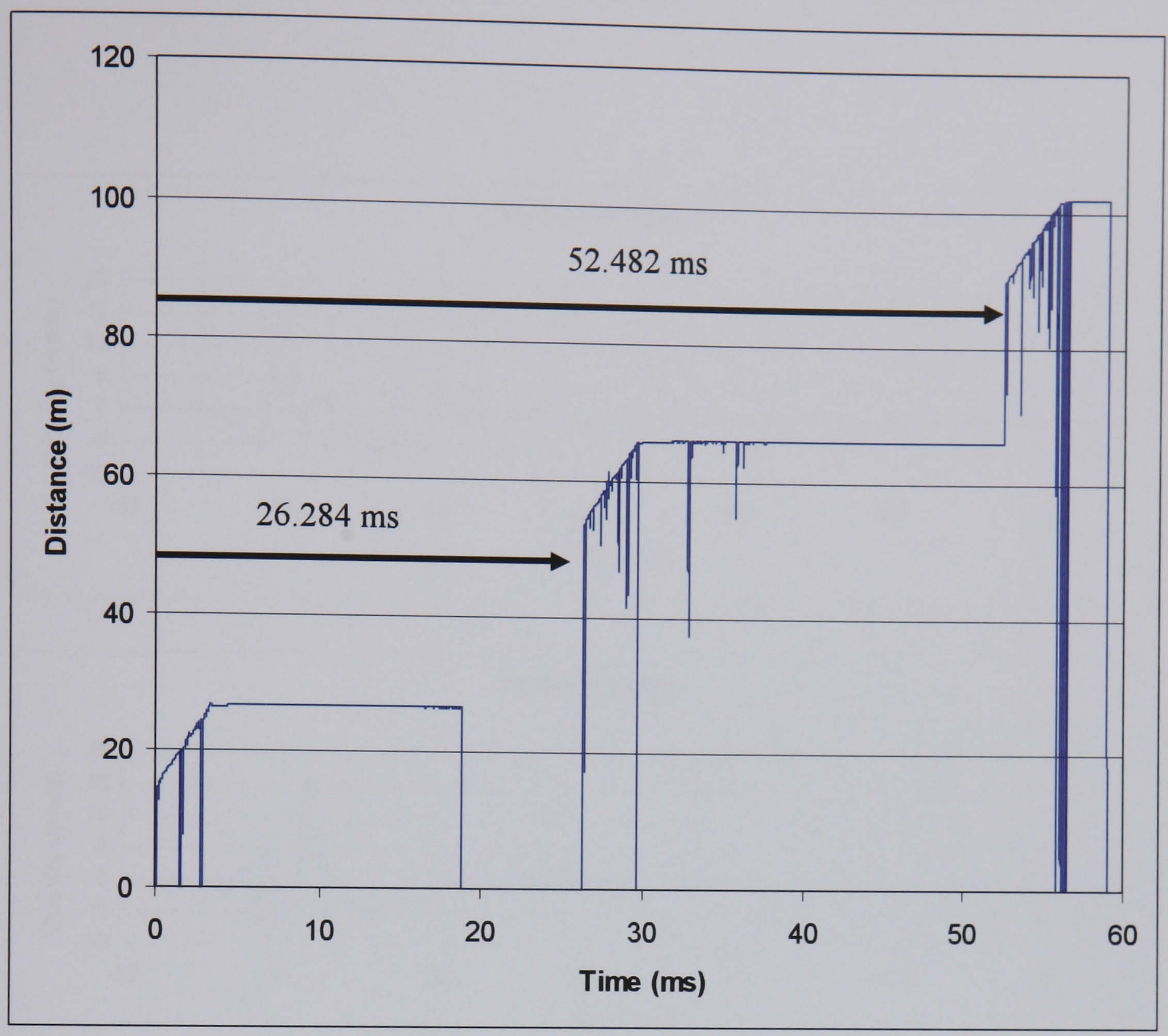

Figure 8.4 VoD recording of three hole blast at Melton Ross Chalk Quarry detailing inter hole timings.

It is difficult to gain any information from the determined second and third holes of the three hole blast as they are still convolved as one waveform. However if the theory explored in Chapter 7 holds true then it should be possible to disassemble the second and third holes by using an inversion of the single hole shot. This should only apply to the radial and transverse directions.

Chapter 8 - Determination Of The Signal Produced By Individual Holes Of A Multi-Hole Shot.

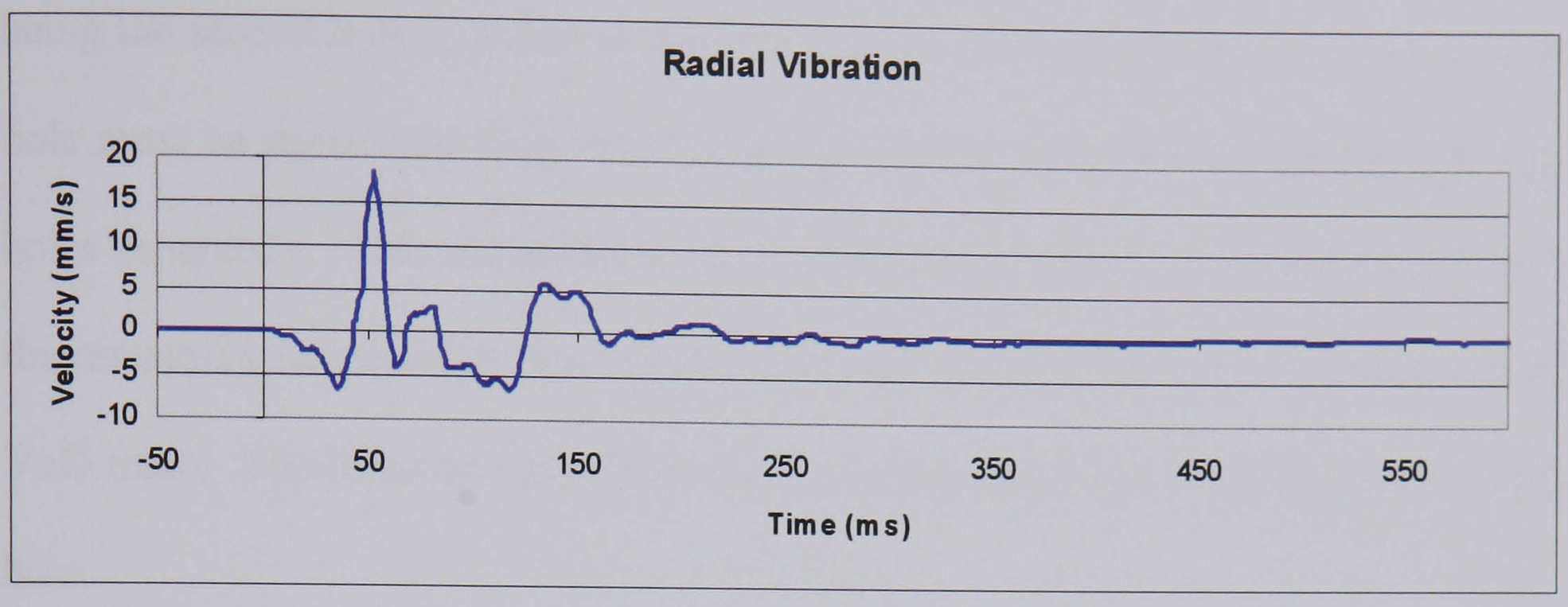

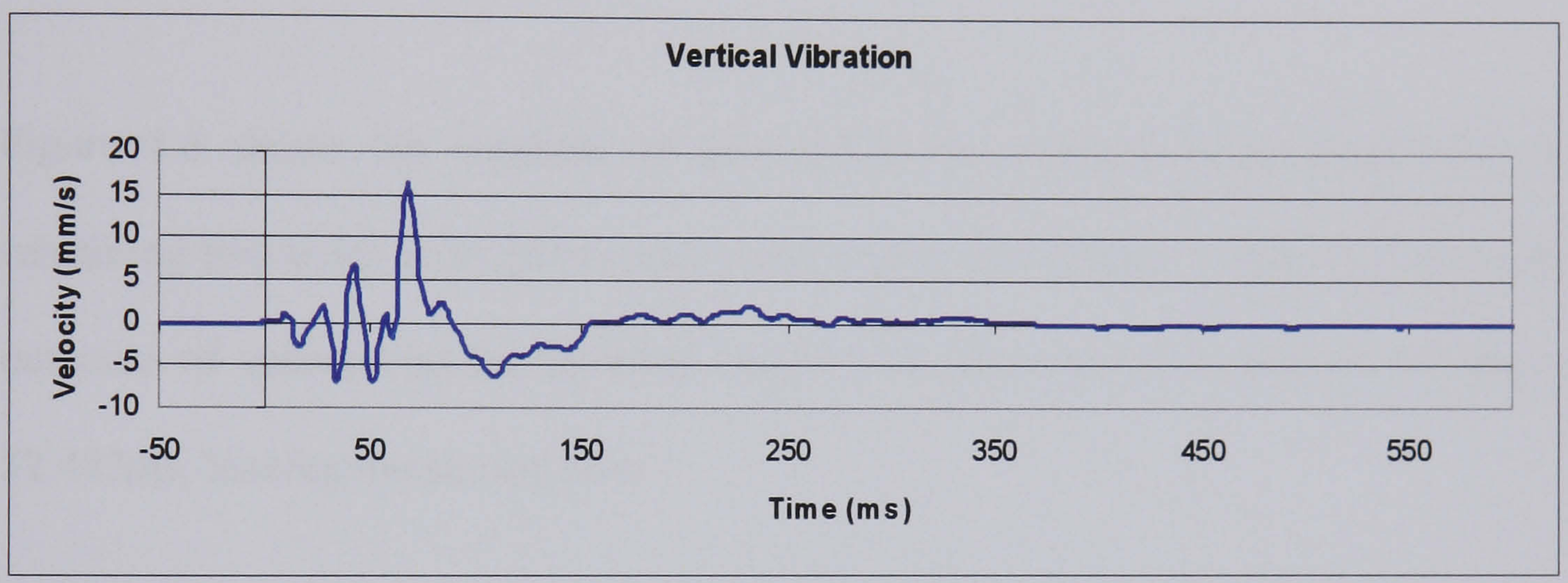

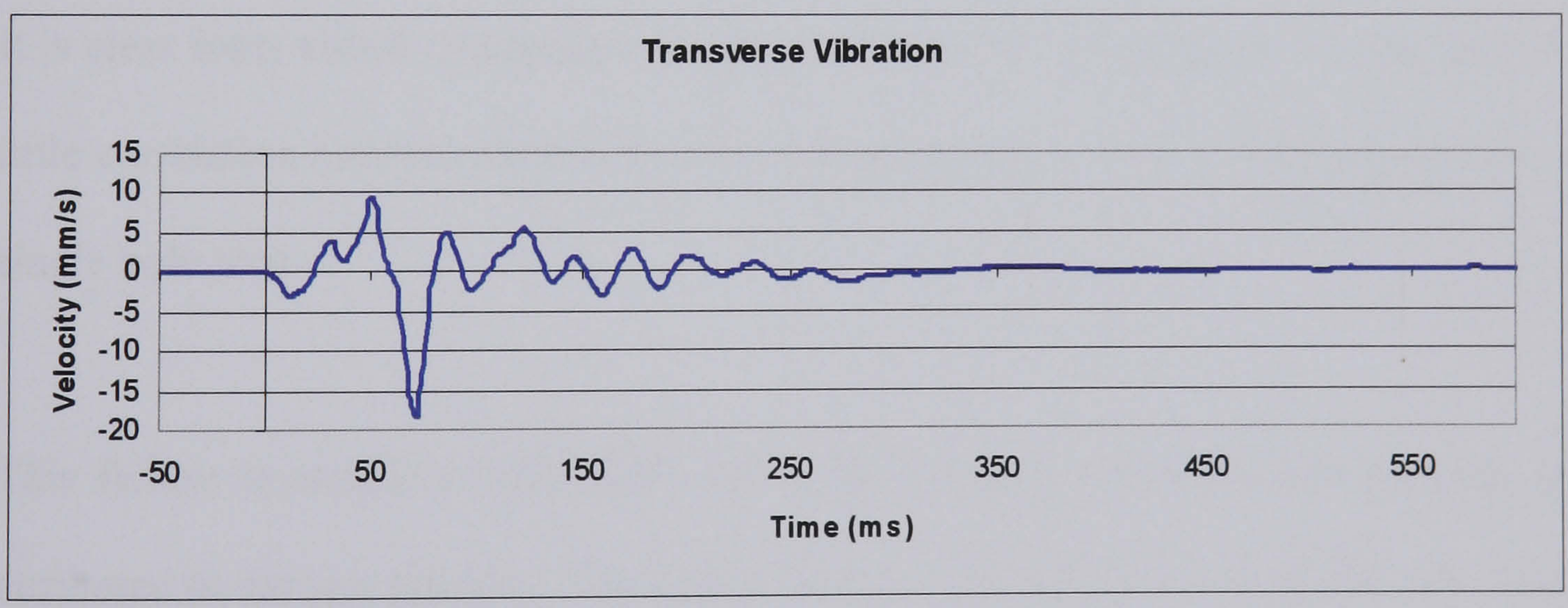

Figure 8.5 Determined second and third holes of a three hole recording from Melton Ross Chalk Quarry at 60 Metres

It is important to note that it is not known whether the inversion is a function of being the second hole in a shot or the last hole in a shot, therefore the inverted single hole must be subtracted from the remaining two holes as both the second and third holes separately. This means that the inverted single hole must be subtracted from the remaining two holes at times coinciding with the initiation times gained from the VoD trace. The times are 26.284ms for the second hole and 52.482ms for the third hole.

Figure 8.6 shows the outcome of subtracting the inverted single hole from the remaining two holes at 26.284ms and so leaving the third hole. Figure 8.7 shows the outcome of subtracting the inverted single hole from the remaining two holes at 52.482ms, leaving the second hole.

It is clear from visual comparison of figures 8.6 and 8.7 with figure 8.2 that there is little correlation between the determined remaining holes of the three hole shot and a single hole shot.

This failure to model a multi-hole shot using the earlier findings can possibly be attributed to various reasons. The first is that it is possible that the single hole blast does not accurately represent the individual holes of a three hole blast. As there is no previous work from this area of this quarry it is impossible to determine whether the single holes are repeatable.

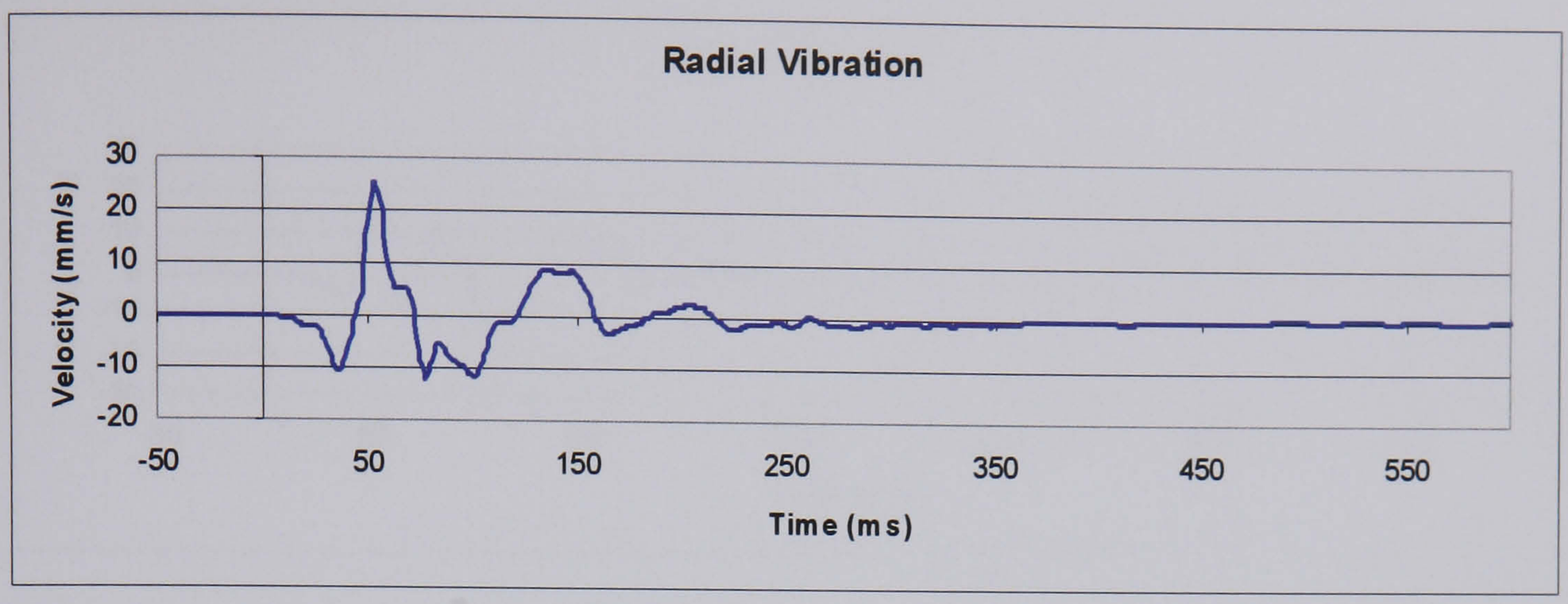

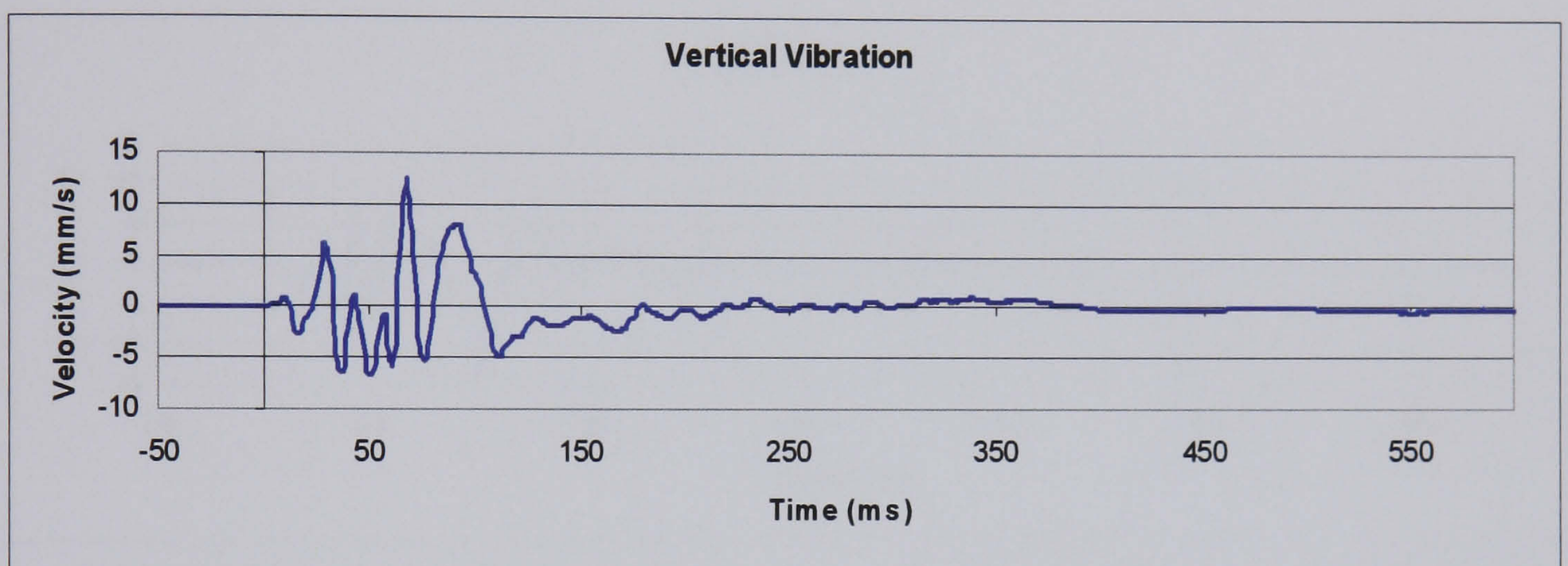

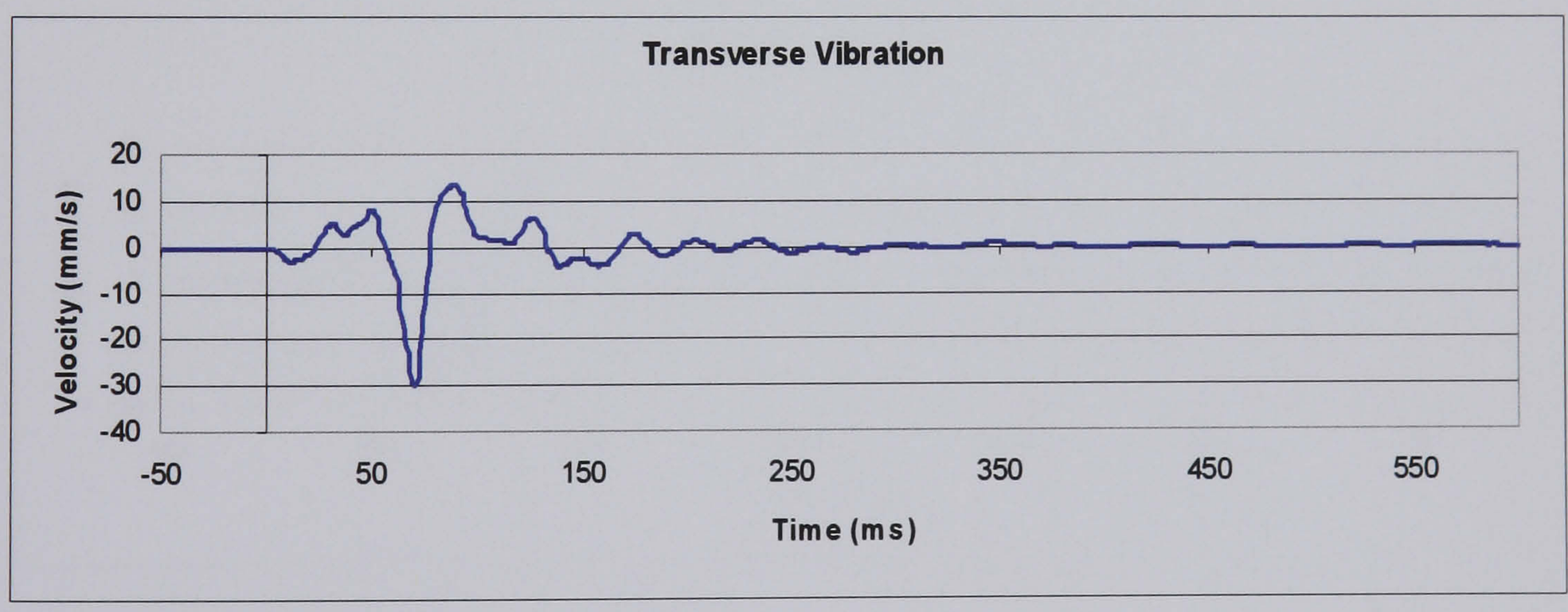

Figure 8.6 Determined last hole of three hole shot obtained by subtracting inverted single hole shot trace at 26.284ms.

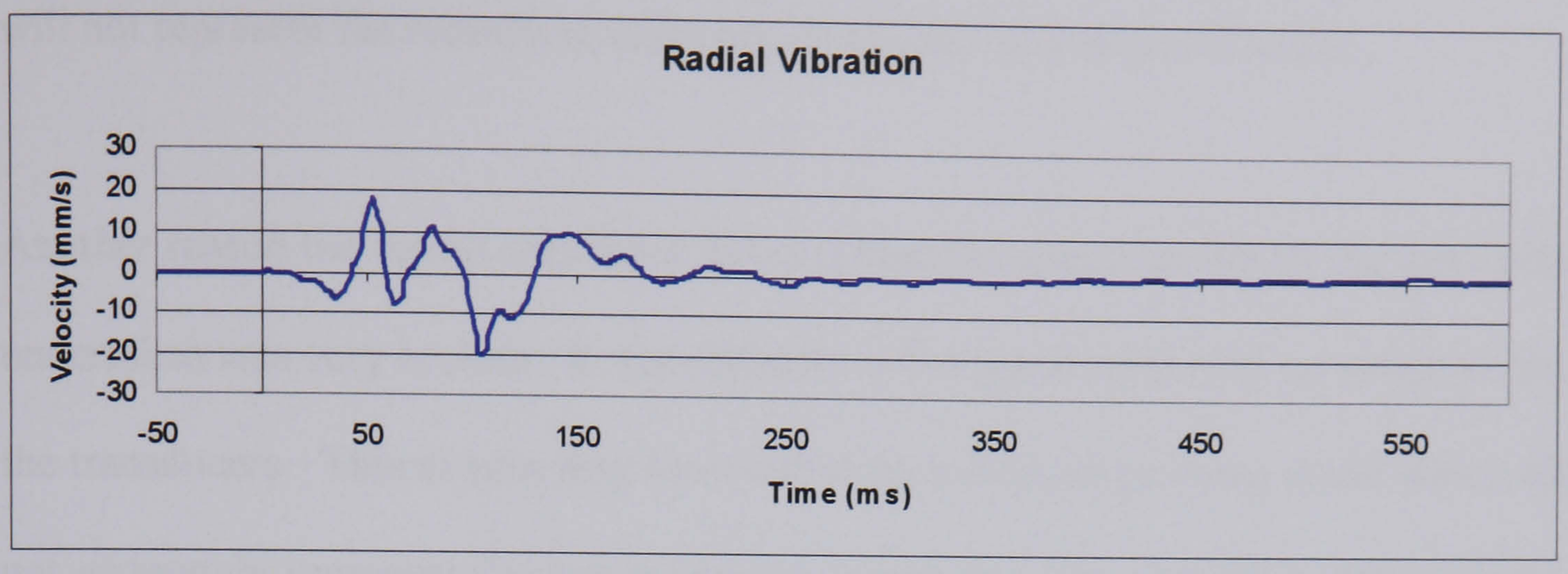

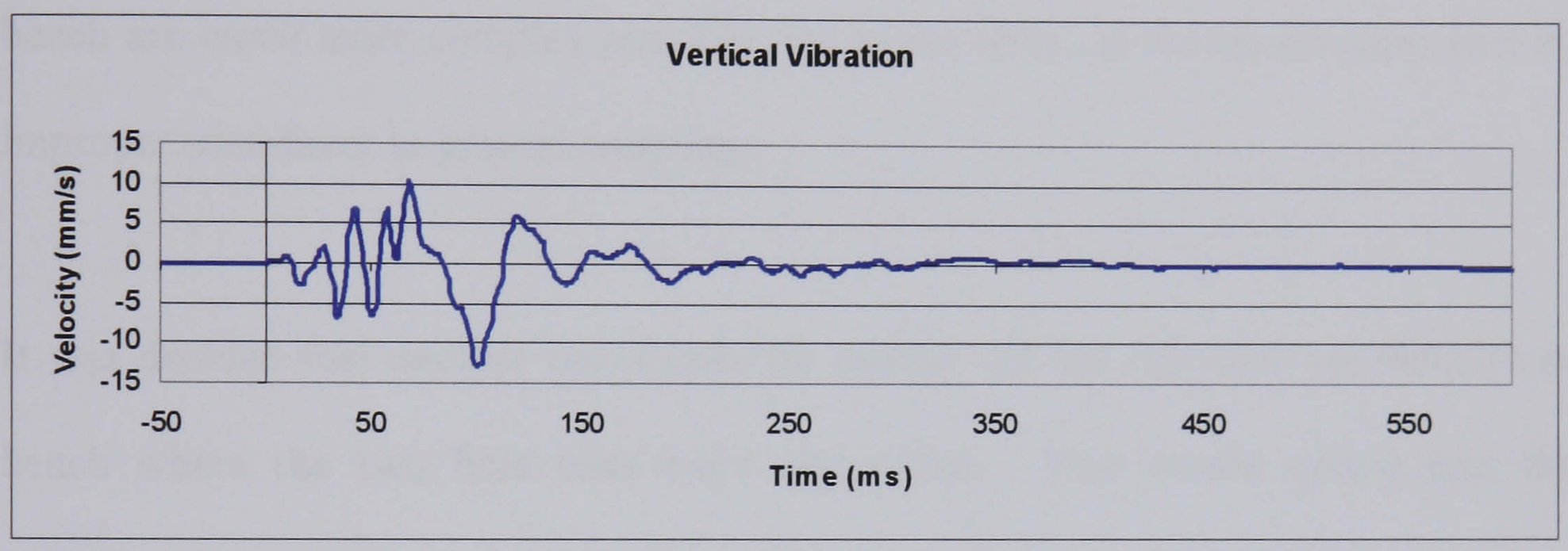

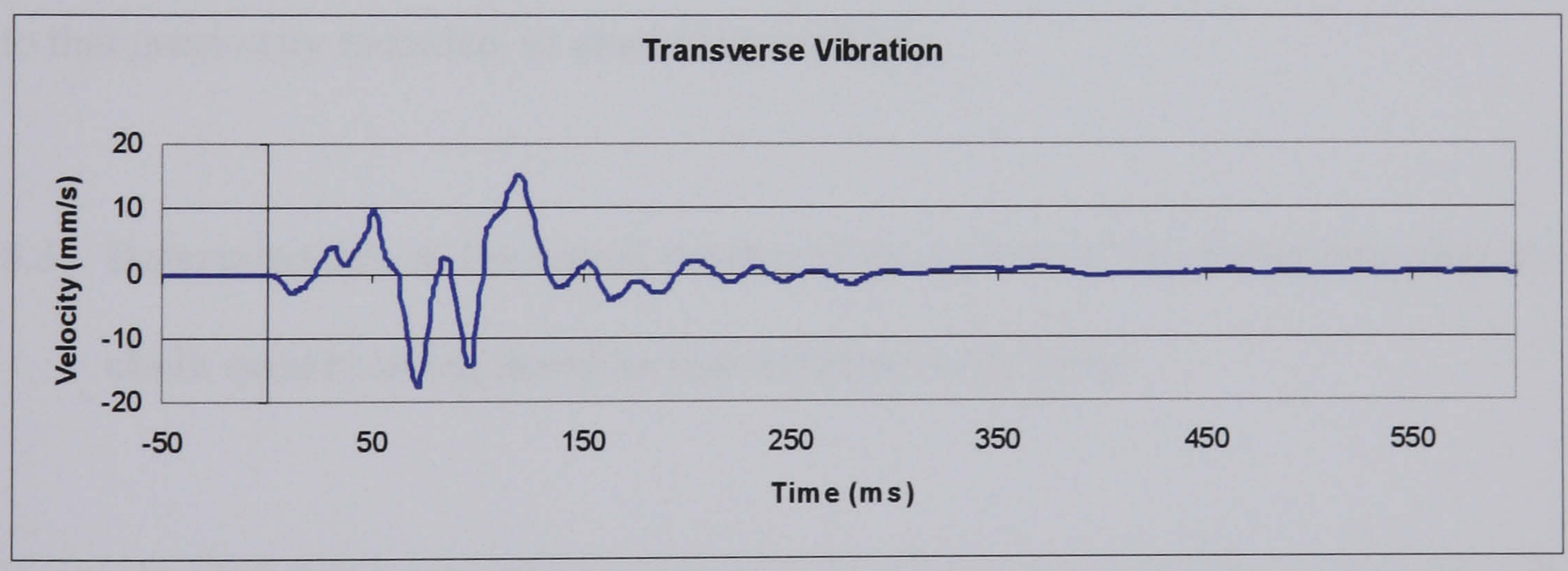

Figure 8.7 Determined second hole of three hole shot obtained by subtracting inverted single hole shot trace at 52.482ms.

If the single hole does not represent the first hole of the shot it stands to reason that it will not represent the remaining holes and the model will not be accurate.

Another reason the model may have failed is that the ground in which the tests were undertaken was very broken. It was difficult to find good solid rock on which to bolt the transducers. This in turn may have led to poor recordings being made which did not accurately represent the actual ground vibration. The recordings from the top bench are much more complex possibly due to the effect of resonance generated by improper transducer to ground coupling.

It was decided that another test should be carried out but this time on the bottom bench where the two hole tests were undertaken. This would ensure that the transducers were bolted to solid rock and the single hole could possibly be compared to that previously recorded, to ensure repeatability.

8.3 Determination of the signal produced by each hole of a three hole shot at a chalk quarry using iterative convolution techniques.

It was decided that a new approach should be used to determine the individual holes of a three hole shot. The main reason for requiring a new method was to determine whether or not there was an inversion of one or more of the holes in the three hole shot and, if not, what was the relationship of the single hole shot to the individual shots?

8.3.1 Iterative convolution method of determining individual holes in a multi-hole shot.

The method which was used to determine the signals produced was an iterative method based on convolving the single hole with a series of time impulse spectra. The time impulse spectra have impulses at each of the three times of initiation varying in magnitude from -2 to 2. This essentially gives a range of each of the holes from double magnitude inverted through to double magnitude non-inverted. The quality of the fit compared to the real three hole shot is then tested using a sum of squares of difference technique. The sum of squares of difference technique for comparing waveforms was chosen as although it is not the best method available it is very fast and the multiple iterations of the system mean that if a more complex system was used the time taken to process the data would render the system unworkable.

A computer program was written in HPVEE to carry out the technique. Figure 8.8 shows the system in action. The top window shows the current simulation and the bottom window shows the best fit between the real and simulated three hole shots.

8.3.2 Experimental work to determine the signal generated by each hole of a multi-hole shot.

A new test was undertaken on the lower bench of the chalk quarry close to the area where the two hole test was carried out in Chapter 7.

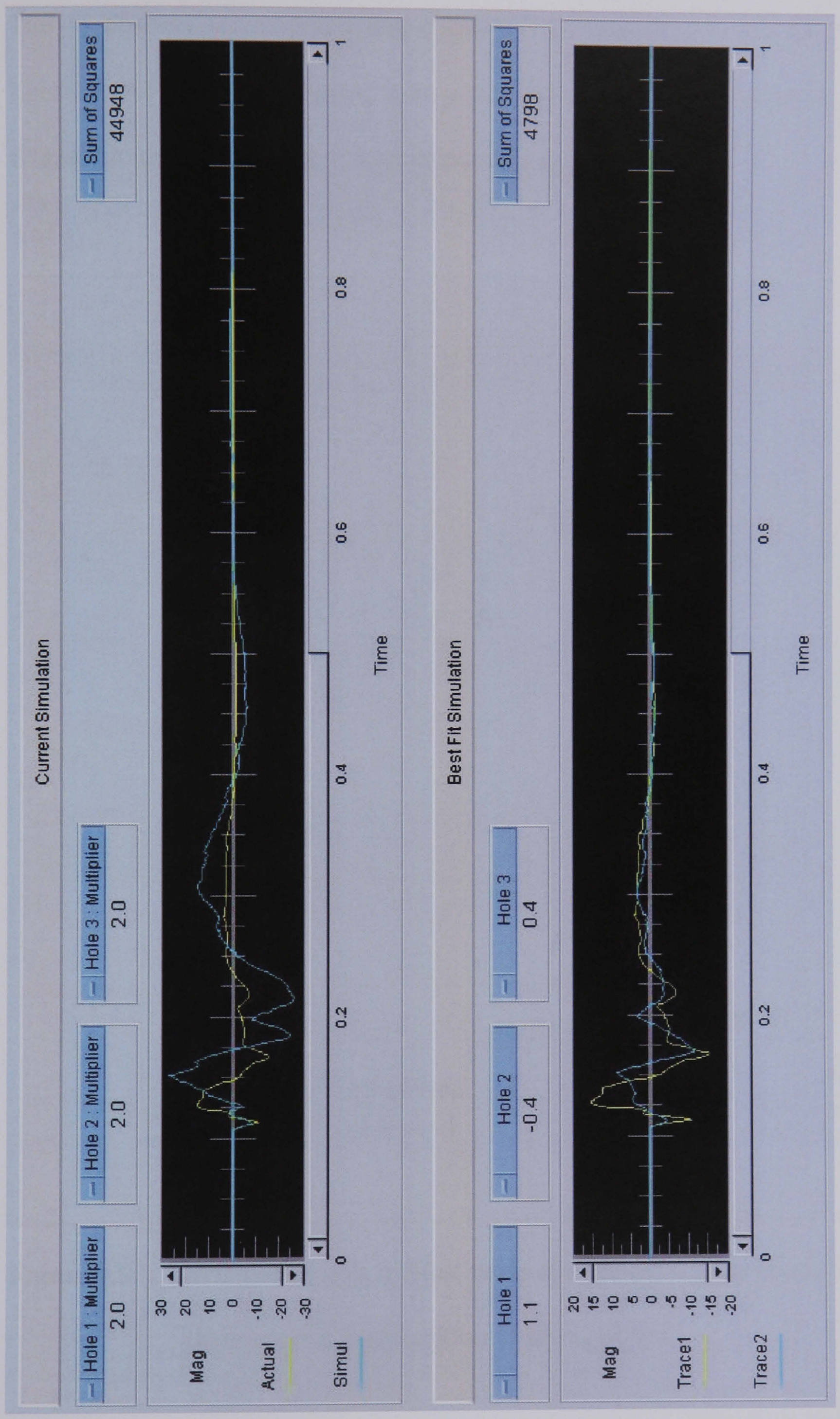

Figure 8.8 Iterative convolution system running in HPVEE.

Chapter 8 - Determination Of The Signal Produced By Individual Holes Of A Multi-Hole Shot.

Figure 8.9 shows the layout of the bench as recorded by the GPS survey equipment. The 15 channel seismograph was installed in locations A2, A3, B2, B3 and C1. Location A1 was instrumented with a triaxial array of accelerometers. Locations B1and A4 were instrumented with White seismographs

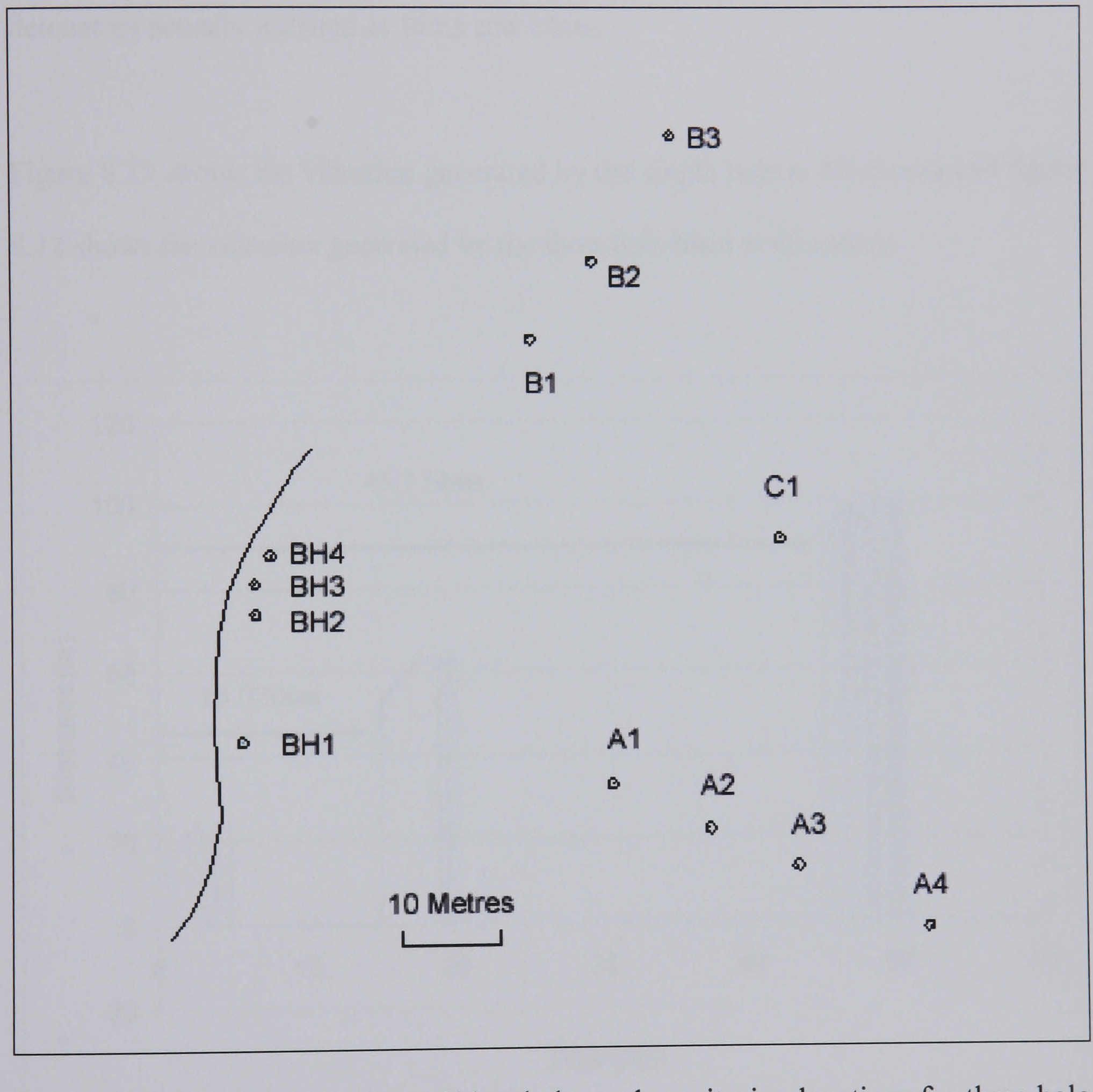

Figure 8.9 GPS survey plot of blast holes and monitoring locations for three hole experiment at Melton Ross Chalk Quarry

The holes were drilled, loaded and fired in a similar manner to previous blasts at this quarry with the exception of a 15ms inter hole delay.

Figure 8.10 shows the VoD recording made from the three hole shot. Note the inaccuracy in the hole firing times. The inter hole delay was nominally 25ms but the detonators actually initiated at 15ms and 45ms.

Figure 8.11 shows the vibration generated by the single hole at 60 metres and figure 8.12 shows the vibration generated by the three hole blast at 60 metres.

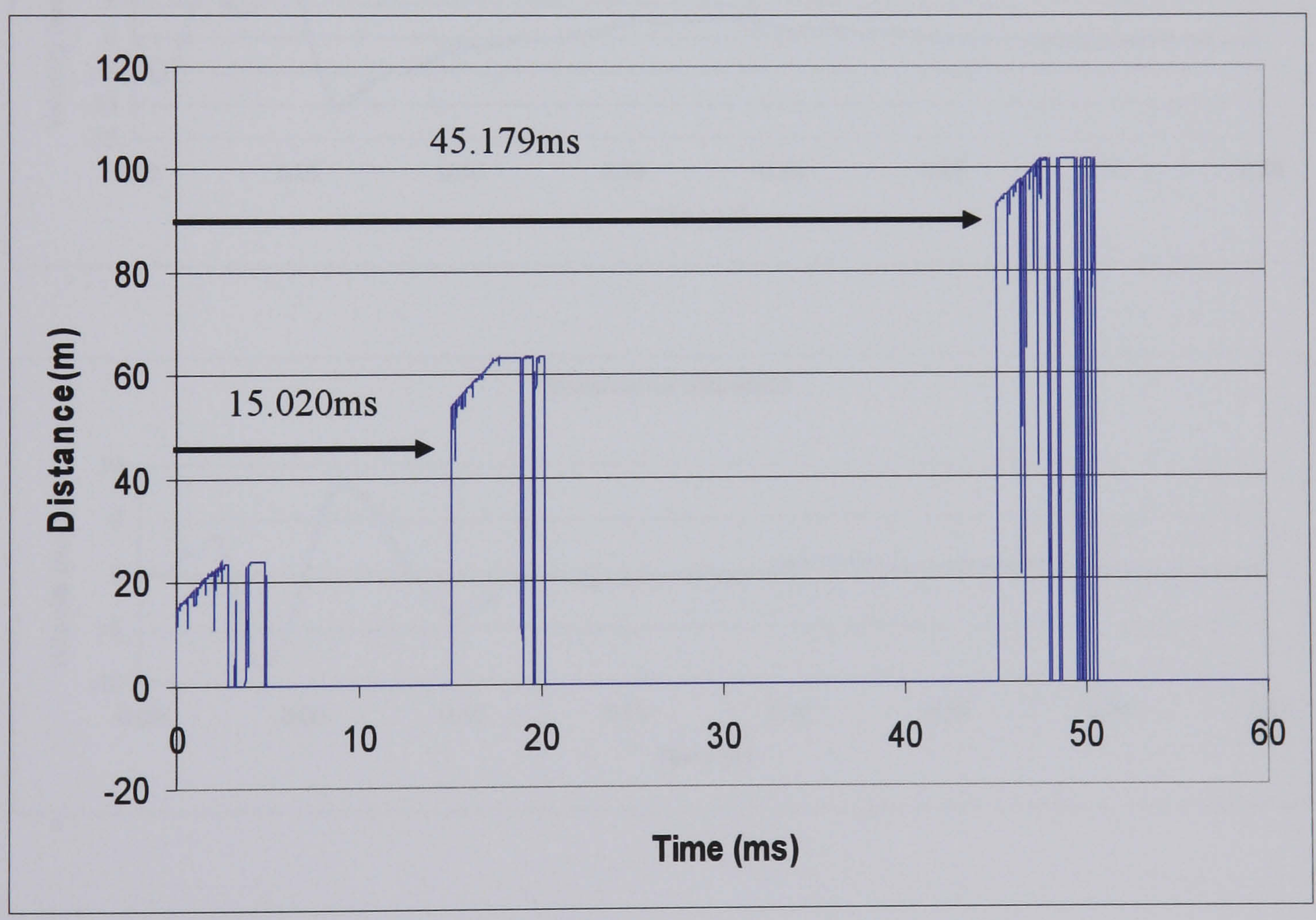

Figure 8.10 VoD recording of three hole blast at Melton Ross Chalk Quarry detailing inter hole timings.

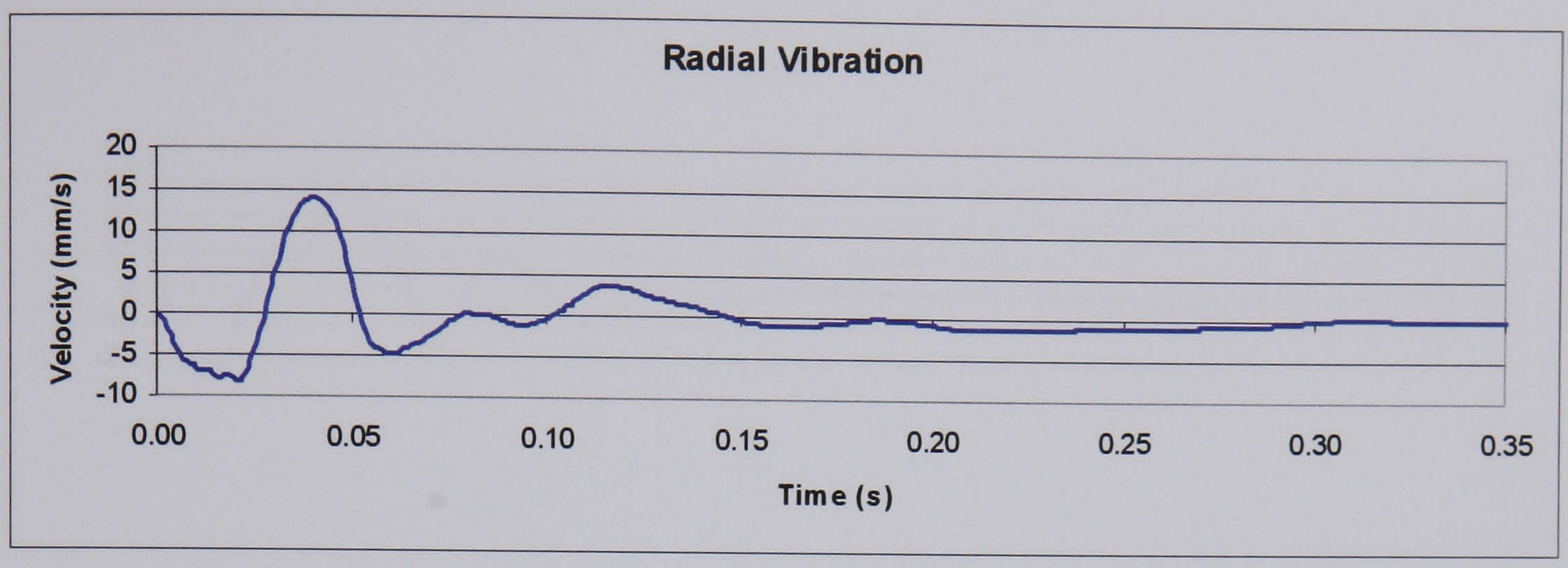

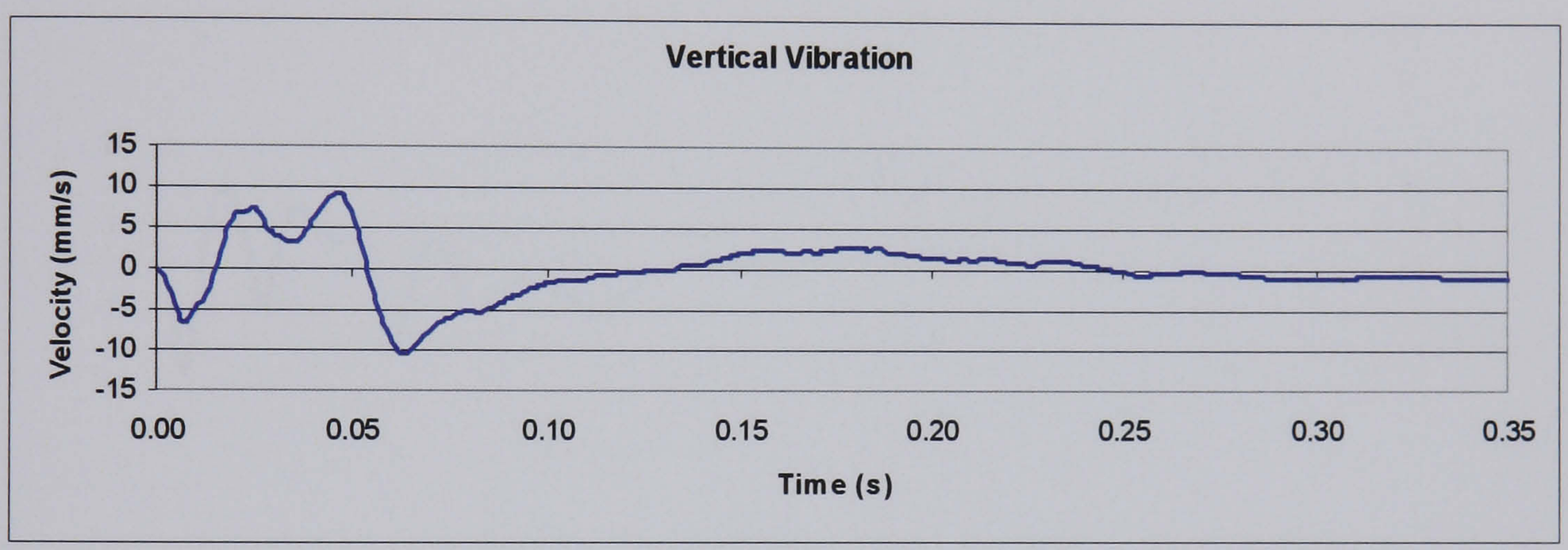

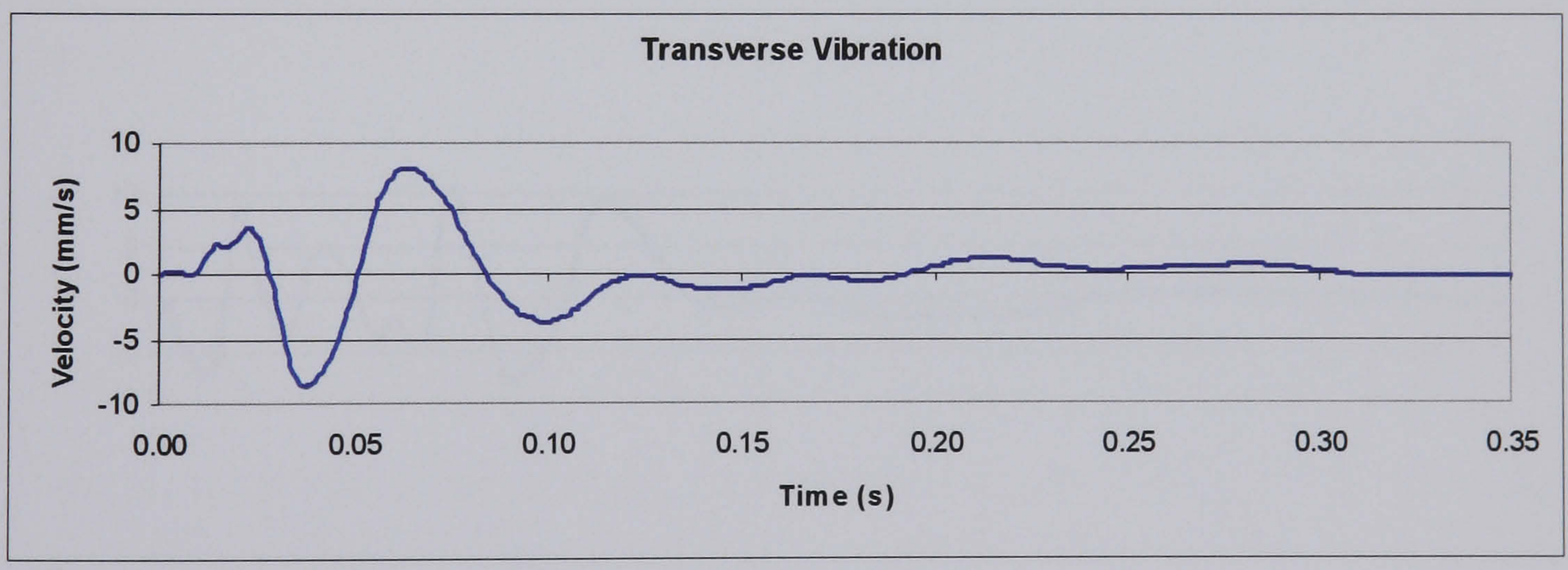

Figure 8.11 Single hole recording from Melton Ross Chalk Quarry at 60 Metres

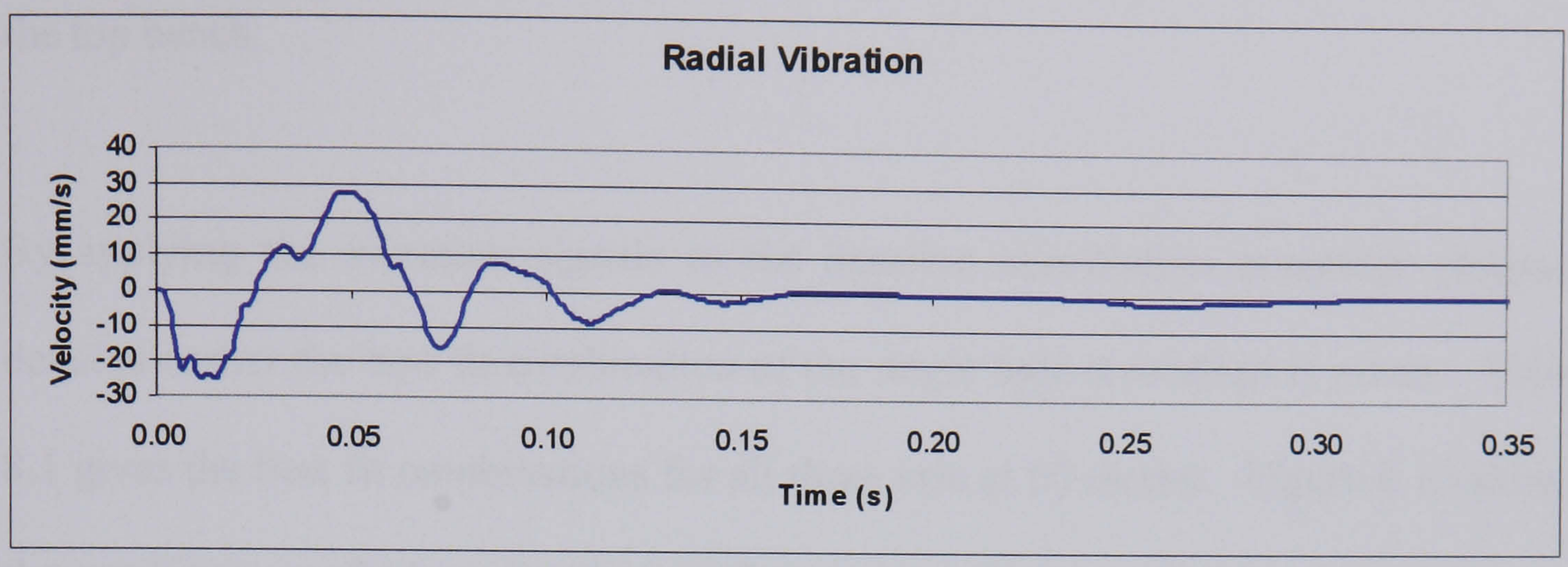

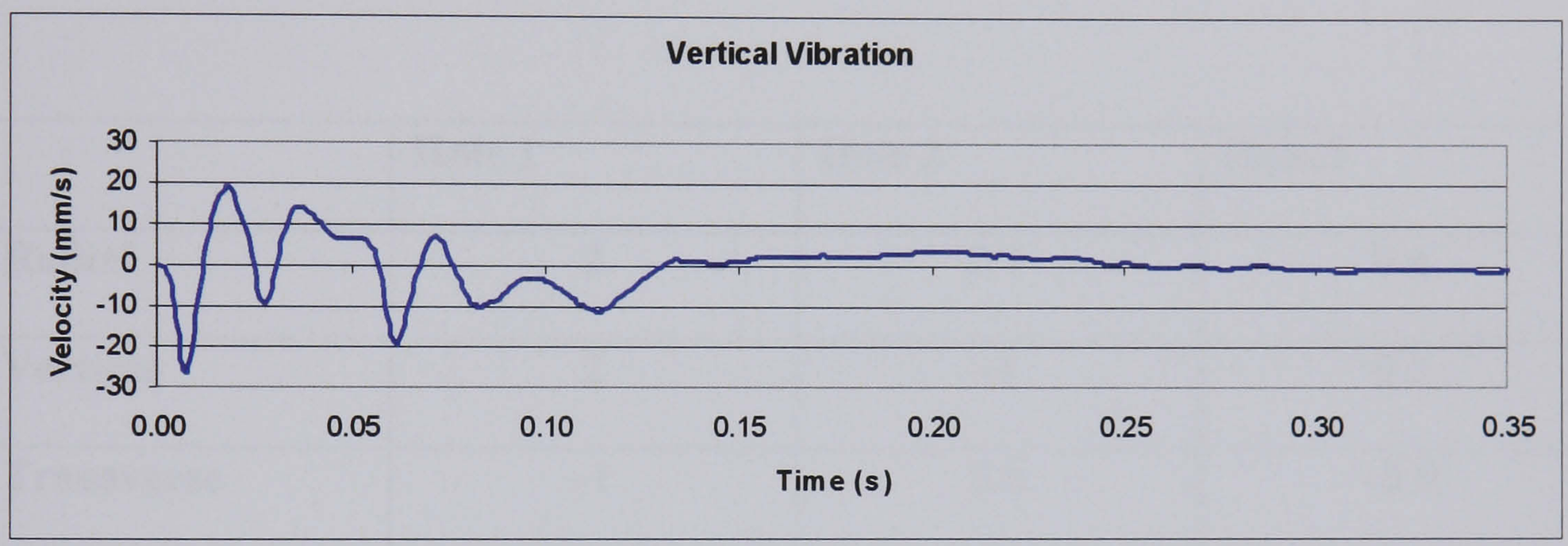

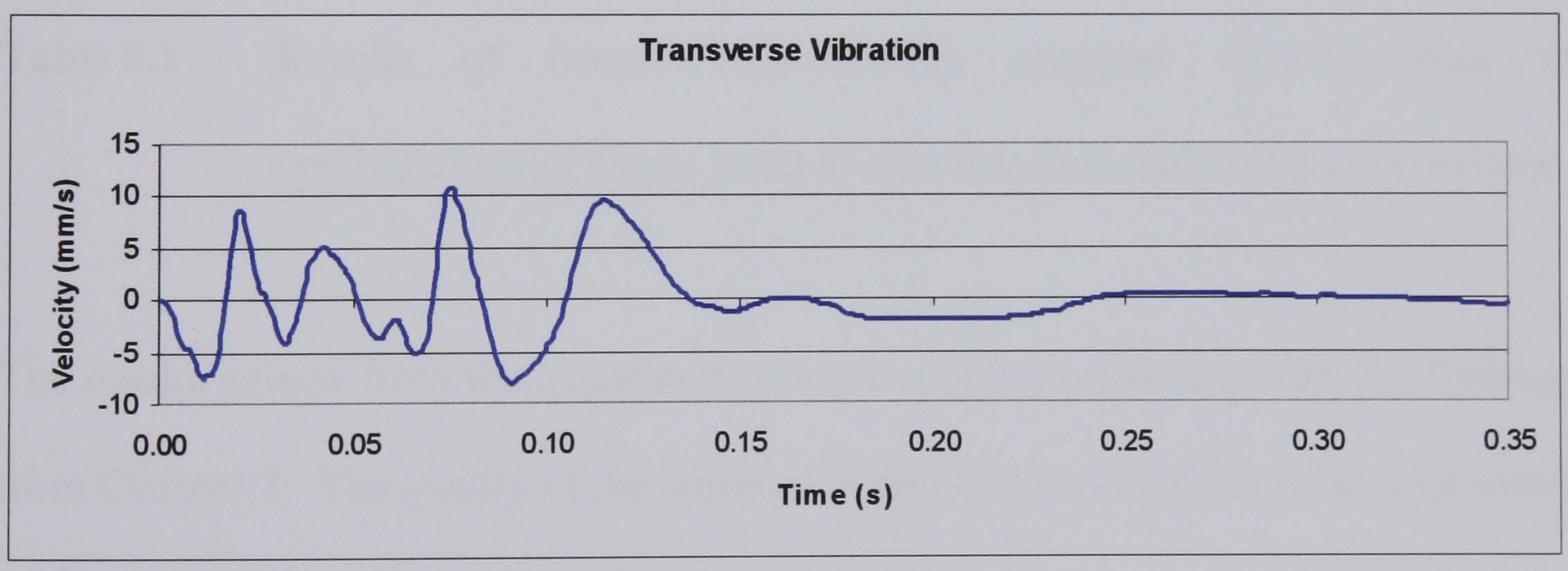

Figure 8.12 Three hole recording from Melton Ross Chalk Quarry at 60 Metres

The single hole recordings from this blast appear similar to those recorded in Chapter 7 in this area of the quarry. They are, however, very different to those recorded on the top bench.

By applying the vibration signals to the iterative convolution computer program detailed earlier the best fit combination of the single hole recordings is given. Table 8.1 gives the best fit combinations for all three axis at 60 metres. Figure 8.13 shows the resulting waveforms using the best fits, compared to the real three hole shot.

	Hole 1	**Hole 2**	**Hole 3**
Radial	2	0.9	0.8
Vertical	2	-1	0.5
Transverse	-1	0.6	-0.9

Table 8.1 Results of iterative convolution program showing best fit combinations of single holes to simulate three hole blast at 60 meters.

The results gained from the experiment do not appear to correlate with the findings from Chapter 7. The quality of the correlation between waveforms is also a lot lower than that seen in Chapter 7. This could possibly be due to the single hole not representing each hole in the blast irrespective of the phase or magnitude of the seed signal.

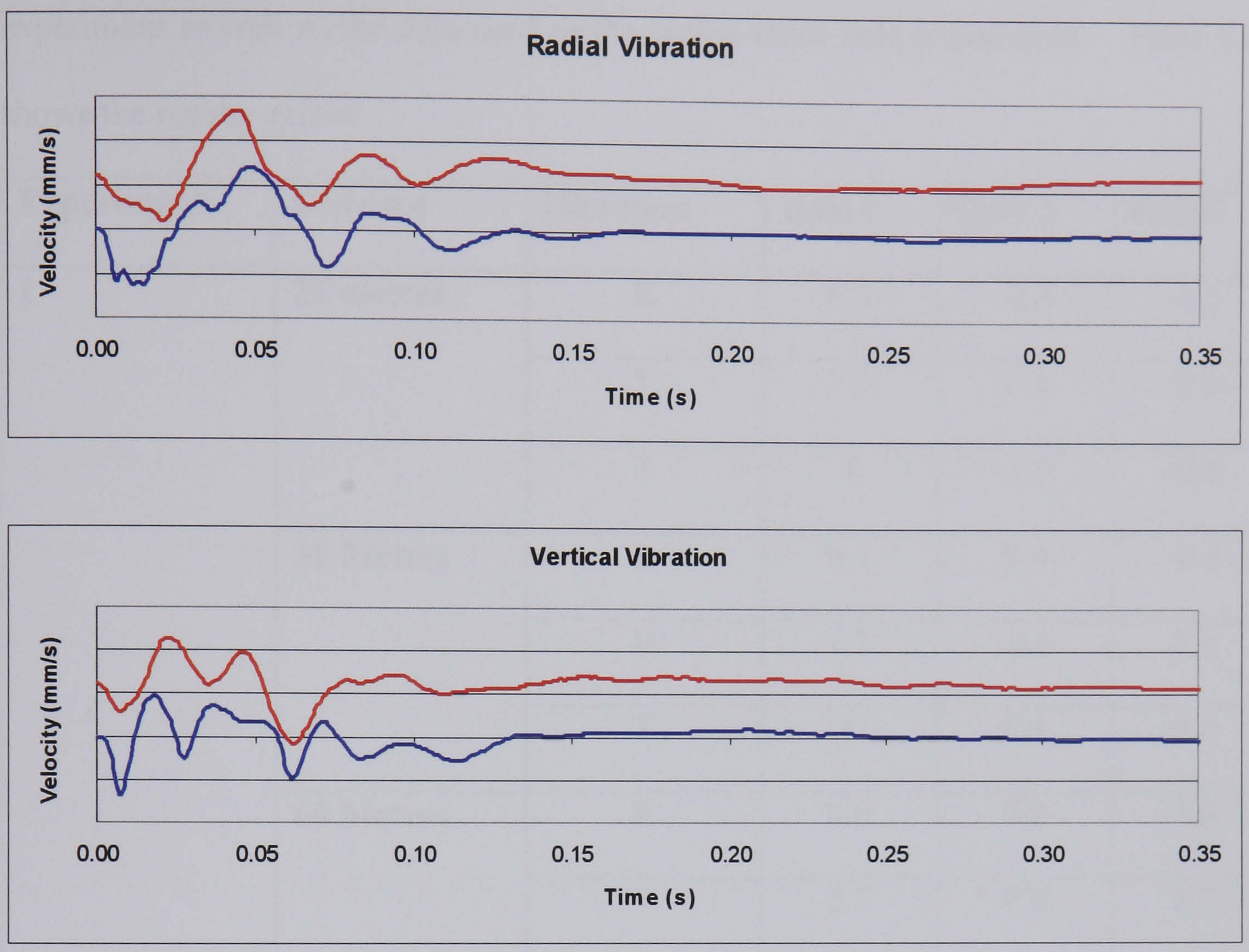

Figure 8.13 Comparison of real three hole shot vibration recording (lower) with that simulated using results from iterative convolution method (upper).

The computer program was run on the remaining useable data from the above experiment as well as the data used in the earlier three hole experiment. Table 8.2 shows the results gained.

Experiment	**Distance**	**Direction**	**Hole 1**	**Hole 2**	**Hole3**
1	**25 metres**	R	0.2	-0.4	-0.5
		V	1.5	0.4	0.6
		T	1	-0.9	-0.8
	35 Metres	R	0.4	0.4	-0.4
		V	1.2	-0.6	0.4
		T	1	0.4	0.6
	60 Metres	R	0.6	0.2	0.6
		V	0.7	0.8	0.7
		T	0.2	0.7	0.5
2	**50 metres**	R	1	0.6	0.5
		V	1.4	-0.6	0.6
		T	-0.8	0.5	-0.6
	60 Metres	R	2	0.9	0.8
		V	2	-1	0.5
		T	-1	0.6	-0.9

Table 8.2 Results of iterative convolution program showing best fit combinations of single holes to simulate three hole blasts.

The results shown in table 8.2 do not follow any pattern and fail to provide any meaningful data on which a model can be based.

8.3.3 Discussion of failure to determine a model to describe a three hole shot.

This failure to find a model which can be used to determine the vibration generated by a small multi-hole shot is disappointing. There are several explanations of this failure. The most likely reason is that the single hole is not representative of the individual holes of the multi-hole shot at Melton Ross Chalk Quarry. If one studies the recordings taken during the work at Coldstones Quarry detailed in Chapter 7 the waveshape at the beginning of the signal is similar in both the single and two hole shots. At Melton Ross, however, the first parts of the signal look very different, indicating that the single hole may not be representative of the first hole in the blast.

Another possible reason for the failure to find a model is that using different monitoring locations the same distance from two separate blasts may cause problems due to the difference in geology. It was assumed that at Melton Ross this would not be an issue as chalk is a very homogeneous material. However, as chalk is a very weak material there are many cracks caused by previous blasting activities which may affect the vibration transmission.

The differences in the angle at which the transducers are placed will also have an effect. It is possible that the inversion of the signal described in Chapter 7 is due to

reflections from the face. If the two transducers are not at exactly the same angle to the face there may be problems. To determine whether any of these reasons were to blame for the failure it was decided to return to Coldstones Quarry to undertake a similar experiment.

8.4 Determination of the vibration signal produced by individual holes of a multi-hole shot at a limestone quarry.

A five hole shot was undertaken in the same area of the quarry as the previous experiments detailed in Chapters 4 and 7. Due to design restrictions the shot had to be double decked. Each hole was loaded with approximately 80kg of hand mixed ANFO and 25kg of emulsion. The blast was recorded at the site office monitoring point in exactly the same manner as had previously been carried out. The holes were initiated with a 42ms delay between holes and an inter deck delay of 25ms. The actual timings were recorded using the MREL Microtrap VoD recorder. Figure 8.14 shows the nominal and actual firing times of each deck. The errors in firing times are quite substantial. For example, in the final hole both decks fire within 2ms of each other.

The signal generated by the 5 hole blast is shown in figure 8.15. The seed signal used with this recording was the double decked test shot described in Chapter 4.

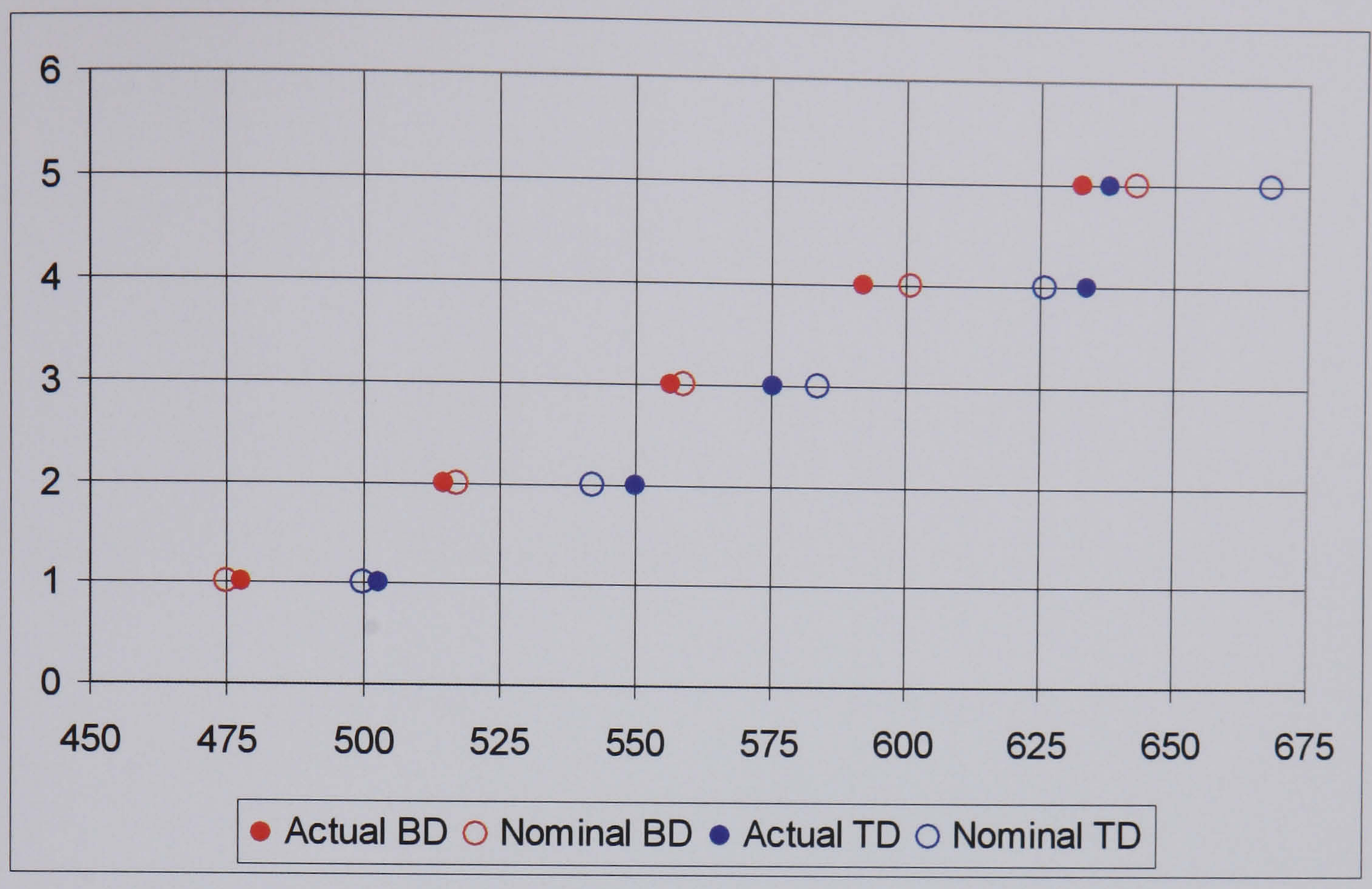

Figure 8.14 Chart of nominal and actual firing times of each deck of a five hole shot.

The 5 hole blast was processed using the iterative convolution computer program to find the best fit combination of the seed signal as had been done previously. The time taken to process each signal, however, increased drastically. Each signal took approximately 3 weeks of processing to determine the best fit with 3.2 million iterations carried out. It is obvious that this method could not be used on any larger blasts. For example if six holes were used there would be a total of 64 million iterations which is estimated would take over a year to complete.

After nine weeks of processing the results were obtained as shown in table 8.3. The signals modelled using this data are shown in figure 8.16.

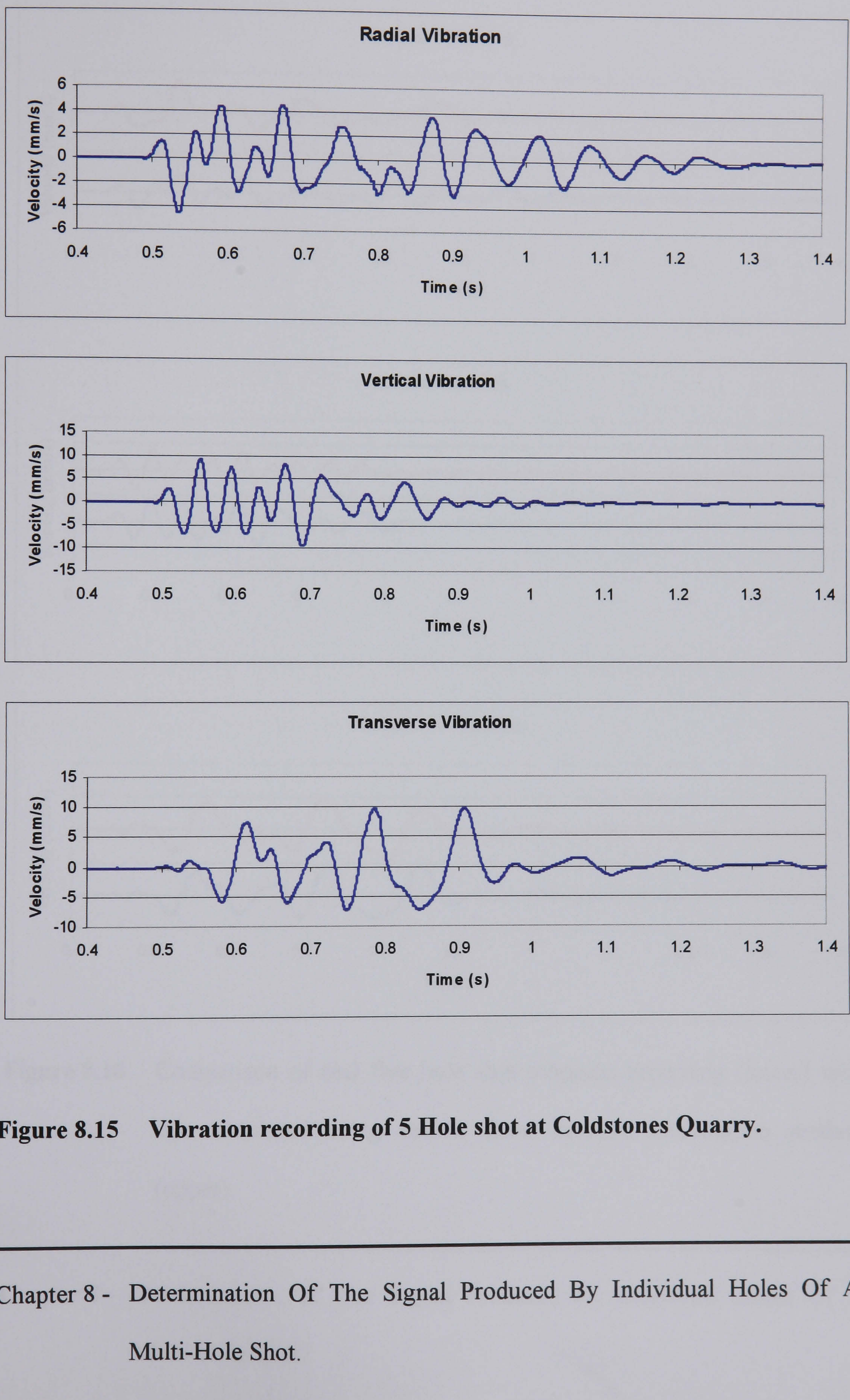

Figure 8.15 Vibration recording of 5 Hole shot at Coldstones Quarry.

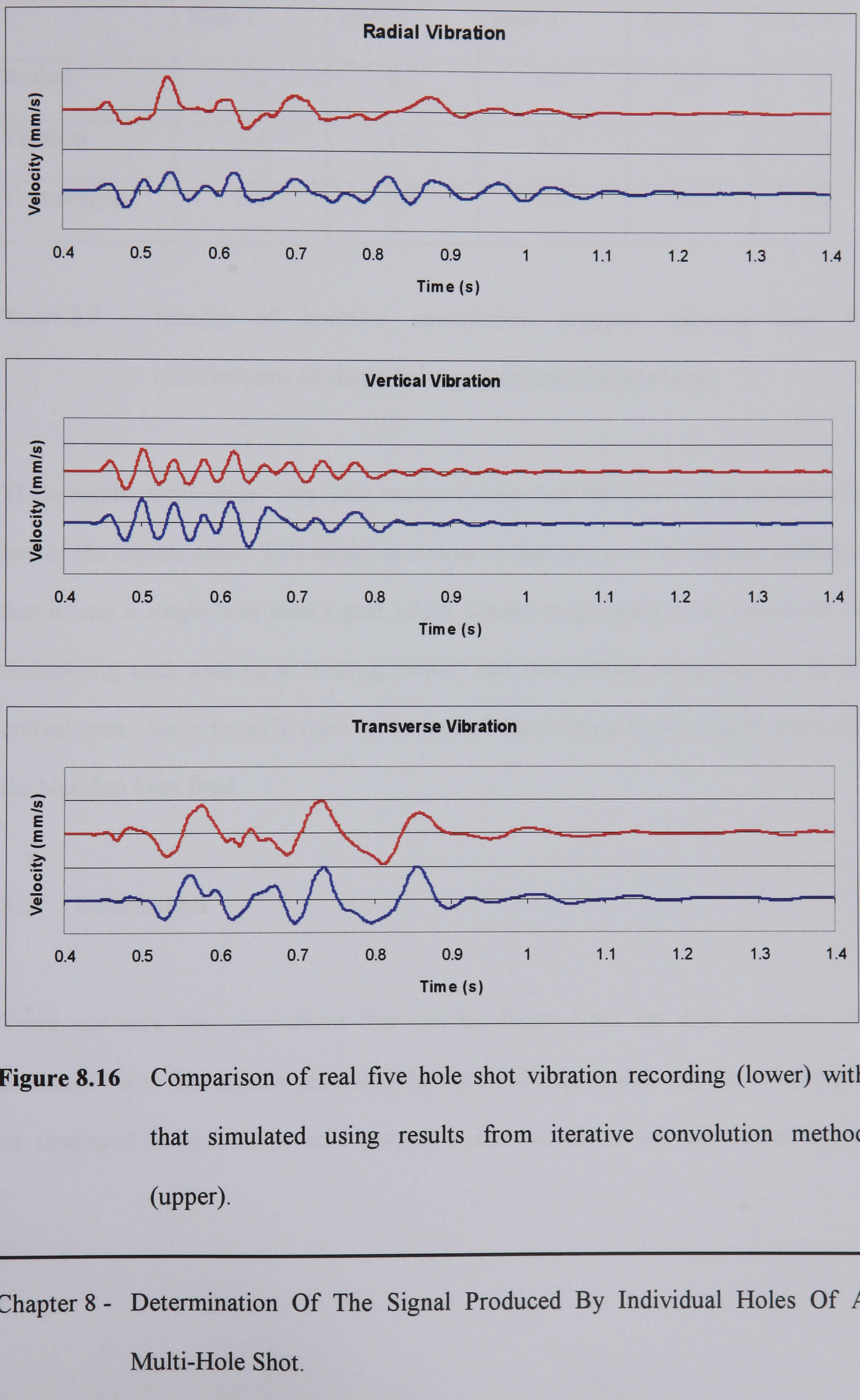

Figure 8.16 Comparison of real five hole shot vibration recording (lower) with that simulated using results from iterative convolution method (upper).

	Hole 1	Hole 2	Hole 3	Hole 4	Hole 5
Radial	1.2	0.7	0.7	0.8	1
Vertical	1.4	1.2	1.3	1.1	0.9
Transverse	0.8	0.3	0.7	0.5	1.2

Table 8.3 Results of iterative convolution program showing best fit combinations of single holes to simulate five hole blast.

These results again show very little except for the fact that there is no inversion of any of the signals seen. This model is similar to that proposed by Hinzen (1988) in that it uses a single hole seed signal which is used to generate a full waveform by multiplying each hole by a "scaling factor" and then adding them together at the correct time. Unfortunately there is no way of determining the scaling factors until the blast has been fired.

8.5 Conclusions

There are very few conclusions that can be drawn from the data gathered and presented here. The signals generated from a multi-hole shot do appear to be able to be simulated using a single hole shot as a seed waveform but only if the correct

scaling factors for each hole are known. These scaling factors can vary wildly between blasts and even between recordings of the same blast.

In order to be able to determine the scaling factors of a hole further study into the effect of dynamic parameters is required. It is also felt that inaccuracies in hole timings will have a large effect on the signal produced. The effect of inter-hole timings should also be investigated.

The failure of the work at the chalk quarry has been attributed to inconsistencies within the quality of the blasts. The VoD was measured and found to be satisfactory, but upon studying video taken of the blasts it is clear that there is much more energy being created in some blasts than others.

Chapter 8 - Determination Of The Signal Produced By Individual Holes Of A Multi-Hole Shot.

9. CONCLUSIONS AND RECOMENDATIONS FOR FURTHER WORK.

This thesis has been primarily concerned with the modelling of blasting vibrations using hybrid techniques. In order to model vibration accurately it is necessary to be able to monitor vibration accurately. The construction of a 15 channel seismograph suitable for recording high resolution blast waveforms was described in Chapter 2. Although this equipment had a few teething problems they were all subsequently addressed satisfactorily and the seismograph is now an essential part of Leeds University Mining Department's vibration monitoring equipment.

Chapter 3 detailed a calibration procedure for the seismograph based on transfer functions which was pioneered by Farnfield (1998). The procedure proposed by Farnfield was refined and made suitable for use in the field. The importance of the casing in which geophones are mounted and the system by which the case is connected to the ground are highlighted and their effect on Farnfield's system is detailed. This calibration system was used extensively throughout the research.

In Chapter 5 the repeatability of single hole shots was studied and a system developed to allow automatic comparison of blasting waveforms. It was generally shown that signals from single hole shots in the same part of a quarry produce very similar waveform shapes even if the design of the hole varies. It was also shown, however, that not all holes produce similar signals. One out of six holes fired produced an inverted signal in the radial and transverse directions.

In Chapter 6 the factors which affect the magnitude of blast vibrations from single holes were studied. It was found that for a similar set of single holes where the charge weight varies very little the most important factors affecting the vibration magnitude are the burden and the number of free faces. This led to the question that if the static burden and number of free faces can have a significant effect on the vibration levels then the dynamic burden and free faces caused by the sequential nature of delay blasting must also have an effect.

Chapter 7 examined the effect that the dynamic parameters could have on a blast by using a two hole shot which was disassembled into the two separate signals. It was found that the second hole of the blast was inverted in the radial and transverse components. This finding calls into question the assumption, in the near field at least, that all holes of a multi-hole shot produce the same vibration signal. This is a possible explanation for the failure of linear superposition techniques in the near field.

Further experimental work is required to determine the cause of this inversion although as it appears to be isolated to the radial and transverse components it can be assumed to be a function of body waves. This could also explain why it is not seen in the far field where surface waves are far more prevalent.

Chapter 8 unsuccessfully attempted to apply the findings from Chapter 7 to a three hole shot. A computer programme was developed by the author which used a single hole vibration as a seed signal to generate thousands of signals by iteratively convolving it with a series of time impulse spectra.

Chapter 9 – Conclusions And Recommendations For Further Work.

The findings from the computer program in the three hole signals were inconclusive, with wildly varying scaling values for each hole being found. The reason for the failure is unclear and more work is required to ascertain what is happening. It is suggested that a hard rock quarry is used rather than a chalk quarry due to the fact that the blasts observed at the chalk quarry appear to vary in quality greatly.

A final test was undertaken at a hard rock quarry firing a five hole blast and attempting to model it using the iterative convolution computer program. This took an extraordinarily large amount of time and could not be used to model blasts on a regular basis.

The results from modelling the five hole shot showed no inversion of the individual holes as had been seen previously with the two hole shots. The individual holes did vary in magnitude a great deal, with no apparent pattern to the scatter of magnitudes.

Further work is required to determine the exact signals produced by individual holes of a blast. Ideally the interaction of two holes should be studied in depth by varying the distance between them until they become two discreet signals. The same could be repeated for the inter-hole timings by changing the timing between the holes from simultaneous initiation to a point where they become discrete signals.

The research in this thesis has been difficult to undertake due to the problems associated with working in commercial quarries. It would be advantageous to be able to fire test shots in a manner far more controlled than has been available to me. Any future project on this subject should choose a test site with care and ensure that

funding is in place to be able to carry out drilling and blasting under the control of the researcher.

At the end of this work it is felt that steps have been made forward in the determination of vibration generated by blasting. Although further research is required to develop this work before it can be applied to hybrid modelling, it has pointed out several areas which current techniques of near field hybrid modelling need to address before they can be considered truly useful tools.

10. ACKNOWLEDGMENTS

I would like to thank my parents for their constant support throughout the course of this research, without them this thesis may never have been completed.

The funding for this research was provided by Geoffrey Walton Practice through an EPSRC grant, and I am extremely grateful to them for it.

My thanks to the Quarries which have let us make a terrible mess of their sites, especially Coldstones Quarry and Melton Ross Quarry.

Special thanks go to Rob Farnfield of Exchem Explosives who has provided many hours of his time to help in this research, and without whom I would have been completely lost.

My gratitude to Bill Birch for the opportunity to do this research and for his supervision throughout.

To everyone who has helped out by providing equipment and services my thanks.

And finally an apology to my girlfriend, who has been extremely patient and understanding despite hardly seeing me and generally being ignored. Sorry Lel.

11. REFERENCES

Abo-Zena, A.M.
"Radiation From A Finite Cylindrical Explosive Source"
Geophysics, Vol 42, No. 7, pp.1384-1393, 1977.

Aitchson, T.C. and Tournay, W.E.
"Comparative Studies Of Explosives In Granite"
RI 5509, United States Bureau of Mines, 1959.

Attewell, P.B. and Farmer, I.W.
"Attenuation Of Ground Vibrations From Blasting"
The Quarry Managers' Journal, pp. 211-215 June 1964.

Barzilai, A., VanZandt,T., Pike, T., Manion, S. and Kenny, T
"Improving The Performance Of A Geophone Through Capacitive Position Sensing And Feedback"
Proc. American Society of Mechanical Engineers International Congress, Nov. 1998.

Bellman, M.A., Mellert, V., Reckhardt, C. And Remmers, H.
"Perception Of Sound And Vibration At Low Frequencies"
J. Acoust. Soc. Amer. 105 Vol. 2, pp. 1297-1230, 1999.

Blair, D.P. and Jiang, J.J.
"Surface Vibrations Due To A Vertical Column Of Explosive"
Int. J. Rock Mech. Min Sci and Geomech. Abstr.Vol 32 pp. 149-154, 1995.

Blair, D.P. and Minchinton, A.
"On The Damage Zone Surrounding A Single Blasthole"
Proc. 6th Int. Symp. Rock Fragmentation by Blasting, Montreal, A.A.Balkema, Rotterdam, pp.121-131, 1996.

Born, W.T.
"The Attenuation Constant Of Earth Materials"
Geophysics, Vol. 6, pp. 132-148, 1941.

Bottenberg, R. A. and J. H. Ward, Jr.
"Applied Multiple Linear Regression"
Technical Documentary Report PRL-TDR-63, Lackland AFB, Texas: U. S. Department of Commerce, Clearinghouse for Federal Scientific and Technical Information, 1963.

Champeney, D.C.
"Fourier Transforms And Their Physical Applications"
Academic Press, London, 1973.

Cooley, J.W. and Tukey, J.W.
"An Algorithm For The Machine Computation Of The Complex Fourier Series"
Mathematics of Computation, Vol. 19, pp. 297-301, April 1965.

Coursen, D.L.
"Proposed Method Of Reducing Ground Vibration From Delay Blasting"
Proc. 11th Res. Symp. On Explosives and Blasting Technique, pp. 205-215, 1995.

Crandell, F.J.
"Transmission Coefficient For Ground Vibrations Due To Blasting"
Journal of Boston Soc. Civil Eng., pp. 152-168, April 1960.

Crenwelge, Jr., O.E.
"Method For Determining Amplitude-Frequency Components Of Blast Induced Ground Vibrations"
Proc. 4Th Symposium on Explosives and Blasting Research, Anaheim, California, pp. 73-90, 1988.

Dare-Bryan P.C., Wade, L. and Randall, M.
"Computer Modelling Of Bench Blasting For Grade Control"
Proc. 27th Annual Conference on Explosives and Blasting Technique, Orlando, ISEE, pp. 13-24, 2001.

Devine, J.F.
"Avoiding Damage To Residence From Blasting Vibrations"
Highway Res. Record, No.135, Highway Res. Board, Natl. Res. Council, Natl. Acad. Sci., 1966.

Devine, J.F., Beck, R.H., Meyer, A.V.C. and Duvall, W.I.
"Effect Of Charge Weight On Vibration Levels From Quarry Blasting"
RI 6774, United States Bureau of Mines, 1966.

Devine, J.F. and Duvall, W.I.
"Effect Of Charge Weight On Vibration Levels For Millisecond Delayed Quarry Blasts"
Earthquake Notes, Eastern Section, Butt. Seismol. Soc. Am., Vol.34, No.2, 1963.

Dietrich, J.H.
"Time Dependant Friction In Rock"
J. Geophys. Res., Vol. 77, pp. 3690-3697, 1972.

Dowding C.H.
"Blast Vibration Monitoring And Control"
Prentice-hall, 1985.

Dowding, C.H.
"ISRM: Suggested Method For Blast Vibration Monitoring"
Int. J. Rock Mech. Min. Sci & Geomech. Vol. 29, No. 2, pp 143-156, 1992.

Duvall, W.I. and Folgeson, D.E.
"Review Of Criteria For Estimating Damage To Residences From Blasting Vibrations"
RI 5968, United States Bureau of Mines, 1962.

Duvall, W.I. and Petkof, B.
"Spherical Propagation Of Explosion Generated Strain Pulses In Rock"
RI 5483, United States Bureau of Mines, 1959.

Farnfield R.A.
"The Application Of Transfer Functions To Blast Vibration Analysis"
PhD Thesis, University of Leeds, January 1998.

Farnfield R.A. and White T.J.
"The Application Of Detonator Timing In Vibration Control: A Case Study"
Proc. Explosives 94, University of Leeds, 1994.

Favreau R.F.
"Generation Of Strain Waves In Rock By An Explosion In A Spherical Cavity"
J. Geophys. Res. Vol. 74, pp. 4267-4280, 1969.

Firth, N.C.
"VIBReX – A Predictive Modelling Code For Assessment Of The Effect Of Blast Design On Ground Vibration"
Proc. Explosives 92, University of Leeds, 1992.

Friedman, M
"The Use Of Ranks To Avoid The Assumption Of Normality Implicit In The Analysis Of Variance"
J. Am. Stat. Assoc. Vol. 32 pp. 675-701, 1937.

Harries, G.
"The Modelling Of Long Cylindrical Charges Of Explosives"
Proc. 1st Int. Symp. On Rock Fragmentation by Blasting, Lulea, Sweden, pp419-438, 1983.

Heelan, P.A.
"Radiation From a Cylindrical source of finite length"
Geophysics, Vol. 18, pp. 685-696, 1953.

Herlufsen, H.
"Dual Channel FFT Analysis (Part 1)"
Brüel and Kjær Technical Review, No. 1, Brüel and Kjær, Denmark, ISSN 007-2621, 1984.

Heusinkveld, M. and Holzer, F.
"Methods Of Continuous Shock Front Position Measurement"
American Institute of Physics, Volume 35, Issue 9, pp. 1105-1107, 1964.

Hinzen K.G.
"Modelling Of Blast Vibrations"
Int. J. Rock. Mech. Min. Sci & Geomech. Abstr. Vol 25, No. 6, pp 439-445, 1988.

Hirai, Y., Yamada, M., Kunimatsu, S., Durucan, S., Farsangi, M.A. and Johnston, G.I.
"A Comparative Study On Numerical Methods Used For The Prediction Of Blast Vibration"
Environmental Issues and Waste Management in Energy and Mineral Production, A.A.Balkema, 1998.

Hogg, D.J.
"Digital Seismographs Are Inaccurate – But Does It Matter?"
Proc. Of Explosives 92, Leeds 1992, pp. 85-92, 1992.

Johnson, C.F.
"Coupling Small Vibration Gauges To Soil"
Earthquake Notes Volume 33, pp 40-47, 1962.

Jordan, D.W.
"The Stress Wave From A Finite, Cylindrical Explosive Source"
Journal of Mathematics and Mechanics, Vol. 11, No. 4, pp. 503-551, 1962.

Kissingler, C, Mateker, E.J., Jr, McEvilly, T.V.
"Seismic Waves Generated By Chemical Explosions, Final Report"
Air Force Cambridge Research Laboratories, 1963.

Kjartansson, E.
"Constant Q-Wave Propagation And Attenuation"
Journal of Geophysical Research, Vol. 84, 4737-4748, 1979.

Krohn, C.E.
"Geophone Ground Coupling"
Geophysics: The Leading Edge, Volume 4, Issue 4, pp.56-60, April 1985.

Langefors, U and Kihlstrom, B.
"The Modern Technique Of Rock Blasting"
Halsted Press, Wiley, New York, 1978.

Lynn, P.A.
"The Analysis And Processing Of Signals"
Macmillan, London, ISBN 0333488865, 1973.

McKenzie, C.K., Scherpenisse, C.R., Arriagada, J and Jones, J.P.
"Application Of Computer Assisted Modelling To Final Wall Blast Design"
Explo'95, pp. 285-292 1995.

Mogi, G, Hoshino, T., Kou, S-Q
"Reduction Of Blast Vibration By Means Of Sequentially Optimized Delay Blasting"
Proc. 1st world conference on Explosives and Blasting Technique, Munich, A.A.Balkema, Rotterdam, 2000.

Morris, G. and Westwater, R.
"Damage To Structures By Ground Vibration Due To Blasting"
Mine & Quarry Eng., pp.116-118, April 1953.

Oppenheim, A.V. and Schafer, R.W.
"Digital Signal Processing"
Prentice-Hall, New Jersey, ISBN 0 13 214635 5, 1975.

Plewman R.P. and Starfield, A.M.
"The Effects Of Finite Velocities Of Detonation And Propagation On The Strain Pulses Induced In Rock By Linear Charges"
J. S. Afr. Inst. Min. Metall. Vol. 66, pp. 77-96, 1965.

Randall, R.B.
"Application Of B&K Equipment To Frequency Analysis"
Brüel and Kjær, Denmark, ISBN 8787355140, 1977.

Ricker, N.
"The Form And Laws Of Propagation Of Seismic Wavelets"
Geophysics, Vol.18, 1953.

Reamer, S.K., Hinzen, K.G., Sifre, Y.
"Case Studies In The Application Of Firing Time Optimization"
Proc. 19th International Symposium of Explosives and Blasting Techniques, ISEE, San Diego, pp.281-293, 1993.

Reamer S.K., Hinzen K.G. and Stump, B.W.
"Near-Source Characterization Of The Seismic Wavefield Radiated From Quarry Blasts"
Int J. Geophysics, pp 435-450, 1992.

Rosenthal, M.F. and Morlock G.L.
"Blasting Guidance Manual''
Office of Surface Mining Reclamation and Enforcement, United States Department of the Interior, 1987.

Rost, A
"Sampling Theroem"
Agilent Technologies Lab Assignment #3,Agilent Technologies, 2001.

Sifre, Y and Bernasconi, P
"The Seismic-Hybrid Modelling (MSH) Theory And Practice(s)"
Proc. Explo 96, University of Leeds, 1996.

Siskind, D. E.
"Frequency Analysis And The Use Of Response Spectra For Blast Vibration Assessment In Mining"
Proc. 12th Symposium on Explosives and Blasting Research, Orlando, Florida, pp. 1-11, 1996.

Siskind, D.E., Stagg, M.S., Kopp, J.W. and Dowding, C.H.
"Structure Response And Damage Produced By Ground Vibration From Surface Mine Blasting"
RI 8507, United States Bureau of Mines, 1980.

Small, A.B..
"Studies In The Generation Of Blast Induced Seismic Waves In The Context Of Opencast Mining And Quarrying"
PhD Thesis, University of Leeds, August 1986.

Stagg, M.S. and Engler, A.J.
"Measurement Of Blast-Induced Ground Vibrations And Seismograph Calibration"
RI 8506, United States Bureau of Mines, 1980.

Starfield, A.M.
"Strain Wave Theory In Rock Blasting"
8th Rock Mechanics Symposium, University Of Minnesota, 1966.

Starfield A.M. and Pugliese, J.M.
"Compression Waves Generated In Rock By Cylindrical Charges: A Comparison Between A Computer Model And Field Measurements"
Int. J. Rock Mech. Min. Sci. Vol. 5, pp. 65-77, 1968.

Walker, S
"The Development Of Techniques To Investigate Structural Damage From Blasting Vibrations"
PhD Thesis, University of Leeds, January 1981.

West, R.M., Tapp, H.S., Spink, D.M., Bennett, M.A. and Williams, R.A.
"Application Specific Optimization Of Regularization For Electrical Impedance Tomography"
Measurement Science and Technology, Vol. 12, pp 1-5, Institute of Physics Publishing, 2001.

White T.J. and Farnfield , R.A.
"Computers and Blasting"
Instn. Min. and Metall. (Sect A : Min Industry), Jan-April 1993.

Wheeler, R.M.
"The Analysis Of Signature Vibrations To Help Control Vibration Frequency"
Proc. BAI 10th High-Tech Seminar on state of the art blasting technology , instrumentation and explosives, Nashville, Tennesee, USA, pp. ix3-ix21, 2001.

Whitaker, K, Chiappetta, F.R, Stump, B.

"Effects Of VOD, Explosive Column Length And Type Of Explosive On Ground Vibration Characteristics Over Distance"

Proc. BAI 10th High-Tech Seminar on state of the art blasting technology , instrumentation and explosives, Nashville, Tennesee, USA, pp. u3-u66, 2001.

Appendix A

Blast Logs From Single Hole Tests At Coldstones

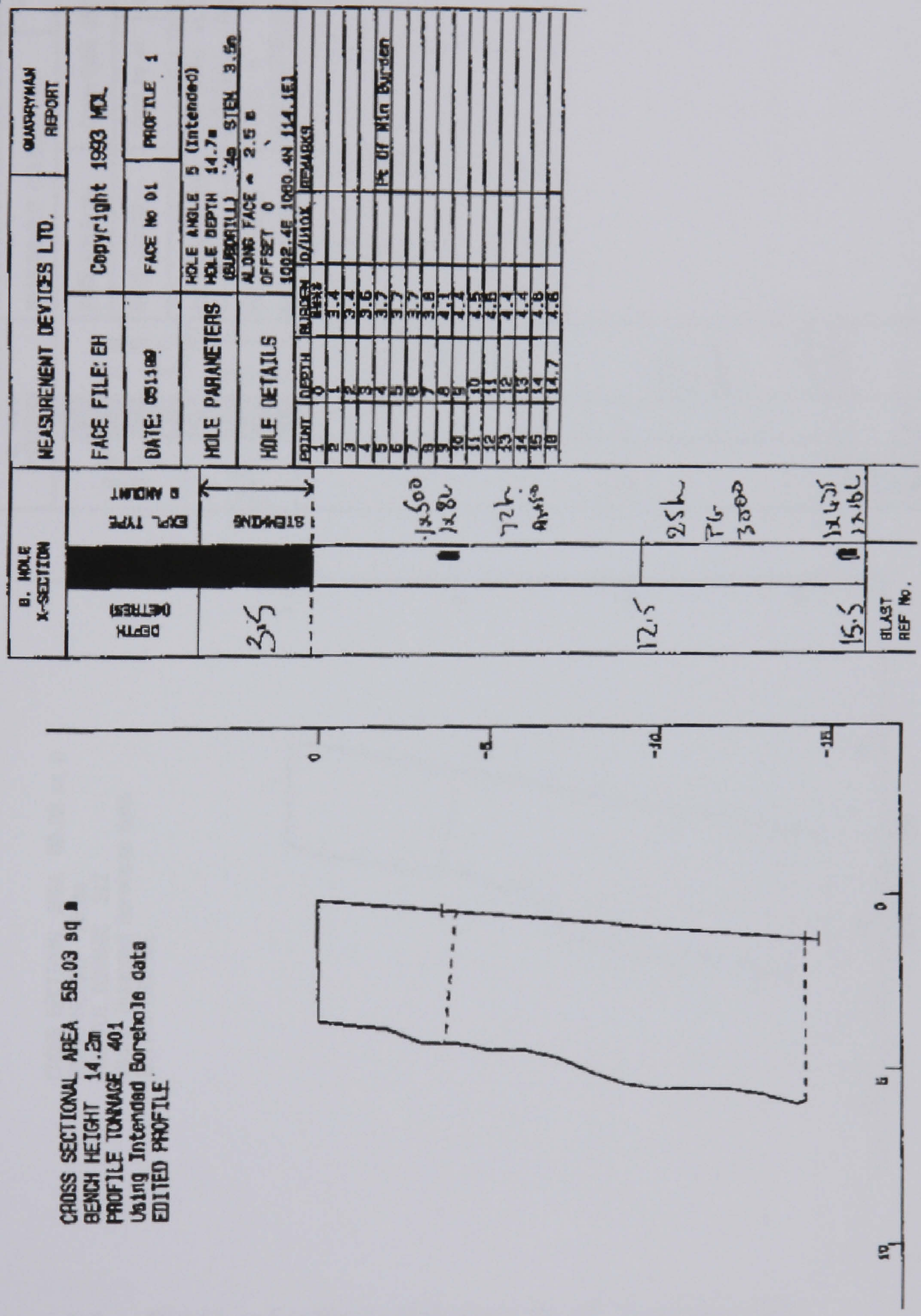

Figure A.1 Blast Log For Single Hole Fired On 8th November 1999

Appendix A

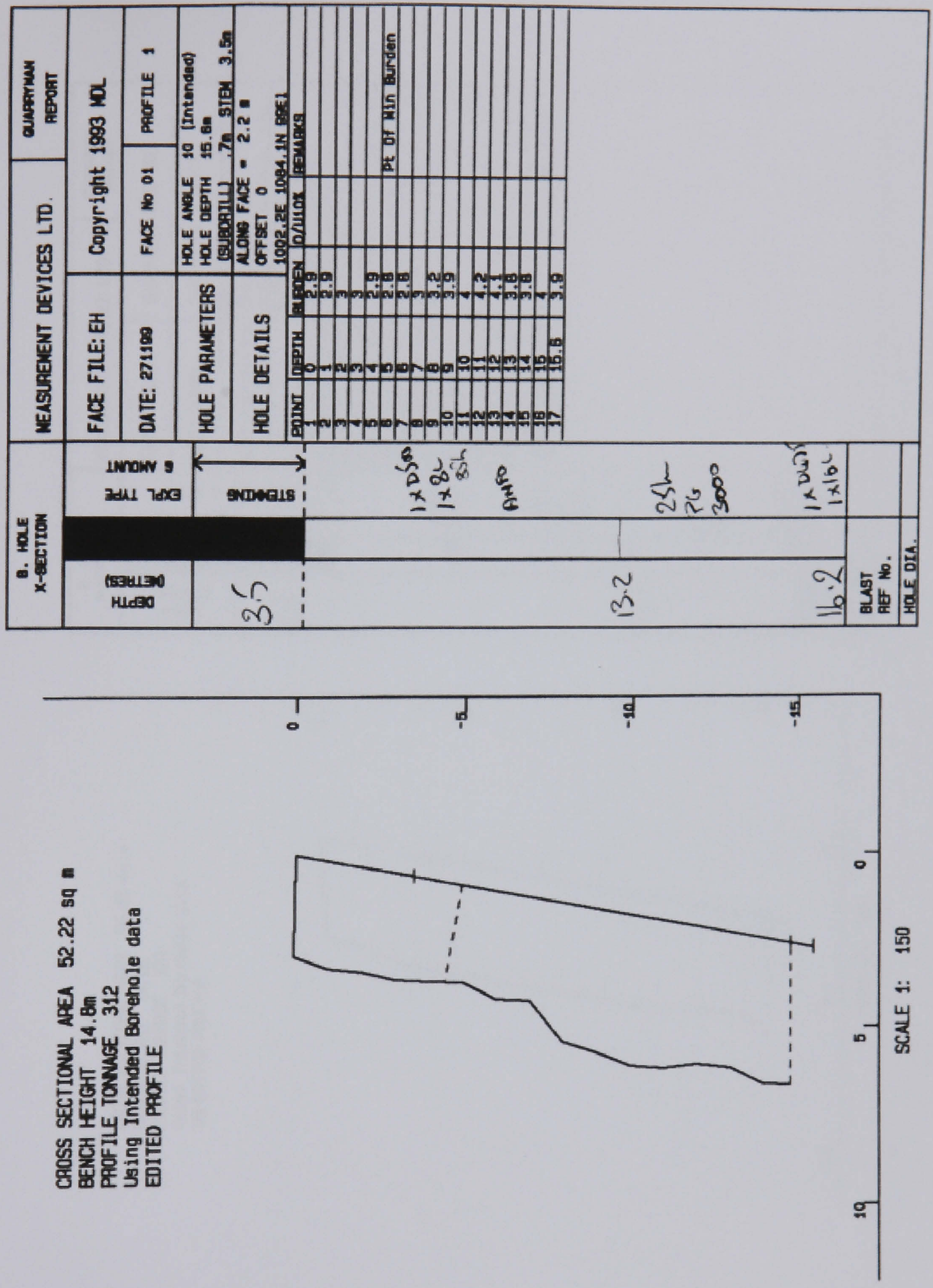

Figure A.2 Blast Log For Single Hole Fired On 29th November 1999

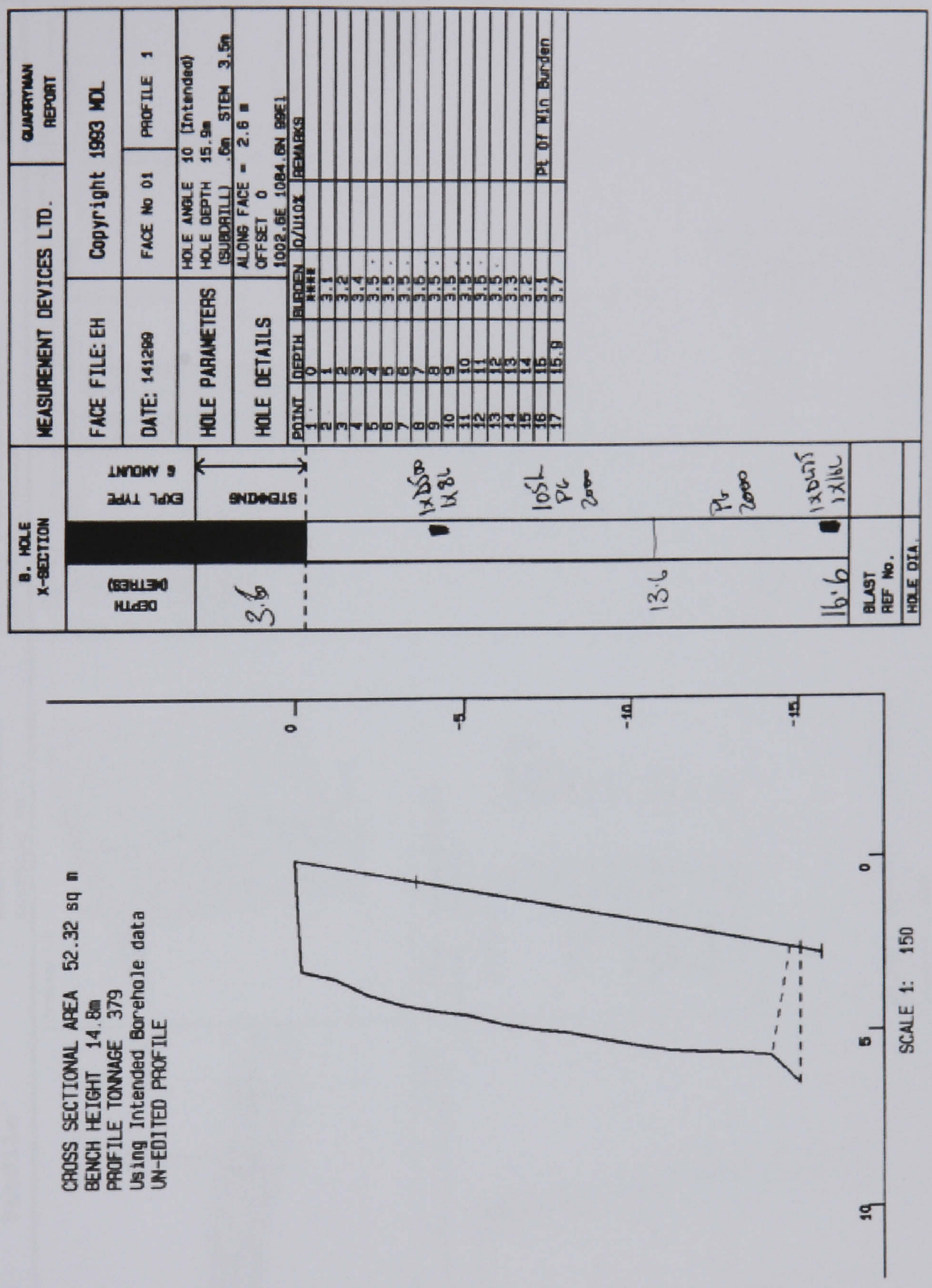

Figure A.3 Blast Log For Single Hole Fired On 15Th December 1999

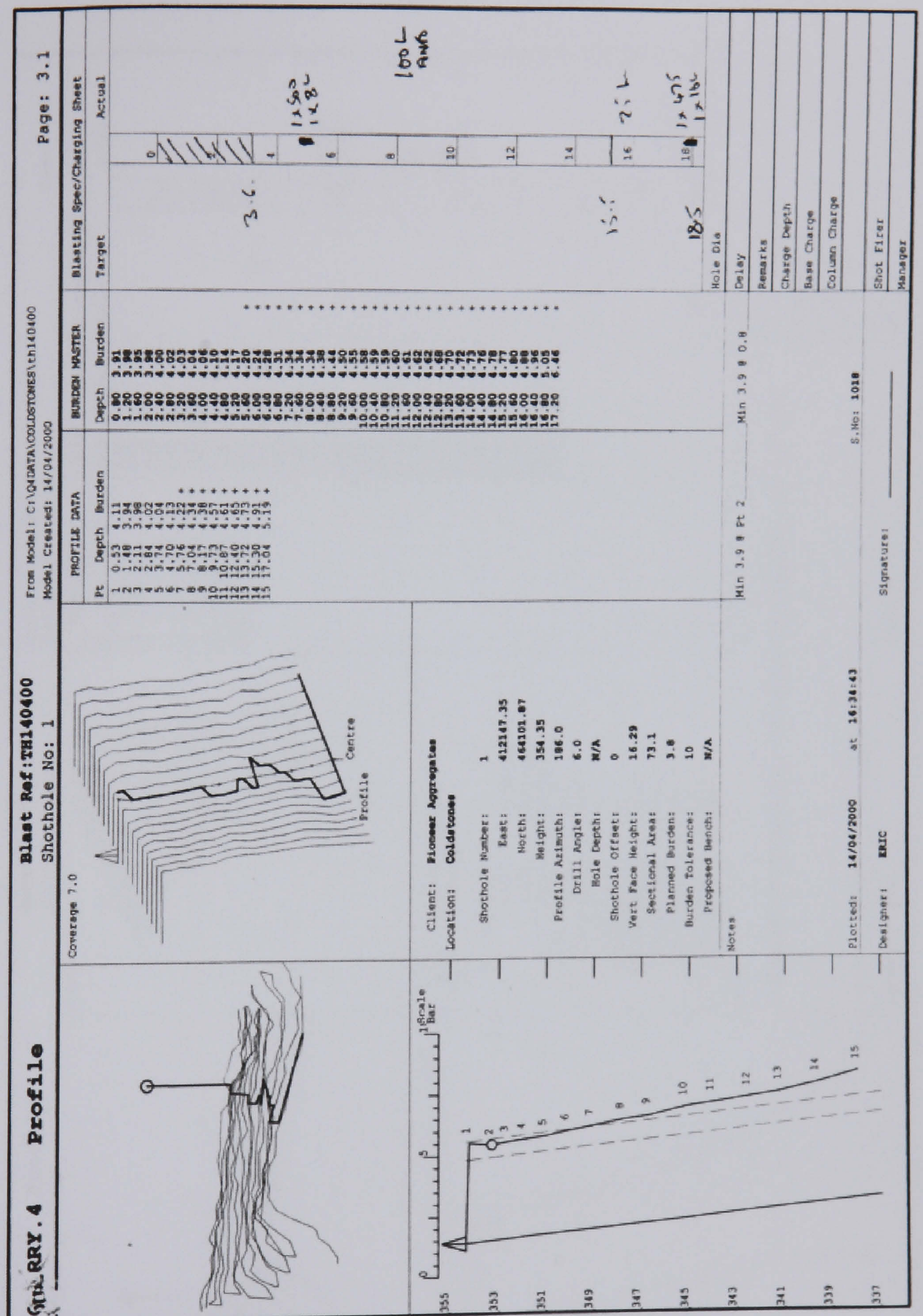

Figure A.4 Blast Log For First Single Hole Fired On 17Th April 2000

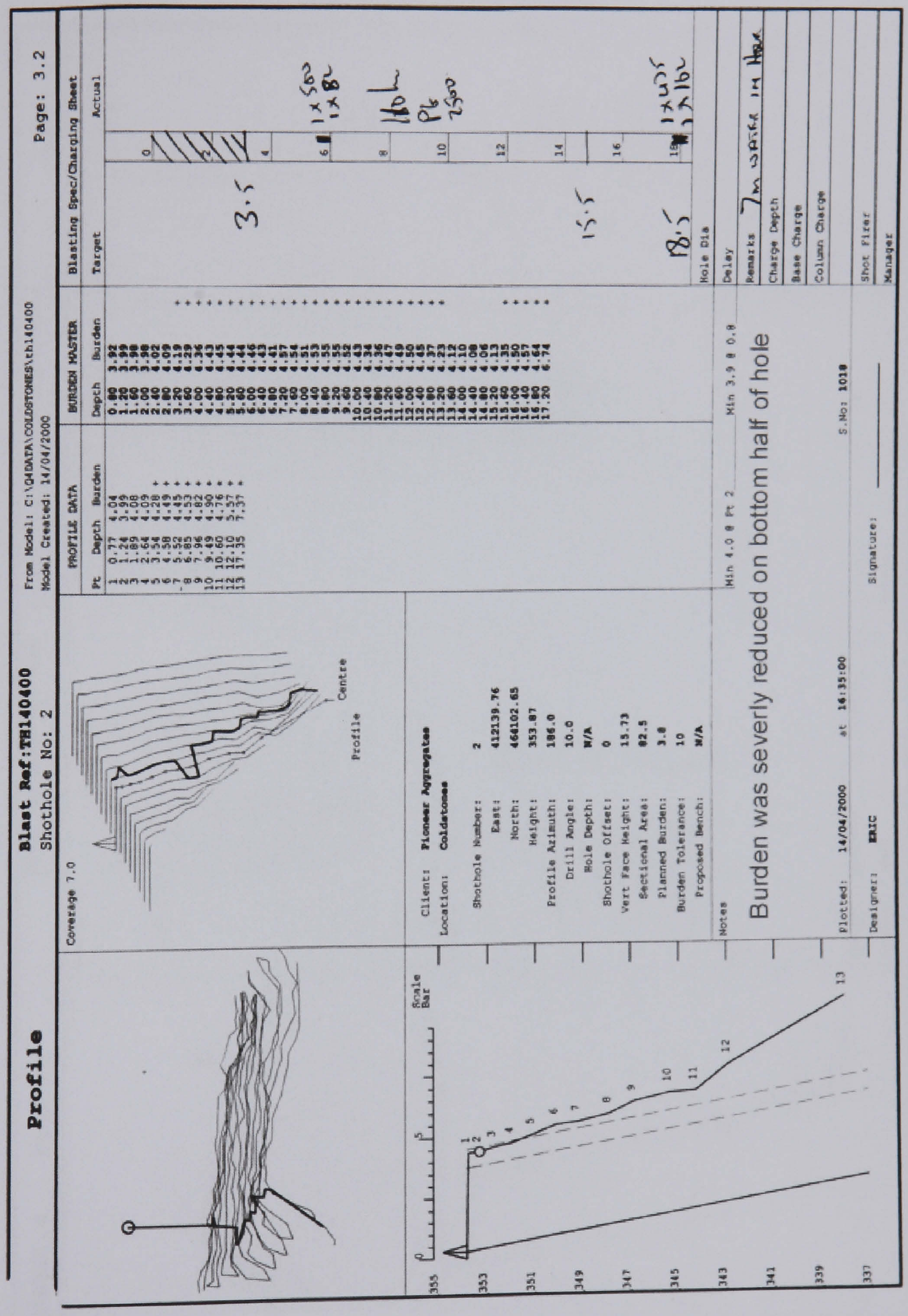

Figure A.5 Blast Log For Second Single Hole Fired On 17th April 2000

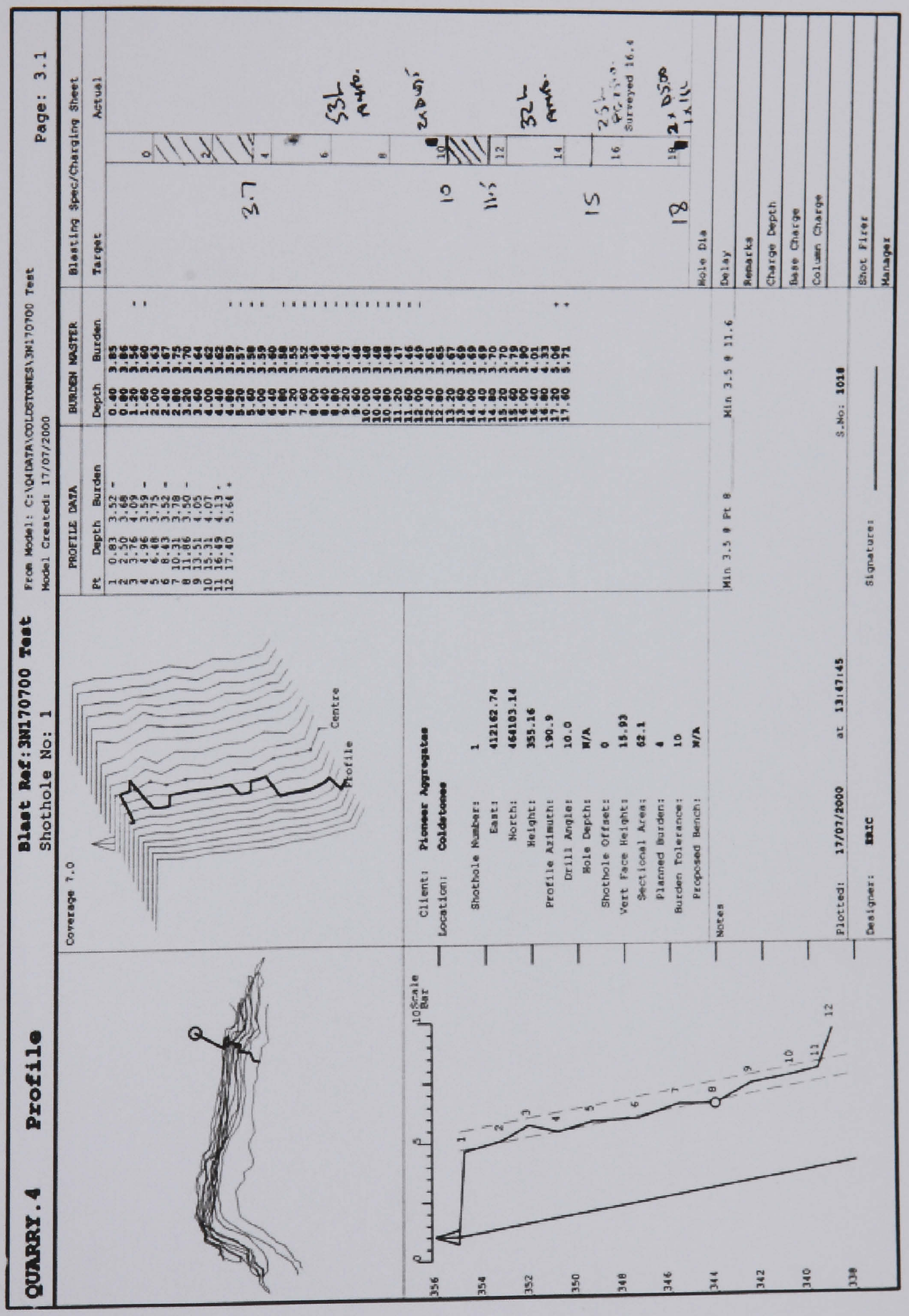

Figure A.6 Blast Log For Second Single Hole Fired On 21st July 2000

Appendix A